Effect of the Gut Environment on the Homeostasis and Function of the Enteric Nervous System

Ana Carina Bon Frauches Oliveira

Development and Homeostasis of the Nervous System Laboratory

The Francis Crick Institute

Supervisor: Vassilis Pachnis

Department of Medicine

University Imperial College London

Supervisor: Guido Franzoso

Thesis submitted to Imperial College London

for the degree of Doctor of Philosophy

April 2019

DECLARATION OF ORIGINALITY

I, Ana Carina Bon Frauches Oliveira, declare that all work presented in this thesis is the result of my own investigation, and all information, data, results, figures have been properly referenced. Besides, I state that all collaborations either experimental or in the provision of materials, including mice, have been rightly acknowledged.

Ana Carina Bon Frauches Oliveira

January 2019

Copyright declaration

The copyright of this thesis rests with the author and is made available under a Creative Commons Attribution Non-Commercial No Derivatives licence. Researchers are free to copy, distribute or transmit the thesis on the condition that they attribute it, that they do not use it for commercial purposes and that they do not alter, transform or build upon it. For any reuse or redistribution, researchers must make clear to others the licence terms of this work.

ABSTRACT

The gastrointestinal (GI) tract performs essential functions that maintain health and homeostasis of organisms. A complex set of tissues of distinct embryological origin (such as epithelial cells and the local immune and nervous systems) interact continuously in order to maintain a functional equilibrium and normal physiology which is constantly threatened by multiple and sometimes severe challenges originating within the wall or the lumen of the gut. The enteric nervous system (ENS) is composed of an intricate and complex network of enteric glial cells (EGCs) and neurons localised into different compartments within the intestinal wall. These cells are involved in controlling virtually all aspects of GI function, including intestinal peristalsis. Due to its positioning at the interface between the internal and external milieu of the body, the ENS shares the same intestinal environment with the highly active immune system and the rich and diverse communities of microbiota and therefore is expected to be influenced by immune responses and microbial dynamics. However, the methodology to study these questions and consequently our understanding of neuro-immune-microbe interactions in the mammalian gut is limited. In this thesis, we examined the effects of the intestinal environment, such as microbiota and adaptive immune system on the homeostasis and function of the ENS in adult animals. We have successfully generated a robust technology to isolate and investigate the molecular profile of enteric neurons from the adult gut, in addition to an *in vitro* system that allows the establishment and maintenance of the adult EGCs. Moreover, by using germ-free (GF) and inflammation mouse models, our experiments demonstrated that subtle changes in the intestinal environment are enough to alter the normal physiology of the ENS. Furthermore, we found that the adaptive immune system is crucial for maintaining the integrity and functional equilibrium of the ENS. Together, our data suggest that the balance between microbiota and adaptive immune system regulates the organisation and homeostasis of the ENS.

I dedicate all work and effort I put in my PhD journey in memory of my forever professional inspiration and dear friend Professor Dr Jane Faria, and my beloved grandpa Ely Frauches, who taught me to be strong and not to be afraid to pursue my dreams.

ACKNOWLEDGEMENTS

"Gosto de ser gente porque inacabado, sei que sou um ser condicionado, mas consciente do inacabamento, sei que posso ir mais além dele." Paulo Freire

I could not have finished or even started this journey without several important people who substantially supported me and my work, and significantly contributed to my personal and professional development. I must say that I would not have been able to go through the most challenging moment of my life, so far, without every single help and support.

I would like to immensely thank Vassilis for not giving up on me and accepting my limitations from even before I started, especially for exposing me to an excellent environment with high-quality science and great people. Vassilis, thank you for your support and guidance during this journey and for sharing your enthusiasm for science, for always being accessible and for teaching me to see "the big picture" and, well, "let's talk about science!". Thank you for the unforgettable experience and opportunity that undoubtedly made me a better person and a better scientist. I could not have gone through in a daily basis without the present and former members from the Pachnis lab. Thank you guys for being friends, family and for teaching me science, drama and English. Thank you Yuuki and Song for sharing your knowledge, teaching me so much and working with me. Our late "MCB" ideas and experiments were essential to bring up great contribution to our lab. Thank you Fränze and Song for reading my thesis and helping me to improve my writing. Thanks Reena and Tiffany for standing up and checking up on me when I needed the most. Thanks Tiffany for believing in me, always. Thanks to the new members of the lab and I hope you keep the vibe up, no pressure. Thanks to the kids, who listened to my dramas and taught me not only science, but all the other important things that make life better and easier. Thanks for supporting me not only in the lab but also in every single "unexpected" thing that "only happens to Ana". Thanks to Colin for the delicious treats and delightful chats in my early mornings. Thank you Werend for sharing your knowledge about the adult ENS with me, as well for being a great friend. I could write an entire book and it would not be enough to thank you all for the experience and friendship. I am lucky and it was a privilege to have worked with you all.

I would like to thank my thesis committee Vivian Li, Victor Tybulewicz and Guido Franzoso for guiding and following my project through, and for giving me helpful feedback to progress and improve throughout my PhD. Thank to my dear Eileen, Shova and Rachel for helping with the administrative bits that I am terrible at. A huge thanks to the former and present student support team at the Crick, especially Donna Brown, Caroline Ransom and Jirina Marková who never let me to miss an important deadline and looked after my university bureaucracy papers so I could focus on my work. Not a single experiment in this thesis was done without the support from the Crick Science and Technology Platform teams. An enormous thanks to the BRF team for providing and looking after my animals, and helping me whenever I needed, especially Murad Miah, Rekha Subramaniam and Jacek Mor. Thanks to the Light Microscopy team, especially Donald Bell for teaching me imaging. Thanks to the Experimental Histopathology, Advanced Sequencing Facility, Metabolomics and Flow Cytometry facilities for the collaboration with my experiments. Thanks to Dr Stefan Boeing from the Bioinformatics and Biostatics team for analysing my samples. A huge thanks to every single colleague from the Crick who was not directly involved in my project but made sure I had the infrastructure I needed to develop my work. Thanks to our collaborators who provided us with animals, reagents and ideas. A big thanks to the Stockinger lab, especially Andrea and Sara who helped me so much with the discussions towards the immunology aspects of my project.

Thanks to the Professors Vivaldo Moura Neto, Jane Faria (who I will miss forever) and Luciana Romão who believed in me and gave me an opportunity back in Brazil to be immersed into neuroscience and who taught me how to hold on a pipette.

Beyond science, I could not have done anything without the love and support from my family. Obrigada pai e mãe por tudo o que vocês fizeram para que eu conseguisse chegar até aqui, por terem acreditado em mim e por me amarem incondicionalmente. Thanks to my brothers João, Dudu, my sister Carol, and my nephew and niece Benício and Duda. You are everything to me, thanks for making my days less painful even from a distance, especially now right at the end. Thank you so much for crossing over the ocean to give me love when I needed the most. I love you. Thanks to the Morey family who embraced me as their own and kindly looked after me. Love you all.

Thanks to all my friends who believed in me and gave me the emotional support I needed to carry on. Thanks Diana for really looking after me always, especially while I was writing my thesis, for checking up every single day, for feeding me, listening to my insane moments. Thank you for keeping me sane (trying). Your help, love and support are vital to me. Love you lots. Thanks Gustavo and Alice for being always there, I love you and I miss you much. Thanks to my favourite Brazilians in London who were very supportive and never let me to give up. Love you Ju, Giu, Lolô, Rodrigo, Pedro, Mari and Deborah. Thanks to my favourite Italians ever, my friends and my brothers Micheal and Andrea for your terrible advices that I never listened to. Thanks to Daria, my dear friend for listening to me and checking up on me. Thanks to my friends Kristina, Fabio and Eva for your care, love and support. Love you. White side of the force, I am so grateful for every single detail since the day I met you. I believe that you know who your real friends are when you are in a challenging and difficult moment and you do not feel lonely… and you have support and love. I know I am very lucky for having the best ones around me.

My dear Jane, I am lucky I could tell you how important you are to me and how inspiring you were as a passionate anatomy professor, nurse and scientist. As a strong woman, mother and dedicated friend. I will never forget every single moment since my first anatomy class when I thought "I want to be this woman". I hope I can be at least half of what you were as a human being and inspire people as you inspired me and continue doing so. I will be forever grateful for having met you and for being your friend, for being the first ones to arrive in the lab and the last ones to leave... for laughing and crying together. Thank you and thank you. You will be forever in my heart and thoughts.

ABBREVIATIONS

5-HT	5-Hydroxytryptamine
α-SMA	α-smooth muscle actin
AAV	Adeno-associated virus
Aβ	β-amyloid
ACh	Acetylcholine
AD	Alzheimer's disease
ADP	Adenosine diphosphate
Adrb2	β2 adrenergic receptor
AH	After-hyperpolarisation
AhR	Aryl hydrocarbon receptor
APC	Antigen presenting cell
APP	Amyloid precursor protein
ATP	Adenosine triphosphate
BBB	Blood brain barrier
BCSFB	Blood-cerebrospinal fluid barrier
BDNF	Brain-derived neurotrophic factor
BFABP	Brain fatty acid binding protein
BMP2	Bone morphogenetic protein 2
BMPRII	Bone morphogenetic protein receptor II
BRB	Blood-retinal barrier
CaMKII	Ca2+/Calmodulin-dependent protein kinase II
CD	Cluster of differentiation
CD	Crohn's disease
CGRP	Calcitonin gene-related peptide
ChAT	Choline acetyl transferase
CM	Circular muscle
CMMCs	Colonic migrating motor complexes
CMV	Cytomegalovirus
CNS	Central nervous system
CSF	Cerebrospinal fluid
CSF1	Colony stimulating factor 1
CSF1r	Colony stimulating factor 1 receptor
CX3CR1	CX3 chemokine receptor 1
DAPI	4',6-diamidino-2-phenylindole
DCs	Dendritic cells
dH20	Distilled water
Dil	1,1'-dioctadecyl-3,3,3',3'-tetramethylindocarbocyanine perchlorate
DIV	Days *in vitro*
DMEM	Dulbecco's modified eagle's medium
DNBS	Dinitrobenzene sulfonic acid

DRG	Dorsal root ganglion
DSS	Dextran sodium sulphate
E-	Embryonic day
EDNRB	Endothelin receptor B
EDTA	Ethylenediaminetetraacetic acid
EGCs	Enteric glial cells
eGFP	Enhanced green fluorescent protein
ENS	Enteric nervous system
EPSPs	Excitatory post-synaptic potentials
eYFP	Enhanced yellow fluorescent protein
FACS	Fluorescence activated cell sorting
FAE	Follicle-associated epithelium
FBS	Foetal bovine serum
FD	Functional dyspepsia
FFPE	Formalin fixed and paraffin embedded
FITC	Fluorescein
FoxD3	Forkhead box d3
FoxP3	Forkhead box p3
FSC	Forward scatter
GABA	Gamma (γ)-aminobutyric acid
GALT	Gut-associated lymphoid tissue
GDNF	Glial derived neurotrophic factor
GF	Germ free
GFAP	Glial fibrillary acid protein
GFP	Green fluorescent protein
GI	Gastrointestinal
gMacs	Gut self-maintaining macrophages
H	Height
H&E	Haematoxylin and eosin
HAND2	Heart and neural crest derivatives expressed 2
HFD	High fat diet
IBD	Inflammatory bowel disease
ICCs	Interstitial cells of Cajal
IELs	Intra epithelial lymphocytes
IFN	Interferon
Ig	Immunoglobulin
IL	Interleukin
ILCs	Innate lymphoid cells
ILFs	Isolated lymphoid follicles
iNKT	Invariant natural killer T
IPANs	Intrinsic primary afferent neurons
ISP	Inner submucosal plexus

KASH	Klarsicht ANC-1 syne homology
L/D	Live and dead
LM	Longitudinal muscle
LMMP	Longitudinal muscle myenteric plexus
LpMs	Lamina propria macrophages
LPS	Lipopolysaccharide
LTi	Lymphoid tissue inducer
M3Rs/M5Rs	Muscarinic receptors
MHC	Major histocompatibility complex
MLNs	Mesenteric lymph nodes
MMCs	Migrating motor complexes
MMs	Muscularis macrophages
MP	Myenteric plexus
MSCs	Mesenchymal stem cells
MUC	Mucosa
Myd88	Myeloid differentiation factor 88
N	Number of independent samples
n.s.	Non-significant
NCCs	Neural crest cells
NDS	Normal donkey serum
NF	Neurofilament
NK cell	Natural killer cell
NMU	Neuromedin U
Nmur1	Neuromedin U receptor 1
NO	Nitric oxide
NOS	Nitric oxide synthase
NPY	Neuropeptide Y
nRNAseq	Nuclear RNA sequencing
NSE	Neuron-specific enolase
O/N	Overnight
OSP	Outer submucosal plexus
P-	Postnatal day
P/S	Penicillin/Streptomycin
P2x7/P2Y4	Purinergic receptors
PACAP	Pituitary adenylyl cyclase activating peptide
PBS	Phosphate buffered saline
PBST	Phosphate buffered saline with triton
PCA	Principal component analysis
PCR	Polymerase chain reaction
PD	Parkinson's disease
PDGFR	Platelet-derived growth factor receptor
PFA	Paraformaldehyde

PGP9.5	Protein gene product 9.5
Phox2b	Paired-like homeobox 2b
PLP1	Proteolipid protein 1
PNS	Peripheral nervous system
PPs	Peyer's patches
PRRs	Pattern recognition receptors
qRT-PCR	Quantitative real-time PCR
RAG	Recombination activating gene
RB1	Retinoblastoma 1
RET	Rearranged during transfection
RFP	Red fluorescent protein
RNA	Ribonucleic acid
RT	Room temperature
SCFAs	Short-chain fatty acids
SD	Standard deviation
SFB	Segmented filamentous bacteria
SILTs	Solitary isolated lymphoid tissues
SMP	Submucosal plexus
SOM	Somatostatin
SOX	SRY (Sex determining Region Y)-box
SP	Substance P
SPF	Specific pathogen free
SSC	Side scatter
TCR	T cell receptor
TGF	Transforming growth factor
TGR5	G-protein-coupled bile acid receptor 1
TH	Tyrosine hydroxylase
Th	T helper
TK	Tachykinin
TLR	Toll-like receptor
TMX	Tamoxifen
TNBS	2,4,6-trinitrobenzene sulphonic acid
TNF	Tumour-necrosis factor
TNFR	Tumour-necrosis factor receptor
Treg	Regulatory T cell
TTX	Tetrodotoxin
Tuj1	Neuronal class III β-Tubulin
UC	Ulcerative colitis
V(D)J	Variable, diversity and joining
VIP	Vasoactive intestinal peptide
W	Weight

TABLE OF CONTENTS

Declaration of Originality **2**
Copyright Declaration **2**
Abstract **3**
Acknowledgements **5**
Abbreviations **8**
Table of Contents **12**
List of Figures **17**
List of Appendices **19**
List of Tables **20**
Chapter 1 | Introduction **22**
1.1 The enteric nervous system (ENS) **22**
1.1.1 Structure and organisation of the adult ENS 23
1.1.2 Functions of the adult ENS 25
1.1.3 Cellular components of the adult ENS 26
1.1.3.1 The enteric glial cells (EGCs) 27
1.1.3.1.1 Localisation and morphology of EGCs 27
1.1.3.1.2 Molecular markers to identify EGCs 29
1.1.3.1.3 Physiological functions of EGCs 32
1.1.3.2 The enteric neurons 35
1.1.3.2.1 Morphology of enteric neurons 37
1.1.3.2.2 Electrophysiology of enteric network 38
1.1.3.2.3 Pan-neuronal markers and chemical coding of enteric neurons .. 38
1.1.3.2.4 Physiological role of enteric neurons 40
1.1.4 Neurogenic control of the colonic motility 44
1.1.5 Enteric Neuropathies/Hirschsprung disease 46
1.1.6 Enteric Neuropathies/Neurodegenerative diseases 48
1.2 An overview of the gut immune system **50**
1.2.1 The adaptive and innate immune systems of the gut 51
1.2.2 Neuroimmune communications 58
1.2.2.1 The immune and central nervous systems 59
1.2.2.2 The gut immune system and the ENS 62

1.3 The microbiome 65
1.3.1 Facts and curiosities about the human microbiota 65
1.3.2 Microbiota and the gut immune system 67
1.3.3 Microbiota and the ENS 70
1.4 Environmental changes that affect the ENS 74
1.4.1 Inflammatory bowel disease 74
1.4.1.1 Genotypic and phenotypic aspects of IBD 76
1.4.1.2. Mouse models for experimental colitis 77
1.4.2 Neuroimmune interactions in a parasitic environment 79
1.5 Models for experimental research 82
1.6 Cell fate restriction and cell plasticity… 84
1.7 Aims of the work performed in this thesis 87
Chapter 2 | Materials and Methods 88
2.1 Materials 89
2.1.1 Reagents 89
2.1.2 Solutions 89
2.2 Methods 89
2.2.1 Animals 89
2.2.1.1 Mouse lines 89
2.2.1.2 Tamoxifen injections 93
2.2.2 Tissue manipulation techniques 93
2.2.2.1 Whole-mount gut preparation 93
2.2.2.2 Dissection of the adult longitudinal muscle myenteric plexus 94
2.2.2.3 Gut sections 94
2.2.3 Primary EGC cultures of dissociated adult LMMPs 95
2.2.4 Adeno-associated virus and labelling of enteric neurons 96
2.2.5 Flow cytometry and fluorescence activated cell sorting 97
2.2.5.1 Immunoprofiling of LMMPs and mucosal layer 98
2.2.5.2 Isolation of lymphocytes from spleen and mesenteric lymph nodes 99
2.2.5.3 Adoptive transfer of lymphocytes 99
2.2.5.4 Adoptive transfer of $CD4^{+}CD45RB^{high}$ T lymphocytes 100
2.2.5.5 Neuronal nuclei isolation from the MP 100
2.2.6 Immunofluorescence assays 101

2.2.7 DiI labelling of neuronal network 104
2.2.8 Histology 105
2.2.9 Microscopy and image processing 105
2.2.10 Images analysis and quantification 105
2.2.11 Total gastrointestinal transit time 105
2.2.12 Stool analysis 106
2.2.13 Live video recording and spatiotemporal analyses of ENS-dependent motility 106
2.2.14 SFB reconstitution 107
2.2.15 Molecular biology techniques 107
2.2.15.1 RNA isolation and cDNA synthesis 107
2.2.15.2 qRT-PCR 108
2.2.15.3 nRNAseq 109
2.2.16 Statistical analysis 110
Chapter 3 | Development of novel experimental approaches for ENS studies 111
3.1 Development of EGC cultures from the adult gut 112
3.1.1 Introduction 112
3.1.2 Aims 114
3.1.3 Results 114
3.1.3.1 Validation of the transgenic mouse line *Sox10::CreER^{T2};R26R-CAG-td^{Tomato}* 114
3.1.3.2 Establishment of a new method to culture adult EGCs 115
3.1.4 Discussion 122
3.2 AAV-based strategies for the characterisation of adult enteric neurons 125
3.2.1 Introduction 125
3.2.2 Aims 128
3.2.3 Results 128
3.2.3.1 AAV9-CaMKII.Cre efficiently transduces enteric neurons from the myenteric and submucosal plexuses following intravenous injection in the adult mice 128

3.2.3.2 AAV9-KASHeGFP drives expression of GFP to the nuclear envelope of neurons from the MP and SMP of adult mouse intestine 130
3.2.3.3 Chemical coding of AAV9-KASHeGFP transduced neurons in the MP and SMP from the small intestine of adult mice 132
3.2.3.4 Efficient isolation of enteric neuronal nuclei from the MP of mice transduced with AAV9-KASH-eGFP/tdT 135
3.2.4 Discussion 138
Chapter 4 | Impact of gut states on ENS physiology 142
4.1 Introduction 143
4.2 Aims 147
4.3 Results 147
4.3.1 Gut microbiota modulates colonic function and homeostasis 147
4.3.2 The microbiota status of different animal facilities impacts on gut motility 156
4.3.3 The ENS response in a model of TNF overexpression prior intestinal inflammation 158
4.3.4 EGCs response in a model of experimental inflammation induced by a disruption in T cells homeostasis 166
4.4 Discussion 169
Chapter 5 | Neuroimmune communication and intestinal function 176
5.1 Introduction 177
5.2 Aims 180
5.3 Results 180
5.3.1 Anatomical positioning between the ENS and the immune system 180
5.3.2 Regional compartmentalisation of the adaptive immune system 185
5.3.3 The ENS network is impaired in absence of the adaptive immune system ..189
5.3.4 The ENS function is reduced in mice lacking adaptive immune system 193
5.3.5 Adoptive transfer of T lymphocytes into immunodeficient mice rescues the ENS-dependent motility 196
5.3.6 Absence of the adaptive immune system alters the ENS transcriptome 200
5.4 Discussion 207
Chapter 6 | Concluding remarks 215

6.1 Impact of the subject and main findings 216
6.2 Outlook and future perspectives 217
Chapter 7 | Bibliography 226
Chapter 8 | Appendices 252

LIST OF FIGURES

Chapter 1 | Introduction

Figure 1.1. Anatomical organisation of the ENS within the intestinal wall 24
Figure 1.2. Localisation and morphology of EGCs within the intestinal wall 29
Figure 1.3. The molecular identity of EGCs 32
Figure 1.4. Topography of the neuronal network within the gut 36
Figure 1.5. Schematic of enteric neuron subtypes in the distal colon of guinea-pigs described by their cell body morphologies and projections, chemical coding and function 41
Figure 1.6. Development of neuronal network and neurogenic motility in the small intestine 46
Figure 1.7. Cellular components of the immune system 53
Figure 1.8. T cell subsets and the adaptive immune response..... 56
Figure 1.9. Regional composition of the gut immune system 57
Figure 1.10. The distribution of microbiota along the gastrointestinal tract 66

Chapter 3 | Development of novel experimental approaches for ENS studies

Figure 3.1. Expression of well-established EGC markers in tdT^+ cells from the *Ser26.tdT* mice..... 115
Figure 3.2. Establishment of a new method to culture tdT^+ EGCs from the adult gut..... 117
Figure 3.3. Immunocytochemical characterisation of myofibroblasts in tdT^+ EGC cultures..... 119
Figure 3.4. *In vitro* expression of EGC-lineage markers in tdT^+ EGCs 121
Figure 3.5. tdT expression in the myenteric and submucosal plexuses and mucosa following intravenous injection of AAV9-CaMKII.Cre into the adult mice 129
Figure 3.6. GFP expression within the MP following tail vein injection of AAV9-KASHeGFP into adult wildtype mice 131
Figure 3.7. Chemical coding of transduced myenteric and submucosal GFP^+ neurons from the small intestine after AAV9-KASHeGFP systemic injection 133
Figure 3.8. Identification of extraganglionic non-neuronal cells in LMMPs of mice transduced with AAV9-KASHtdT and AAV9-KASHeGFP 134
Figure 3.9. GFP^+ and tdT^+ neuronal nuclei isolation from the MP of the small intestine in mice injected with AAV9-KASHeGFP and AAV9-KASHtdT 137

Chapter 4 | Impact of gut states on ENS physiology

Figure 4.1. Comparison of the size of ceca dissected from SPF and GF mice 148
Figure 4.2. Enteric neural network in various segments of the intestines in SPF and GF mice 149
Figure 4.3. Effect of the absence of microbiota on colonic ENS homeostasis and function 153
Figure 4.4. Effect of the absence of microbiota on ENS-specific transcript levels within the colon 155
Figure 4.5. Effect of changes in microbiota composition on ENS transcriptional profile and function 157
Figure 4.6. Analysis of ENS structure and function in $TNF^{\Delta ARE/+}$ mice at 4 weeks 161
Figure 4.7. Analysis of ENS structure and function in $TNF^{\Delta ARE/+}$ mice at 16 weeks 165
Figure 4.8. T cell transfer model of chronic inflammation and its impact on ENS homeostasis 168

Chapter 5 | Neuroimmune communication and intestinal function

Figure 5.1. Intestinal compartmentalisation of local neuroimmune interactions 184
Figure 5.2. Analysis of T cell subsets within the mucosa and LMMPs of the small intestine and colon from C57Bl/6 mice 188
Figure 5.3. Morphological analyses of the ENS network in mice lacking the adaptive immune system 192
Figure 5.4. Absence of adaptive immune cells impairs the neurogenic intestinal peristalsis 195
Figure 5.5. Regulatory T cells modulate the ENS-dependent colonic motility 199
Figure 5.6. Effect of the absence of the adaptive immune system on ENS-specific transcript levels within the colon 202
Figure 5.7. Impact of the absence of T lymphocytes on the transcriptional profile of enteric neurons 206

LIST OF APPENDICES

Appendix 1. Localisation and morphology of EGC subsets within the intestinal wall 252
Appendix 2. Neuronal network within the gut 252
Appendix 3. *In vitro* expression of EGC markers in tdT$^+$ cells at DIV3 254
Appendix 4. eGFP expression in neurons from the SMP of the colon 255
Appendix 5. Number of HuC/D$^+$ neurons within the MP of GF and SPF mice 255
Appendix 6. Localisation of MMs relative to the ENS within different layers of the intestinal wall 256
Appendix 7. Neuronal network at the level of Peyer's Patches 256
Appendix 8. CD8$^+$ T cells localisation within the intestinal wall 257
Appendix 9. Flow cytometry plots of spleen after adoptive transfer of lymphocytes into mice lacking T cells 257
Appendix 10. Neurogenic intestinal motility of mice lacking T and B cells after adoptive transfer of lymphocytes 258

LIST OF TABLES

Table 1.1 Proportion of enteric neuron subtypes in the distal colon of guinea-pigs described by their cell body morphologies and projections, chemical coding and function 43

Table 2.1 Mouse lines used in this thesis 91

Table 2.2 Antibodies used for flow cytometry and FACS experiments 97

Table 2.3 Table of primary antibodies used in this study 103

Table 2.4 Table of secondary antibodies used in this study 104

Table 2.5 List of Taqman assays used in this thesis 109

Table 3.1 Quantification of GFP^+ neurons within the MP 131

Table 4.1 Quantification of EGC populations in the small intestine of SPF and GF mice. 151

Table 4.2 Quantification of enteric neurons in the small intestine of SPF and GF mice ... 151

Table 4.3 Quantification of CMMCs in SPF and GF mice 152

Table 4.4 Quantification of $Ki67^+Sox10^+$ EGCs in the model of TNF overexpression 162

Table 5.1 Proportion of T and B lymphocytes within the mucosal and LMMPs of small intestine and colon 186

Table 5.2 Total numbers of isolated nuclei from C57Bl/6 and *Tcrα*$^{-/-}$ colonic LMMPs ... 204

Chapter 1

Introduction

1. Chapter 1 | Introduction

1.1 The enteric nervous system

One of the earliest published observation of the enteric nervous system (ENS) was first described by Bayliss and Starling in the late 19th century. They reported two distinct movements in the gut wall. The first one was called the pendulum movement, described as a rhythmic contraction with a myogenic origin that affects muscle layers and is propagated by muscle fibres. The second one was named peristaltic contraction. That was the very first concept of coordinated peristalsis executed by a local and intrinsic nervous system localised within the gut wall. Bayliss and Starling also proposed that these peristaltic waves travelled in only one direction and that occurred partially independent of the commands from the central nervous system (CNS). Moreover, they suggested that this coordinated peristalsis was induced by local and mechanical stimulation within the gut wall that promoted excitation above and inhibition below the stimulated site. They called this event "The Law of the Intestine" (Bayliss & Starling, 1899). The law of the intestine was supported 18 years later by Ulrich Trendelenburg using *in vitro* studies showing the intestinal peristaltic reflex, confirming that the gut had its own nervous system (see (M. D. Gershon & Erde, 1981)).

Furthermore, Langley acknowledged those findings in 1921 and classified the ENS as a third subdivision of the autonomic nervous system based on histological differences from other peripheral nerve cell types, and the lack of evidence that the intrinsic intestinal nervous system was indeed connected to the CNS (Langley, 1921).

For many years, the research and progress on ENS science were not adequately appreciated. Later on, however, due to its complexity and also due to structural and functional similarities to the CNS, the ENS was described as a subdivision of the peripheral nervous system (PNS) and named as the second brain by Professor Dr Michael Gershon in his book "The Second Brain" (Michael D. Gershon, 1998).

Although the ENS was first mentioned more than 150 years ago and several studies have now demonstrated its importance in the gastrointestinal (GI) function and participation in diseases, there is still a small amount of reliable information about this system when compared to others. The role of the neural connections within the ENS and their functional interactions with the surrounding systems are only starting to be unravelled. From this point

on, we will describe what it has been proposed about the composition, structure and organisation of the ENS so far, as well as its interactions with the intestinal environment.

1.1.1 Structure and organisation of the adult ENS

Most aspects of the GI function including digestion, epithelial absorption and secretion, intestinal blood circulation, defence and mixing peristalsis have been shown to be controlled by the ENS. The ENS is the largest subdivision of the PNS, and it functions in concert with commands originated from the CNS, working partially independent of inputs from the brain (M. D. Gershon & Erde, 1981). Although many studies have revealed the autonomy of the ENS to respond itself to external stimuli, the activation of extrinsic nerve fibres from sympathetic and parasympathetic nervous systems also plays a role in proper the gut function (Luckensmeyer & Keast, 1998; Powley, 2000).

The ENS is an extensive and complex network composed of a vast and diverse number of intrinsic neurons and enteric glial cells (EGCs), which are located within the GI wall, starting from the oesophagus to the rectum. In the mammalian gut, these cells are anatomically localised within two major interconnected and ganglionated plexuses. The myenteric plexus (MP) (or Auerbach's) is confined between the longitudinal and circular muscle layers, and it extends along the entire length of the GI tract **(Figure 1.1)**. The MP is subdivided into three smaller components: the primary, secondary and tertiary plexuses. The primary plexus includes the ganglia containing neuronal cell bodies and two or three times as many EGCs, in addition to interganglionic neuronal fibres and glia that connect multiple ganglia (Gabella, 1972). The size and shape of each ganglion varies according to the number of cells and area of the gut (Gabella & Trigg, 1984). The secondary plexus consists of finer nerve bundles embedded in parallel with the circular muscle, and it lies below the primary plexus. The tertiary plexus includes thinner fibres arising from primary and secondary bundles that fulfil areas between the primary plexus (John Barton Furness, 2006).

The submucosal plexus (SMP) (or Meissner's) is a smaller network of ganglia and nerve fibres localised beneath the mucosal layer, mainly found in the small and large intestines in mammals **(Figure 1.1)** (John Barton Furness, 2006). However, the presence of isolated submucosal ganglia was reported in the oesophagus and stomach of cats and opossum (Christensen & Rick, 1985). In large mammals and humans, the SMP is further subdivided into two distinct ganglia, an outer (outer submucosal plexus, OSP - close to the

circular muscle layer) and inner (inner submucosal plexus, ISP - close to the mucosal layer) components, that differ from each other in both morphological and neurochemical features. The functional significance of those two ganglia still remains unclear (Timmermans, Hens, & Adriaensen, 2001).

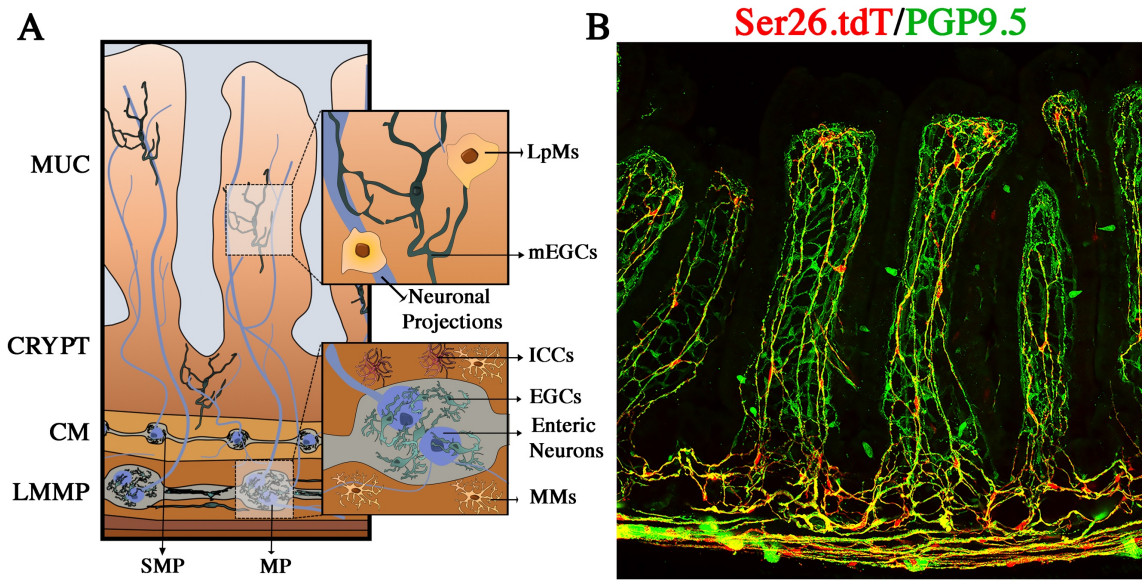


Figure 1.1. Anatomical organisation of the ENS within the intestinal wall. (A) Schematic represents a transverse overview of the intestinal layers and ENS niche. Enteric neurons and EGCs are localised within the MP and SMP. EGCs are found within the mucosal layer in close proximity to enteric neuronal fibres. **(B)** Visualisation of neuroglia network within the intestinal wall. Transverse section of the ileum from the Ser26.tdT mice showing tdT^{+} EGCs (red) immunostained for the neuronal marker PGP9.5 (green). Muc: Mucosa, CM: circular muscle, LMMP: longitudinal muscle myenteric plexus, SMP: submucosal plexus, MP: myenteric plexus, MMs: muscularis macrophages, EGCs: enteric glial cells, ICCs: interstitial cells of Cajal, mEGCs: mucosal enteric glial cells and LpMs: lamina propria macrophages.

Although the anatomical organisation of neurons and EGCs into myenteric and submucosal ganglia is very clear in mammals (Christensen & Rick, 1985; John Barton Furness, 2006), birds (Burns & Douarin, 1998; Goldstein & Nagy, 2008) and reptiles (Timmermans et al., 1991), in teleost like zebrafish the submucosal structure is absent. Also, in zebrafish, the neuronal organisation is found to be much less complex. In this species, neurons are arranged as single or paired structures in the interconnected cell network, and

the presence of EGCs is still unknown (Heanue, Shepherd, & Burns, 2016; Wallace & Burns, 2005).

The adult enteric ganglia network is highly compact and devoid of any connective tissue, blood vessels or collagen fibres. Neurons and ECGs are located within the ganglia in close proximity, and the absence of connective tissue in between those cells is one of the features that resemble the structure of the CNS (Gabella, 1972, 1981).

Furthermore, it is important to emphasise that in the mammalian GI tract, neuronal cell bodies are only found within the myenteric and submucosal ganglia. However, enteric neurons do extend their fibres along the muscle layers, and their projections are also observed deep into the mucosa. Individual EGCs, on the other hand, can be found in the extra ganglionic space, and single cells are present within the lamina propria of the intestines (see more details in section 1.1.3.1) **(Figure 1.1)** (Boesmans, Lasrado, Vanden Berghe, & Pachnis, 2015; John Barton Furness, 2006).

1.1.2 Functions of the adult ENS

Recently, interest in developing new strategies to study the function of the ENS has increased exponentially. Despite significant advances in technologies and approaches to explore ENS function in more detail, the field still lacks specific knowledge of how enteric neurons and EGCs integrate and respond to environmental cues and surrounding tissues, both in homeostatic and pathological conditions. However, it is clear that the ENS has a crucial role in many activities that control GI function, such as regulation of blood flow, propulsion and mixing of gut contents in intestinal peristalsis, absorption and secretion of luminal substances and gut barrier during inflammation and against pathogens (Goyal & Hirano, 1996; Kunze & Furness, 1999). Although the ENS has a primary function in controlling GI activities, the influence of sympathetic and parasympathetic neuronal fibres enhances the enteric neural input in the gut (Phillips & Powley, 2007).

In small mammals, the MP controls mainly the gut motility whereas the SMP primarily regulates the submucosal vasculature, absorption and secretion of nutrients. Nevertheless, in large mammals, the SMP also contributes to regulating intestinal motility. This observation could be explained because the SMP has a more complex subdivision into OSP (outer) and ISP (inner) structures. Some studies have suggested that neurons from the

OSP are motoneurons and resemble those from the MP whereas the neurons in the ISP are likely to be sensory neurons (Timmermans et al., 2001).

It has been reported that the ENS is involved in mechanisms responsible for modulating intestinal blood flow. In support of the role of the ENS in regulating blood flow, submucosal neurons in the small intestine of guinea-pigs were found to extend their projections onto submucosal arterioles and release acetylcholine to promote vasodilation (Neild, Shen, & Surprenant, 1990). In the distal colon, submucosal cholinergic and non-cholinergic neurons control vasodilation of submucosal arterioles. The non-cholinergic neurotransmission of colonic vasodilation is predominant and possibly controlled by neuronal Substance P and vasoactive intestinal peptide (VIP) (Vanner & Surprenant, 1991).

Additionally, the ENS also plays a critical role in gut motility. Neurons and glial cells in combination with smooth muscle cells and interstitial cells of Cajal (ICCs) control and modulate each pattern of motility. This function will be further discussed below.

The ENS has fundamental importance in maintaining GI homeostasis. Its presence and function are critical during all stages from development to postnatal life. It has been shown that mice lacking ENS throughout the GI tract due a depletion of Sox10 (Southard-Smith, Kos, & Pavan, 1998), Phox2b genes (Pattyn, Morin, Cremer, Goridis, & Brunet, 1999) or, in RET and Mash-1 isoforms, have a lifespan of 24 hours after birth (de Graaff et al., 2001; Schuchardt, D'Agati, Larsson-Blomberg, Costantini, & Pachnis, 1994), suggesting that the normal ENS development is vital for the survival of mice.

Other functions of the adult ENS such as integration with immune system, interactions with microbiota, response to diet uptake and pathological insults will be further discussed (sections: 1.2.3.2, 1.3.3 and 1.4).

1.1.3 Cellular components of the adult ENS

The adult ENS is composed of an intricate network of neurons and glial cells. Similar to other nervous systems, enteric neurons and glial cells are in close contact and form complex circuits that regulate GI functions. Our understanding of reciprocal and specific functional interactions between these two types of cells are still rudimentary. However, the anatomical positioning and proximity between enteric neurons and glial cells and their responses to internal and external challenges, have provided some clues on how these cells

could communicate to maintain intestinal homeostasis, which will be further elaborated in the following sessions.

1.1.3.1 The enteric glial cells (EGCs)

For over 70 years after their discovery, EGCs were minimally noted. They were first described by Dogiel in 1899 as nucleated satellite cells surrounding ganglionic enteric neuronal cell bodies, and frequently compared to Schwann cells (Ruhl, 2005). Only in the early 1970s, Gabella started an accurate morphological analysis of EGCs, recognising them as a unique and distinct peripheral glia population (Gabella, 1970).

1.1.3.1.1 Localisation and morphology of EGCs

EGCs are the major cellular component of the ENS. In the MP, EGCs outnumber neurons by around 3 to 1, but this proportion varies according to the size of species and observed area of the gut (Gabella, 1971, 1972). These cells are in close association with enteric neuronal cell bodies and their processes. However, in contrast with the sympathetic ganglia, EGCs do not entirely form an envelope around neurons (Gabella, 1981). When compared to enteric neurons, EGCs are smaller and extensively branched, usually elongated and thin, with several irregular processes in shape and size (Gabella, 1972). They present bundles of gliofilaments in their cytoplasm, which are a prominent characteristic of a glial cell. Detailed morphological analyses described EGCs as a distinct subset of peripheral glia, different from Schwann cells as they do not myelinate neuronal axons. On the other hand, because of their morphology and close association with neuronal cell bodies, EGCs were compared to astrocytes from the CNS (Gabella, 1971).

Overall, the EGC network is widespread along the entire extension of the GI tract, including all layers of the gut wall. EGC bodies reside within the myenteric and also the submucosal plexuses (**intraganglionic** EGCs), as well as in the interganglionic strands between multiple ganglia. EGCs are also found in extraganglionic spaces embedded within muscle layers (**intramuscular**), surrounding intestinal crypts forming a basket-like structure, and also as single units within the mucosal layer (**subepithelial**) **(Figure 1.2 and Appendix 1)** (M. D. Gershon & Rothman, 1991; Gulbransen & Sharkey, 2012; Ruhl, 2005).

After many years of progress on deciphering the role of EGCs on gut homeostasis, features of these cells based on their distinct location and morphology have not revealed

much further their unique functions. It is believed that the intestinal micro-environment could dictate the morphology of EGCs as they are derived from a common progenitor; however, this theory is still to be proven. Morphometrical analyses of EGCs have suggested that these cells are very heterogenic and their morphology varies accordingly to compartments they are localised within the gut wall. EGCs can be classified into four distinctive subtypes based on their morphology and position: type I or "protoplasmic" glial cells are intraganglionic, star-shaped, with short and branched processes and resemble astrocytes from the CNS. The type II or "fibrous" EGCs, in turn, are elongated, branched and localised within interganglionic fibre strands. They are similar to fibrous astrocytes (Hanani & Reichenbach, 1994). The type III or mucosal EGCs are found within the lamina propria, surrounding intestinal crypts, wrapping around blood vessels and in the extraganglionic space. These cells have four extensive and branched processes. Finally, the type IV or intramuscular EGCs are bipolar with two long processes, running along with muscular fibres in the gut wall **(Figure 1.2 and Appendix 1)** (Boesmans et al., 2015; Gulbransen & Sharkey, 2012).

Although the morphological and distinct positioning of EGCs along different compartments of the gut is evident, the correlation with their molecular profile and physiology remain unclear.

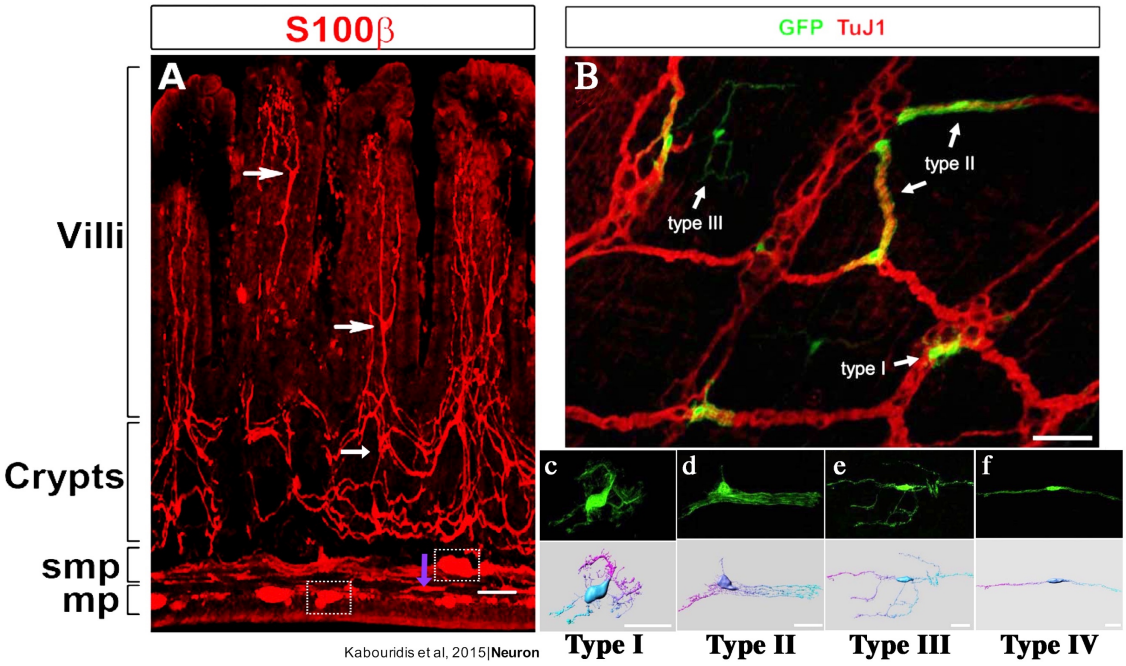


Figure 1.2. Localisation and morphology of EGCs within the intestinal wall. (A) Transverse section of the ileum showing the localisation of S100$^+$ EGC subsets (red). Image highlights subepithelial EGCs within the lamina propria and surrounding crypts (white arrows); intramuscular EGCs (lilac arrow) and intraganglionic EGCs within the SMP and MP (white dotted squares). **(B)** Flat preparation of LMMP from Sox10Cre|MADM mice showing the localisation of GFP$^+$ EGC subtypes (green) within the MP highlighting type I, type II and type III subsets. Tuj1$^+$ neurons are labelled in red. Morphology of type I **(c)**, type II **(d)**, type III **(e)** and type IV **(f)** EGCs. Scale bars: 100 µm **(A)**, 50 µm **(B)** and 20 µm **(c-f)**. MP: myenteric plexus, SMP: submucosal plexus, LMMP: longitudinal muscle myenteric plexus. Modified from Kabouridis et al., 2015 **(A)** and Boesmans et al., 2015 **(B-f)** with publishers' permission.

1.1.3.1.2 Molecular markers to identify EGCs

Nowadays, a variety of molecular markers are available to identify EGCs. Nonetheless, these markers are also shared with other glial populations such as astrocytes of the CNS and Schwann cells of the PNS. Because the expression of glial markers is shared among several glial cell types, their physiological role in EGCs specifically and on GI function remains a challenge to be defined. Discovering new molecules to identify EGC populations specifically would bring new insights into their physiological role in GI function.

During development in rodents, enteric glial progenitors first express the *Brain Fatty Acid Binding Protein* (BFABP) around embryonic stage (E) E11.5. BFABP expression

starts even before glial differentiation, suggesting that this is a possible marker for a committed enteric glia lineage (Veerkamp & Zimmerman, 2001; Young, Bergner, & Muller, 2003). The transcription factor Sox10, in turn, is expressed by undifferentiated neural crest progenitors, and its expression is maintained throughout the ENS development, while exclusively labelling mature EGCs (Hoff et al., 2008; Laranjeira et al., 2011; Young et al., 2003). Likewise, Sox2 levels first appear in migrating progenitor ENS cells, and its expression is maintained in mature EGCs, overlapping almost completely with Sox10 (Heanue & Pachnis, 2011). Adult EGCs also express the intermediate filament protein GFAP (glial fibrillary acidic protein) (Jessen & Mirsky, 1980), the calcium-binding protein S100β (Ferri et al., 1982) and glutamine synthetase (Jessen & Mirsky, 1983). S100β is first detected at E14.5, and it is exclusively expressed in EGCs, while its expression is absent in neurons. S100β is found in the cytoplasm of glial cells, working as a regulator of Ca^{2+} homeostasis, as well as of the cytoskeletal structure and function. Similarly, GFAP is also a specific glial cell marker, and its expression in EGCs starts around E16.5 (Young et al., 2003). Sox10, GFAP and S100β are the most used markers to identify EGCs in the adult gut **(Figure 1.3)**. Quantitative analysis of Sox10-expressing cells in combination with GFAP and S100β antibodies showed that adult EGC populations differentially express these markers in the MP, and often in a dynamic fashion (Boesmans et al., 2015).

Additionally, in the past few years, efforts to identify new adult EGCs markers have yielded new insights. Joseph et al. successfully used CD49b (integrin α2) antibody to isolate EGCs from the adult MP by flow cytometry. These studies showed that $CD49b^+$ cells co-expressed Sox10, GFAP and S100β, but not the neuronal marker HuC/D while exhibiting the expected cell morphology and sharing the same location as EGCs. Moreover, the group suggested that $CD49b^+$ EGCs are quiescent in the adult gut as only 1% of this population incorporated the cell-cycle marker propidium iodide. Intriguingly, isolated $CD49b^+$ cells were able to generate neurospheres *in vitro*. The group further showed that CD49b is first detected at E13 guts at low levels, and its expression increases throughout the development and remains expressed in the adult EGCs (Joseph et al., 2011). Despite the significant advance in targeting EGCs using CD49b, the isolation of these cells requires a combination of antibody staining as CD49b is widely expressed by other cell types, such as immune and stromal cells (Gagliani et al., 2013).

Recently, Rao et al. proposed proteolipid protein 1 (PLP1) as a new and specific molecular marker expressed in EGCs within the adult intestine. However, PLP1 is not uniquely expressed in EGCs, but also by glial cells in other parts of the nervous system, such as Schwann cells of the PNS (Rao et al., 2015).

Lastly, another molecular marker expressed in EGCs that still needs to be better explored is the forkhead transcription factor 3 (FoxD3). Similar to Sox10, FoxD3 is one of the earliest genes expressed by neural crest progenitors until they colonise the GI tract, and it is maintained in differentiated EGCs (Labosky & Kaestner, 1998; Mundell et al., 2012; Teng, Mundell, Frist, Wang, & Labosky, 2008). Studies have revealed that the early depletion of this gene specifically in the neural crest cells (NCCs) results in several defects in their derivatives, including the complete absence of ENS (Teng et al., 2008). Moreover, additional data have further shown that the late depletion of FoxD3 in a subset of vagal neural crest progenitors triggered a compensatory mechanism to induce another $FoxD3^{+}$ EGCs subset to proliferate and differentiate to diminish the damage on the ENS development (Mundell et al., 2012). Although it is evident that FoxD3 is crucial for the development and homeostasis of EGCs, its role on the adult glia is still unclear. Ongoing *in vivo* studies in our lab have proposed that FoxD3 is maintained in mature EGCs and its expression colocalises with Sox10 and Sox2 in the small and large intestines. The expression of FoxD3 in EGCs appear to be dispensable for the survival of these cells once their identity is established following the deletion of this gene *in vivo* (Ana Oliveira and Song Hui Chng, experimental observations).

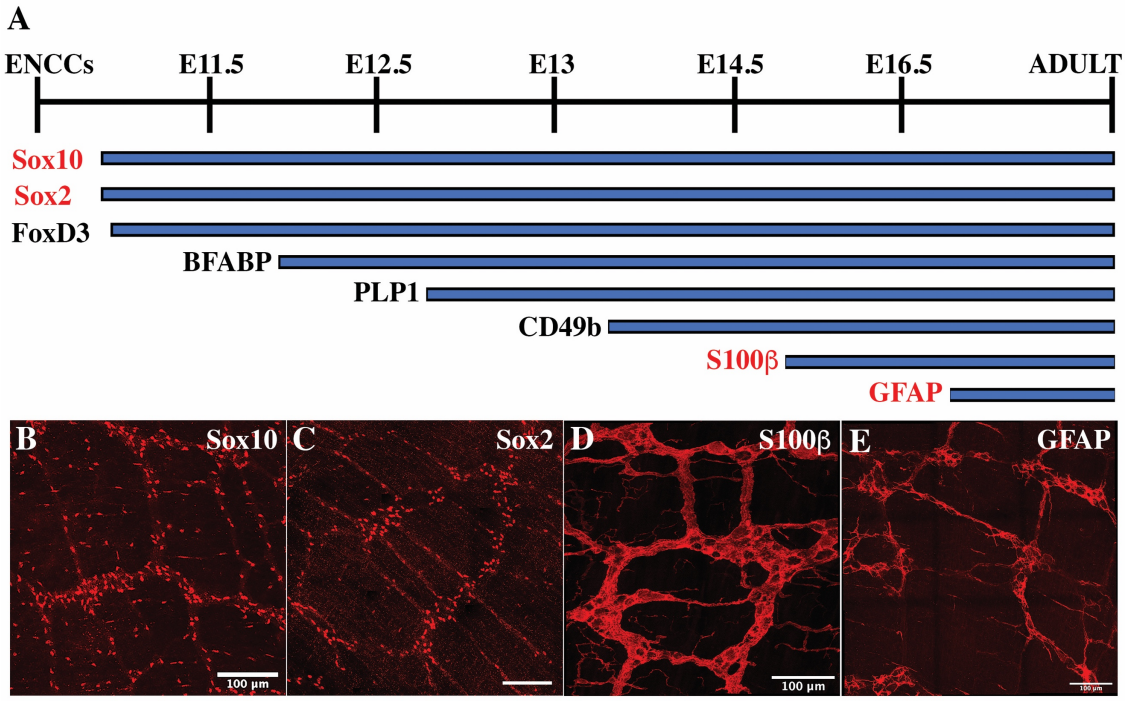


Figure 1.3. The molecular identity of EGCs. (A) Schematic representing the molecular markers expressed in EGCs throughout the development and adulthood. Whole-mount immunohistochemistry of LMMPs showing in red the most commonly used molecular markers to identify EGCs in the adult gut such as Sox10 **(B)**, Sox2 **(C)**, S100β **(D)** and GFAP **(E)**. Scale bars: 100 µm. ENCCs, enteric neural crest cells.

1.1.3.1.3 Physiological functions of EGCs

For a long time, little was known about the physiological functions of EGCs. These cells were originally described as being mere supportive cells for the neuronal machinery, and many times defined as having an adjuvant role in maintaining the function of neuronal circuitry. Studying EGCs has been challenging, as they present a very plastic and heterogeneous phenotype, being able to promptly respond to many insults and integrate signals emanating from different systems, such as the immune system.

One of many approaches to study the role of EGCs on GI function is to use genetic tools to ablate these cells and analyse their contributions to the integrity and homeostasis of the system. Studies using mice expressing herpes simplex virus thymidine kinase under the control of GFAP promoter depleted EGCs, resulting in disruption of the mucosal integrity, severe intestinal inflammation and necrosis, as well as degeneration of enteric neurons (Bush et al., 1998). Moreover, Cornet et al. observed a robust inflammatory phenotype comparable to Crohn's Disease in humans by using a double mutant mouse line, in which EGCs

expressed a virus antigen, with most of $CD8^+$ T cells being specific for this antigen (Cornet et al., 2001). Together, these data could possibly suggest that EGCs play a crucial role in maintaining the integrity of the mucosal barrier. However, both models lack direct evidence to support the necessity of EGCs for the intestinal barrier function rather than the effect of inflammation itself on the mucosal permeability (Bush et al., 1998; Cornet et al., 2001).

To further test the contribution of these cells on intestinal barrier function, EGCs were disrupted, but not entirely depleted by using mice expressing haemagglutinin (HA) in $GFAP^+$ cells with an injection of activated HA-specific $CD8^+$ T cells. With this strategy, no observable signs of inflammation were detected. In this study, EGC disruption resulted in changes in motor and mucosal functions as well as in neurochemical coding of enteric neurons (Aube et al., 2006). Similarly, Nasser et al. have shown that chemically ablating EGCs by using gliotoxin fluorocitrate leads to changes in GI contractility and motility *in vivo* and *in vitro*, without any evident signs of inflammation (Nasser et al., 2006). Subsequently, recent data using an inducible $PLP1^{CreERT2};Rosa26^{DTA}$ mouse model to ablate EGCs, did not demonstrate any deleterious effects on epithelial function but did show altered intestinal motility in a sex-dependent manner (Rao et al., 2017). Thus, taken together, these data remain contentious for reasons highlighted here: 1. All transgene expression to target EGCs in these approaches was performed using glia promoters that are not specific to the ENS but also affect glia of the PNS and CNS; 2. GFAP is not expressed by all enteric glial subtypes, which means that the phenotype observed in these models could be caused by a subtype-specific ablation of EGCs; 3. Age/sex and environmental conditions of mice used in the experiments which could have an impact on the effect of EGCs ablation in the development of inflammatory conditions. There are still many variables to be considered on the use of genetic tools to study EGCs, including the lack of a specific marker to label these cells.

EGCs are also expected to assist neuronal function by providing structural support, delivering neurotrophic factors and assuring a protective microenvironment to these cells. Because of their shape and multiple gliofilaments, EGCs play an essential role in keeping the ganglionic structure by providing a partial coating on neuronal cell bodies and wrapping around bundles of enteric neurites (Gabella, 1981; Ruhl, 2005). Intramuscular (Type IV) EGCs express P2X7 receptors that are important for myelin coverage of axons in the CNS, suggesting a possible role of these cells in maintaining the structure of neuronal fibres

(Vanderwinden, Timmermans, & Schiffmann, 2003). Indeed, Rudolf Virchow first named these cells *glia*, which in Greek means "glue", first suggesting their role in keeping neuronal structures together. The neuroprotective role of EGCs has been suggested using *in vivo* and *in vitro* assays.

Recent studies have also demonstrated that adult EGCs can generate neurons *in vitro* and *in vivo*. However, the potential neurogenic ability of these cells under physiological conditions remains controversial. It has been shown that EGCs can undergo neurogenesis during pathological conditions, upon chemical ablation of the ENS network. Nonetheless, the proportion of newborn neurons derived from EGCs was very low (Laranjeira et al., 2011). Interestingly, using various physiological and pathological conditions, Joseph et al. did not observe any newborn neurons derived from $GFAP^+$ lineage-marked EGCs *in vivo*. Instead, it was observed that the majority of EGCs *in vitro* were multipotent, with a high neurogenic capacity (Joseph et al., 2011). More recently, it has been shown that $Sox2^+$ and $PLP1^+$ EGCs generate neurons following colitis in mice (Belkind-Gerson et al., 2017), suggesting that different environmental cues can modulate the neurogenic ability of EGCs to maintain ENS homeostasis.

It has been proposed that EGCs are involved in neurotransmission either by synthesis and/or inactivation of neurotransmitters. EGCs express glutamine synthase, and this is essential for neuronal GABA and glutamate synthesis (Fletcher, Clark, & Furness, 2002). Additionally, EGCs may be taking part in neuropeptidergic and nitrergic neurotransmission by expressing peptide transporter 2 (PEPT2) and L-arginine respectively (Nagahama, Semba, Tsuzuki, & Aoki, 2001; Ruhl, Hoppe, Frey, Daniel, & Schemann, 2005). Furthermore, EGCs participate in nucleotide signalling by controlling the availability of ATP and ADP as they express NTPDase2 on their surface (Braun et al., 2004). It has been shown that EGCs can intrinsically respond to neuronal-released ATP through P2Y4 receptors by increasing intracellular Ca^{2+} (Gulbransen & Sharkey, 2009), in addition to sympathetic neuronal activation (Gulbransen, Bains, & Sharkey, 2010). *In vitro* studies have also provided evidence that acetylcholine (ACh) and serotonin (5-HT) increase EGCs intracellular Ca^{2+} transients, supporting once again their participation in signalling mechanisms (Boesmans, Cirillo, et al., 2013). EGCs intracellular Ca^{2+} transients were reported to be responsive to many factors released by neurons, i.e. KCl, caffeine, nicotine and substance P, and may play a key role in intestinal motility (Broadhead, Bayguinov,

Okamoto, Heredia, & Smith, 2012; J. L. McClain, Fried, & Gulbransen, 2015), mediated by connexin 43 (J. McClain et al., 2014). EGCs also express muscarinic receptors M3Rs and M5Rs that detect ACh from neurons, leading to the release of gliotransmitters that actively participate in gut motility (Delvalle, Fried, Rivera-Lopez, Gaudette, & Gulbransen, 2018).

It has been implied that EGCs actively cooperate in immune responses in the gut (Chow & Gulbransen, 2017). However, the cellular and molecular mechanisms that underlie those responses by EGCs in gut pathologies remain unclear. EGCs express the major histocompatibility complex class II (MHCII), a molecule usually expressed by antigen presenting cells (Geboes et al., 1992). It has been shown that this marker is upregulated in EGCs under inflammatory conditions (Koretz, Momburg, Otto, & Moller, 1987; Turco et al., 2014), conferring an immunological role of these cells in a pathological environment. Moreover, EGCs may modulate inflammatory responses by producing, secreting or responding to cytokines, such as IL-1β, IL-6 and IL-10 (Ruhl, Franzke, Collins, & Stremmel, 2001; Ruhl, Franzke, & Stremmel, 2001) and nitric oxide (I. A. M. Brown, McClain, Watson, Patel, & Gulbransen, 2015). Recently, Ibiza et al. showed that GNDF derived from EGCs could modulate the release of anti-inflammatory IL-22 from type 3 innate lymphoid (ILC3)-RET expressing cells *in vitro* and *in vivo* (Ibiza et al., 2016). *In vitro* studies have also proposed the potential role of human EGCs in inhibiting T lymphocytes proliferation, suggesting an immunosuppressive property of these cells (Kermarrec, Durand, Neunlist, Naveilhan, & Neveu, 2016). Therefore, it is evident that EGCs play a substantial role in modulating gut inflammation and mediating neuroimmune interactions. Understanding specific contributions of these cells in controlling gut homeostasis can be a useful tool to decipher their roles in inflammatory disorders.

1.1.3.2 The enteric neurons

The enteric neuronal network is composed of a vast number of neurons that are displayed into two rings of ganglia and interconnect by neuronal projections. Enteric neurons are involved in several GI functions that will be discussed below. These cells and their connections with the surrounding tissues, including their partners EGCs, are vital for the accurate performance of the GI tract.

It has been estimated that the number of neurons within enteric ganglia is equivalent to those found in the spinal cord (J. B. Furness & Costa, 1980), and even higher than the

total number of sympathetic and parasympathetic neurons altogether (J. B. Furness, 2012). The estimated number of enteric neurons in the myenteric and submucosal ganglia was established by counting single cell bodies per area of the gut. Those numbers may vary according to species analysed and size of the gut. It is predicted that the mammalian adult ENS is composed of around 500 thousand neurons in mice (Gabella, 1987), extrapolating to about 600 million in humans within the MP (John Barton Furness, 2006). In the SMP of mice, in turn, neuronal numbers can reach about 330 thousand **(Figure 1.4 and Appendix 2)** (J. B. Furness, 2012; J. B. Furness & Costa, 1980).

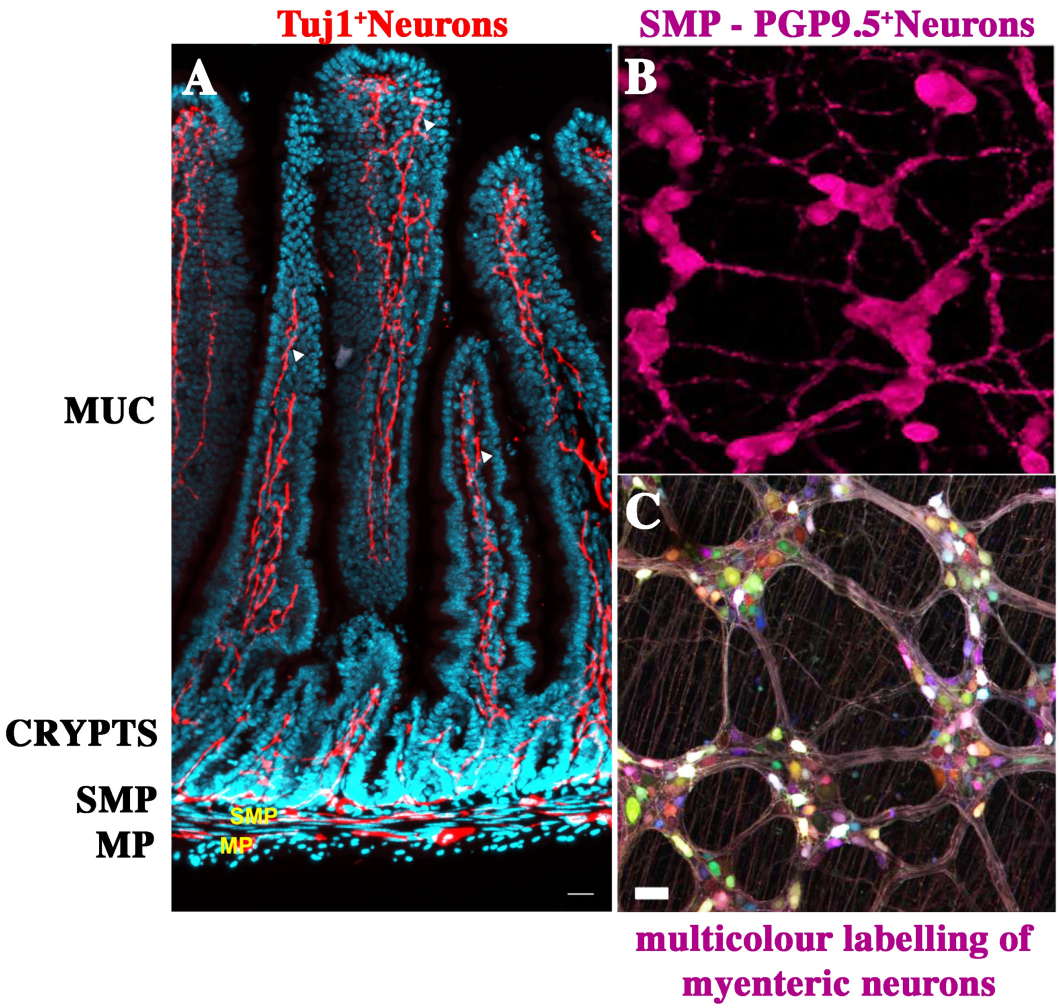


Figure 1.4. Topography of the neuronal network within the gut. Muc: Mucosa, SMP: submucosal plexus, MP: myenteric plexus. **(A)** Image shows the neuronal network in a cross-section of the small intestine labelled for the neuronal marker Tuj1 (red). **(B)** Image demonstrates the neuronal network stained for the neuronal marker PGP9.5 in flat preparation of the SMP (magenta) of the mouse colon. **(C)** Image shows the topography

of the colonic neuronal network within the MP of mice injected with multicolour ssAAV-PHP.S:hSyn1-3XFP vector containing a neuronal specific promoter. Adapted from (Chan et al., 2017; Hao et al., 2016; Uesaka, Nagashimada, & Enomoto, 2015).

The ENS contains different neuronal subtypes, including interneurons, sensory and motoneurons that project to muscle cells, arterioles and epithelium. The classification of enteric neurons subtypes is mainly based on their morphology, electrophysiology, neurochemical and pharmacological properties. However, in order to accurately unravel the neuronal circuitry, a combination of techniques to identify those neuronal properties must be taken into consideration (J. B. Furness, 2000).

Using the criteria mentioned above, studies have identified about 20 distinct subtypes of enteric neurons, in which 14 have been found in the small intestine of guinea-pigs (J. B. Furness, 2000). The characterisation of those neurons is described below.

1.1.3.2.1 Morphology of enteric neurons

Based on their shapes, Dogiel was the first one to provide a detailed morphological description of myenteric and submucosal enteric neurons as Dogiel types I, II and III. Dogiel type I group of neurons are flat, slightly elongated with stellate or angular cell bodies and only one axon with multiple dendrites. Their axons are at the same level of the MP, and most of them can extend through up to 4 ganglia before entering to the circular muscle layer. Functionally, they can be classified as excitatory and inhibitory motoneurons and interneurons. Following, the most prominent class of neurons in the myenteric and submucosal ganglia is the Dogiel type II, covering about 10-25% of the myenteric population in the small intestine and colon. These neurons have a prominent round or oval cell bodies, and multiple long axons with fine varicose branches. In the MP, their long processes travel into the same or neighbouring ganglia in a circumferential manner, but they can occasionally project anally from 2 to up to 100 mm, including into the mucosa. In the submucosal ganglia, their fibres run shorter distances, about 2 mm long, along with the adjacent ganglia orally and anally, and they also project into the mucosal layer. Physiologically, they are classified as myenteric and submucosal intrinsic primary afferent neurons (IPANs). Lastly, the Dogiel type III or filamentous neurons are branched with short axons that begin from a protrusion of their cell bodies and stay within the ganglion of origin. They are functionally classified

as descending interneurons involved in migrating myoelectric complex (Brehmer, Schrodl, & Neuhuber, 1999; John Barton Furness, 2006).

More recently, another four classes of neurons were described by using new methods and techniques to single-label neurons. Type IV neurons have a single axon that projects vertically through the circular muscle layer to the mucosa, with short and one-sided polarised dendrites, and function as secretomotor neurons. Type V neurons are non-nitrergic, uniaxonal neurons with long branch dendrites localised within the myenteric and external submucosal ganglia. Type VI are nitrergic neurons, and they were found within the myenteric and outer submucosal plexuses in the small intestine. They are monoaxonal with branched dendrites that project from their proximal part and cell bodies. In the MP, they project aborally to the same level of the ganglia, whereas the ones in the outer submucosal plexus project vertically, crossing the circular muscle layer up to the MP (Brehmer et al., 1999). There is still not much information regarding the type VII and giant neurons.

1.1.3.2.2 Electrophysiology of enteric network

Intracellular recordings of neuronal electric activities are an essential approach to understand the function of their connections. However, because this property is susceptible to environmental changes, such as neurotransmission, infections and nutrition, its reliability can be limited. Based on their electrophysiological features, neurons have been classified into two main types: Synaptic (S-type) and after-hyperpolarisation (AH-type) neurons. S-type neurons show large-amplitude and fast excitatory post-synaptic potentials (EPSPs) when stimulated and exhibit brief action potentials. They usually present only one axon, and they vary in shape, including Dogiel type I and III morphologies. In contrast, AH-type neurons have prominent action potentials with prolonged duration, exhibiting slow EPSPs with small amplitude. Morphologically, they were described as Dogiel type II neurons (John Barton Furness, 2006).

1.1.3.2.3 Pan-neuronal markers and chemical coding of enteric neurons

Enteric neurons are generated from NCCs and differentiate throughout the embryonic life until early postnatal stages (Pham, Gershon, & Rothman, 1991). The occurrence of adult neurogenesis in homeostatic conditions is still under an extensive debate (Joseph et al., 2011; Kulkarni et al., 2017; Laranjeira et al., 2011). Enteric neurons express

a broad range of molecular markers that identify their developmental stage, and some of these markers are maintained during adulthood. Here, we are going to focus on markers that are expressed by mature enteric neurons.

Molecular markers to identify enteric neurons

Though several antibodies have been currently identified and routinely used as pan-neuronal markers, controversies related to their ability to label neurons specifically, covering different areas of the ENS and efficiently labelling all subtypes of adult neurons have been taken into consideration (Phillips, Hargrave, Rhodes, Zopf, & Powley, 2004). Nowadays, the most used marker to identify enteric neurons is HuC/D. HuC/D antigens are a member of the Elav-like RNA-binding protein family (Lin et al., 2002), and its expression is already observed in neural crest-derived cells by E10, E10.5 (Hao & Young, 2009). HuC/D protein typically resides in the neuronal cytosol and nuclei but not in their processes, what is a practical advantage of its use to quantify neuronal cell numbers. HuC/D positive neurons are found both in the myenteric and submucosal ganglia from the small and large intestines (Lin et al., 2002). Hu proteins usually interact with adenine uridine-rich sequences in the 3' untranslated region, stabilising specific mRNAs (Perrone-Bizzozero & Bird, 2013), and may be involved in motoneuron differentiation and axogenesis (Tebaldi et al., 2018). However, its role on enteric neurons is still not clear.

Another widely used protein expressed in adult enteric neurons is the protein gene product 9.5 (PGP9.5). PGP9.5 immunoreactivity is found in neuronal cell bodies and processes, which allows the visualisation of the neuronal network (Krammer, Karahan, Rumpel, Klinger, & Kuhnel, 1993). However, this protein is only present in about 80% of enteric neurons in the MP (Eaker & Sallustio, 1994). Moreover, the receptor tyrosine kinase (RET), heart and neural crest derivatives expressed 2 (Hand2), Peripherin (Szabolcs, Visser, Shelanski, O'Toole, & Schullinger, 1996) and the neuron-specific class III beta tubulin (Tuj1) are also expressed in the majority of mature enteric neurons. However, the characterisation of those markers in the adult gut has not yet been performed.

Chemical coding of enteric neurons

Chemical properties of enteric neurons are known as chemical coding and include a combination of molecular markers expressed in different subtypes of neurons. Together with

their electrophysiological and morphological features, the chemical coding of neurons define the functional subtype of these cells. This unique group of molecules includes enzymes to synthesise neurotransmitters (TH – tyrosine hydroxylase, ChAT – choline acetyl-transferase, NOS – nitric oxide synthetase), neurotransmitters (NO - nitric oxide, 5-HT – hydroxytryptamine, ACh – acetylcholine), neuropeptides (NPY – neuropeptide Y, VIP, CGRP – calcitonin gene-related peptide, SOM - somatostatin, TK - tachykinin), calcium-binding proteins (calretinin and calbindin) and axonal markers (NF – neurofilament). Some of these molecules are expressed in a high percentage of neurons (ChAT and Calretinin), whereas others in a small group of cells (5-TH). The level and percentage of expression of those markers vary according to the layer of the ganglia, area of the gut as well as species analysed. Moreover, some neurons express a combination of those molecules (Boesmans, Hao, & Vanden Berghe, 2018; J. B. Furness, 2000).

1.1.3.2.4 Physiological role of enteric neurons

Enteric neurons were further classified into physiologically defined subgroups by combining their distinct features, such as morphological characterisation and target of their projections, electrophysiology and neurochemical coding. Considering those properties, studies done in the ileum of guinea-pig have identified about 14 subtypes of enteric neurons (Brookes, 2001; J. B. Furness, 2000) that are conserved in mouse model **(Table 1.1)** (Boesmans et al., 2018), and about 17 in the colon **(Figure 1.5)** (Lomax & Furness, 2000).

The complexity of this further classification is due to the lack of methods and models to study enteric neurons at the level of a single cell within the mosaic of the ENS network. The role and positioning of those subtypes could vary according to the area of the GI tract and species. Overall, it is well known that ***motoneurons*** from the MP innervate both longitudinal and circular muscle layers, performing excitatory (ACh/TK/Calret) and inhibitory (NOS1/VIP/NPY) commands to those cells, having a crucial role in gut peristalsis. In the SMP, motoneurons also innervate enteroendocrine cells and are involved in controlling mucosal secretion. They are classified as cholinergic (ACh/CGRP/SOM/Calret) and non-cholinergic (VIP/NPY/Calret/TH) secretomotor neurons. It has also been suggested that motoneurons from the SMP supply the muscularis mucosae, but those studies were only performed in dogs. Vasodilator neurons (VIP/NPY/Calret) are involved in the control of submucous arterioles. ***Interneurons*** are located within the MP and are divided into four

subgroups as it follows: Ascending interneurons (ACh/TK/Calret) are orally directed and are involved in ascending excitation. Descending interneurons are anally directed and are involved in descending inhibition (ACh/NOS), descending excitation of secretomotor reflex (ACh/5-HT) and propagation of migrating motor complexes (ACh/Calret/SOM). ***IPANs*** are sensory neurons located within both plexuses. These types of neurons function sensing chemical environment, movements of the villi and distension of the gut (CGRP/ACh/Neurofilament/Calb/Calret) (Boesmans et al., 2018; J. B. Furness, 2000; Lomax & Furness, 2000).

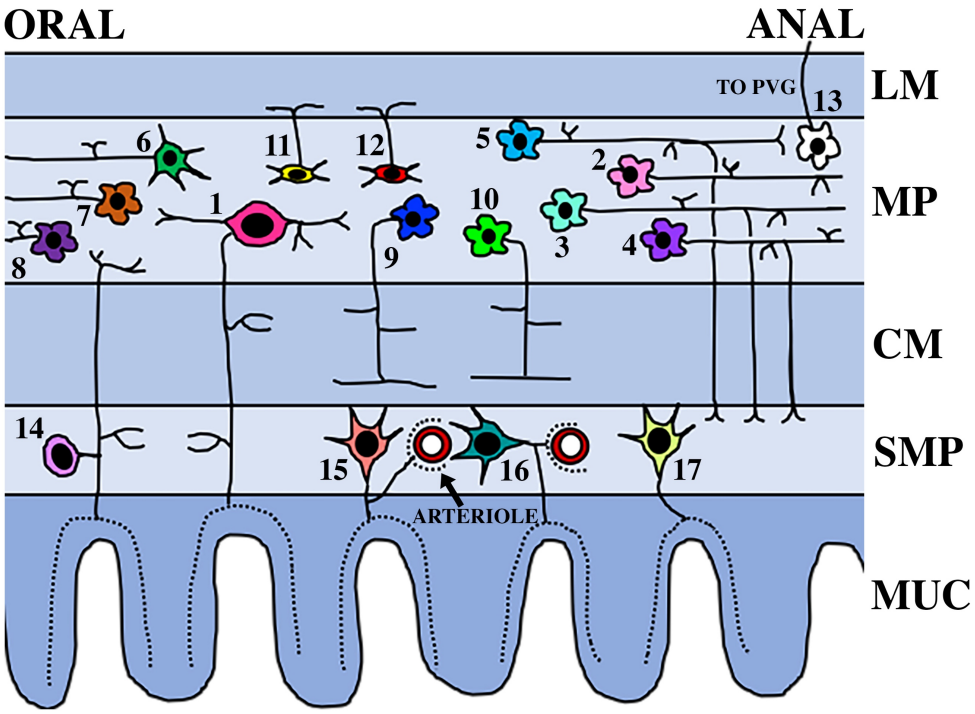


Figure 1.5. Schematic of enteric neuron subtypes in the distal colon of guinea-pigs described by their cell body morphologies and projections, chemical coding and function. LM: longitudinal muscle layer, MP: myenteric plexus, CM: circular muscle layer, SMP: submucosal plexus, Muc: muscosal layer, PVG: paravertebral ganglia. *Neurons within the myenteric plexus*: 1. Intrinsic primary afferent neuron (ACh/Calbindin/TK); 2. Descending interneuron (ACh/VIP); 3. Descending interneuron (NOS); 4. Descending interneuron (ACh/5-HT/CGRP/Calbindin/±Calretinin); 5. Descending interneuron (ACh/VIP/CGRP/±NOS/±Calbindin); 6. Filamentous ascending interneuron (ACh/SOM/Calretinin/VIP); 7. Ascending interneuron (ACh/TK/ENK/±VIP/±Calretinin); 8. Ascending interneuron (ACh/NPY/±TK/±SOM/±Calretinin); 9. Excitatory circular muscle motor neuron (ACh/TK/±ENK); 10. Inhibitory circular muscle motor neuron (NOS/VIP/±GABA/±NPY); 11. Excitatory longitudinal muscle motor

neuron (ACh/TK/Calretinin); 12. Inhibitory longitudinal muscle motor neuron (NOS/±VIP/±ENK); 13. Intestinofugal neuron (ACh/±NOS/±VIP/±CGRP/±Calbindin/±Calretinin). *Neurons within the submucosal plexus:* 14. Intrinsic primary afferent neuron (ACh/TK/Calbindin); 15. Non-cholinergic secretomotor neuron (NOS/VIP/±Calbindin); 16. Cholinergic secretomotor (ACh/Calretinin); 17. Cholinergic secretomotor neuron (ACh/NPY/CGRP/SOM). Modified from (Lomax & Furness, 2000) authorised by Springer.

Table 1.1 Proportion of enteric neuron subtypes in the distal colon of guinea-pigs described by their cell body morphologies and projections, chemical coding and function

Neuronal Subtype	Proportion	Neurochemical Coding	Shape	Function
Myenteric plexus				
Excitatory circular muscle motor neurons	21%	ACh / Tachykinin ± Calretinin	Dogiel type I	Promotes Contraction of circular muscle
Inhibitory circular muscle motor neurons	23%	NOS1 / VIP / NPY	Dogiel type I	Inhibits contraction of circular muscle
Excitatory longitudinal muscle motor neurons	13%	ACh / Calretinin ± Tachykinin	Small Dogiel type I	Promotes Contraction of longitudinal muscle
Inhibitory longitudinal muscle motor neurons	3%	NOS1 / VIP	Dogiel type I	Inhibits contraction of longitudinal muscle
Descending interneurons (local reflex)	3%	ACh / NOS	Dogiel type I	Descending Inhibition
Descending interneurons (secretomotor and motility reflex)	1%	ACh / 5-HT	Dogiel type I	Descending Excitation
Descending interneurons (migrating myoelectric complex)	4%	ACh / Somatostatin / Calretinin	Dogiel type III (filamentous)	Propagation of migrating motor complexes
Ascending interneurons	4%	ACh / Calretinin / Tachykinin	Large Dogiel type I	Ascending Excitation
Intrinsic sensory neurons or intrinsic primary afferent neurons (IPANs)	26%	CGRP / ACh / Neurofilament / Calbindin ± Calretinin	Dogiel type II	Majority senses chemical and mechanical changes in the gut lumen
Submucosal Plexus				
Cholinergic secretomotor neurons	30%	ACh / CGRP / Somatostatin / Calretinin	Stellate/Type IV	Control secretion in the mucosa
Non-cholinergic secretomotor neurons	22%	VIP / NPY / Calretinin / TH	Dogiel type I	Control secretion in the mucosa
Vasodilator neurons	30%	VIP / NPY / Calretinin	Dogiel type I	Vasodilation of submucous arterioles
Intrinsic primary afferent neurons (IPANs)	-	Not identified in murine submucosal plexus	-	-
Cholinergic neurons	10%	ACh	Dogiel type I	Unknown
Unknown markers	8%	Unknown	Unknown	Unknown

Note that some regional differences might occur in different parts of the GI tract, including colon. ACh: acetylcholine, NOS1: nitric oxide synthase, VIP: vasoactive intestinal peptide, NPY: neuropeptide Y, TH: tyrosine hydroxylase, 5-HT: 5-hydroxytryptamine, CGRP: calcitonin gene-related peptide. Table modified from (Boesmans et al., 2018) and (John Barton Furness, 2006) with permission from Springer and Wiley, respectively.

Despite many advances in unravelling neuronal properties taking into consideration their morphology, electrophysiology, chemical coding and overall function of a group of these cells, the field still lacks on knowledge about the complexity of single neurons and their connections with surrounding tissues in adult intestines.

1.1.4 Neurogenic control of the colonic motility

A unique feature of the ENS is the ability to independently coordinate the propulsion of intestinal contents in isolated pieces of the gut without inputs from the CNS and spinal cord (Bayliss & Starling, 1899). However, this synchronised intestinal movement involves a complex interaction between ICCs, smooth muscle cells (longitudinal and circular layers), platelet-derived growth factor receptor (PDGFR)α^+ cells and enteric neural network (EGCs and neurons) (Bayguinov, Hennig, & Smith, 2010). ICCs are considered the pacemakers of the gut since they generate slow electrical waves that control depolarisation and hyperpolarisation of longitudinal and circular muscle layers (Sanders, Kito, Hwang, & Ward, 2016; Ward, Burns, Torihashi, & Sanders, 1994). Smith et al. have proposed a model which suggests that the generation of rhythmic motor patterns in the colon is dependent on activation of serotoninergic neurons, IPANs, EGCs, muscle cells and ICCs by enterochromaffin-derived 5-HT (Smith & Koh, 2017). Although this function is influenced by other cell types, the neural control of colonic motility will be more specifically discussed in this section.

Peristalsis and migrating motor complexes (MMCs) are the two motility patterns responsible for mixing and expelling luminal contents. Peristalsis involves synchronised movements of longitudinal and circular muscle layers to simultaneously contract and relax. Peristaltic waves occur with no regular frequency and usually stop after few centimetres (Spencer, 2001). In the colon, the faecal pellet is propelled into a relaxed gut segment by an oral contraction of both muscle layers. This movement is dependent on excitatory neuronal response to promote contraction upstream, and descending inhibitory activation to promote relaxation downstream the bolus (Smith & Robertson, 1998).

Colonic migrating motor complexes (CMMCs) are spontaneous, anally propagating contractions that migrate over more than a half of the colonic length. It has been suggested that CMMCs are essential for pellet formation, size, shape and consistency (Costa et al., 2015). CMMCs are not observed in early postnatal colons, even though the neuronal network

is already present. The development of CMMCs occurs around P10 (10 days after birth) when the innervation of muscle layers by cholinergic neurons increase considerably **(Figure 1.6)**. However, slow waves of rhythmic depolarisation called "ripples" are already observed in embryonic guts, and they are enough to expel intestinal contents (Roberts, Murphy, Young, & Bornstein, 2007). CMMCs are likely to have neuronal origin as they were abolished by the use of neuronal blockade tetrodotoxin (TTX) (Fida, Lyster, Bywater, & Taylor, 1997). Little is known about mechanisms associated with formation and propagation of CMMCs. Studies have suggested that ACh, TK, NO and ATP may be involved in formation of CMMCs (Brierley, Nichols, Grasby, & Waterman, 2001), and mucosal 5-HT is necessary to activate those neurons to generate CMMCs (Bayguinov et al., 2010). The mechanisms that underlie intestinal peristalsis and formation and propagation of CMMCs remain still unclear. Recently, studies using optogenetic to stimulate a subtype of excitatory neurons (Calretinin) showed an increase in colonic function without the use of pharmacological agents (Hibberd et al., 2018).

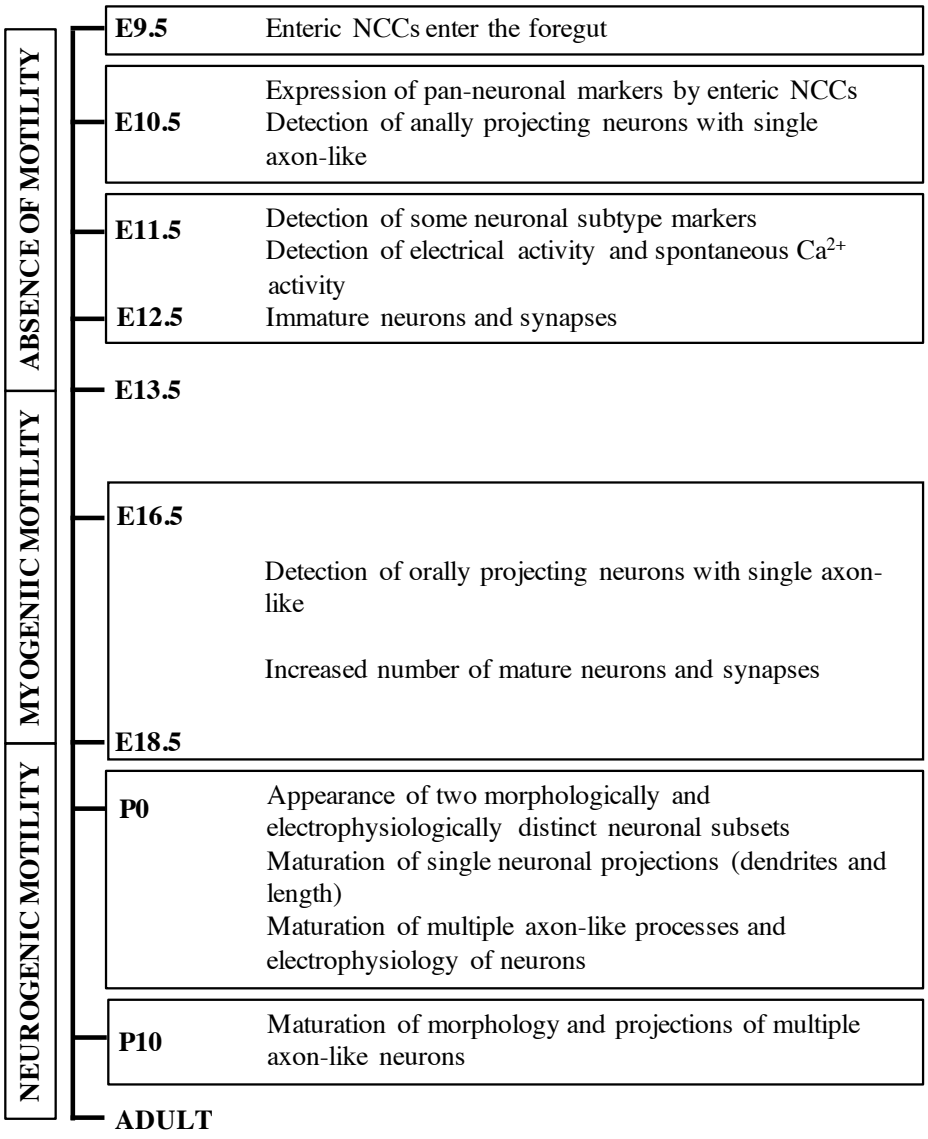


Figure 1.6. Development of neuronal network and neurogenic motility in the small intestine. Schematic shows de timeline of the maturation of enteric neurons, neuronal connection and neurogenic motility in the mouse intestine. Modified from (Hao et al., 2013) with permission from Springer.

1.1.5 Enteric Neuropathies/Hirschsprung disease

Enteric neuropathies comprise a wide range of disorders that disrupt the ENS function. Neuropathies can be caused by direct alterations on ENS components (primary neuropathies), resulting from genetic aberrations, i.e. HSCR disease, with symptoms that manifest in childhood. Secondary neuropathies, on the other hand, are caused by a disruption in related systems, such as the immune system, resulting in secondary effects on ENS function, for example, as observed in chronic inflammation and diabetic neuropathy.

Nonetheless, the aetiology of many primary enteric neuropathies is still unclear, and the severity of human phenotype may involve multiple causes (Knowles, Lindberg, Panza, & De Giorgio, 2013). Here, we are going to discuss what is known about the aetiology and pathogenesis of HSCR disease.

The most common and best known congenital ENS neuropathy is HSCR disease, which occurs on average in 1:5,000 live births and its incidence varies among ethnic groups. The disease presents an elevated heritability (>80%) and evident sex differences (male:female ratio is 4:1) (Amiel et al., 2008; Badner, Sieber, Garver, & Chakravarti, 1990). Approximately 18% of patients with HSCR disease have been diagnosed in combination with multiple anomalies, and about 12% of cases have been associated with major chromosomal abnormalities, for example, Down syndrome. Besides, HSCR disease includes a familial occurrence in a non-mendelian manner, and about 3 to 17% of sibling recurrence risk (Amiel et al., 2008). However, HSCR can also develop from a single mutation (also known as nonsyndromic HSCR) in genes affecting the control of ENCC proliferation, differentiation and migration. Genomic-wide association studies have identified the *RET* gene as one of the critical genetic factors implicated in the genesis of HSCR, with heterozygous mutations in its locus accounting for up to 50% of familial cases. Nonetheless, other single or combined mutations in members of RET pathway such as *GDNF* and *GFRα1*, and in other genes that regulate the development of ENCCs such as *NRTN*, *EDNRB*, *ET3*, *PHOX2b* and *SOX10* can also account in the pathogenesis of HSCR disease (Butler Tjaden & Trainor, 2013; Heanue & Pachnis, 2007; Tilghman et al., 2019).

HSCR disease is characterised by the absence of the myenteric and submucosal plexuses of the gut due to an incomplete rostrocaudal colonisation of colonic segments by ENS progenitor cells. The incomplete colonisation of intestinal layers by EGCs and neurons in patients is classified as short (about 80% of cases), long (15-20%) or total colonic aganglionosis (5%), rarely extending to the small intestine (Parisi, 1993). However, it is still unclear the causality of these distinct phenotypes in the segment length of the aganglionic colon. One of the main functions of the ENS is to promote intestinal peristalsis, and the absence of ENS network in patients with HSCR disease leads to impaired tonic contraction causing prominent functional obstruction. This is responsible for dramatic distension of the large intestine, a marked condition in HSCR disease referred as megacolon. Other symptoms that are detected in this condition are constipation, emesis, abdominal pain or distention,

vomiting and occasionally diarrhoea. In most cases, HSCR disease is diagnosed within the first 48 hours of life by the failure of the intestine in eliminating meconium, but it can also be later diagnosed when individuals report severe constipation (Butler Tjaden & Trainor, 2013; Parisi, 1993).

Children with HSCR are predisposed to enterocolitis (HAEC - HSCR associated enterocolitis) (Gosain, 2016; Vieten & Spicer, 2004). This fact may be due to defects in either the epithelial integrity or mucosal immune system, possibly due to direct regulation of the adaptive and innate intestinal immune system (Genton & Kudsk, 2003; Neunlist, Van Landeghem, Bourreille, & Savidge, 2008; Ruhl, 2005) or changes in gut flora (Frykman & Short, 2012). Alternatively, this link may reflect direct involvement of the RET gene in the immune system, as has been demonstrated for Peyer's patches and immune cell function (Almeida et al., 2012; Rusmini et al., 2013; Veiga-Fernandes et al., 2007).

Altogether, this overview on the aetiology and pathology of HSCR disease highlights the complexity of the genetic nature of this disorder, exemplifying multifactorial and complex inheritances, although distinct molecules that participate in the pathogenesis of HSCR have been identified. Nonetheless, more extensive genetic-wide association studies need to build on recent findings to integrate the contribution of epigenetic, environmental, immune and microbiological factors to reveal more details regarding the risks, pathophysiology and treatment to patients with HSCR disease.

1.1.6 Enteric Neuropathies/Neurodegenerative diseases

Recently, several hypotheses have emerged determining the participation of ENS in neurodegenerative diseases. Understanding the pathological alterations in the ENS and the course of neurodegenerative disorders could lead to potential and promising targets for early diagnosis and prevention of symptoms progression.

Parkinson's disease (PD) is a long-term degenerative disorder defined by selective damage in dopaminergic neurons in the *substantia nigra* in the brain and by the atypical accumulation of α-synuclein (Lewis bodies) aggregates in those surviving neurons, affecting the motor system. It has been suggested that patients with PD develop abnormal GI motility and severe constipation (Fasano, Visanji, Liu, Lang, & Pfeiffer, 2015). Interestingly, α-synuclein depositions are also found in the myenteric and submucosal neurons of patients with PD in age-dependent manner (Chen et al., 2018), and GI manifestation of this disease

was reported to precede motor symptoms by several years (Holmqvist et al., 2014). This suggests that the ENS may be the opening door for α-synuclein accumulation and spreading throughout the vagal nerve fibres until it reaches the brain (Holmqvist et al., 2014). However, it has been recently shown that submucosal neurons in the duodenum are not affected by α-synuclein deposition and display of normal function in PD patients (Desmet, Cirillo, Tack, Vandenberghe, & Vanden Berghe, 2017). Nonetheless, PD patients have a decreased number of VIP^+ neurons within the SMP in the colon (Giancola et al., 2017). Furthermore, the levels of genes expressed in EGCs are increased in PD patients, such as *Gfap*, *Sox10* and *S100b*, as well as of proinflammatory cytokines, suggesting that the progression of PD involves EGCs regulation and intestinal inflammation (Devos et al., 2013).

The contribution of the ENS for the spreading of PD and how microbiota influences the gut-brain transport of the disease, the GI symptoms and the specific loss of dopaminergic neurons in the brain are still to be further investigated. PD patients exhibit dysbiosis, but it is unclear whether this causes the dysmotility in the GI tract or it is a consequence of a deficient mechanism for bacteria elimination (Perez-Pardo et al., 2018; Scheperjans et al., 2015). Recent data have suggested that the microbiota or microbial products are necessary to initiate α-synuclein pathology, neuroinflammation and motor impairment. Oral administration of microbial-derived metabolites or faecal transplantation of microbiota from PD patients into α-synuclein overexpressing mice enhanced the pathophysiology of this disorder (Sampson et al., 2016). On the other hand, depleting microbiota with antibiotics in this mouse model ameliorated the symptoms of PD (Lombardi et al., 2018). Interestingly, it has been reported that patients with PD have low levels of brain-derived neurotrophic factor (BDNF) in the CNS and ENS. BDNF is a crucial factor to support neuronal survival and differentiation of dopaminergic neurons. BDNF can also regulate the immune system by playing a role in anti-inflammatory responses. Moreover, intestinal microbiota produces increased levels of BDNF (Lombardi et al., 2018). Collectively, these data could imply a potential role of this neurotrophic factor in the progression of PD, by functioning in the neuronal, microbial and immune regulations. The diagnosis of PD usually happens very late, when a loss of dopaminergic neurons followed by motor symptoms have already occurred. Understanding the role of the ENS and microbiota on the initiation and progression of PD could potentially be the opening door for the discovery of new targets to control this disorder.

Alzheimer's disease (AD) is a neurodegenerative disorder that promotes an impairment in the cognitive and loss of working memory. In the brain, AD is characterised by aggregation of β-amyloid (Aβ) plaques and intracellular hyperphosphorylated tau protein. Aβ is derived from the amyloid precursor protein (APP) also shown to be expressed in enteric neurons and glia, suggesting that AD pathology could affect the ENS. However, recent studies showing the pathophysiology of AD in ENS are limited and controversial (Chalazonitis & Rao, 2018). Post-mortem data using samples from AD patients showed no difference in neuronal loss or tau pathology when compared to controls (Shankle et al., 1993). An additional study demonstrated an increase in colonic Aβ immunoreactivity in patients with AD (Chalazonitis & Rao, 2018). Moreover, in a model in which overexpression of APP caused AD brain pathology (AβPP/PS1), mice exhibited Aβ accumulation and phosphorylated tau overexpression in enteric neurons (Han et al., 2017; Puig et al., 2015), followed by a decreased proportion of nitrergic and cholinergic neurons in the MP, with no significant changes in neuronal numbers (HuC/D^+) or density ($Tuj1^+$) (Han et al., 2017; Puig et al., 2015). Increased intestinal macrophage density and levels of pro-inflammatory cytokines were also observed in this model (Puig et al., 2015). Additionally, Semar et al. suggested that the levels of nestin, GFAP and TLR4 were increased in adult mice in a model of APP overexpression. Myenteric neurons exhibited Aβ accumulation, reduced neuronal density that potentially cause intestinal dysmotility. Altogether, this study suggests that the ENS undergoes several changes that precede the brain manifestations of AD pathology (Semar et al., 2013). Furthermore, AD patients exhibit less microbiota diversity that could contribute to the pathophysiology of this disease. In mice model of AD, antibiotic treatment led to a reduction of amyloidosis. Similar to PD, patients with AD have reduced levels of BDNF, suggesting a potential role of this molecule in the progression of disease (Lombardi et al., 2018).

1.2 An overview of the gut immune system

The GI tract is continuously exposed to high amounts of external antigens from dietary and bacterial sources due to its localisation and interface between the internal and external environment in the body. As a result, the GI contains a highly diverse microbiome and an extremely active immune system (Doe, 1989). The gut contains the most significant number of immune cells in the body. Although the intestinal epithelia form a tight barrier

against intraluminal contents, the gut remains susceptible to pathogens and requires additional defence machinery. An essential component of a such protective apparatus is the immune system. The immune system includes a network of cells from the innate and adaptive immune systems, such as macrophages/monocytes and T and B lymphocytes, respectively. These cells compose an orchestrated line of defence against pathogenic microorganism invasions and harmful antigens (Sansonetti, 2004).

Most of all intestinal immunological processes take place in the mucosa that comprises of the epithelial layer, the lamina propria underneath and the *muscularis* mucosa. The **lamina propria** includes a bundle of connective tissue and contains blood and lymph vessels, neural cells and processes, and many cells from the immune system. The **submucosa** is located just beneath the mucosal layer, and contains the Peyer's Patches (PPs) and colonic patches. The **gut-associated lymphoid tissue (GALT)** includes all subepithelial lymphoid aggregates localised within the mucosa and submucosa, such as a) **follicle-associated epithelium (FAE)** that is a layer of epithelium that covers the PPs and the isolated lymphoid follicles and it is also rich in immune cell populations; b) **subepithelial dome (SED)** that is localised just under the FAE, and it contains many antigen-presenting cells and B cells; c) **PPs** which are localised opposite to the mesenteric border in the small intestine. They contain many B lymphoid follicles surrounded by T cells; d) **colonic patches** are organised lymphoid tissues and consist of T and B cells. GALTs also comprises **solitary isolated lymphoid tissues (SILTs)** such as - **crypto patches** which are small areas of lymphoid tissue and contain dendritic cells and lymphoid tissue inducer cells and **isolated lymphoid follicles (ILFs)** containing numerous B cells but no clear T cell zone (Agace & McCoy, 2017). However, interestingly none of those structures is located within the muscle layers of the gut.

1.2.1 The adaptive and innate immune systems of the gut

Innate immunity comprises cellular mechanisms that contribute to the first line of defence from insults in the gut, in a non-specific manner. Innate immune responses are usually rapid and independent of antigen. This system comprises a group of cells that have distinct roles in gut homeostasis and pathology. Intestinal **macrophages** are the most abundant innate cell type within the lamina propria. They have phagocytic function and work as antigen-presenting cells, producing different mediators (IL-10, IL-1β) that activate other

immune cells to repair and maintain the gut environment. Macrophages highly express the markers CD11c, MHCII, CX3CR1, F4/80, CD163 and CD68 in mice (Agace & McCoy, 2017; Mowat & Agace, 2014). Recent studies have identified a novel population of *muscularis* macrophages (MMs) that are localised within the longitudinal muscle layer, distinct from those in the lamina propria, and were reported to be involved in tissue protection (Gabanyi et al., 2016; Muller et al., 2014). **Dendritic cells** (DCs) share some molecular and physiological features with macrophages and they both have been implicated in the antigen presentation in the gut. They are $MHCII^+$ and $CD11c^+$ but lack the expression of the macrophage marker F4/80. Four subtypes of these cells were described in the gut that can be identified by using a combination of markers. It has been suggested that those subsets of DCs have different roles in the gut. DCs were found within the lamina propria as well as in the GALTs. In homeostasis, **mast cells** ($CD69^+$) and **eosinophils** ($LY6C^+$) are very abundant in the small intestine lamina propria and are involved in allergic reactions and immunological response to worm infections. **ILCs** are derived from the common lymphoid progenitor, but they do not express T or B cell receptors as they lack recombination activating genes (*Rag*). ILCs do not share myeloid markers. They are identified by the expression of RORγt. These cells are involved in many immunological functions, and they promptly respond to insults and rapidly produce cytokines. They are subdivided into three groups with specific pivotal roles in different pathologies (ILC1, ILC2 and ILC3). Other types of innate immune cells are **basophils**, **neutrophils**, and **natural killer** cells **(Figure 1.7)** (Mowat & Agace, 2014; Spits & Cupedo, 2012).

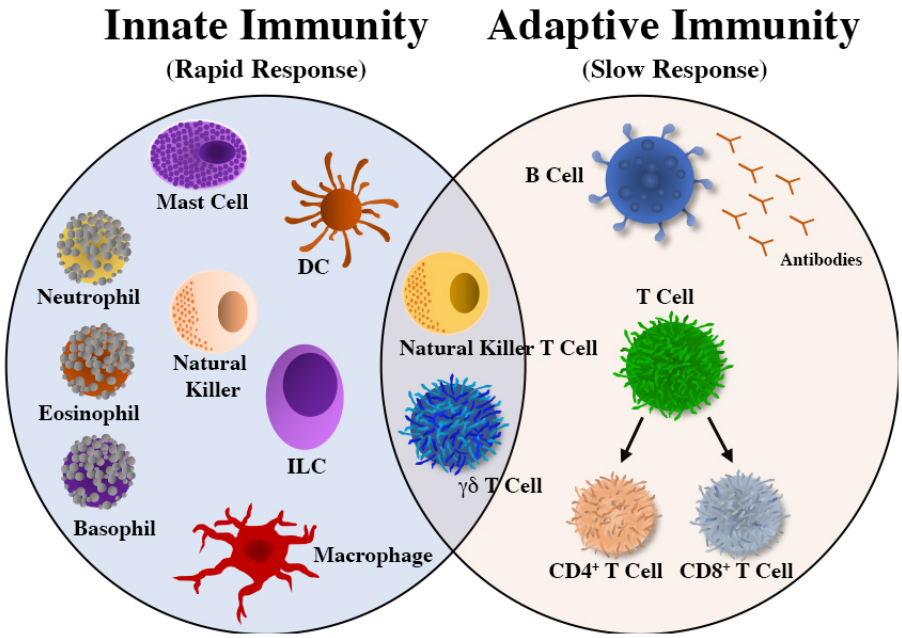


Figure 1.7. Cellular components of the immune system. The adaptive immune system (slow response) contains T (cellular) and B (humoral) lymphocytes. The innate immune system (rapid response) is composed of phagocytes such as macrophages, dendritic cells, mast cells, natural killer, basophil, eosinophil, neutrophil and innate lymphoid cells.

Adaptive immunity is the protective mechanism that detects specific epitopes (antigens). It is mediated by lymphocytes and is the basis of immunological memory to specific epitopes. In contrast to innate immunity, adaptive immunity is specific to a determined antigen and the activation and response of those cells are highly adaptable. The adaptive immune system includes antigen-specific receptors that are expressed by T and B lymphocytes. T cell express the highly variable T cell receptor (TCR) associated to the CD3 signalling receptor complex and are further subdivided into $CD4^+$ and $CD8^+$ cells. B cells express a highly variable BCR in the form of a membrane associated immunoglobulin IgM. Both TCR and BCR are generated following a cascade of molecular events that are unique to their development and include DNA somatic recombination, mutation at junctions and affinity maturation.

T lymphocytes are derived from haematopoietic stem cells (HSC) produced in the bone marrow. These T cell progenitors migrate and colonise the thymus, upon which they undergo different maturation steps that can be identified based on the expression of cell surface markers such as CD4, CD8, CD44 and CD25. It is also in the thymus that thymocytes

will give rise to αβ T cells (about 95% of the T cell receptor - TCR expressing cells) and γδ T cells (5% of T cells). In the thymic cortex, the successful binding of MHC proteins expressed on the cell surface of epithelial cells to immature thymocyte receptors positively select double-positive thymocytes ($CD4^+CD8^+$) to continue differentiation while those which cannot bind, undergo apoptosis. During positive selection, cells will refine into CD4 or CD8 and become MHCII and I restricted respectively. These positively selected cells will then migrate to the thymic medulla, where negative selection takes place. Thymocytes that bind to self-antigens presented by antigen presenting cells (APCs) are killed by apoptosis to prevent autoimmune responses and the ones left are thymocytes that can bind to MHC molecules with foreign presented antigens (H. Liu, Rhodes, Wiest, & Vignali, 2000; OpenStax, 2013).

$CD4^+$ and $CD8^+$ T cells are further classified into several subgroups and have distinct functions. It has been suggested that the ratio of $CD4^+$ and $CD8^+$ T cells within the lamina propria is around 2:1, respectively. One type of T cell that has successfully undergone both positive and negative selections is the **naïve T cells** (Th_0 cell). Naïve T cells are negative for the activation markers CD25, CD44 and CD69 and circulate from the blood to the lymph nodes and back to the blood every 12-24 hours, thus having high chances to encounter a given antigen. They initiate an effective activation program by up-regulating those markers if they find an APC expressing MHC/peptide to which they can bind. Activated $CD4^+$ T cells become helper T cells (Th) due to their ability to help other cells from the immune system to eliminate pathogens by secreting cytokines that help to suppress or regulate immune responses. Th cells are classified into distinct and specialised subgroups depending on the cytokines that induce their differentiation, master transcriptional regulators and their production and secretion of cytokines, conferring them different roles in adaptive immunity (Agace & McCoy, 2017). Here, we are going to briefly discuss five main subsets of Th cells **(Figure 1.8)**.

Briefly, upon insult such as viral or bacterial infection, APCs secrete IL-12 and migrate from the site of infection to a lymphoid tissue (PPs and MLN), presenting antigens to naïve $CD4^+$ T cells. Once these antigens are recognised, IL-12 induces more signals that differentiate naïve $CD4^+$ T cells into **T helper type 1 (or Th1 cells)**. Th1 cells secrete IFNγ that activates macrophages to eliminate phagocytosed pathogens and stimulates the production of antibodies that further promote the phagocytosis of pathogens. Besides IFNγ,

Th1 cells also produce IL-2, an important cytokine for promoting proliferation and differentiation of other T cell subsets. **T helper type 2 (or Th2)** differentiate from naïve $CD4^+$ T cells when there is an infection caused by parasites in which cells from the innate immune system release IL-4. Th2 cells themselves also secrete IL-4 that stimulates B lymphocytes to produce antibodies, followed by secretion of IL-5 that activates mast cells and eosinophils, together with IL-13 that induces the production of mucus in the intestinal lumen. Altogether, these cytokines promote the killing and elimination of parasites within the intestines. Moreover, when there is an infection by fungi or extracellular bacteria, innate immune cells produce IL-6, IL-21 and TGFβ that differentiate naïve $CD4^+$ T cells into **T helper 17 (or Th17)**. Th17 cells produce and secrete IL-17 recruiting neutrophils to the site of infection, inducing inflammation. Th17 cells also secrete IL-22 that stimulates epithelial cells to produce antimicrobial peptides. **Regulatory T cells (or suppressor T cells or Tregs)** have a pivotal role to limit tissue damage caused by the immune response once a pathogen is eradicated and they also prevent autoimmunity. Tregs mainly express CD4, CD25 and the transcription factor Forkhead box P3 (FOXP3). These cells mainly secrete TGFβ and IL-10 that respectively induce the generation of more Tregs and suppress macrophage functions. They have been reported to closely interact with Th17 cells. Studies using segmented filamentous bacteria (SFB) showed an inverse correlation between the number of Th17 and $Foxp3^+$ Treg cells (Denning et al., 2011). **Follicular helper T cells (or T_{FH} cells)** differentiate from naïve $CD4^+$ T cells upon stimulation with IL-6 and IL-21. These cells also produce IL-21 that guide B cells to produce appropriate antibodies to defeat specific infections.

$CD8^+$ T cells are the **cytotoxic T cell (or killer T cell or Cytotoxic T lymphocytes - CTLs)**. These cells play a crucial role in recognising and destroying cells that present antigens using their MHCI-molecule complex expressed on their surface. At the same time, Th1 cells secrete IL-2 that combined with the recognition of MHCI molecules by $CD8^+$ T cells triggers the differentiation and proliferation of cytotoxic T cells and memory T cells. Cytotoxic T cells produce more IL-2 for its self-stimulation, migrate to the site of infection to recognise foreign antigens presented by MHCI molecules and release granules to kill target cells. These cells also secrete cytokines such as IFNγ and TNFα that activate and recruit macrophages to the site of infection **(Figure 1.8)**.

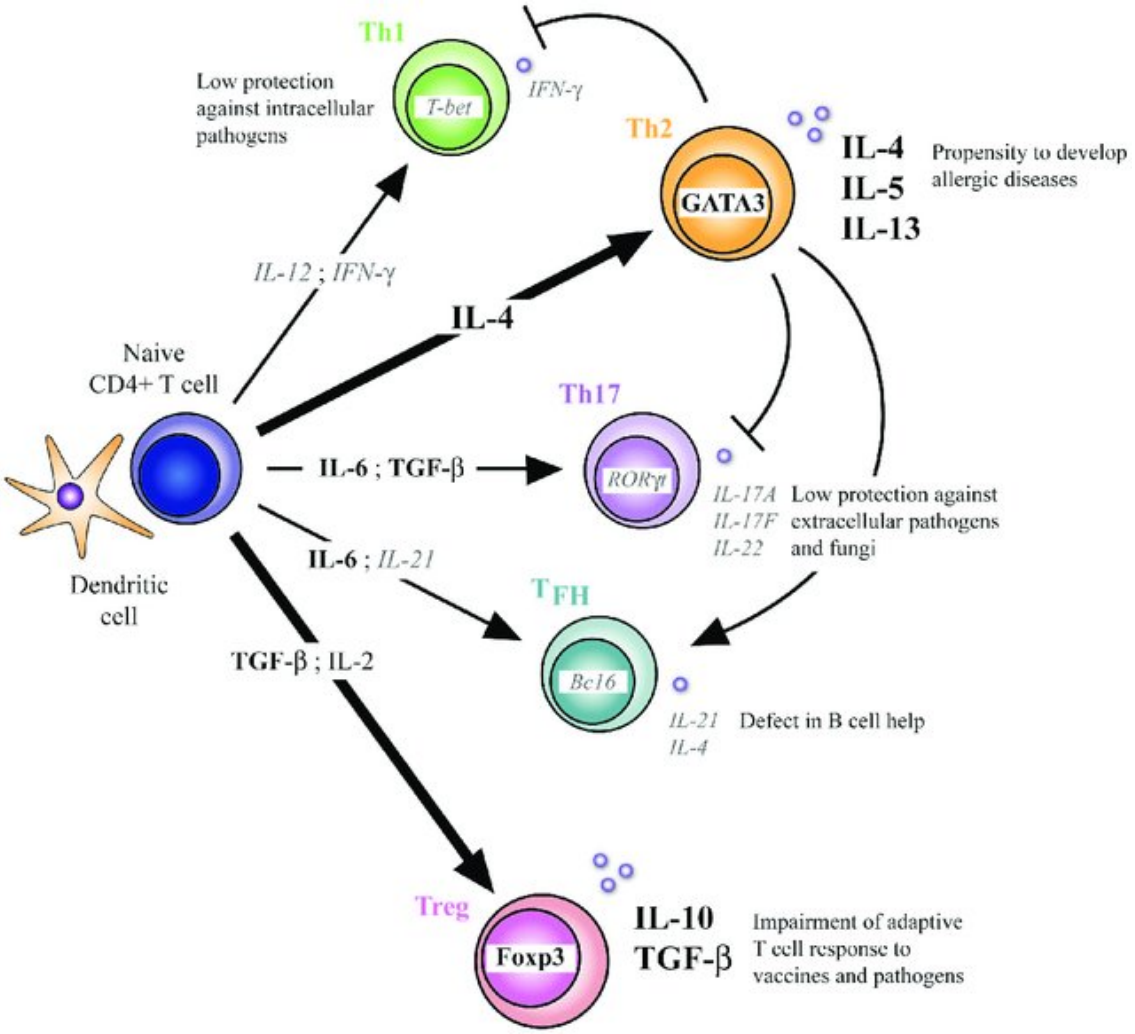


Figure 1.8. T cell subsets and the adaptive immune response. Schematic shows subtypes of helper T cells upon stimulation of naïve $CD4^+$ T cells with different cytokines triggering the differentiation of these cells into Th1, Th2, Th17, T_{FH} and cytotoxic T cells. Th, helper T cells. Schematic from (Debock & Flamand, 2014).

Intestinal **B cells** (B lymphocytes) are extremely abundant within the intestinal lamina propria and GALTs. They express a diverse range of immunoglobulin receptors (secrete antibodies), that bind to specific antigens, then functioning in the humoral immunity. The majority of mature B cells express CD19 and Immunoglobulin M (IgM). Most of the plasma cells produce IgM, however, in the colon, they produce about 90% of Immunoglobulin A (IgA). The production of IgA is dependent on microbiota and it is

released in the gut lumen following transcytosis through the epithelium (Agace & McCoy, 2017; LeBien & Tedder, 2008; Mowat & Agace, 2014).

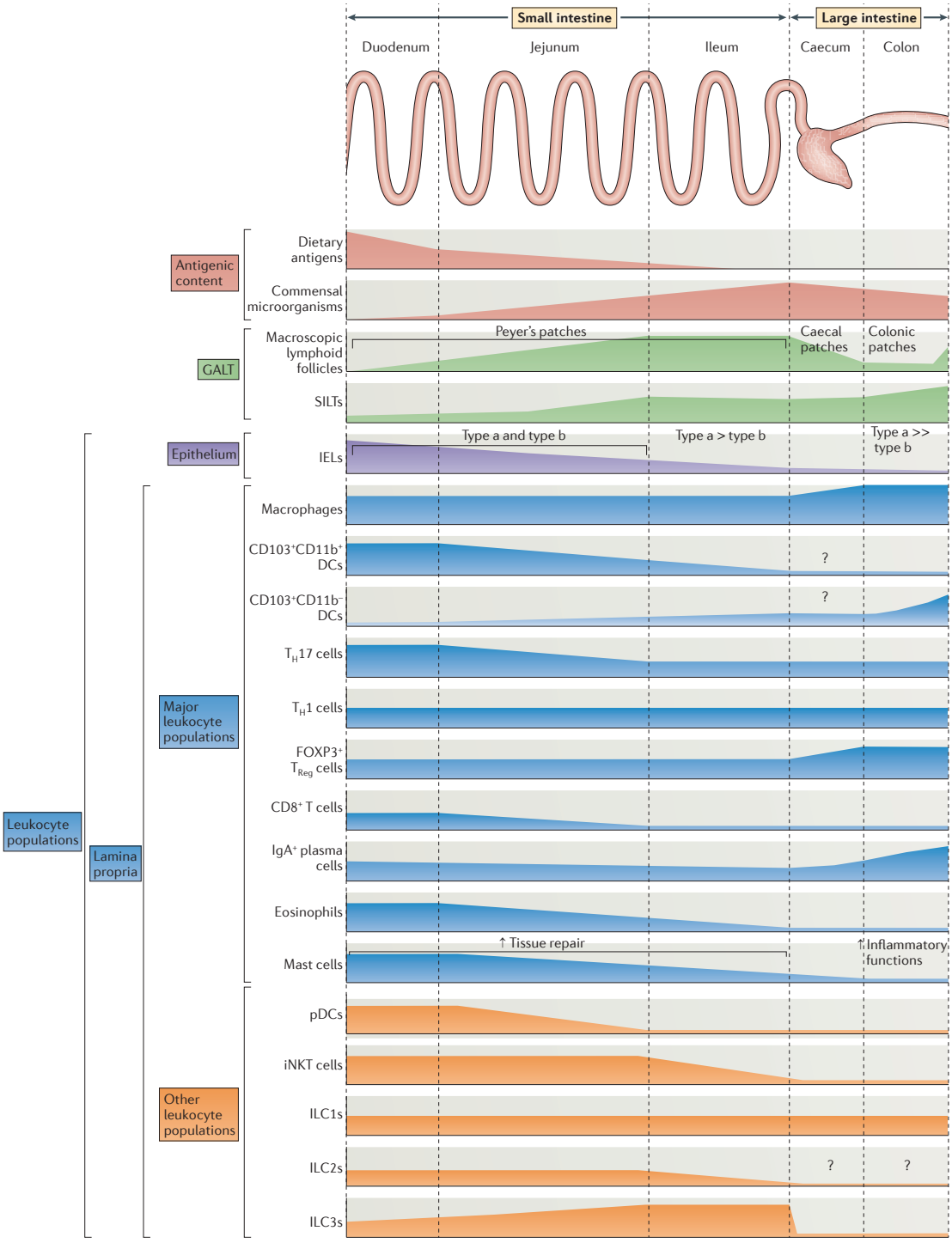


Figure 1.9. Regional composition of the gut immune system. The diagram shows the compartmentalised frequency of the immune apparatus in the GI tract. Antigenic content such as dietary antigens and commensal

microorganisms (red), GALT (green) showing the macroscopic lymphoid follicles and SILTs. Leukocyte populations are divided in epithelium IELs (purple), and different leukocyte populations within the lamina propria (blue and orange). GALT: gut-associated lymphoid tissue, SILT: solitary isolated lymphoid tissue, IEL: intra epithelial lymphocyte, ILC: innate lymphoid cell, Th: T helper, iNKT: invariant natural killer T, DC: dendritic cell, pDC: plasmacytoid DC, CD: cluster of differentiation. From (Mowat & Agace, 2014) and authorised by Springer Nature.

The balanced presence and function of each cell from the gut immune system are essential for its homeostasis. Intestinal immune cells are primed to defeat any possible threats that disturb the stability of the gut system, working for or against those challenges. One example of this is the gut microbiome. The colon has the highest resident population of microorganisms, containing about 10^{12} microbes per gram of luminal contents. The gut microbiota together with antigenic load produced by food provides more antigens to the gut immune system than any other parts of the body. Besides, the intestinal microbiota work along with the immune system to control inflammation, suggesting once again that the crosstalk between microbiota and immune system is essential for the physiology of host tissue (Blander, Longman, Iliev, Sonnenberg, & Artis, 2017). The gut immune system participates in many other events to control health and disease as it has been recently reviewed, such as aging (Nikolich-Zugich, 2018), oncobiology (Palucka & Coussens, 2016), neurodegenerative diseases (Song & Colonna, 2018), food allergies (Tordesillas, Berin, & Sampson, 2017). In this thesis, we are going to focus on neuroimmune interactions, which is relevant to our subject.

1.2.2 Neuroimmune communications

Over the past few years, interest in studying neuroimmunology has increased exponentially, especially with the fast progress in developing advanced strategies to explore and understand neuroimmune interactions at high resolution. Because the immune and nervous systems share the same environment in health and disease, it is expected that these cells work in concert to maintain tissue homeostasis. Such interactions can be anatomical by the positioning of these cells within the tissue, expressing complementary ligands and receptors that suggest physiological function, and also by responding to environmental cues during inflammation, for instance. However, deciphering mechanisms by which immune and

neural cells interact and respond to infection and inflammation is still a challenge to be addressed.

1.2.2.1 The immune and central nervous systems

The brain is considered a privileged organ because it contains a resistant blood-brain barrier (BBB) that protects this organ from physical trauma, pathogens and antibodies from immune cells. The BBB, blood-cerebrospinal fluid barrier (BCSFB) and the blood-retinal barrier (BRB) form an intricate physical mechanism to protect the CNS from external insults. Besides physical barriers, the CNS is also endorsed with a potent immunological barrier that provides continuous immune surveillance necessary to control insults and maintain the CNS homeostasis. The activation of immunological responses in the CNS is very limited since there are few antigen-presenting cells within the parenchyma and adaptive immune cells need to be activated prior to crossing physical barriers. Microglia are the most abundant immune cells within the brain parenchyma and colonise this organ early during development. It is suggested that microglial cell numbers within the brain do not change under physiological conditions (Wraith & Nicholson, 2012). On the other hand, the role of the adaptive immune system in the CNS in a steady-state environment need further study. The presence and function of adaptive immune cells in a non-pathological CNS condition is ambiguous and lacks conclusive evidence. Immune surveillance is essential to control infections in the CNS. Nonetheless, adaptive immune responses in the CNS may be advantageous or detrimental to the system. It has been reported that T lymphocytes enter the cerebrospinal fluid (CSF) and travel around the meninges and perivascular spaces, not reaching the brain parenchyma unless required after an insult. In healthy individuals, it was demonstrated by flow cytometry that around 150 000 T cells in the CSF routinely penetrate the choroid plexus maintaining a constant flux of cells through the CNS (Engelhardt & Ransohoff, 2005; Wraith & Nicholson, 2012).

Infiltration of immune cells through a leaky BBB has been documented in autoimmune diseases, ageing and gestation in which there is an increased level in cytokine production which activates and recruits these cells (McAllister & van de Water, 2009). Moreover, several pieces of data have shown the role of adaptive immune cells in CNS diseases. For instance, using patch-clamp experiments, Meuth et al. have demonstrated that $CD8^+$ T lymphocytes induce impaired electrical patterns in neurons, increasing intracellular

Ca^{2+} concentrations that precede neuronal death (Melzer, Meuth, & Wiendl, 2009; Meuth et al., 2009).

One suggestion that supports the idea of neuroimmune interactions is the fact that some immune cells secrete neurotransmitters or express their receptors, which could have an autocrine or paracrine role in immune function. It has been reported that Substance P and its receptor NK-1 are expressed by human lymphocytes (Lai, Douglas, & Ho, 1998) and mononuclear phagocytes (Lai, Douglas, & Ho, 2002; Mashaghi et al., 2016). T cells also express dopamine receptors, and different subtypes of these cells have distinct responses to dopamine (Levite, 2016). It has been suggested that not only T and B cells (Bergquist, Tarkowski, Ekman, & Ewing, 1994), but macrophages and neutrophils can also produce and release catecholamines that enhance inflammatory responses (Flierl et al., 2007). Furthermore, studies have reported an intrinsic and functional role of GABA in human lymphocytes (Dionisio, Jose De Rosa, Bouzat, & Esandi Mdel, 2011). CGRP inhibits myeloid cell function and activates Th2, Tregs and Th17 cells. VIP is a peptide hormone produced by neurons. Studies have revealed the presence of this neuropeptide in many cells from the immune system including mast cells and lymphocytes (Gomariz et al., 1993). Moreover, given the appropriate stimuli, macrophages, DCs, $CD4^+$ T cells and B cells could also produce and secrete ACh in order to control physiological processes (Reardon et al., 2013; Reardon, Murray, & Lomax, 2018; Rinner, Kawashima, & Schauenstein, 1998). In addition to production and release of ACh, immune cells also express both muscarinic and nicotinic ACh receptors that have different functions in immune response (Reardon et al., 2018). The production of neurotransmitters by immune cells supports the evidence of a robust neuroimmune partnership to maintain tissue homeostasis.

On the other hand, it has been described that important molecules that mediate immune responses and were thought to be expressed exclusively in cells from the immune system are also expressed by neural cells. For instance, MHCI is expressed by developing and mature CNS neurons when stimulated with IFNγ (Corriveau, Huh, & Shatz, 1998; Neumann, Cavalie, Jenne, & Wekerle, 1995) and actively participate in neuronal synaptic function and structure (Goddard, Butts, & Shatz, 2007). Besides MHCI, the receptor complex for this molecule CD3ζ and β2-microglobulin are also expressed by CNS neurons (Corriveau et al., 1998). TCRβ expression was also identified in cortical neurons even though its function on these cells has not yet been elucidated (Syken & Shatz, 2003).

Moreover, *Rag1*, a fundamental gene involved in the generation of a diverse receptor repertoire in T and B lymphocytes, was also identified in murine neurons (Chun, Schatz, Oettinger, Jaenisch, & Baltimore, 1991) and in a subset of olfactory neurons in zebrafish (Feng, Bulchand, Yaksi, Friedrich, & Jesuthasan, 2005). However, its role in neuronal homeostasis is unclear as no neuroanatomical, physiological or behavioural phenotypes were observed in mice lacking expression of this gene (Mombaerts, Iacomini, et al., 1992). Instead, Rag1 was described to play a role neuronal apoptosis in a model of optic neuropathy (Hirano, Murata, & Hayashi, 2015) and recently been suggested to act in long-term memory in fear conditioning (Castro-Perez et al., 2016). Not only neurons but astrocytes also participate in immune response by expressing pattern-recognition receptors (PRRs) that are involved in recognition of microbial and danger signals (Farina, Aloisi, & Meinl, 2007).

Another important aspect of the nervous system is the ability to form synaptic connections that permit chemical and electrical information to pass from one neuron to another or targeted cell. In the CNS, microglia have a crucial role during formation and development of synaptic circuits by engulfing and pruning synaptic debris via microglia-specific phagocytic signalling pathway, complement receptor 3(CR3)/C3. Impaired microglial function in synapses engulfment and pruning could contribute to neurodevelopmental disorders (Paolicelli et al., 2011; Schafer et al., 2012). Likewise, cleaning of synaptic debris by microglia was also observed after optic nerve injury (Norris et al., 2018). Additionally, it has been shown that the anatomical positioning between microglia and neuronal dendrites induces filopodia formation. Recent findings have reported that microglial depletion reduces spine density, excitatory synapses and neuronal connectivity (Miyamoto et al., 2016). Moreover, studies with the CX3CR1^{CreER} microglia depletion model, have suggested an essential physiological role of microglia in learning and memorising synapse formation via the BDNF pathway (Parkhurst et al., 2013). Studies in the CNS have also proposed a "quad-partite" synaptic function of microglia working mutually with neurons and astrocytes via fractalkine, TNFα and L-serine signalling (Schafer, Lehrman, & Stevens, 2013). Recently, another mechanism for a "quad-partite" synapse has been revealed. Vainchtein et al. have proposed that IL-33 secreted by developing astrocytes primes microglia to promote synapse engulfment during neuronal circuit maturation and remodelling (Vainchtein et al., 2018).

Although several indications have been recently published about the potential role of

the immune system on the development, homeostasis and response of the CNS to injury, the interaction between immune cells and the ENS remains poorly explored.

1.2.2.2 The gut immune system and the ENS

Different from the CNS that is considered an immune-privileged organ, the ENS is continuously exposed and interacts with the external (microbiota, diet, metabolites) and internal (immune and stromal cells) environment of the gut. Emerging studies have proposed that the gut immune system interacts with the ENS by sharing the same anatomical location within the GI wall and by sharing physiological functions in order to defeat pathogens and keep the gut homeostasis.

Recently, two types of tissue-resident macrophages with distinct roles were identified within the intestinal wall. Lamina propria macrophages (LpMs) are the most abundant cell group localised just beneath the epithelium. Using a transcriptional profiling approach, these cells were identified to preferentially express a pro-inflammatory phenotype (Gabanyi et al., 2016). Along with EGCs, neuronal processes, epithelial and stromal cells and other immune cell types, LpMs form a physical and functional barrier against pathogens. The exact mechanism by which these cells functionally interact with ENS cells is still to be further investigated.

The other group of macrophages, MMs, are closely associated with the MP. Recent data have suggested that MMs secrete the growth factor bone morphogenetic protein 2 (BMP2) that binds its receptor BMPRII on neurons. This process influences the differentiation of ENS precursors, neurite fasciculation and ganglion formation, in addition to enteric neurons activation and peristalsis modulation (Chalazonitis et al., 2008; Muller et al., 2014). In turn, enteric neurons produce the colony stimulatory factor 1 (CSF1), a growth factor necessary for macrophage/monocytes development. At the same time, it has been suggested that the microbiota also interacts with macrophages and neurons, since the presence of bacteria upregulates both CSF1 and BMP2 (Muller et al., 2014). Although CSF1 is mainly secreted by enteric neurons in adulthood, the development of MMs was reported to not be dependent on neuronal CSF1. MMs colonise the gut prior to neuronal network formation. Recent data have shown that numbers, distribution and phenotype of MMs do not differ from controls in a mouse model of ENS aganglionosis ($Ret^{-/-}$) or patients with Hirschsprung's disease (Avetisyan et al., 2018).

Moreover, by using a double reporter to label macrophages (*Cx3CR1*$^{GFP/+}$) and enteric-associated neurons (*Hand2*^{Tomato}), Gabanyi et al. recently identified that MMs are anatomically associated with enteric neuron cell bodies and fibres along the gut wall. When compared to LpMs, MMs display a tissue-protective phenotype. This data has also revealed that activated MMs highly expressing *Adrb2* (encoding b2 adrenergic receptors) reside adjacent to enteric neurons in the MP (Gabanyi et al., 2016), once again suggesting the interaction between immune and enteric nervous systems. It has been proposed that MMs exhibit a similar function to microglia in the CNS by phagocytosing neuronal debris in a healthy environment. Kulkarni et al, using a flow cytometry approach, isolated macrophages from a reporter mouse line that labels a subgroup of enteric neurons (*CHAT-Cre:td*^{Tomato}) and identified td$^{Tomato+}$ neuronal debris in these cells. They further proposed that this is a unique function of MMs from both small and large intestines as they did not observe accumulation of neuronal debris either in submucosal or LpMs (Kulkarni et al., 2017). Furthermore, it has been shown that genetic (*Csf1r*$^{-/-}$) and antibody depletion (αCSF1R) of MMs *in vivo* results in intestinal dysmotility (Muller et al., 2014).

Another population of gut self-maintaining macrophages (gMacs) was recently identified, and they present a unique transcriptional profile depending on their location within the gut wall. These macrophages were reported to be crucial for ENS homeostasis since the genetic depletion of gMacs (Cx3cr1^{CreERT2};Rosa26-iDTR) led to a loss of enteric neurons and reduced intestinal transit time (De Schepper et al., 2018).

Moreover, recent studies have described a new mechanism by which enteric neurons and ILC2 integrate to promote type 2 immune responses in the gut. It has been shown that ILC2 selectively express neuromedin U receptor 1 (Nmur1) and enteric neurons secret the neuropeptide neuromedin U (NMU). The functional interaction between neuron-ILC2 unit by neuronal NMU binding to Nmur1 is essential for cytokine production and inflammation repair. Accordingly, *in vitro* stimulation with NMU induced activation and proliferation of ILC2 and type 2 cytokine secretion. *In vivo* administration of this neuropeptide, in turn, accelerated worm expulsion. In contrast, Nmur1 ablation in ILC2 caused an impaired type 2 response and increased worm burden (Cardoso et al., 2017; Klose et al., 2017).

Not only neurons but also EGCs appear to cooperate with immune responses, but so far, the impact of EGCs on immune cells is still relatively unexplored under homeostatic conditions. Latterly, an exciting study has discussed that glial-derived neurotrophic factors

(GDNF) produced by EGCs orchestrate IL-22-producing ILC3 activation through Ret signalling (Ibiza et al., 2016). Moreover, it has been shown that Ret is an essential regulator for PPs organogenesis, highlighting the potential role of glial cells in regulating innate immune functions in the gut (Veiga-Fernandes et al., 2007). Also, experiments performed in the SMP from patients with functional dyspepsia (FD) showed impaired calcium response in neurons when compared to control samples. Cirillo et al. identified morphological changes both in EGCs and neurons in FD patients, suggesting that these abnormalities are due to an increased number of eosinophil and mast cell within the SMP (Cirillo et al., 2015). These data suggest the participation of EGCs in neuroimmune interactions in order to maintain intestinal homeostasis.

In the gut, however, interactions between the adaptive immune system and ENS in the healthy GI tract are poorly elucidated. It has been suggested that different subset of enteric neurons innervate the PPs based on observations in which submucosal enteric neurons project to around and inside PPs follicles (Chiocchetti et al., 2008; Vulchanova, Casey, Crabb, Kennedy, & Brown, 2007). It has been shown that neuropeptides participate in immune modulation and proliferation of lymphocytes in the PPs by controlling the production of immunoglobulin isotypes (Stanisz, Befus, & Bienenstock, 1986). The reason why lymphocytes respond to some neuropeptides is that they express receptors that bind to these molecules, for instance, receptors for VIP and NPY. The exact role of neurotransmitters directly on lymphocytes remains unclear, but they seem to modulate the response of these cells to inflammation (S. Schneider, Wright, & Heuckeroth, 2018). It has been shown that neurons and EGCs express the cytokine IL-7. After exposure to pro-inflammatory cytokines such as IL-1β and TNFα, EGCs upregulate the expression of IL-7. This study also suggests that IL-7-EGCs protects T cells from cell death (Kermarrec et al., 2018). Kermarrec et al. have examined the direct effect of human EGCs on T cells using a co-culture system. They suggested that EGCs inhibit T cell proliferation, raising the possibility that EGCs have immunosuppressive characteristics in Crohn's disease (Kermarrec et al., 2016).

Emerging and interesting data have suggested that neuroimmune interactions are crucial to maintain the intestinal homeostasis and protect the gut from physical and pathogenic insults. However, many studies have explored more in-depth those interactions in a pathological context, and that will be further discussed below (session 1.4).

1.3 The microbiome

1.3.1 Facts and curiosities about the human microbiota

The human body is colonised by a vast number of microbes that generally live in harmony with other tissues, occupying the gut, skin and other mucosal cavities. The collection of microbes in health and disease is called microbiome. In adulthood, the number of bacteria is about ten times greater than the number of cells in the human body, and it encodes at least 100-fold more genes than the ones found in the human cells. It is well-known nowadays that the types and numbers of microbes in the human body vary extensively among different ethnic groups as they are influenced by diet, genetic background, exposure to environmental challenges and lifestyle, as well as pathological conditions. The proximity between these microorganisms and human cells is so tight that they are expected to communicate by exchanging nutrients and metabolic products in both directions.

Sequencing studies have shown that there are about 1.000 bacterial species in the human gut, even suggesting that humans contain two genomes. The gut microbiota is composed of around 1.5 kilograms of bacteria colonising this tissue in a symbiotic manner. However, environmental factors are crucial in establishing and defining the microbiota colonisation of the gut lumen. Emerging evidence has claimed that gut microbiota is essential to human health and may be involved in diseases. Nonetheless, further research unravelling the interactions between this system and host tissues are required to understand the physiological contribution of the gut microbiome to human health as well as its contribution to the progression of diseases (Human Microbiome Project, 2012; Zhao, 2010; Zhu, Wang, & Li, 2010).

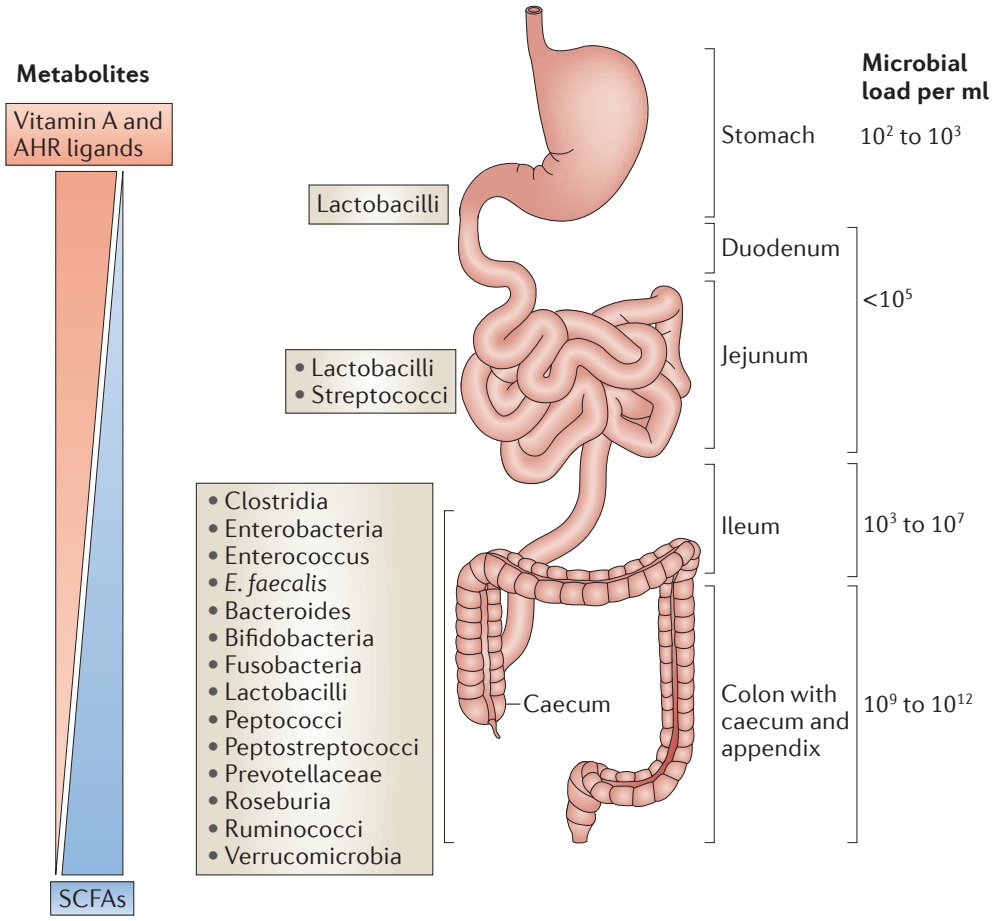


Figure 1.10. The distribution of microbiota along the gastrointestinal tract. Schematic illustrates the regional localisation of different species of bacteria within the gastrointestinal lumen and the estimated total numbers of microbial load per mL of luminal content. The number of species of bacteria increases from oral to anal segments of the GI tract. The composition of bacterial species in different segments of GI is due to the availability of energy sources that are consumed by the microbiota. Microbiota take up energy products to generate metabolites that participate in GI function. AhR, aryl hydrocarbon receptor; SCFAs, short-chain fatty acids; mL, millilitres (Mowat & Agace, 2014) authorised by Springer Nature.

The GI tract contains the highest number of commensal microorganisms in the body. The number of microbes as well as the number of distinct bacterial species usually increases from the oral to the anal parts of the GI tract, going from about 10^2 to 10^3 per mL of luminal content in the stomach and up to 10^{12} per mL in the colon. The gradient of microbiota within the intestinal lumen could be due to the availability of energy sources that are used by those microorganisms to produce metabolites such as vitamins and short-chain fatty acids (SCFAs) provided mainly by food uptake in this part of intestine. The composition and

arrangement of microbiota in different parts of the GI tract as well as their role in the tissue homeostasis is still a challenge to be addressed. However, it is known that the most prevalent phyla groups found in the GI tract are the Firmicutes, Bacteroidetes, Proteobacteria and Actinobacteria. Additional data has reported that due to oxygen availability, aerobic bacteria are more dominant in the upper small intestine whereas anaerobic species are found in the colon. The distribution of environmental factors reflecting changes in microbiota composition within the GI tract could influence immunological activity and function, and be associated with different diseases (**Figure 1.10**) (Costea et al., 2018; Mowat & Agace, 2014).

1.3.2 Microbiota and the gut immune system

Commensal bacteria strongly influence the intestinal immune system. The colonisation of the GI tract by microbiota during early stages of life plays an instrumental part in the development and function of the immune system. Transfer of mammalian maternal microbiota to their progeny begins *in utero* during pregnancy, and it is rapidly increased after birth. Recent studies have implicated the importance of maternal vaginal microbiota for the development of a competent immune system within a critical "window of exposure" of the offspring to maternal microbes. Lack of contact of neonates with vaginal microbiota caused irreversible defects in the development and maturation of immune cells. It has been suggested that children delivered by caesarean section (C-section) have much less microbial diversity which present high risk of developing immune and metabolic disorders (Dominguez-Bello et al., 2016). Labour induces intra-utero concentration of inflammatory cytokines such as IL-1β, IL-6, IL-8 and TNFα that are important for activation of the foetal immune system. The modulation of intra-utero cytokines is absent in case of elective C-section. Development and maturation of Tregs, iNKTcells, T helper cells and DCs are impaired in newborn children delivered by C-section, in addition to an increased humoral immune response and strong production of IgA, IgG and IgM by B cells (Francino, 2018). Moreover, PPs, mesenteric lymph nodes (MLN) and ILFs require signals from intestinal microbiota to adequately differentiate and recruit complement immune cells. Lymphoid tissue inducer (LTi) cells are essential for prenatal organisation of these lymphoid tissues and development of immune responses, and they greatly depend on microbiota to develop (Maynard, Elson, Hatton, & Weaver, 2012).

One of the first sources of antigen-specific immune protection comes from the breast milk that contains many antimicrobial and immunomodulatory products. In mammals, breastfeeding has an immunological benefit including the prevention and protection against infection, development of microbiota and maintenance of intestinal barrier homeostasis in the progeny via the secretory IgA (SIgA) found in breast milk (Rogier et al., 2014). Moreover, breastfed offspring have a more stable and less diverse intestinal microbiota and twice as many bacterial cells than formula-fed infants. Breast milk also appears to modulate the differentiation of B cells, a necessary event for antibody production (Andreas, Kampmann, & Mehring Le-Doare, 2015).

The dynamic and mutual partnership between the microbiota and the immune system is essential for maintaining intestinal homeostasis. When this relationship is perturbed by an imbalanced microbiota or immune response, the outcome is a detrimental dysbiosis or inflammatory conditions that harm GI functions.

Human studies have been supported by experimental work using germ-free (GF) mice, which are devoid of microbial colonisation, showing a late development, decreased diversity and low activity of immune cells. Striking structural changes were also observed in the development of GALTs. For instance, the presence of ILFs is reduced, and PPs and MLN are smaller under GF conditions. Although microbiota can be restored at any stage after birth and many abnormalities corrected by introducing microbes back to the system, the ability to modulate cellular components and their normal activity is restricted to early postnatal life. This suggests that the colonisation of gut microbiota and development of a competent immune system is dependent on a critical window of establishment of those commensal microbes. It has been shown that GF mice exhibited reduced $CD4^+$ and $CD8^+$ T cell subtypes (Th1 and Th2) and $TCR\alpha\beta^+$ intraepithelial lymphocytes. Th17 is absent in GF mice but can be restored after colonisation with SFB or infection with *Citrobacter rodentium*. Also, GF mouse colon contains reduced numbers of Tregs, and that can be restored with conventionalisation of GF mice with intestinal microbes. GF mice present normal B lymphocyte numbers and phenotype. However, the production of IgA and IgG1 is decreased, and IgE increased in these mice. The microbiota also regulates intestinal ILC functions, but their numbers appear to be normal in GF conditions (Gensollen, Iyer, Kasper, & Blumberg, 2016; Rooks & Garrett, 2016).

Furthermore, the microbiota is involved in controlling haematopoiesis and the establishment of the innate immune system. Studies using antibiotics to ablate the GI microbiota showed reduction in frequency and numbers of neutrophils, macrophage colony formation and macrophage progenitors. This could be explained by the fact that antibiotic treatment also reduces levels of IL-17 and granulocyte colony stimulating factor (G-CSF), important factors for the development of myeloid cells. Basophil and monocyte-derived macrophages within the mucosa are also regulated by intestinal microbiota. Additionally, GF mice show a defective innate immune composition (Bain et al., 2014; Belkaid & Harrison, 2017).

Microbe and host immune interactions are essential to the homeostatic modulation and function of immune cells in early-life. Disruption in balance and diversity of gut microbes may result in potential immune abnormalities and susceptibility to diseases. Emerging evidence has suggested that children raised in farm environments have reduced risk of developing allergies. Similar immune protection is observed in the offspring of pregnant mothers exposed to the same environment. These protective microbial/immune mechanisms could be explained by the ability of microbes to prime and generate diversity of immune cells. On the other hand, early exposure to antibiotics potentiates the risk of respiratory infections, eczema and allergies in the childhood, in addition to increased chances for development of celiac disease and inflammatory bowel disease. It has been reported that early exposure to antibiotics also increases the susceptibility of developing other diseases in adulthood such as obesity and type 1 and 2 diabetes *mellitus*. The use of antibiotics to treat bacterial infections is still vital for human health care. However, the risks of its overuse and collateral effects should be taken into consideration. A variety of data indicates that antibiotic exposure disrupts the diversity of microbiota (biodiversity loss) leading to metabolic alterations that directly affect the normal development of the immune system (Blaser, 2016; Gensollen et al., 2016).

The metabolic profile produced by the gut microbiota is extremely rich and diverse, and they can access the subepithelial layer and interact with host cells, influencing the intestinal immune response. The bacterial metabolic repertoire is a product of dietary components that are used as an energy source by the microbiota. Diet is an environmental and life-style related factor that impacts on bacterial composition and therefore the immune system. Primary metabolites generated by the gut microbiota include SCFAs, AhR ligands

and polyamines. It has been shown that GF mice have reduced levels of SCFAs in the intestinal lumen. These intestinal metabolites were reported to be involved in immune modulation, shaping the production and release of cytokines and activating different subsets of immune cells (Geuking, Koller, Rupp, & McCoy, 2014; Rooks & Garrett, 2016).

1.3.3 Microbiota and the ENS

The ENS is immersed in the GI tract and shares the same rich environment with a complex and diverse community of microorganisms and microbial products, which have been described to control host physiology. Given the location of ENS cells and their proximity to intestinal microbiota, it is expected that microbes can influence the ENS development and homeostasis. It has been extensively reported that the intestinal microbiota controls many aspects of the GI physiology such as immunity, production of metabolites and dietary modification, as well as they actively participate in the progression of diseases. The intestinal microbiota is also involved in controlling the gut-brain-axis by modulating vagal afferent sensory neurons that project to the villi (Williams et al., 2016). However, the direct and indirect involvement of microbiota on ENS organisation and homeostasis still remains unclear.

Although GF animal models are not physiological and cannot be translated into human conditions, this mouse model is still a useful tool for investigating the influence of microbiota on host homeostasis, including on the ENS. Research data on GF mice have suggested that the microbiota is essential for the development and maturation of ENS network. Studies using early postnatal GF mice have shown decreased numbers of enteric neurons in the jejunum and ileum and reduction in nerve density, in addition to increased proportions of nitrergic neurons relative to specific pathogen-free (SPF) mice. The defective neuronal network in GF mice led to decreased frequency and amplitude of gut contractility (Collins, Borojevic, Verdu, Huizinga, & Ratcliffe, 2014). These studies suggest the importance of microbiota for ENS maturation even when the diversity of microbes has not yet been established. Furthermore, a recent study has suggested that the colonisation of mucosal EGCs within the villi is concomitant with the maturation of microbiota and happens after weaning under homeostatic conditions. Moreover, GF mouse ileum showed reduced numbers and density of S100β^+ mucosal EGCs relative to conventionally raised controls, but no apparent differences were noticed in the MP and SMP between those groups.

Interestingly, adult colonisation of GF mice with microbiota restored the mucosal EGC network within the villi, suggesting that the development of these cells is dependent on microbiota (Kabouridis et al., 2015). Similar data were found after ablation of microbiota with antibiotics (De Vadder et al., 2018; Kabouridis et al., 2015).

In adult stages, microbiota is involved in modulating the homeostasis of the ENS via 5-HT pathway. De Vadder et al. found that GF mice have reduced intestinal transit and 5-HT levels in the colon, and both phenotypes can be restored after long-term colonisation with bacteria. However, no differences in neuronal numbers were observed in the colon of GF mice, but the ENS network within the villi was reduced, consistent with previously published data (De Vadder et al., 2018). Furthermore, the jejunum of GF mice showed decreased immunoreactivity for calbindin in enteric neurons which was rescued following microbiota colonisation. Excitability of IPAN sensory neurons was also reduced in GF mice, which was corrected after conventionalisation with microbiota (McVey Neufeld, Perez-Burgos, Mao, Bienenstock, & Kunze, 2015). Moreover, the action potential of enteric neurons (McVey Neufeld, Mao, Bienenstock, Foster, & Kunze, 2013) and migrating motor complex (MMC) are decreased in GF mice, followed by a reduced concentration of NPY in rat cecum (Husebye, Hellstrom, Sundler, Chen, & Midtvedt, 2001). The morphology of enteric neurons within the MP in the cecum of GF mice were found to be 3-fold larger compared to the control group (Dupont, Jervis, & Sprinz, 1965). The colonisation of GF animals with human microbiota also improved the total transit time. Additional and complementary experiments showed that diet modifications led to changes in microbiota composition followed by an alteration in GI transit time (Kashyap et al., 2013). Controversially, Lomasney et al. claimed that the secretomotor function of enteric neurons is largely preserved in GF mice after testing the colonic electrical parameters in response to epithelial, neural and bacterial stimulation (Lomasney et al., 2014).

Complementary to studies ablating the intestinal microbiota (GF mice and antibiotic treatment), the use of metabolic and dietary products and probiotic microorganisms have also been applied to analyse the microbiota-ENS interactions. Piglets on a supplemented diet with probiotic yeast *Saccharomyces boulardii* showed decreased number of Calbindin$^+$ neurons in the MP of the jejunum (Kamm, Hoppe, Breves, Schroder, & Schemann, 2004), while those fed with *Pediococcus acidilactici* had increased numbers of Galanin$^+$ and CGRP$^+$ enteric neurons in the SMP of the ileum, followed by an increased EGCs

immunoreactivity for GFAP (di Giancamillo, Vitari, Bosi, Savoini, & Domeneghini, 2010). Intriguingly, the probiotic *Lactobacillus paracasei* attenuated visceral hypersensitivity induced by alterations in the intestinal microflora following the use of antibiotics (Verdu et al., 2006). Likewise, *Lactobacillus acidophilus* inoculation promoted an analgesic effect in colonic hypersensitivity by increasing the levels of cannabinoid and opioid receptors (Rousseaux et al., 2007). Animals fed with *Lactobacillus reuteri* displayed increased excitability in AH neurons while S-type, or motor neurons did not respond to this microbe (Kunze et al., 2009). Dependent on the viability of bacteria strain, mice exposed to *Lactobacillus rhamnosus* exhibited decreased colonic motility. Furthermore, medium from *Bifidobacterium longum* influenced the activity of neurons in the MP of the ileum by reducing sensory nerve activity (Hyland & Cryan, 2016). These data suggest that the ENS network is dynamic and continues to develop after birth, depending on microbiota or their products to further maturate.

Moreover, microbial factors such as butyrate, a SCFA, can modulate EGCs *in vitro* and *in vivo*, by inhibiting EGC proliferation (Cossais et al., 2016), in addition to increasing neuronal excitability (Bertrand, Kunze, Bornstein, Furness, & Smith, 1997) and GI motility (Soret et al., 2010). However, mice fed with resistant starch diet (RSD), which enhances the concentration of SCFA in the intestinal lumen, showed a selective increase in the proportion of colonic excitatory cholinergic neurons but resulted in decreased intestinal transit time. Administration of butyrate showed a similar effect (Moreau et al., 2004). One of the causes of gut dysbiosis is the consumption of high-fat diet (HFD) which alters bacterial metabolites. It has been shown that HFD causes intestinal dysmotility by inducing loss of nitrergic myenteric neurons and consequent constipation. Depletion of TLR4 (*Tlr4*$^{-/-}$) prevented neuronal damage, suggesting that this receptor might mediate the survival and function of enteric neurons (Reichardt et al., 2017). G-protein-coupled bile acid receptor 1 (TGR5) is highly expressed in enteric neurons. *Tgr5*$^{-/-}$ mice exhibited slower colonic transit time and reduced defecation frequency compared to wildtype controls. Moreover, TGR5 stimulation with agonists enhanced colonic motility in wildtype mice, but not in *Tgr5*$^{-/-}$ (Poole et al., 2010).

Components derived from intestinal microbes are in part sensed by pattern recognition receptors (PRRs) expressed by host cells, such as immune, epithelial and ENS cells. Toll-like receptors (TLRs) are one of PRR subgroups and have been involved in

maintaining symbiotic homeostasis between the intestinal microbiota and host cells. Enteric neurons and glial cells have been reported to express TLR3 and TLR7 that recognise viral RNA, and TLR2, TLR4 and TLR9, which recognise bacterial products, suggesting that the ENS has the potential to directly respond to inputs derived from the gut microbiota (Hyland & Cryan, 2016; Kabouridis & Pachnis, 2015; Obata & Pachnis, 2016). Studies using *Tlr4*$^{-/-}$ mice have shown abnormal intestinal motility and reduced number of inhibitory nNOS^{+} neurons in the ileum. Furthermore, the same study demonstrated that GF and antibiotic-treated mice exhibited a similar phenotype to that reported in mice lacking TLR4. To support these experiments, MyD88, a molecule essential for TLR signalling was specifically deleted from Wnt1 expressing ENS cells (Wnt1Cre$^{+/-}$/Myd88$^{fl/fl}$), and the same phenotype was observed thereby suggesting the importance of ENS-microbiota communication in maintaining ENS physiology and survival (Anitha, Vijay-Kumar, Sitaraman, Gewirtz, & Srinivasan, 2012). Another separate report demonstrated that deletion of TLR2, expressed in enteric neurons and EGCs, also resulted in fewer neuronal numbers, a decreased nitrergic neuronal subset, and alterations in cholinergic fibres in the myenteric ganglia. This phenotype was characterised further by intestinal dysmotility and reduced chloride secretion by ileal explants. The EGC markers GFAP and S100β, as well as the levels of GDNF were also diminished within the MP of *Tlr2*$^{-/-}$ mice. However, it is not evident whether the mutation affected the numbers of EGCs or the levels of protein expression in these cells. In this study, exogenous addition of GDNF surprisingly restored many ENS alterations both in the *Tlr2*$^{-/-}$ and antibiotic-treated mice, suggesting that the physiology and organisation of the ENS are potentially driven by microbiota/TLR2 production of neurotrophic factors (Brun et al., 2013). Moreover, TLR9 is expressed by enteric neurons but not EGCs. Stimulation of TLR9 with ligands induced cytokine production by enteric neurons, suggesting that these cells can participate in the gut defence against pathogens (Burgueno et al., 2016).

The influence of microbiota on homeostasis and function of the ENS in maintaining intestinal health was previously appreciated above. However, a recent study has proposed that the ENS can also modulate the intestinal microbiota. Studies in the zebrafish gut showed that the depletion of the allele t3 in the *Sox10* gene (*sox10*^{t3}) caused a complete ablation of the ENS, leading to dysbiosis and intense intestinal inflammation. The intestinal pathology was corrected by restoring anti-inflammatory bacterial lineages or transplanting wildtype ENS progenitors back to the gut (Rolig et al., 2017).

1.4 Environmental changes that affect the ENS

It is evident that microbiota, immune and nervous systems of the gut work in cooperation in order to maintain the GI physiology. It is also expected that together these systems encounter many challenges that disturb the integrity of their natural environment. It is believed that these systems work alongside in many pathological conditions, either to control the spreading of diseases or to promote its progression. Some aspects of those communications in a pathological context will be highlighted below.

1.4.1 Inflammatory bowel disease

Inflammatory bowel disease (IBD) is the term referring to a chronic intestinal pathology causing inflammation in the GI tract. IBD includes two main conditions: ulcerative colitis (UC) and Crohn's disease (CD). Patients with IBD experience functional GI disorders including diarrhoea, abdominal pain, bloating and bleeding. Moreover, IBD has a remarkable impact on patients' quality of life as they are often dealing with symptoms and relapsing clinical care (de Souza & Fiocchi, 2016). The incidence of IBD is increasing worldwide, and it is estimated that around 2.5-3.0 million people have IBD in Europe (Kaplan, 2015). It is still unclear what drives the pathogenesis of IBD, however, in addition to immunological and genetic conditions, the progression of IBD has been recently linked to environmental exposures in industrialised societies. Lifestyle, stress, diet and smoking habits all seem to influence the pathogenesis of this disease (Allendoerfer et al., 1994).

IBD is characterised by marked immune cell infiltration and the activation of pathways that modulate epithelial cell turnover leading to permeability changes and disruption of intestinal barriers. Alterations in epithelial barrier contribute to the pathogenesis of IBD, and this can also initiate immune responses. IBD is also related to intestinal dysbiosis and immunological imbalance mainly associated with the adaptive immune system. Other factors that enhance the pathogenesis of IBD are the unbalanced levels of Th1 and Th2 cytokines in the gut mucosa, secretion of TNFα, TGFβ and IFNγ and response to self-antigens (de Mattos et al., 2015). In addition to immunological alterations, it has been reported that IBD induces structural changes in the ENS (Geboes & Collins, 1998).

CD primarily manifests in the terminal ileum, but it can also affect any other regions of the GI tract and can spread transmurally. Increased levels of cytokine release such as IL-

12, IL-17, TNFα and IFNγ have been implicated in the progression of this disease (de Mattos et al., 2015). In paediatric patients with CD submucosal neurons exhibit increased immunoreactivity for VIP and decreased expression of nNos whereas, in the MP, the proportion of $nNos^+$ neurons was reported to be augmented. No differences in the number of VIP^+ neurons were observed in the MP, as well as the total number of neurons (HuC/D) in both plexuses were similar in the **colon** (Boyer, Sidpra, Jevon, Buchan, & Jacobson, 2007). In the **ileum** of patients with CD, however, there was an increased immunoreactivity for many subtypes of enteric neurons within the MP, such as TH, 5-HT, NPY, NF, VIP, nNOS and pituitary adenylate cyclase-activating polypeptide (PACAP) (Belai, Boulos, Robson, & Burnstock, 1997). Likewise, no neuronal loss (neuron-specific enolase – NSE^+) was detected in non-inflamed intestinal biopsies from CD patients, although the proportion of VIP^+ neurons and colocalization of $nNOS^+/ChAT^+$ neurons increased in these patients, followed by an increase in CGRP fibre thickness (J. Schneider et al., 2001). Due to the degree of intestinal damage followed by the impact in the lifestyle of patients and high recurrence of CD, new methods to diagnose this pathology early have been evaluated to prevent its further progression. Based on this, scientists have raised the possibility of investigating the role of the ENS on the pathogenesis of CD by analysing the submucosal and myenteric plexitis that happens prior clinical symptoms. It has been suggested that these lesions in the ENS precede severe mucosal inflammation after surgery, making the ENS a potential system to early diagnose the progression of CD (Ferrante et al., 2006; Sokol et al., 2009).

UC is characterised by intensive superficial ulcerations. Different from CD, ulcerative colitis manifests only in the mucosal layer of the colon. It has been suggested that IL-13 is the main cytokine involved in the progression of this disease, but other cytokines also play a role in UC pathogenesis (de Mattos et al., 2015). Patients with UC showed increased numbers of SP^+ neurons in the MP with no differences in total numbers of NSE^+ neurons (Neunlist et al., 2003; Villanacci et al., 2008). Samples from patients with IBD also showed increased SP^+ and $TRPv1^+$ and decreased SOM^+ neuronal fibres surrounding the intestinal vasculature (de Fontgalland, Brookes, Gibbins, Sia, & Wattchow, 2014). Besides, the levels of mucosal iNos and nNOS were respectively up- and down-regulated in patients with inflamed and non-inflamed UC, suggesting that perhaps, these molecules could predict the course of the disease (Menchen et al., 2004). Increased production of mucosal iNos was

reported to be partially mediated by EGC-derived S100B (Cirillo et al., 2009). Moreover, S100β⁺ EGC numbers are significantly increased in the MP of patients with UC, but not in the SMP (Villanacci et al., 2008), followed by increased gene and protein expressions and release of S100B in these patients (Cirillo, Sarnelli, Esposito, et al., 2011). In patients with UC, EGCs produce low levels of 15-HETE, which controls the permeability of the intestinal epithelial cells, suggesting the potential role of EGCs in participating of the stability of mucosal barrier (Pochard et al., 2016). These data together suggest that EGCs have a critical role in controlling the progression of pathogenesis in human UC.

Human studies highlighting the effect of IBD on the ENS are still scarce, and answers regarding how the ENS respond to inflammation are limited. One of the reasons for this is the accessibility of human samples in addition to the invasiveness of procedures. Animal models to mimic those diseases have been generated in order to facilitate the access and the understanding of molecular mechanisms that drive the progression of diseases. Among others, some models that were suggested to affect the ENS will be further discussed below (session 1.4.1.2).

1.4.1.1 Genotypic and phenotypic aspects of IBD

In humans, IBD comprises a heterogeneous group of patients that can display a variable course of pathology. A range of challenges such as immunological status, genetic alterations, microbiological and environmental factors could have a significant impact on the development and progression of IBD. Recently, genome-wide association studies have been employed in an effort to understand the genetic influence on the progression of IBD. Although the majority of identified susceptibility genes in IBD control responses to host-immune-microbes interactions (T. C. Liu & Stappenbeck, 2016), the molecular mechanisms that correlate the involvement of genetic mutations together with environmental factors on the progression of IBD remain still unclear. Further, GWAS studies have suggested that hundreds of different mutations could contribute to the susceptibility for the development of both CD and UC demonstrating the complexity of this disease. For instance, it has been reported that mutations in the *NOD2* gene (also known as *CARD15*), localised on chromosome 16, increases the susceptibility for the development and progression of IBD. It has been shown that patients carrying at least one mutation in variants of *NOD2* had an aggressive clinical course and need for surgery. *NOD2* encodes the NOD2 protein that is

involved in recognition of bacteria and activation of immune cells, suggesting that perhaps, mutations in variants of this gene could implicate in altered immune responses to bacterial infections (Annese et al., 2005; Norouzinia, Chaleshi, Alizadeh, & Zali, 2017). Other mutations in genes such as *PRDM1*, which is involved in the regulation of T and B cells differentiation, *NDP52* related to selective autophagy of intracellular bacteria and signalling molecules, *IL-10* and *IL-23* receptor genes that also participate in immune responses were reported to be implicated in the susceptibility to IBD (Norouzinia et al., 2017).

Nonetheless, studies are still scarce in relating specific mutations and environmental factors to the variability in the phenotype of human IBD. One of the reasons is the complexity in measuring the level of exposure of individuals to external factors. Another reason is that some patients are ineligible to participate in study cases due to their comorbidities and use of medications. However, it is well-recognised that malnutrition and obesity have important roles in the susceptibility and progression of IBD, together with smoking habits and lifestyle (Bhat et al., 2009; Moran, Sheehan, & Shanahan, 2016).

Although most of these risk loci have been linked to host-microbe-immune dysfunction, the participation of the ENS in the pathogenesis of IBD cannot be excluded. For instance, our lab has recently discovered that Ser26.tdT^{+} EGCs also express certain IBD susceptibility genes, such as *nod2* and *Il10rb* (Fränze Progatzky, unpublished observation), suggesting a possible involvement of this cell type.

1.4.1.2 Mouse models for experimental colitis

Trinitrobenzene sulfonic acid (TNBS) is a common and widely used chemical to induce colitis, which models CD-like inflammation. Inflammation induced by TNBS includes loss of body weight, intestinal damage and intensive infiltration of immune cells within the mucosa that can be extended transmurally (Dou et al., 2018). In guinea pig, TNBS induced neuronal cell loss in the MP which persisted for 56 days after treatment, followed by increased infiltration of neutrophils in the region. The observed neuronal loss was not associated with a reduction of any specific neuronal subtype; however, the proportion of VIP^{+} neurons was increased in this study (Linden et al., 2005). Decreased protein and transcript levels of the neuronal markers ChAT, nNOS and PGP9.5, were also observed in TNBS colitis (Winston, Li, & Sarna, 2013). At the peak of inflammation and mucosal damage, TNBS induced different responses dependent on neuronal physiology, by altering

excitability and synaptic transmission in the MP and causing damage in neuronal processes projecting to the ileal mucosa (Linden, Sharkey, & Mawe, 2003; Nurgali, Nguyen, Thacker, Pontell, & Furness, 2009; Nurgali et al., 2011). Moreover, it has been recently shown that vasopressin via the vasopressin receptor V_{1a} expressed in enteric neurons, evokes prostaglandin release from mast cells that are in close contact to cholinergic neuronal fibres in the intestinal mucosa (Dou et al., 2018). TNBS-induced colitis promoted upregulation of transglutaminase by enteric neurons, followed by increased neuronal activity in the MP. Transglutaminase are involved in several neuronal processes including neuronal survival. *In vitro* experiments showed that the induction of transglutaminase led to a significant increase of neuronal apoptosis (Sarnelli et al., 2009).

Mesenchymal stem cells (MSCs) have been used as a new therapeutic possibility to attenuate symptoms of neurodegenerative diseases by controlling inflammation and exhibiting anti-inflammatory, immunomodulatory and neuroprotective properties. Treatment with human MSCs in mice with TNBS-induced colitis reduced the numbers of immune cell infiltration, diminished damage in neuronal processes in the colon (Tuj1), prevented neuronal loss in the MP, changes in neuronal subtypes (nNos and ChAT) (Robinson et al., 2017; Stavely et al., 2015b) and increased $CGRP^+$ neurons (Stavely et al., 2015b). Similar results were observed using guinea pig MSCs transplantation. TGFβ1 produced by gpMSCs was found to be the main factor to regulate and attenuate the neuropathy caused by inflammation (Stavely et al., 2015a).

Dinitrobenzene sulfonic acid (DNBS) is also a well-established model to study CD for sharing the same features as the human disease. The induction of colitis with DNBS promoted significant and rapid neuronal (HuC/D) loss in the MP of mice (Boyer et al., 2005; Sanovic, Lamb, & Blennerhassett, 1999) analysed by the expression of poly (ADP-ribose) polymerase (PARP), resulting in increased colonic propulsive function. However, no changes in neuronal density (PGP9.5) were observed (Boyer et al., 2005). Eosinophils were found within the MP, and extensive infiltration of neutrophils in the muscle layers was observed (Sanovic et al., 1999). Neuronal cell death and inflammatory immune response were partially attenuated after treatment with anti-neutrophil serum, suggesting the potential modulatory role of neutrophil in neuronal survival and function (Boyer et al., 2005). Neurons express Neurokinin 2 receptors (NK2Rs) that are involved in the progression of inflammation. It has been recently shown that antagonising NK2Rs in DNBS model

prevented intestinal dysmotility, neuronal loss and reactive gliosis by restoring the levels of GFAP in EGCs during colitis (Delvalle, Dharshika, et al., 2018). Moreover, increased levels of NO produced during inflammation induced by DNBS triggered EGC to release ATP through connexin-43, driving neuronal death. Inhibition of connexin-43 in glial cells resulted in neuroprotection and prevented intestinal inflammation (I. A. Brown, McClain, Watson, Patel, & Gulbransen, 2016).

The oral administration of dextran sodium sulfate (DSS) mimics several aspects of UC. DSS-colitis mice showed a significant neuronal loss, followed by substantial increase in colonic transit time. Administration of GDNF by adenovirus partially prevented the loss of enteric neurons and rescued the intestinal transit somewhat, followed by decreased infiltration of leukocytes and reduction in levels of TNFα and IL-1β. These data suggest a potential participation of EGC-derived molecules in constraining inflammation caused by DSS and modulating immune response (G. X. Liu et al., 2014). Moreover, DSS promoted loss of cholinergic regulation of epithelial secretion via muscarinic receptors, accompanied by increased expression of nicotinic receptors in enteric neurons, resulting in release of nitric oxide (Green, Ho, Sharkey, & McKay, 2004). DSS also induced the expression of ChAT (Green et al., 2004; Winston et al., 2013) and PGP9.5, but no changes were observed in levels of nNOS in myenteric neurons (Winston et al., 2013). Furthermore, infiltration of IgA-producing lymphocytes was observed close to VIP^+ neuronal fibres that had less density within the colonic mucosa after the administration of DSS, in parallel with the progression of the intestinal inflammation (Ueno, Hisajima, Nakano, Goris, & Funakoshi, 2011).

Also, *in vitro* studies showed that the supernatant from individuals with IBD altered the levels of VIP in the ENS, mediated by IL-6 (Soufflet et al., 2018).

1.4.2 Neuroimmune interactions in a parasitic environment

It has been hypothesised that regulatory immune responses and activation of the ENS have fundamental importance in eradicating parasite infection, limiting tissue damage and restoring gut homeostasis. Parasitic infections change ENS homeostasis either by modifying the distribution of neuronal fibres, by altering neurotransmission and by consequence, disturbing GI functions. However, the mechanisms by which immune cells work alongside the ENS to control infection and expel parasites remain unclear.

Several studies have described the consequences of *cryptosporidium* infection in the GI function. Cryptosporidiosis causes neutrophil influx and induces prostacyclin (PGI_2) within the mucosa, and that is controlled by VIPergic and cholinergic neurons. NK1 receptor and SP levels are also increased during this infection. SP stimulates pro-inflammatory cytokines such as IFN-γ, IL-1β and TNFα, suggesting that neurons can prime immunological responses against parasitic invasion. Moreover, in a giardiasis model, nNOS and 5-HT appear to participate in the elimination of *Giardia* by modulating intestinal motility (Halliez & Buret, 2015).

It has been shown that *Nippostrongylus brasiliensis* infection induces Th2 responses by increasing levels of IL-4 and IL-13. The IL-13 response has been suggested to be triggered by neuronal stimulation via ACh and SP transmission (Halliez & Buret, 2015). Another recently described mechanism of Th2 response against this worm was reported to involve ILC2 activation, eosinophil recruitment via neuronal secretion of NMU. Both mechanisms were suggested to contribute to the nematode expulsion (Halliez & Buret, 2015; Klose et al., 2017). Enteric neurons participate in the gut contractility by regulating protease-activated receptor 2 (PAR2) in immune cells after nematode infection (Shea-Donohue et al., 2010).

During *Trichinella spiralis* infection there is an increase in SP levels that is associated with impaired lymphocyte response. The ablation of high levels of SP significantly prevented the intestine from initiating pathological processes associated with this nematode, suggesting that SP is a critical neuroimmune mediator of GI inflammation. ENS-derived motility is changed after *T. spiralis*-infection consistent to neuronal ACh imbalance. Moreover, MMs and EGCs also increase the production of pro-inflammatory cytokines that can directly regulate neurotransmitter release by enteric neurons affecting gut motility. In a mast cell-deficient mouse model, however, both SP and ACh levels are normal, suggesting that mast cells could be involved in neuronal neurotransmission remodelling in this model (Leng et al., 2010). At a late stage, after worm infection with *Trichinella spiralis,* there is still low-grade inflammation in the intestines that causes alterations in neuro-epithelial barrier and disturbance in GI functions. Studies to support this have shown an accumulation of mast cells in the gut tissue, increased mucosal permeability and ion secretion, in addition to a reduced response to 5-HT and IgE. It has been suggested that Substance P and capsaicin are involved in late neuronal response to parasitic infection after

neuronal blockade with TTX (Fernandez-Blanco, Barbosa, Sanchez de Medina, Martinez, & Vergara, 2011; Halliez & Buret, 2015).

Schistosoma infections change gut motility via ACh, 5-HT and SP pathways. This can be due to a significant accumulation of mast cells and eosinophils (responding to SP and VIP) at the level of the MP or within the mucosa. Increased numbers of mast cells within the villi can be correlated to an up-regulation of CGRP in neuronal fibres in this area. Purinergic receptors present in immune cells can modulate ACh release by enteric neurons. Mast cells at the site of inflammation modulate purinergic ligands (ATP/ADP) that can act in positive feedback degranulating these cells. Excessive exposure to purines during inflammation caused by the loss of immunomodulation can be harmful to enteric neurons (Halliez & Buret, 2015).

Further, infection with *Trypanosoma cruzi* causes autoimmune response and neuronal damage by an excessive production of antibodies that binds to neuronal fibres. It has been reported that T cells preferentially target myelin basic protein in neurons leading to damage in the GI function (Oliveira et al., 2009). A recent study has shown that neuronal damage could also be associated with increased immune reactivity to tryptase in mast cells. Tryptase$^+$ mast cells were found close to neuronal fibres within the mucosa of patients with chagasic megacolon (Martins et al., 2018). EGC numbers are also decreased in patients infected with *T. cruzi*. ACh was the only neurotransmitter reported to be affected in this disease (Halliez & Buret, 2015).

Studies also reported that infection with *Toxoplasma gondii* changed the numbers and morphology of nitrergic, VIPergic and serotoninergic enteric neurons in the small intestine and colon associated to an increased number of mast cells (D. M. Sant'Ana et al., 2012; D. M. G. Sant'Ana et al., 2017; Vicentino-Vieira et al., 2017).

In summary, parasite infections in the GI tract trigger a cascade of neuroimmunomodulatory events that includes the release of neuropeptides and cytokines by immune and neural cells within the gut wall. That includes activation/inhibition of different immune cell types and ENS morphological and physiological damage with severe consequences to the GI function and tissue repair. In this context, neurotransmitters such as ACh, SP, 5-HT and VIP participate in the regulation of gut motility after parasite exposure, and myeloid and EGCs appear to initiate pro-inflammatory responses.

1.5 Models for experimental research

Scientific research moves forward when the experimental hypothesis and data can be verified. The use of animal models for research has an essential impact in avoiding false interpretation and misleading concepts, by providing accurate collection and representation of data that can be reproducible. It is well-established that the choice of species used in experimental research has to be primarily determined by the nature of each experiment, suitability for questions to be addressed in a particular type of research, and available facilities.

The use of animal models has different advantages and disadvantages for biomedical research. Distinct models such as simple organisms including yeast, fruit flies, *C. elegans* have been useful tools in underlying mechanisms implicated in the development of a system because they normally have a short lifespan, they are easier to manipulate and cost less to maintain, although sharing many genes with other more complex mammals. However, their small level of complexity when compared with other models hampers the understanding of more elaborated physiological and non-physiological events related to human biology. As an alternative, mice are still the most widely used animal model for understanding human biology, especially for drug targeting in many human diseases as they play an essential role in preclinical trials. One of the reasons is because mice and humans are biologically very similar, qualifying this model for scientists to study the physiology of a system assembling information regarding how a specific system grows, develops diseases and ages. Mice also have a shorter lifespan when compared to humans, making it possible to understand the development and progression of diseases and processes of ageing. Moreover, mice are relatively small and breed well, and are reasonably economical to maintain. Most importantly, by using molecular tools, scientists can manipulate the mouse genome to mimic most of human conditions and diseases.

Mouse lines can be studied in research by using inbred strains and outbred stocks. Inbred mouse strains have undergone more than 20 generations of mating between brother and sister, with all individuals having at least 98.6% genetic similarities with parents. They are genetically stable, providing more accurate and repeatable experiments, and are widely used in toxicological research. Additionally, they and are the first choice in science as they provide a stable genetic background for the generation of mutants and genetically altered mice. The key advantages of inbred strains are their isogenicity, homozygosity, phenotypic

uniformity, long-term stability, identifiability and individuality (Beck et al., 2000; Festing, 2010). Nevertheless, quiet mutations may appear over time slightly changing the phenotypic characteristics of inbred strains (Stevens, Banks, Festing, & Fisher, 2007). The drawback of using inbred strains is that it is unclear whether the experimental data will be extrapolated to other mouse strains or humans, but it increases the chances of reproducing the data. On the other hand, in order to specifically test genetic diversity, some experiments require the use of outbred stocks, in which each animal in the colony will be genetically different with the degree of genetic variation depending on the history of the colony. Most scientists claim that outbred mice should not be considered for research as no individuals are genetically alike and external factors could disguise the actual data acquired. However, it has been recently suggested that inbred strains and outbred stocks can be phenotypically very similar depending on the experimental approach of choice (Jensen, Porsgaard, Lykkesfeldt, & Hvid, 2016; Tuttle, Philip, Chesler, & Mogil, 2018).

As previously mentioned in this section, many experimental models can be used. Alternative studies can be done by using zebrafish models, which minimises the debate in using inbred and outbred mouse models, since all strains are markedly genetically different. This genetic diversity needs to be taken into consideration when designing experimental plans (Guryev et al., 2006). The zebrafish model represents a powerful resource in science as they are genetically similar to humans, easier to house and breed than rodents, and are amenable to genetic modification and drug studies. Additionally, many human diseases can be investigated by using zebrafish models, such as diabetes, obesity, metabolic diseases, atherosclerosis, intestinal inflammation among others (Seth, Stemple, & Barroso, 2013).

Although they have been widely used in research to predict and investigate human development and disease, animal models are not an alternative to replace human trials, but when appropriately used for research, they are an elegant complementary strategy, together with computational science, tissue studies and *in vitro* systems. Distinct methods, complementary cross-species analysis approaches can provide insightful and compelling results to build our knowledge and understanding of the mechanisms that underlie human health and disease, in addition to testing novel drug therapies.

1.6 Cell fate restriction and cell plasticity

The challenge in developmental biology is to understand how a particular cell develops and gives rise to a specified cell type. Cell fate is determined by the expression of a complex set of intrinsic molecular markers, and is influenced of neighbouring cells and environmental factors, which over time and space work combinatorically to specify a determined cell type. Recently, significant progress has been achieved by the generation and implementation of cell fate mapping tools combined with high-throughput sequencing technologies to label and unveil the molecular state of cells, for example, ENS cells (Lasrado et al., 2017; Memic et al., 2018).

Based on molecular identity, morphology, spatial location and function it has been determined in enteric neuroscience that cells from the mature ENS derive from a common group of NCCs that enter the foregut and give rise to mature EGCs and neurons. Undifferentiated NCCs highly express molecular markers such as Sox10, p75, Ret and Phox2b that later on are differentially expressed in mature EGCs and neurons (Hao et al., 2016; Lasrado et al., 2017; Young et al., 2003). For instance, during mouse development EGCs downregulate Ret and Phox2b, but maintain the expression of factors that are expressed in ENCCs such as Sox10, p75, Sox2 and FoxD3, and acquire the expression of well-known differentiated glial cell markers such as GFAP and S100β (Mundell et al., 2012; Young et al., 2003). These cells upregulate EGC markers and downregulate neuronal markers behind the migratory wavefront of NCCs (Young et al., 2003), suggesting that these expression changes may be associated with changes to the local environment of these NCC derivatives. Enteric neurons, in contrast, maintain the expression of Ret and Phox2b, upregulate other pan-neuronal markers such as HuC/D, and then subtype-specific markers such as ChAT, nNOS, VIP, CGRP, 5-HT, Calretinin and Calbindin from E10 onwards (Hao et al., 2016; Young et al., 2003). These established neural markers characterise the identity of these neurons, which like EGCs have distinct phenotypes and physiological roles. However, very little is known about the factors influencing EGC and ENS neuron cell fate choices or how ENS cells in the adult gut respond to environmental cues changing their cellular fate. This will be further discussed below.

In contrast to the ENS, the development and establishment of immune cells is rapid and continuous, taking place during gestation and also in postnatal life. Immune cells develop from pluripotent hematopoietic stem cells in the foetal liver, spleen and thymus

(early during gestation) and bone marrow (later in gestation and postnatally) and generate lymphoid (adaptive immune system) and myeloid (innate immune system) progenitor cells, that later will give rise to many different subsets of immune cells based on the milieu of cytokines and differentiation factors they are exposed to, as well as master key transcription factors (for the development of adaptive immune cells see section 1.2.1) (Landreth, 2002). Using advanced technologies, the transcriptional profile of many subsets of immune cells has been well characterised bringing new insights into the plasticity of their cellular states and identities.

Cell plasticity defines the capacity of some cells to acquire the molecular phenotype and functional features of other cells in an organism, outside their natural repertoire of differentiation. Mechanisms that underlie cell plasticity guarantee cell heterogeneity in a determined system. For instance, key cytokines orchestrate the differentiation of naïve $CD4^+$ T cells into different Th cell subsets with different functions to quickly adapt to alterations in their microenvironment and surrounding molecular signals in order to provide immunity. For instance, it has been shown that inflammatory conditions *in vivo* shape the fate of Th17 cells. In experimental autoimmune encephalomyelitis, Th17 cells produce high levels of IFNγ and do not express the IL-17A protein, thus acquiring a similar phenotype to Th1 cells. However, in the case of acute infection with *Candida albicans*, the expression of IL-17A is downregulated with no production IFNγ by Th17 cells (Hirota et al., 2011). Th17 cells can also acquire a T_{FH} phenotype in PPs by inducing the development of Ig-A-producing B cells and experiments using mice lacking Th17 cells showed an impaired production of IgA in this lymphoid tissue (Bluestone, Mackay, O'Shea, & Stockinger, 2009; Hirota et al., 2013; Saravia, Chapman, & Chi, 2019). Together, these data suggest that T cells can be plastic. However, it is not clear whether a given subtype of T cells can acquire phenotypes of any and every other T cell subset *in vivo*. Similarly, innate immune cells such as macrophages and neutrophils can acquire different phenotypes and adapt to environmental cues. Researchers have been trying to identify and characterise macrophages by their functional profile, by which M1 macrophages have inflammatory functions, and M2 macrophages are essential for maintaining tissue integrity (Mills, Kincaid, Alt, Heilman, & Hill, 2000). However, this paradigm of polarisation of macrophages has been questioned as M1 macrophages can be activated and adopt an M2-like phenotype, and vice versa. Similarly, by using flow cytometry assay to isolate cells from the intestine of *Cx3cr1*$^{GFP/+}$ reporter

mouse line, stained for macrophage lineage markers, and by using transcriptional profile tools, Gabanyi and colleagues showed that LpMs preferentially display a pro-inflammatory phenotype while MMs express a tissue-protective gene profile at steady state conditions (Gabanyi et al., 2016). Altogether, these data suggest plasticity of immune cells by adapting and responding to environmental challenges.

Likewise, the ENS is also exposed to a volatile array of challenges that could drive the plasticity and activation of EGCs and neurons. However, our knowledge regarding the adult ENS is still very limited as the field lacks molecular markers that could identify the state of activation of these cells. In steady state conditions, enteric neuroscience research has yet not succeeded in showing how enteric neurons, for instance, could change their molecular fate and acquire different phenotypes. It is clear, however, that they can respond to stimuli by altering the motor activity in the intestinal wall (De Schepper et al., 2018; Muller et al., 2014; Rao et al., 2017). Adult EGCs, are very diverse in their molecular profile and present four distinct subtypes according to their morphology. It is so far unclear whether different morphologies reflect the state and function of these cells, as they seem to equally express all molecular markers that are currently available to identify these cells. However, GFAP was reported to preferentially label type I intraganglionic EGCs, although it is also expressed by a small group of other EGC subtypes. (Boesmans et al., 2015). Reactive gliosis is a hallmark of activation of several glial cell types in different pathologies, and it is characterised by upregulation of GFAP (Sofroniew, 2009). Increased GFAP expression has been demonstrated in many pathologies that affect the ENS, including in patients with IBD (Cornet et al., 2001; Devos et al., 2013; Semar et al., 2013). Although the expression of GFAP could suggest a certain degree of EGC plasticity or a mere fluctuation of this protein in response to environmental changes, direct evidence of a regulation of glial markers conferring them distinct phenotypes at the level of single cell analysis in the adult ENS is not yet available. Besides, a certain degree of EGC plasticity has been suggested by using experimental injury models, which have demonstrated that EGCs undergo neurogenesis (Belkind-Gerson et al., 2017; Laranjeira et al., 2011). However, the rates of enteric neurogenesis in the adult gut are remarkably low, and the ability of all subtypes of EGCs to give rise to neurons remains elusive. Further progress in unravelling the potential plasticity of ENS cells is expected in the near future with the implementation of single-cell fate mapping combined with high-throughput sequencing technologies.

1.7 Aims of the work performed in this thesis

The ENS, the main focus of this thesis, is comprised of a specialised network of enteric neurons and glial cells that are essential for the function of the GI tract. Novel insight emerging from the transcriptional profile and dynamics of the organisation of enteric neuroglia networks have shed new light on the developmental principles that control the assembly of the ENS. However, the elucidation of physiological aspects of the mature ENS lags behind, mainly due to the complexity and heterogeneity of enteric neural and glial networks, the paucity of tools to unravel the properties of the constituent lineages and the complexity of tissue circuitry the ENS is part of.

The overall aim of this thesis is to investigate the effect of the gut tissue and luminal environment on the homeostasis and function of the ENS in adult mice.

Towards this goal we have three specific aims:

1) The development of new methodology that can interrogate at high resolution the properties of enteric neurons and glial cells.
2) The evaluation of the impact of experimental changes in the intestinal tissue and luminal environment on the organisation and physiology of the ENS.
3) The characterisation of the effects of adaptive immune system deficits on the organisation, molecular properties and function of the ENS.

Chapter 2

Materials and Methods

2. Materials and Methods

2.1 Materials

2.1.1 Reagents

All reagents used in this thesis are highlighted within the experimental sections described below with their respective catalogue numbers and companies.

2.1.2 Solutions

Some solutions used in this project were prepared at the Francis Crick Institute following well stablished protocols using reagents from Sigma or Thermo Fisher Scientific. Others were acquired in ready-to-use formats from research companies. Solutions used in specific experiments are described in their respective sections in methods.

Common solutions used in different experiments:

PBS – phosphate buffered saline, pH 7.4, 137 mM NaCl (Sigma, S7653), 3 mM KCl (Sigma, P9333), 8 mM Na_2HPO_4 (Sigma, 255793-50G), 1.5 mM KH_2PO_4 (Sigma, NIST200B) in dH_2O

PFA – paraformaldehyde (PFA, Sigma, P6148), 4% in PBS

PBT – 0.3%, 0.5% or 1% TritonX-100 (Sigma, X100) in PBS

2.2 Methods

2.2.1 Animals

All animal procedures were approved and held under the Animals Act 1986 (Scientific Procedures) by the UK Home Office project license and The Francis Crick Institute Animal Ethics Committee. Animals were appropriately housed and maintained on a 12/12 hours light/dark cycle at ambient temperature (22ºC-24ºC). Standard food and water were provided *ad libitum*. All mice used in this thesis were sacrificed by a Schedule One method before dissections.

2.2.1.1 Mouse lines

Specific Pathogen Free (SPF) breeding units (The Francis Crick Institute) generated and provided C57BL/6Jax, *Rag1*$^{-/-}$ (B6/JRag1KO-MOM) (Mombaerts, Iacomini, et al.,

1992), *Rag2*$^{-/-}$ (B6.CD45.1-Rag2KO) (Shinkai et al., 1992), *Tcr*$\alpha^{-/-}$ (TCRalphaKO.B6) (Mombaerts, Clarke, et al., 1992) and *B6.muMT*$^{-/-}$ (N15) (Kitamura, Roes, Kuhn, & Rajewsky, 1991) mice. TNF$^{\Delta ARE/+}$ mutant mice were kindly provided by Professor George Kollias at the Fleming Institute (Athens) and bred at The Francis Crick Institute animal facility (Kontoyiannis, Pasparakis, Pizarro, Cominelli, & Kollias, 1999). The Quadram Institute (Norwich) provided SPF and GF mice (C57Bl/6 raised in GF isolators) that were tested and found negative for both aerobic and anaerobic bacteria as well as fungi. *Il17*α*.Cre:R26R*^{eYFP} (Hirota et al., 2011) and *Foxp3.mRFP* (Wan & Flavell, 2005) mice were kindly provided by Brigitta Stockinger (The Francis Crick Institute). *Tg(Csf1r-iCre)1Jwp* mice (Deng et al., 2010) were imported and bred with the *Rosa26-lsltdTomato* line to generate the *Csf1r.iCre;R26tdT* mouse line maintained at The Francis Crick Institute. The *Sox10::CreER*^{T2} tamoxifen inducible mouse line (*Ser26*) was generated in our lab (Laranjeira et al., 2011) and crossed with *Rosa26R-CAG-tdTomato* (The Jackson Laboratory) to generate *Ser26.tdT* heterozygotes **(Table 2.1)**. Male mice aged between 8-14 weeks were preferentially used for experiments. Experimental genotypes were determined by Transnetyx using real-time Polymerase Chain Reaction (PCR).

Table 2.1 Mouse lines used in this thesis

Name of strain	Gene names	Phenotype	Source	Reference
C57Bl/6	-	-	Breeding Units at The Francis Crick Institute	-
SPF	-	-	Quadram Institute (Norwich)	-
Germ Free	-	Absence of microbiota	Quadram Institute (Norwich)	-
Mutant mice				
Rag1$^{-/-}$	*recombinantion activating gene 1/Rag1*	Lack of T and B lymphocytes	Breeding Units at The Francis Crick Institute	Mombaerts et al., 1992
Rag2$^{-/-}$	*recombinantion activating gene 2/Rag2*	Lack of T and B lymphocytes	Breeding Units at The Francis Crick Institute	Shinkai et al., 1992
Tcra$^{-/-}$	*T cell receptor alpha/Tcra*	Lack of T lymphocytes	Breeding Units at The Francis Crick Institute	Mombaerts et al., 1992
muMT$^{-/-}$	*immunoglobulin heavy chain 6/IgM/mu*	Lack of B lymphocytes	Breeding Units at The Francis Crick Institute	Kitamura et al., 1991
TNF$^{\Delta ARE/+}$	*tnf delta ARE element*	Overexpression of TNF	Vassilis Pachnis Lab, The Francis Crick Institute	Kontoyiannis et al., 1999
Transgenic mice				
Il17a.Cre:R26R^{eYFP} *(Il17a.eYFP)*	*Interleukin 17a*	Labels cells that once expressed Il17a, such as Th17 lymphocytes	Gitta Stockinger Lab, The Francis Crick Institute	Hirota et al., 2011
Foxp3.mRFP	*Forkhead box P3*	Labels regulatory T cells	Gitta Stockinger Lab, The Francis Crick Institute	Wan & Flavell, 2005
Csf1r.iCre;R26tdT (Csf1r.tdT)	*Colony stimulating factor receptor 1/Csf1r*	Labels macrophages	Vassilis Pachnis Lab, The Francis Crick Institute	Deng et al., 2010
Sox10::CreER^{T2}*;R26R-CAG-td*^{Tomato} *(Ser26.tdT)*	*SRY-related HMG-box 10/Sox10*	Labels EGCs	Vassilis Pachnis Lab, The Francis Crick Institute	Laranjeira et al., 2011

Constructs used for generating previously published transgenic reagents

***Rag1*$^{-/-}$** - A 1356 bp genomic fragment of the Rag1 gene, encoding the nuclear localization signal and the zinc-finger motif in the 5'end of the coding sequence of RAG-l, was replaced by a neomycin cassette by homologous recombination, resulting in a null mutation (Mombaerts, Iacomini, et al., 1992).

Rag2$^{-/-}$ - A 0.85 kb fragment of the Rag2 gene open reading frame from 4.0 kb Rag2 genomic DNAλ phage clone was replaced with a neomycin resistance cassette eliminating the region encoding of 286 of the 527 amino acids of the protein. This large deletion results in a null mutation (Shinkai et al., 1992).

Tcrα$^{-/-}$ - The insertion of the transposon Tn5 neomycin selection cassette disrupted the coding potential of the first Cα exon (CI) element of the Tcrα gene, resulting in a null mutation (Mombaerts, Clarke, et al., 1992).

muMT$^{-/-}$ - A 9 kb of genomic DNA spanning exons 1 and 2 of *μM* and the first three exons of the constant (C) region of the δ gene encoding immunoglobulin heavy chain of the class mu (IgM) were disrupted by a neomycin resistance cassette, causing a null mutation (Kitamura et al., 1991).

TNF$^{\Delta ARE/+}$ - A 69 bp fragment of the AU-rich elements (ARE) were deleted by homologous recombination of a floxed neo cassette, and subsequent *in vitro* Cre mediated excision. The resultant allele contained a single loxP site in place of the ARE sequence, resulting in a null mutation. ELISA of mutant mice showed high levels of protein compared to wild-type mice, indicating a suppressive role of the AREs in controlling TNF expression (Kontoyiannis et al., 2002).

Il17a.eYFP – Knock-in, a targeting vector underwent homologous recombination in R1 cells so that the codon-improved Cre recombinase sequence was expressed by the Il17a locus. Point mutations were introduced into exon 2 of the Il17a gene to modify internal ATG-site. A neo resistance cassette was excised by FLPe-mediated recombination to generated the final allele. R26R^{eYFP}, a construct containing a floxed PGK-neo cassette and an enhanced yellow fluorescent protein (EYFP) gene was inserted into the Gt(ROSA)26Sor locus via homologous recombination. The floxed neo cassette contains a strong tpA stop sequence which prevents the transcription of EYFP (Hirota et al., 2011).

Foxp3.mRFP – Targeted Reporter, knock-in of a bicistronic fluorescent reporter into the endogenous Foxp3 locus (Wan & Flavell, 2005).

Csf1r.tdT - Transgenic construct for *Tg(Csf1r-iCre)jwp*, the improved Cre (iCre) sequence was inserted into ApaI and NotI sites using blunt-ended ligation downstream from the colony-stimulating factor-1 receptor promoter (Deng et al., 2010).

Ser26.tdT – The coding sequence of Sox10 in a phage artificial chromosome (PAC; RP21-529-16) was replaced with a Cre/ERT2 cassette by homologous recombination in bacteria.

The targeting vector also contained an Frt-flanked chloramphenicol resistance gene, which was removed by transient activation of Flp in bacteria. A construct was generated that encodes tamoxifen-inducible Cre under control of the Sox10 regulatory sequences. These animals were crossed to Rosa-CAG-LSL-tdTomato-WPRE targeting vector was designed with (from 5' to 3') a CMV-IE enhancer/chicken beta-actin/rabbit beta-globin hybrid promoter (CAG), an FRT site, a loxP-flanked STOP cassette, tdTomato sequence, a woodchuck hepatitis virus post-transcriptional regulatory element (WPRE), a polyA signal, and an attB/attP-flanked PGK-FRT-Neo-polyA cassette. The construct was inserted between exons 1 and 2 of the Gt(ROSA)26Ser locus (Laranjeira et al., 2011).

2.2.1.2 Tamoxifen injections

Tamoxifen (TMX) (Sigma, T5648) was used to induce Cre recombination in the *Ser26.tdT* adult mouse line. Stock concentrations of TMX (10 mg/mL) were prepared from powdered stock, dissolved in 9 parts of corn oil (Sigma, C8267) and 1 part of ~99% ethanol. TMX solution was covered in foil, stored at 4°C and used within two weeks. Adult *Ser26.tdT* mice were given intraperitoneal injections of 0.1 mg/g TMX per body weight one day before they were humanely sacrificed for subsequent tissue harvesting.

2.2.2 Tissue manipulation techniques

2.2.2.1 Whole-mount gut preparation

Whole-mount gut preparations were used for immunostaining to visualise the entire ENS structure and surrounding tissues. We opted for using this technique in several experiments, as tissue manipulation is minimal; isolation is fast and integrity of intestinal architecture well preserved. Another practicability of using whole-mount intestinal preparations is the prospect of imaging intestinal layers from the same area of the gut, for instance, visualisation of the ENS network from serosal to mucosal layers. This technique is useful to visualise the MP, SMP and the ENS network within the mucosal layer after immunohistochemistry or genetic labelling of ENS cells. For this, small and large intestines were isolated and washed with ice-cold PBS. Intestinal small segments of around 2 cm long were dissected to remove adipose tissues and opened at the mesenteric border. Tissues were then stretched and pinned flat (0.2 mm insect pins – Agar Scientific, L4494) onto Sylgard 184 Elastomer (Dow Corning, Sylgard 184) coated dishes and fixed overnight (O/N) in 4% PFA at 4ºC on a shaker.

2.2.2.2 Dissection of the adult longitudinal muscle myenteric plexus (LMMP)

Adult prewashed portions of small and large intestines (2 cm long) were collected, cleared of adipose tissues and then placed and stretched over a 1 mL serological pipette. A longitudinal incision was gently made on the external muscle layer, and a cotton swab immersed in PBS was used to dissect the adherent outer layer containing the myenteric plexus. Once dissected, muscle strips with the MP attached were either processed for RNA isolation or/and stretched and pinned flat (0.2 mm insect pins) onto Sylgard 184 Elastomer coated dishes and fixed for 2 hours in 4% PFA at 4ºC on a shaker. After fixation, LMMPs were washed in PBS (3 times at Room Temperature - RT) and used for immunohistochemistry. The dissection of LMMPs allows the collection of sufficient material that can be efficiently used for transcriptional analysis of ENS markers by quantitative PCR. Additionally, this technique enables a more precise visualisation of ENS network within this layer. However, information about the ENS network found within other layers is missing when this dissection method for immunostaining is used.

2.2.2.3 Gut sections

Intestine segments were collected, washed in PBS and fixed O/N in 4% PFA at 4ºC. In the following day, tissues were processed either for cryo-, gelatin- or paraffin-sectioning.

For cryo-sectioning: samples were exposed to a gradient of sucrose solution (VWR, 27480.294) of 10%, 15% until tissues settle down, followed by 30% O/N. Samples were next embedded in OCT (Tissue-Tek 25608-930), snap-frozen in liquid nitrogen and transversally sectioned at 14 µm thick slices using a Microm HM 560 CryoStar cryostat (Thermo Scientific). Sections were then collected and mounted onto SuperFrost Plus glass microscope slides (J1800AMNT, Thermo Scientific) and stored at -80ºC until used for immunostaining.

For paraffin-sectioning: after fixation, samples were kept O/N in 70% ethanol and submitted to the Histology Facility at The Francis Crick Institute for processing and staining. 5 µm thick transversal sections were collected onto glass microscope slides and used for H&E staining.

For vibratome-sectioning: samples were embedded in 3% agarose-PBS (Roche, 11388991001) and cross-sectioned at 200 µm thick floating slices in PBS using a Leica vibratome. Tissue sections were collected in sequence in 24-well plates containing PBS and

immediately used for immunohistochemistry or stored in PBS with 0.01% sodium azide at 4^0C for up to a month.

2.2.3 Primary EGC cultures of dissociated adult LMMPs

Dissection Medium - Dulbecco's Modified Eagle's Medium (DMEM/F12, Thermo Scientific 11320033) containing 12.5 mM HEPES (Thermo Scientific 15630080), 2% fetal bovine serum (FBS, HyClone SH30070.030E), 1% penicillin/streptomycin (P/S, Life Technologies, 15140-122).

Digestion Medium - Dissection media containing 0.5 mg/mL collagenase I (Wako, 9001-12-1) and 0.5 mg/mL DNAse I (Grade II; Roche, 10104159001).

FBS Medium – DMEM/F12 containing, 10% FBS, 1% P/S (Life technologies, 25030- 024).

G5 Medium - DMEM/F12 containing 1% P/S, 1% N2 (Thermo Scientific, 17502048), 1% G5 (Thermo Scientific, 17503012) and nerve growth factor-7s (NGF 50 ng/mL, Thermo Scientific, 13257019).

The protocol for EGCs isolation and culture was adapted from (Boesmans et al., 2015). *Ser26.tdT* mice were used for EGC culture experiments since the vast majority of EGCs within the intestinal tissue can be labelled with the fluorescent reporter tdTomato (Laranjeira et al., 2011). Mice were injected with TMX to induce activation of the fluorescent reporter in EGCs at least 24 hours prior to performing experiments (section 2.2.1.2). The small intestine of *Ser26.tdT* mice older than 8 weeks of age was collected and washed in ice-cold PBS to remove luminal contents. To maintain high viability of isolated EGCs, the following dissections were done on ice. Mesentery and adipose tissues were removed from the full extension of the intestine, which was cut into 2 cm long pieces and placed in a new plate with ice-cold **dissection medium**. LMMPs were gently isolated following the protocol for dissection of LMMPs (section 2.2.2.2). Next, in the tissue culture hood, LMMPs were washed three times in sterile **dissection medium**, transferred into 50 mL conical tube (Nunc™ 339652) containing 15 mL **digestion medium** and incubated for 35 minutes at 37ºC on a shaker (200 rpm). After incubation, tissue suspensions were mechanically triturated 60x using a glass pasteur pipette, and 15 mL of sterile **digestion**

medium was added into the tube containing EGCs. The suspension was then centrifuged at 500 g for 5 minutes at 4ºC, washed with **dissection medium** and once again centrifuged. Cells were then plated onto 6 cm diameter dishes coated with fibronectin (Sigma, F1141) in DMEM/F12 containing, 10% FBS, 1% P/S O/N and kept in an incubator at 37ºC continuously supplied with 5% CO_2. The following day, media was carefully removed with any remaining floating tissue, and replaced with new media according to the experimental condition desired, in this case G5 or FBS-containing media. At day *in vitro* 3 (DIV3), half of the media was replaced with respective fresh media. At DIV4, cells were passaged, filtered using 40 μm (Corning®, CLS431750-50EA) to remove remaining tissue clumps and plated onto 8-well Lab-Tek permanox chamber (Thermo Fisher Scientific, 177445) slides pre-coated with fibronectin. At DIV6, cells were fixed with 4% PFA for 10 minutes at 4ºC and processed for immunocytochemistry.

2.2.4 Adeno-associated virus (AAV) and labelling of enteric neurons

Dr Yuuki Obata generated the AAV9-CaMKII-eGFP-KASH/tdT (AAV9.KASHeGFP/tdT) to transduce the expression of fluorescence reporters on the outer nuclear membrane of enteric neurons *(Obata et al., in preparation)*. Briefly, adeno-associated viral vectors encoding enhanced GFP (eGFP) or tdTomato (tdT) reporter proteins driven by the CaMKII promoter were packaged into AAV9 serotype. Virus was packaged by transfection of 293AAV cells with three plasmids containing pAAV-CaMKII-eGFP-KASH/tdT, pFdelta6 (Adenovirus-helper plasmid) and the capsid plasmid (including the AAV9 Rep and Cap sequences). Vectors were purified using AAVpro® Purification Kit (All Serotypes, TAKARA) and purity of viral particles assessed by SDS-PAGE. Large-scale production of AAV particles were performed by AAV packaging service of the Penn Vector Core (University of Pennsylvania, USA). Other AAVs used in this study, such as AAV9-CaMKII-Cre and AAV9-CAG-eGFP were purchased from Penn Vector Core (University of Pennsylvania, USA) or Cyagen Biosciences Inc (CA, USA).

AAV particles were diluted with 5% sucrose in H_2O. Volume of injection was adjusted to 150 μL of solution containing AAV per animal. AAV9.KASHeGFP/tdT was intravenously injected in the tail vein of 6 weeks old C57Bl/6, *Rag2*$^{-/-}$ or *Tcrα*$^{-/-}$ mice (chapter 5). AAV9-CaMKII-Cre was injected in the tail vein of *Rosa26.tdT* mice to label the majority of neuronal cell bodies and processes (chapter 3). Intestinal tissues were collected 4 weeks after the injection with AAV for immunohistochemistry or nuclei RNA-sequencing

(nRNAseq). The concentration of viral particles was determined based on ddPCR-GC titre (>2.5e14 GC/mL for labelling of most enteric neurons).

2.2.5 Flow cytometry and fluorescence activated cell sorting (FACS)

All samples were processed for flow cytometry on a BD™ LSRII Fortessa machine (BD Biosciences) and analysed using FlowJo 10.5.0 Java Version: 1.8.0_151-b12 software (© FlowJo). Cell suspensions were sorted using FACS on a FACS Aria (BD Biosciences) machine. Table 2.2 shows the list of fluorophore-conjugated antibodies used in the experiments described below.

Table 2.2 Antibodies used for flow cytometry and FACS experiments

Antibody	Clonality	Conjugate	Cat number	Host	Supplier	Concentration
CD19	6D5	Alexa Fluor 647	115522	Rat	BioLegend	0.5 mg/ml
CD19	6D5	Alexa Fluor 488	115521	Rat	BioLegend	0.5 mg/ml
CD19	6D5	PE-Cy7	115520	Rat	BioLegend	0.2 mg/ml
CD25	PC61	Alexa Fluor 488	102017	Rat	BioLegend	0.5 mg/ml
CD3ε	17A2	PerCP-Cy5.5	100218	Rat	BioLegend	0.2 mg/ml
CD3ε	17A2	APC-Cy7	100222	Rat	BioLegend	0.2 mg/ml
CD4	RM4-5	APC	100516	Rat	BioLegend	0.2 mg/ml
CD4	GK1.5	FITC	100406	Rat	BioLegend	0.5 mg/ml
CD45	Monoclonal (Clone 30-F11)	Alexa Fluor 700	103128	Rat	BioLegend	0.2 mg/ml
CD45	30-F11	PE	103106	Rat	BioLegend	0.2 mg/ml
Foxp3	FJK-16s	APC	17-5773-80	Rat	Life Technologies	0.2 mg/ml
RORγt	Clone Q31-378	BV421	562894	Mouse	BD Bioscience	0.2 mg/ml
TCRβ	H57-597	PerCP/Cy5.5	109228	Armenian Hamster	BioLegend	0.2 mg/ml
Viability						
Zombie Aqua™ Fixable Viability Kit	-	-	423101	-	BioLegend	1:200

20EH buffer - 20 mM EDTA, 12.5 mM HEPES, 1% P/S, and 1 mM DTT (Promega, P1171) pH 7.4 in HBSS (Thermo Scientific, 14170088).

2R buffer - Collagenase (0.5 mg/mL, Wako 9001-12-1) and 0.5 mg/mL DNase I (Grade II; Roche, 10104159001) in 2% FBS (HyClone SH30070.030E), 12.5 mM HEPES in RPMI 1640 (Thermo Scientific, 11875093).

Washing buffer - 2% FBS in PBS.

Cell washes - In this case, cell wash stands for centrifugation of cell suspensions at 1800 rpm for 5 minutes at 4°C in washing buffer (2% FBS in PBS).

2.2.5.1 Immunoprofiling of LMMPs and mucosal layer

We developed in our lab a protocol to analyse and characterise immune cells from the mucosal and muscle layers. To separate the mucosa from longitudinal muscle layer, segments of both small and large intestines were dissected following the protocol described in section 2.2.2.2. In the small intestine, the mucosal layer was first incubated in **20EH buffer** (described above) for 30 minutes on ice to remove epithelial cells. Next, the remaining attached epithelial cells were removed using a dissection blade. LMMPs and mucosal layers from both small intestine and colon were mechanically triturated and incubated in **2R buffer** containing collagenase (described above) for 30 minutes on a shaker at 37ºC. Cell suspensions both from mucosal and muscle layers were washed (washing buffer) and filtered using 100 µm cell strainers (Corning®, CLS431752-50EA) into a 50 mL conical tube. Then, samples were centrifuged (1800 rpm at 4°C for 10 minutes) and incubated with cell membrane fluorophore-conjugated antibodies for 30 minutes. After incubation with cell membrane antibodies, cell suspensions were washed in PBS, followed by incubation with cell viability markers **(Table 2.2)** for 40 minutes. Of note, at this step only it is essential to use a serum-free buffer for washing cell membrane antibodies prior incubation with viability markers, since serum binds these markers impairing the efficiency of staining. Next, cells were then fixed for 1 hour (Thermo Scientific, 00-5523-00) and incubated with intracellular antibodies for 30 minutes when necessary. Cells were washed twice in washing buffer, filtered into a conical bottom polystyrene tube with a cell strainer cap (BD, 352235) and processed for flow cytometry analysis. Single colour staining was used for setting FACS gates and compensation parameters.

2.2.5.2 Isolation of lymphocytes from spleen and MLNs

For isolation of lymphocyte populations within lymphoid tissues, spleen and MLNs were dissected and any remaining adipose tissues removed. Next, tissues were injected with a solution containing collagenase (2R buffer) and incubated for 30 minutes at 37ºC. After collagenase incubation, tissues were homogenised and filtered using a 100 μm cell strainer into a 50 mL conical tube in washing buffer. Samples were then centrifuged at 1800 rpm for 10 minutes at 4ºC. To remove red blood cells from our samples, we incubated splenic cell suspensions with ACK lysing buffer (Thermo Scientific, A1049201) for 3 minutes at RT, followed by a wash in PBS. Next, splenic and MLN suspensions were incubated with cell membrane fluorophore-conjugated antibodies for 30 minutes. Samples were then washed in PBS and incubated with cell viability markers for 40 minutes.

For flow cytometry: after incubation with viability markers, cell suspensions were fixed for 1 hour, incubated with intracellular antibodies, washed twice in washing buffer, and processed for flow cytometry analysis.

For adoptive transfer (rescue experiments section 5.3.5): after incubation with viability markers, cells were washed filtered and submitted for FACS analysis (section 2.2.5.3).

2.2.5.3 Adoptive transfer of lymphocytes (rescue experiments section 5.3.5)

Lymphocytes from spleen and MLNs of 8 C57Bl/6 mice were isolated as previously described in section 2.2.5.2. Cell suspensions were stained with the viability dye Zombie Aqua to exclude dead cells; CD45 Alexa Fluor 700 to detect the total immune cell population; CD3 PerCP-Cy5.5 to identify the total population of T lymphocytes; CD4 APC to detect naïve T cells and CD25 Alexa Fluor 488 to detect Tregs. Cell suspensions were gated on singlet $CD3^+CD45^+$ living lymphocytes and separated into $CD25^+CD4^+$ Tregs and $CD25^-CD4^+$ naïve T cells. 3 x 10^6 $CD25^+CD4^+$ Tregs and $CD25^-CD4^+$ naïve T cells were sorted from MLN and spleen into 15 mL tubes containing 5 mL FBS. Cell suspensions were centrifuged at 1800 rpm for 10 minutes at 4ºC, resuspended in sterile saline solution, and 6 x 10^5 $CD25^+CD4^+$ Tregs or 6 x 10^5 $CD25^-CD4^+$ naïve T cells were intravenously injected into $Tcr\alpha^{-/-}$ mice (5 mice/group). Recipient mice were analysed 10 weeks after the transfer together with C57Bl/6 and $Tcr\alpha^{-/-}$ controls. The efficiency of adoptive transfer was

confirmed by the identification of lymphocytes within the MLNs and spleens isolated from individual mice from each group and analysed by flow cytometry (section 2.2.5.2).

For the adoptive transfer experiments into *Rag2*$^{-/-}$ mice: 8 C57Bl/6 donor mice were used in this experiment. T and B lymphocytes isolation from spleen and MLNs was performed as described in section 2.2.5.2. Cell suspensions were stained for L/D Zombie Aqua to exclude dead cells; CD45 PE was used to detect the total immune cell population; TCRβ PerCP-Cy5.5 to identify the total population of T lymphocytes; CD19 Alexa Fluor 647 to identify B lymphocytes. Total of 5.6 x 10^6 and 4 x 10^6 T and B cells, respectively were sorted from C57Bl/6 donors into 15 mL tubes containing 5 mL FBS. Cell suspensions were centrifuged at 1800 rpm for 10 minutes at 4ºC, resuspended in sterile saline solution and 7 x 10^5 $CD45^+TCR\beta^+CD19^-$live T lymphocytes and 5 x 10^5 $CD45^+TCR\beta^-CD19^+$live B lymphocytes cells were injected into *Rag2*$^{-/-}$ mice. Mice were collected 9 weeks post-transfer, and the efficiency of adoptive transfer was confirmed by the identification of lymphocytes within the MLNs and spleens isolated from individual mice from each group and analysed by flow cytometry (section 2.2.5.2).

2.2.5.4 Adoptive transfer of $CD4^+CD45RB^{high}$ T lymphocytes (chronic colitis model section 4.3.4)

The isolation of $CD4^+CD45RB^{high}$ naïve T lymphocytes from the spleen of C57Bl/6 donor mice, transfer of cells into 3 *Rag2*$^{-/-}$ recipient mice and monitoring of these animals after transfer were carried out by Dr Mark Wilson at the NIMR Institute, who kindly provided these animals along with 3 *Rag2*$^{-/-}$ mice used as controls for our experiments. Animals were collected for immunohistochemistry when the colitis group had reached 20% body loss from their original body weight and presented signs of diarrhoea.

2.2.5.5 Neuronal nuclei isolation from the MP

NIM2 buffer - 1.5 M sucrose, 1 M KCl, 1 M Tris buffer - pH 8.0, nuclease-free water (Thermo Scientific, 4387936), 1 mM DTT, 50x protease inhibitor (Roche, protease inhibitor cocktail - #11697498001) and DAPI (1:1000, Thermo Scientific D1306).

The protocol for isolation of enteric neuronal nuclei was adapted from a method of single-nuclei isolation of neurons from post-mortem brain tissues (Krishnaswami et al., 2016). For labelling of the outer membrane of enteric neuronal nuclei, 6 weeks old C57Bl/6

and *Tcrα*$^{-/-}$ male mice were systemically injected with AAV9.KASHeGFP (section 2.2.4). Four weeks after injection, small or large intestines were collected, and LMMPs dissected as described in section 2.2.2.2. Next, LMMPs were transferred into a 1.5 mL plastic tube and mechanically triturated using fine scissors. Tissues were then transferred into a homogeniser (Pestle and Mortar, Scientific Laboratory Supplies, HOM3512/HOM3532) containing a small volume of NIM2 buffer and further gently triturated. Samples were next filtered using a 100 μm cell strainer into a 50 mL plastic conical tube. Remaining tissues retained in the cell strainer were transferred into a 1.5 mL plastic tube and further macerated using a plastic pestle (Sigma, Z359947 – 100EA). Cell suspensions from the 1.5 mL tube were transferred into the 50 mL with remaining cell suspension and centrifuged at 4ºC for 8 min at 1000 g. The precipitate was then resuspended in NIM2 and submitted for nuclei sorting by FACS.

The gating strategy for neuronal nuclei isolation by FACS is based on the integrity of nuclei analysed by DAPI staining. Singlet DAPI^{+} nuclei selected in cell suspensions from C57Bl/6 and *Tcrα*$^{-/-}$ mice were then separated into eGFP^{+} and eGFP^{-} populations and sorted into 1.5 mL plastic tubes containing TRIzol™ LS (Invitrogen, 10296028) for the isolation of intact nuclear RNA for RNA sequencing (nRNAseq).

Of note, the numbers of nuclei isolated per mice vary from 15-50K eGFP^{+} nuclei (observed in n>5 experiments) associated with the efficiency of transduction, length of the gut, nuclei isolation technique and gating strategy. Generally, at least about 15,000 intact nuclei should be isolated from the adult small intestine and colon when using this strategy. AAV9-KASH-tdT viruses were also used for pilot experiments, and the FACS profile of neuronal nuclei was similar to the eGFP mice.

2.2.6 Immunofluorescence assays

Immunofluorescent assays were performed on whole-gut (section 2.2.2.1), whole-LMMP preparations (section 2.2.2.2), transverse cryo- and vibratome sections (section 2.2.2.3) as well as in cultures of dissociated EGCs (section 2.2.3).

For whole-mount gut staining and vibratome sections: after fixation, about 1-2 cm pieces of intestines or floating gut sections were transferred into a 48-well plate and washed 3x with 1% PBT (PBS + Triton X-100, Sigma X100). All incubation and wash steps were performed on a shaker at RT. Next, samples were permeabilised with 1% PBT for 1 hour. Non-specific binding sites were then blocked by exposing tissues to 10% normal donkey

serum (NDS, Jacksons ImmunoResearch Laboratories 017-000-121) diluted in 1% PBT for 1 hour. Samples were next incubated with primary antibodies diluted in the blocking buffer **(Table 2.3)** for 1 or 2 O/N (to detect cytoskeleton or nuclei proteins, respectively). After incubation with primary antibodies, samples were then washed in 1% PBT (3x, 1 hour each) and incubated with appropriate fluorophore-conjugated secondary antibodies **(Table 2.4)** containing DAPI (1:1000, Thermo Scientific D1306) O/N. Finally, to reduce background staining, tissues were extensively washed in 1% PBT (at least 3x, 2 hours each) and flat-mounted onto glass slides using Vectashield™ Mounting Medium with or without DAPI (Vector Labs, H-1200/H-1000).

For whole-mount LMMP preparations: all procedures for immunostaining on LMMPs were similar to the one described above, apart from incubation times: permeabilisation, 30 minutes; blocking, same as above; primary antibodies, O/N; secondary antibodies, 2 hours; and washes, 3x of 30 minutes/each.

For cryo-sections: glass slides with 14 μm gut sections attached were placed in a container with PBS for 20 minutes to remove any remaining OCT. After that, sections were permeabilised with 0.5% PBT for 10 minutes at RT followed by incubation with a blocking buffer (10% NDS in 0.5% PBT) for 1 hour at RT in a humidified chamber. After that, sections were incubated with primary antibodies diluted in blocking buffer O/N at RT. Next, samples were washed in PBT (3x, 30 minutes) and incubated with secondary antibodies for 1 hour at RT. Samples were then washed in PBT (3x, 2 hours at RT) and mounted using Vectashield™ Mounting Medium.

For cell culture: same protocol as described above for cryosections, except for the concentration of PBT (0.3%) and incubation times: permeabilisation, 20 minutes; blocking, 1 hour; primary antibodies, 1 O/N at 4ºC; secondary antibodies, 1 hour at RT.

In the case of Ki67-antigen detection, the immunofluorescence protocol on LMMPs was followed by antigen retrieval treatment before incubation with the Ki67 antibody. For this, LMMPs were placed into 1.5 mL plastic tubes containing sodium citrate buffer (10 mM, Sigma W302600) and kept on a shaker at RT for 5 minutes. Following, plastic tubes were placed in a water bath set at 80ºC for 10 minutes in citrate buffer. Next, plastic tubes containing LMMPs were exposed to the same buffer at RT for 20 minutes. Finally, LMMPs were washed in 1% PBT, incubated with blocking solution and the general protocol was again followed as described above.

Table 2.3 Table of primary antibodies used in this study

Antigen	Expected target	Host	Company and Catalogue number	Dilution
BrdU [CloneBU 1/75(ICR1)]	Proliferating Cells	Rat	AbDSerotec, OBT0030CX	1:1000
c-KIT	ICCs	Goat	R&D systems, AF1356	1:250
Calbindin	IPAN neurons	Rabbit	Chemicon, AB1778	1:500
Calretinin	Excitatory neurons	Goat	Swant, CG1	1:500
CD3-ε	T cells	Armenian Hamster	Santa Cruz, sc-18871	1:200
CD4	T cells mainly	Rat	BD Biosciences, 550280	1:200
ChAT	Sensorimotor neurons	Goat	Millipore (Chemicon), AB144P	1:100
FoxD3	EGCs	Rabbit	Labosky lab	1:500
GFAP	EGCs	Chick	Abcam, AB4674	1:500
GFP	-	Rat	Nacalai Tesque (Gentaur), 04404-84	1:500
HuC/D	Pan neuronal	Mouse	Molecular Probes, A-21271	1:400
IBA1	Macrophages	Goat	Abcam, AB5076	1:500
Ki67	Proliferating Cells	Mouse	BD Biosciences, 550609	1:200
mCherry	-	Goat	SICGEN (2BScientific), AB0040-200	1:400
nNOS	Inhibitory neurons	Rabbit	Santa Cruz, sc-1025	1:500
NPY	Inhibitory/secretomotor/ vasodilator neurons	Rabbit	Peninsula Laboratories, T-4070	1:100
PGP9.5	Pan neuronal	Rabbit	Biogenesis, 7863-0504	1:500
S100β	EGCs	Rabbit	DAKO, z-0311	1:500
SMA Clone MY-32	Myofibroblasts	Mouse	Sigma, M4276	1:200
Sox10	EGCs	Goat	Insight Biotechnology (Santa Cruz), sc-17342	1:400
Sox2	EGCs	Goat	Immune Systems (ISL), GT15098	1:200
TCRβ	T cells	Armenian Hamster	BioLegend, 109228	1:200
TNFR1	TNF receptor I	Goat	Santa Cruz, sc-1069	1:100
Tuj1	Pan neuronal	Mouse	Biolegend (previously Covance), MMS-435P (801201)	1:500
VIP	Inhibitory/secretomotor/ vasodilator neurons	Rabbit	Immunostar, 20077	1:500

Table 2.4 Table of secondary antibodies used in this study

Host	Primary specificity	Fluorophore	Company and Catalogue number	Dilution
Donkey	anti-Chick	Alexa Fluor 488	Jackson ImmunoResearch, 703-545-155	1:500
Donkey	anti-Goat	Alexa Fluor 647	Life Technologies, Invitrogen, Molecular Probes, A21447	1:500
Donkey	anti-Goat	Alexa Fluor 488	Life Technologies, Invitrogen, Molecular Probes, A11055	1:500
Donkey	anti-Goat	Alexa Fluor 568	Life Technologies, Invitrogen, Molecular Probes, A11057	1:500
Donkey	anti-Mouse	Alexa Fluor 488	Life Technologies, Invitrogen, Molecular Probes, A21202	1:500
Donkey	anti-Mouse	Alexa Fluor 568	Life Technologies, Invitrogen, Molecular Probes, A10037	1:500
Donkey	anti-Mouse	Alexa Fluor 647	Life Technologies, Invitrogen, Molecular Probes, A31571	1:500
Goat	anti-Mouse IgG1	Alexa Fluor 647	Life Technologies, Invitrogen, Molecular Probes, A21240	1:500
Donkey	anti-Rabbit	Alexa Fluor 647	Jackson ImmunoResearch, 711-606-152	1:500
Donkey	anti-Rabbit	Alexa Fluor 488	Life Technologies, Invitrogen, Molecular Probes, A21206	1:500
Donkey	anti-Rabbit	Alexa Fluor 568	Life Technologies, Invitrogen, Molecular Probes, A10042	1:500
Donkey	anti-Rat	Alexa Fluor 488	Life Technologies, Invitrogen, Molecular Probes, A21208	1:500

2.2.7 DiI labelling of neuronal network

DiI neurotracer labelling of enteric network was performed as previously described (Sasselli et al., 2013). LMMPs were dissected from the colon of C57Bl/6, *Rag2*$^{-/-}$ and *Tcrα*$^{-/-}$ adult mice (section 2.2.2.2), about 2 cm pieces of tissues were stretched flat onto Sylgard-coated plates using 0.2 mm insect pins by pinning the edges of each LMMP onto the dish and fixed in 4% PFA in 0.1% EDTA/PBS for 2 hours at 4°C on a shaker. Next, one additional pin which was dipped into DiI tissue labelling paste (Molecular Probes, N 22883) was placed in the middle part of the total length of the isolated LMMP. Finally, tissues were covered in 4% PFA/0.1% EDTA/PBS and incubated in a 37°C oven for 14 days. LMMPs labelled with neuronal tracer DiI were monitored every other day and an extra 4% PFA/0.1% EDTA/PBS solution added into the plates when required. At the end of incubation period, LMMPs were washed in PBS, mounted onto glass slides and examined using a confocal microscope.

2.2.8 Histology

H&E staining was performed on 5 μm paraffin-embedded intestinal sections (section 2.2.2.3) by the Histology Facility at the Francis Crick Institute.

2.2.9 Microscopy and image processing

Bright field images of intestinal cross-sections stained with H&E (section 2.2.8) were acquired with a colour camera (Prog Res C14) in a bright field Zeiss epifluorescence Axioplan microscope using the OpenLab software (PerkinElmer). Images and routine following up of EGC cultures were performed using a Nikon Eclipse TS100 microscope. All confocal images were acquired using either the Leica microscope fitted with multiphoton spectra physics (SP5) Mai Tai Ti:Sapphire Deep Sea Laser system with a DM6000 microscope or upright Olympus Confocal Laser Scanning Microscope FV3000. Leica confocal was run by the Leica Application Suite Advanced Fluorescence (LAS AF) software. Olympus confocal was run by the FV31S-SW software. Images were taken with 2x, 4x, 10x, 20x and 40x dry or 20x and 40x oil objectives. All images were processed using Fiji ImageJ (2.0.0-rc-68/1.52h) and Adobe Photoshop (CC 2015.5). Brightness and contrast were finely adjusted when required to improve the clarity of images. The same adjustments were applied to all images for experiments requiring a direct comparison between experimental groups. Adobe Photoshop was used to compose final figures.

2.2.10 Images analysis and quantification

Cells were manually quantified using the Cell Counter plugin in Fiji ImageJ software. The presence of a determined marker in a DAPI expressing cell was counted in single z-stacks per acquired image. At least 8 random images were acquired per tissue and a minimum of 3 mice were used per experimental group analysed. Tissues were collected and images acquired from the approximate matching area of the gut from each experimental group.

2.2.11 Total gastrointestinal transit time

The protocol for the total gastrointestinal transit time was performed and measured as previously described (Sasselli et al., 2013). Mice were individually placed into cages devoid of bedding and fasted for an hour. Next, 300 μL of 6% (w/v) carmine red dye (Sigma-Aldrich, C1022-25G) and 0.5% (w/v) methylcellulose (Sigma, M0512-500G) in dH_20 was

administrated by oral gavage, and the animals returned to their individual cages. The total intestinal transit time was calculated by the time from gavage until the extrusion of the first red-coloured pellet (Nagakura, Naitoh, Kamato, Yamano, & Miyata, 1996). A maximum period of observation was 5 hours in all experiments and mice that fail to expel the red pellet within this time were quantified as ending point at 5 hours.

2.2.12 Stool analysis

Animals were placed individually in cages devoid of bedding. Produced faecal pellets over a period of 5 hours were counted and collected into 1.5 mL plastic tubes and immediately snap-frozen in liquid nitrogen. Afterwards, stools were weighed (average wet weight) and dehydrated using a lyophiliser O/N to define their dry weight (average). Stool water content was calculated as the difference between the wet and dry weights and expressed as a percentage.

2.2.13 Live video recording and spatiotemporal analyses of ENS-dependent motility

Whole *ex vivo* colonic motility was recorded and analysed as previously described (Roberts et al., 2007). Entire colons were carefully isolated, luminal contents emptied and placed loosely pinned onto an organ bath chamber. Colons were then continuously infused (4 mL/min) with Krebs solution (120.9 mM NaCl, 5.9 mM KCl, 1.2 mM $MgCl_2$, 2.5 mM $CaCl_2$, 1.2 mM NaH_2PO_4, 14.4 mM $NaHCO_3$, 11.5 mM Glucose in dH_2O), constantly supplied with 95% O_2 and 5% CO_2 at 37°C. During the entire procedure, colons were continually submerged in carboxygenated-Krebs solution and allowed to rest for 30 minutes before the beginning of video recordings. After that, intestinal spontaneous activity was recorded (2.5 Hz frame rate) using a QICAM-Fast camera and QCapture Pro 6.37 software (Q-Imaging). Spatiotemporal maps of colonic motility were generated using Igor Pro (WaveMetrics) and analysed using custom-written algorithms plugin generated by Dr Peter Vandenberghe (KU, Leuven). The intestinal edges were determined and width computed and mapped over time. Spatiotemporal maps generated in the software represent the CMMCs and allow the quantification of frequency (the number of CMMCs within the total recording time), travel distance (the distance of propagation of CMMCs), and speed (measured as the average speed over the total propagated distance).

Analysing CMMCs is an efficient model to study the participation of the ENS on intestinal motor behaviour, and the spatial and temporal evaluation of ENS-dependent activity allows a precise examination of aspects responsible for propulsive motility.

2.2.14 SFB reconstitution

SFB reconstitution in mice used in this thesis was performed by Dr Sara Omenetti (Stockinger lab, The Francis Crick Institute). C57Bl/6 SFB^- male mice were colonised with SFB strains by oral gavage of faecal material immediately after weaning. Faecal pellets from SFB^+ mice were collected and snap-frozen in liquid nitrogen. Prior to colonisation, pellets were homogenised in PBS (1 mL/pellet) using 1 mL syringes to solubilise the faecal material. One pellet was sufficient to reconstitute SFB populations in 3 mice (200-300 µL of faecal solution/mice). The efficiency of SFB inoculation was confirmed by analysing the genomic DNA of SFB and total bacteria load (Eubacterial primers, UniF3240/UniR514) in faecal samples by qRT-PCR.

2.2.15 Molecular biology techniques

2.2.15.1 RNA isolation and cDNA synthesis

LMMPs (section 2.2.2.2) from different segments of the adult gut and distinct experimental groups were triturated and homogenised using a pestle (Sigma, Z359947 – 100EA) in lysis buffer (provided with the kit) containing β-mercaptoethanol and processed for RNA isolation using RNeasy Mini Kit (Qiagen, 74104) according to the manufacturer's instructions. Briefly, tissue lysates obtained after homogenisation were treated with 70% ethanol and passed through RNeasy MinElute columns. RNA was purified after a series of washes to eliminate DNA, proteins and other contaminants. Finally, RNA was eluted in RNase-free H_2O and either stored at -80ºC until further use or processed for reverse transcription. The quantification of concentration and quality of RNA was performed using a spectrophotometer Nanodrop™ 1000 (Thermo Scientific). The purity of extracts was determined by the ratio of absorbance at 260 nm and 280 nm (A_{260}/A_{280}), and RNA was considered pure with A_{260}/A_{280} ratio of 1.9-2.1. At least 100 ng of total RNA was used for reverse transcription using High- Capacity cDNA Reverse Transcription Kit (Applied Biosystems 10249814) and the protocol was followed according to the manufacturer's instructions on a DNA Engine Dyad programmable thermal converter (BioRad).

FACS-sorted GFP^+ neuronal nuclei and GFP^- non-neuronal populations for nRNAseq analysis were lysed and homogenised in TRizol and processed using PureLink™ RNA Micro Kit (Life Technologies, 12183018A) for RNA isolation according to the manufacturer's instructions. Since the concentration of RNA in these samples is very small, samples were directly submitted for nRNAseq (section 2.2.15.3).

2.2.15.2 qRT-PCR

Relative quantification of gene expression levels for transcripts of interest was performed using Taqman gene expression-based real-time PCR technology (Life Technologies). This assay involves pre-made fluorescent probes and primers for a specific gene of interest. Reactions contained 5 µL of Taq fast universal 2x PCR Master Mix (Applied Biosystems, 4352042), 0.5 µL of 20x Taqman Gene Expression assays **(IDs listed in table 2.5)**, 1 µL of cDNA and 3.5 µL of RNase-free water. qRT-PCR reactions in our experiments were prepared in triplicates in 96-well plates (Applied Biosystems, 4346906) for each cDNA template and negative control, using a 7500 Fast Real-time PCR system (Applied Biosystems). Ct (cycle threshold) values for transcripts of interest were normalised to Ct values of the housekeeping gene *Actinb*, used as an endogenous control. For relative quantification of transcript levels, samples were normalised to one control sample using the standard $2^{-\Delta\Delta Ct}$ formula expressed as relative expression of the transcript.

Table 2.5 List of Taqman assays used in this thesis.

Gene name	Taqman assay identification code
Actb	Mm01205647_g1
Ascl1	Mm03058063_m1
Calb1	Mm00486647_m1
Calb2	Mm00801461_m1
Cgrp	Mm00801462_m1
Chat	Mm01221882_m1
Elavl3	Mm01176703_m1
Elavl4	Mm01263580_mH
Erbb3	Mm01159999_m1
Foxd3	Mm02384867_s1
Gdnf	Mm00599849_m1
Gfap	Mm01253033_m1
Hand2	Mm00439247_m1
Hes5	Mm00439311_g1
Nos1	Mm00439311_g1
Npy	Mm03048253_m1
Phox2b	Mm00435872_m1
Plp1	Mm01297210_m1
Ret	Mm00436304_m1
S100b	Mm00485897_m1
Sox10	Mm01300162_m1
Sox2	Mm03053810_s1
Tac1	Mm00436881_m1
Tph2	Mm00557715_m1
Vip	Mm00660234_m1

* *Calb2* encodes the protein calretinin and *Elavl3* and *Elavl4* the protein HuC/D.

2.2.15.3 nRNAseq

RNA was isolated from FACS-sorted nuclei samples from colonic LMMPs of C57Bl/6 and *Tcrα*$^{-/-}$ mice (n=4 mice/group) using TRizol and PureLink Columns as previously described in section 2.2.15.1. Samples were submitted to The Crick Advanced Sequencing Facility. NuGEN Ovation Ultralow v2 library preparation kit (NuGEN) was used to amplify the total RNA transcriptome for low input RNA and libraries generated using the HiSeq4000 sequencer (Illumina). Sequencing was performed as 75bp read length fragment, single read and *Mus musculus* genome was used as reference. The most variable 20000 genes between the groups were represented in the analysis. Bioinformatics analyses were carried out by Dr Stefan Boeing at the Bioinformatics and Biostatistics Science Technology Platform of the Crick Institute.

The 'Trim Galore!' utility version 0.4.2 was used to remove sequencing adaptors and to quality trim individual reads with the q-parameter set to 20 (www.bioinformatics.babraham.ac.uk/projects/trim_galore/). Then sequencing reads were aligned to the mouse genome and transcriptome (Ensembl GRCm38 release-89) using RSEM version 1.3.0 (Li & Dewey, 2011) in conjunction with the STAR aligner version 2.5.2 (Dobin et al., 2013). Sequencing quality of individual samples was assessed using FASTQC version 0.11.5 (https://www.bioinformatics.babraham.ac.uk/projects/fastqc/) and RNA-SeQC version 1.1.8 (DeLuca et al., 2012). Differential gene expression was determined using the R-bioconductor package DESeq2 version 1.14.1 (Love, Huber, & Anders, 2014; Team, 2014). Gene set enrichment analysis (GSEA) was conducted as described in Subramanian et al (Subramanian et al., 2005).

2.2.16 Statistical analysis

All experiments were performed using at least 3 mice per experimental group and data were represented as mean ± standard deviation (SD). All statistical analysis was carried out using GraphPad Prism 8.0 software (GraphPad software, CA, USA). Since the size of the samples used in this thesis was small, and our data did not follow a specific distribution, non-parametric statistic tests were preferentially used to compare differences between experimental groups. Mann-Whitney test was used to compare two groups and, Kruskal Wallis test followed by a Dunn's multiple comparison test was used when comparing more than two groups. P values of less than 0.05 were considered statistically significant with * $p < 0.05$, ** $p < 0.01$, *** $p < 0.001$ and **** $p < 0.0001$.

Chapter 3

Development of novel experimental approaches for ENS studies

3. Chapter 3 | Development of novel experimental approaches for ENS studies

This chapter presents my collaborative work with other lab members for the development of new approaches for studies on the ENS, which are currently being applied to several projects in the lab. This work forms part of two major collaborative projects. However, all data presented in this chapter is the result of my own experiments and collection of my own data. All information, data, results, figures have been collected and analysed by me. My collaborations, either experimental or in the provision of materials, have been rightly acknowledged in the figure legends.

The development and establishment of EGC cultures were carried out in collaboration with Dr Song Hui Chng who continues to use this system to investigate the mechanisms that drive EGCs plasticity and neurogenic potential (Chng et al., *manuscript in preparation*). Together, we originated a robust and reproducible *in vitro* system that can be further explored to unravel the molecular and physiological features of EGCs.

In addition, because of the lack of experimental strategies to efficiently and quickly isolate enteric neurons, in collaboration with Dr Yuuki Obata we developed a method to efficiently deliver viral particles expressing fluorescent reporters to specifically target enteric neurons (Obata et al., *manuscript in preparation*). In addition to its ongoing application to several lab projects, this method was also applied in experiments performed in this thesis.

It is our firm belief that the development of robust and effective experimental methods to study the adult EGCs and enteric neurons will be critical for the advancement of research in enteric neuroscience.

3.1 Development of EGC cultures from the adult gut

3.1.1 Introduction

Identifying the properties of EGCs is fundamental to the understanding of their physiological roles in the development and homeostasis of the ENS, as well as their participation in and response to diseases. So far, the lack of robust models to unravel the molecular mechanisms that take part in these processes has delayed progress in understanding the properties and physiological roles of this cell population.

EGCs are originated from NCCs and are firstly identified at E11.5 by expression of the molecular markers Sox10, p75 and BFABP (Young et al., 2003). In addition, FoxD3 is one of the earliest NCC markers, and its expression is maintained in adult EGCs (Mundell

et al., 2012). Moreover, Sox10 and Sox2 expression largely overlap with FoxD3 levels during development and in the adult gut (Heanue & Pachnis, 2011). Adult EGCs also express S100β after E14.5 and GFAP from E16.5 onwards (Jessen & Mirsky, 1980). Although the function of some of these molecules remains unclear, it has been shown that deletion of Sox10 and FoxD3 at embryonic stages results in a complete loss of the ENS, suggesting that the expression of these transcription factors in ENS progenitors and EGCs plays essential roles on ENS development and cell survival (Southard-Smith et al., 1998; Teng et al., 2008).

Furthermore, the physiological function of EGCs in the healthy gut remains unclear as they were reported to be very plastic and heterogeneous. EGCs are localised in different layers within the GI tract and present distinct morphological subtypes. EGCs within the mucosa are exposed to intestinal fluids, microbial products and immune cells. EGCs within muscle layers, in turn, closely interact with enteric neurons and are involved in providing factors to neuronal survival and function (Boesmans et al., 2015; Gulbransen & Sharkey, 2012). Different locations of EGCs within the gut wall and their close anatomical association with other cell types are restrictive factors that withhold the isolation and purification of these cells, due to increased chances of contamination with other cell types.

EGCs are very branched, presenting multiple filaments that closely interact with other cell types (Gabella, 1981). The morphological aspects of EGCs and their deep localisation inside ganglionic structures, muscle fibres and mucosal lamina propria hamper the isolation of these cells. Moreover, EGCs are very sensitive to the gut environment, rapidly responding to mechanical insults such as breaking down of the epithelial layer (Bush et al., 1998), neuronal damage (Laranjeira et al., 2011) and activation of immune system (Chow & Gulbransen, 2017). These factors may also contribute to changes in EGC phenotype during dissection and processing of the gut tissue.

One aspect that facilitates the visualisation of EGCs dynamics *in vivo* and *in vitro* is the endogenous genetic labelling of these cells. Progress in ENS research has emerged from the evaluation of transgenic mouse models in which the expression of a molecular marker is labelled with fluorescent reporters. This enables the permanent and selective labelling of a specific gene in cells of interest. In our experiments described below, we took advantage of the Sox10 transgenic mouse line (*Sox10::CreER*^{T2}) generated in our lab (Laranjeira et al., 2011) combined with the reporter line *R26R-CAG-td*^{Tomato} to label and culture EGCs *in vitro*.

3.1.2 Aims

Here, we have generated and tested a new culture system that enriches the population of EGCs in a short period. The purpose of developing this technique was to create a robust protocol that could be used in the field to analyse the dynamics of EGCs *in vitro*.

In this part of the thesis, we aimed to:

1. Generate a robust protocol to isolate EGCs from the adult gut.
2. Characterise the identity of EGCs *in vitro* by the expression of well-known glial markers.

3.1.3 Results

3.1.3.1 Validation of the transgenic mouse line *Sox10::CreER^{T2};R26R-CAG-td^{Tomato}*

Experimental set-up

To establish a culture system of adult EGCs we took advantage of the *Sox10::CreER^{T2};R26R-CAG-td^{Tomato}* mouse line generated in our lab, from now on referred here as *Ser26.tdT*. In this line, the Sox10 transgene is expressed about 95% of adult EGCs and its expression is restricted to this population. Although it is efficient, tdT does not label all EGCs, since small group of GFAP^{+}tdT^{-} was previously observed within the MP (Boesmans et al., 2015; Laranjeira et al., 2011). We still do not know the molecular and functional features of the tdT^{-} EGCs. Adult mice, older than eight weeks of age were used for all experiments.

Before performing the *in vitro* experiments, we first evaluated the *in vivo* specificity in expression of EGC lineage markers by tdT^{+} cells. We isolated LMMPs from the small intestine of the *Ser26.tdT* reporter mouse line and performed immunohistochemistry to detect FoxD3, S100β, GFAP, Sox10 and Sox2 expression. We observed that the vast majority of tdT^{+} cells *in vivo* also express FoxD3 **(Figure 3.1A)**, S100β **(Figure 3.1B)**, GFAP **(Figure 3.1C)**, Sox10 **(Figure 3.1D)** and Sox2 **(Figure 3.1E)**, endorsing the EGC identity of the tdT expressing cells within the LMMPs.

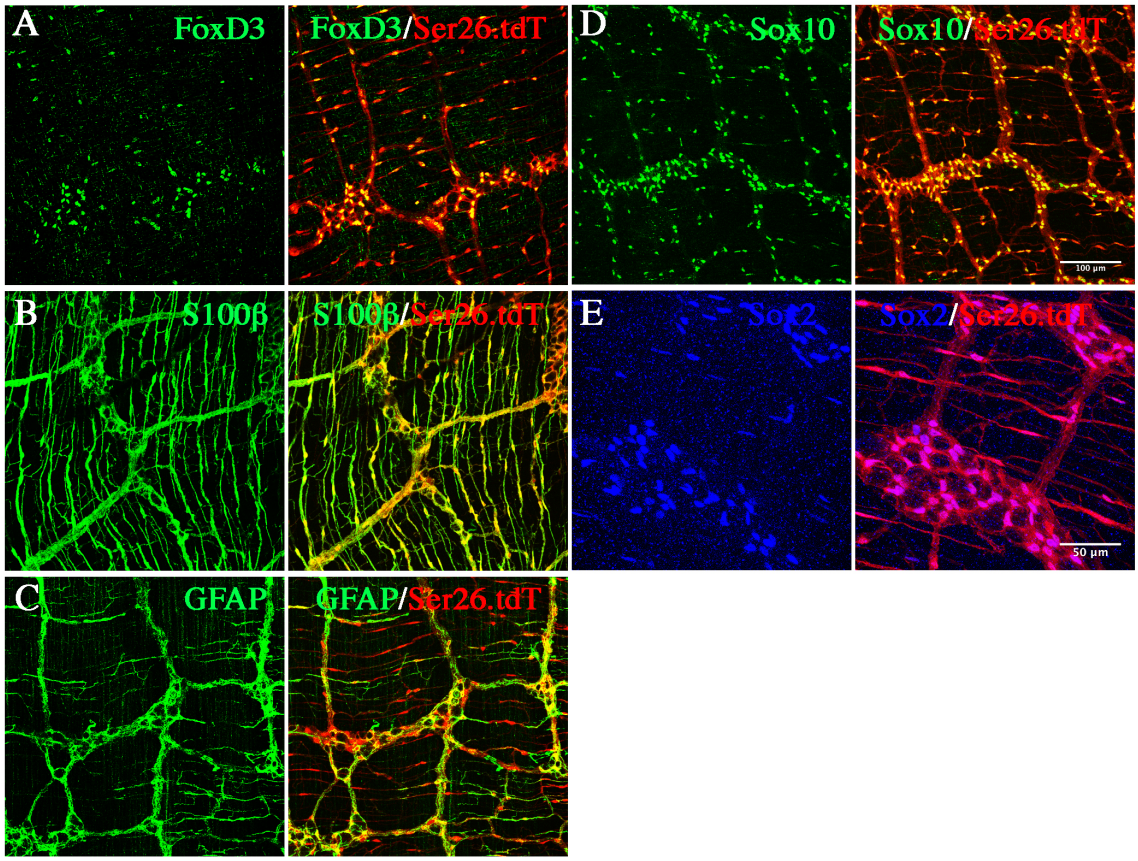


Figure 3.1. Expression of well-established EGC markers in tdT⁺ cells from the *Ser26.tdT* mice. (A-E) Confocal images of dissected LMMPs from the small intestine of the *Ser26.tdT* reporter mouse line (red) immunostained for the EGC markers FoxD3 (green) **(A)**, S100β (green) **(B)**, GFAP (green) **(C)**, Sox10 (green) **(D)** and Sox2 (blue) **(E)**. Scale bars: 100 µm **(A-D)** and 50 µm **(E)**. Representative of at least three experiments.

3.1.3.2 Establishment of a new method to culture adult EGCs

Since we confirmed the EGC identity of tdT⁺ populations, we next proceeded with the isolation the establishment of an *in vitro* system to culture these cells. To determine which culture condition was most efficient for the establishment of EGCs *in vitro*, we compared EGCs grown in the presence of foetal bovine serum (FBS medium) or serum-free medium (G5). The protocol for EGCs isolation was adapted from Boesmans et al. and is as follows (Boesmans et al., 2015).

The small intestine of the *Ser26.tdT* mice was collected, and the efficiency of EGC labelling was confirmed under a conventional fluorescence microscope. Intestines were then placed in ice-cold PBS and flushed to eliminate any remaining luminal contents. Thereafter, the mesentery was removed from the full extension of the gut. The intestines were next cut into about 2 cm long pieces and placed in a new plate with DMEM/F12 media containing

12.5 mM HEPES, 2% FBS and 1% P/S **(dissection media)**. LMMPs were then isolated by using cotton swabs to gently separate this layer from the remaining intestinal wall. In tissue culture hood, LMMPs were subsequently washed three times in a new and sterile **dissection media**. LMMPs were cut into small pieces by using fine scissors and next incubated in **digestion media** (0.5 mg/mL collagenase I and 0.5 mg/mL DNAse I in sterile dissection media) for 30 minutes at 37ºC on a shaker. Following that, the remaining tissues were mechanically triturated for about 60 times by using a glass pipette, washed once again in **dissection media** and spun down at 500 g for 5 minutes. Finally, cell suspensions were plated onto 6 cm dishes coated with fibronectin and incubated with DMEM/F12 containing, 10% FBS and 1% P/S for the first 24 hours in an incubator at 37ºC continuously supplied with 5% CO_2 **(Figure 3.2A)**.

On the following day **(DIV1)**, the media and all remaining floating pieces of tissue were carefully removed, and new media offered to the cells according to different experimental conditions chosen for these experiments. The FBS group was changed into a new DMEM/F12 + 10% FBS and the G5 group into DMEM/F12 containing 1% P/S, 1% N2, 1% G5 and NGF (50 ng/mL). N2, G5 and NGF are well-known growth factors used for the establishment of neural cell cultures. At **DIV3**, half of the media was replaced with fresh media. At **DIV4**, cells were passaged and plated onto fibronectin pre-coated dishes and at **DIV6** cell cultures were more stable and ready to be used **(Figure 3.1B)**.

EGCs under different culture conditions

To assess the expansion of cultured cells under different media conditions, tdT^+ cells were followed over six days after seeding. Morphological characterisation of tdT^+ cells in FBS and G5 conditions from DIV2 to DIV6 was performed by using a conventional fluorescence microscope. At DIV2, EGCs appear to be small and have short processes and form modest colonies in both groups **(Figures 3.2C and 3.2D)**. The morphology of these colonies already differs in the DIV2 by comparing the two groups. Colonies from FBS-cultured EGCs grow in small islands, forming compact structures **(Figures 3.2C)**. Conversely, cells from the G5 group expand out from the core of colonies **(Figures 3.2D)**. By DIV3 and DIV4 the expansion of these cells follows the same trend, in which in the FBS group, colonies are still compact **(Figures 3.2C' and 3.2C")** while in the G5 group tdT^+ cells migrate from the colony **(Figures 3.2D' and 3.2D")**. By DIV6, EGCs in the FBS group start to expand and are morphologically heterogeneous, presenting multiple and highly

branched processes (**Figure 3.2C'''**). In turn, colonies from the G5 group form structures that resemble enteric plexuses *in vivo*. EGCs present a triangular body shape with short processes or they are bipolar with two elongated processes (**Figure 3.2D'''**).

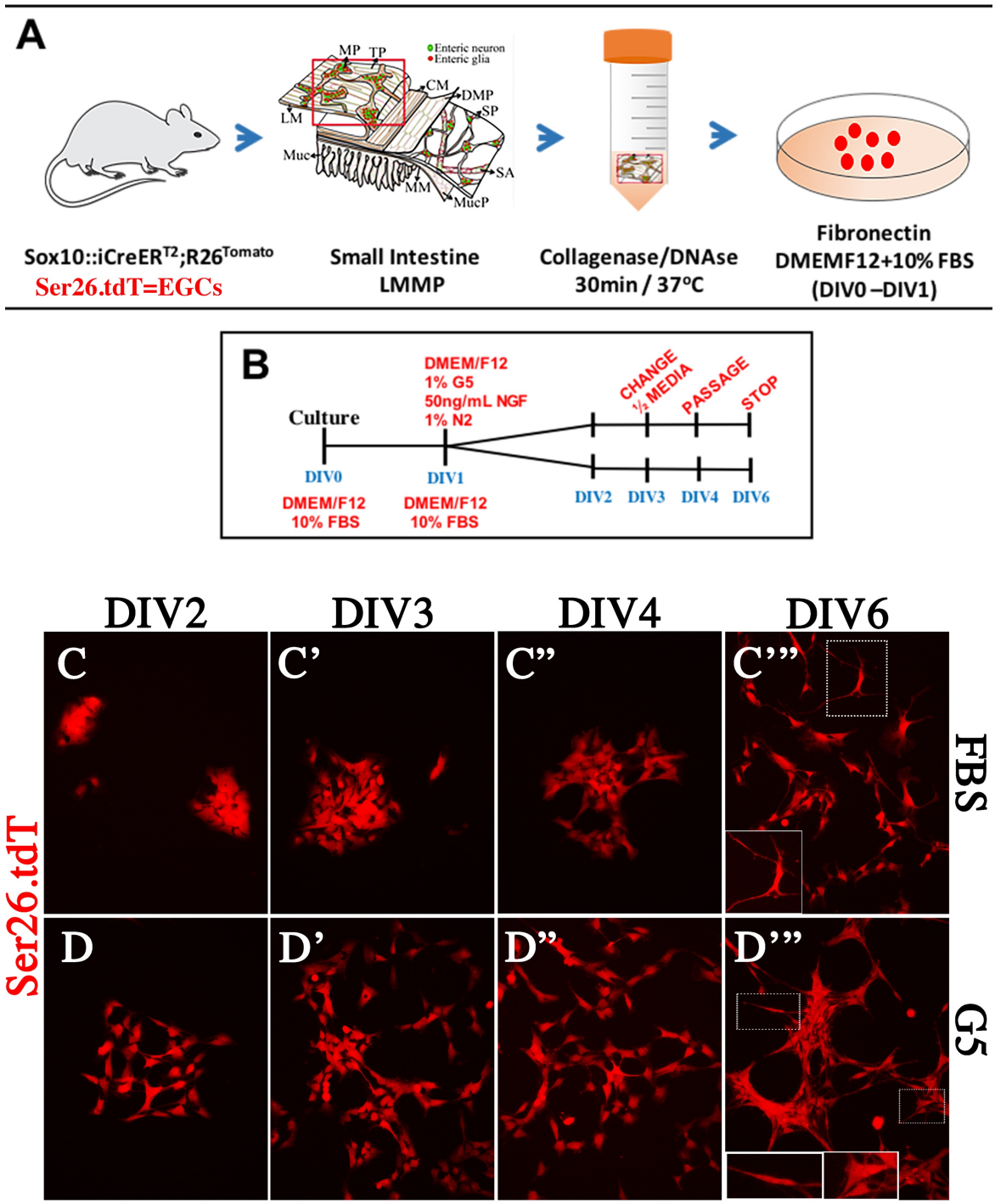


Figure 3.2. Establishment of a new method to culture tdT$^+$ EGCs from the adult gut. (A) Simplified schematic illustrating the steps for tdT$^+$ EGCs isolation from the adult gut. *Ser26.tdT* adult mice were used for

the visualisation of tdT$^+$ EGCs. LMMPs from the small intestine were dissected, digested using collagenase/DNAseI and placed onto fibronectin-coated dishes in presence of DMEM/F12 and 10% FBS for 24 hours. **(B)** Time-course of tdT$^+$ EGCs cultures from DIV0 to DIV6. DIV1 - medium was changed to either FBS or G5. At DIV3, half of the culture media was replaced. DIV4 – tdT$^+$ EGCs were passaged, and cultures stopped at DIV6. Images of tdT$^+$ EGCs expansion from the *Ser26.tdT* (red) mice over six days *in vitro* in FBS **(C-C'")** and G5 **(D-D'")** media. Insets highlight the morphology of tdT$^+$ EGCs. Images were acquired by using a 20x objective. LMMP, longitudinal muscle myenteric plexus; FBS, foetal bovine serum; DIV, days *in vitro*; NGF, nerve growth factor. Representative of at least three experiments.

This result suggests that EGCs are heterogenous under differing *in vitro* conditions and the culture environment can modulate their morphology and formation of colonies, even when they come from the same animal source.

Characterisation of the adult EGC cultures

Smooth muscle cells are one of the most persistent contaminants in primary cultures. The overgrowth of these cells represents a major obstacle to establishing EGC cultures. Given the primary culture conditions in which the dissection of LMMP layers comprises different cell types, including smooth muscle cells, it had to be ensured that our culture preparations were devoid of other cell contaminants and enriched with EGCs. To test the homogeneity of EGC cultures, cells were fixed at DIV3 and DIV6 and immunocytochemistry was performed using a monoclonal antibody to detect smooth muscle α-actin (SMA), expressed in myofibroblasts. SMA$^+$ cells were detected in both groups at DIV3 **(Figures 3.3A and 3.3B)** and DIV6 **(Figure 3.3C and 3.3D)**, and appear to be enriched in the group supplemented with FBS at DIV6 **(Figure 3.3C)** relative to the G5 **(Figure 3.3D)**. This data suggests that the FBS media favours the outgrowing of SMA$^+$ myofibroblasts when compared to the G5 group.

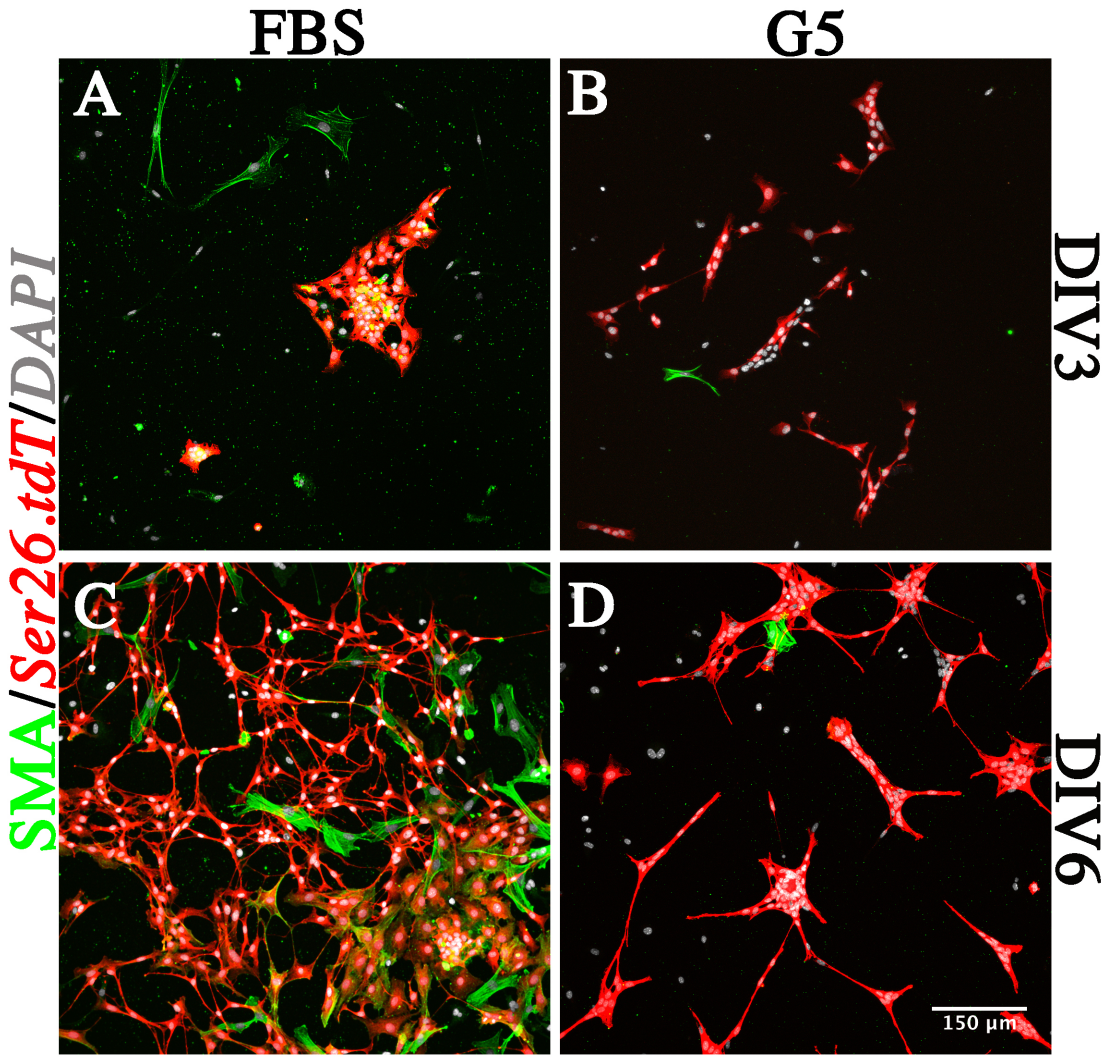


Figure 3.3. Immunocytochemical characterisation of myofibroblasts in tdT⁺ EGC cultures. Confocal images show the presence of tdT⁺ EGCs (red) and SMA⁺ myofibroblasts (green) *in vitro* under FBS **(A and C)**, and G5 **(B and D)** supplemented media. SMA⁺ cells are identified in DIV3 in the FBS **(A)**, and the proportion is increased in DIV6 **(C)** in the same group. **(B and D)** SMA⁺ cells were virtually absent in the G5 supplemented culture at DIV3 and DIV6. Nuclei were stained with DAPI (grey) **(A-D)**. Scale bar: 150 µm. Representative of more than three experiments.

EGCs express lineage-specific markers such as Sox10 (Southard-Smith et al., 1998), Sox2 (Heanue & Pachnis, 2011) and FoxD3 (Mundell et al., 2012) at early stages during development and the expression of these markers are maintained in adult glia, along with GFAP (Jessen & Mirsky, 1980) and S100β, which together identify these cells. To confirm the lineage-specificity of tdT expressing EGCs, we performed

immunocytochemistry for EGC lineage-markers in cultures that were exposed to FBS and G5 media at DIV6.

At DIV6, FoxD3 expression was observed in the nuclei of tdT-expressing cells in both the FBS **(Figure 3.4A)** and G5 **(Figure 3.4A')** conditions. Moreover, its expression almost completely overlapped with GFAP expression that was detected in the cytoskeleton of EGCs in both conditions **(Figures 3.4A and 3.4A')**. Furthermore, the expression of Sox10 and S100β co-localised with tdT^+ cells in the FBS **(Figure 3.4B)** and G5 **(Figure 3.4B')** groups. Sox10 marked the nuclei and S100β labelled the cellular body and processes of tdT expressing cells. Likewise, the majority of $Sox2^+$ cells were also $S100\beta^+$ and almost fully overlapped with tdT^+ cells in the FBS **(Figure 3.4C)**, and G5 **(Figure 3.4C')** supplemented media. A small population of tdT^- cells expressed EGC lineage markers, but this could be explained by the inefficiency of this line to label the total population of EGCs. The expression of these molecules by tdT^+ cells were also detected in EGC cultures at DIV3 **(Appendix 3)**.

In addition to characterisation of the molecular profile of EGCs *in vitro*, these experiments confirmed the typical morphological differences in the ganglia formation noted between the cells that were exposed to FBS and G5 **(Figure 3.4)**.

Altogether, these experiments suggest that we have successfully generated an *in vitro* system to grow and expand EGCs that maintain the molecular properties of these cells. Moreover, by selecting the seeding conditions to grow these cells in G5 media, we could decrease the overgrowth of myofibroblasts *in vitro*.

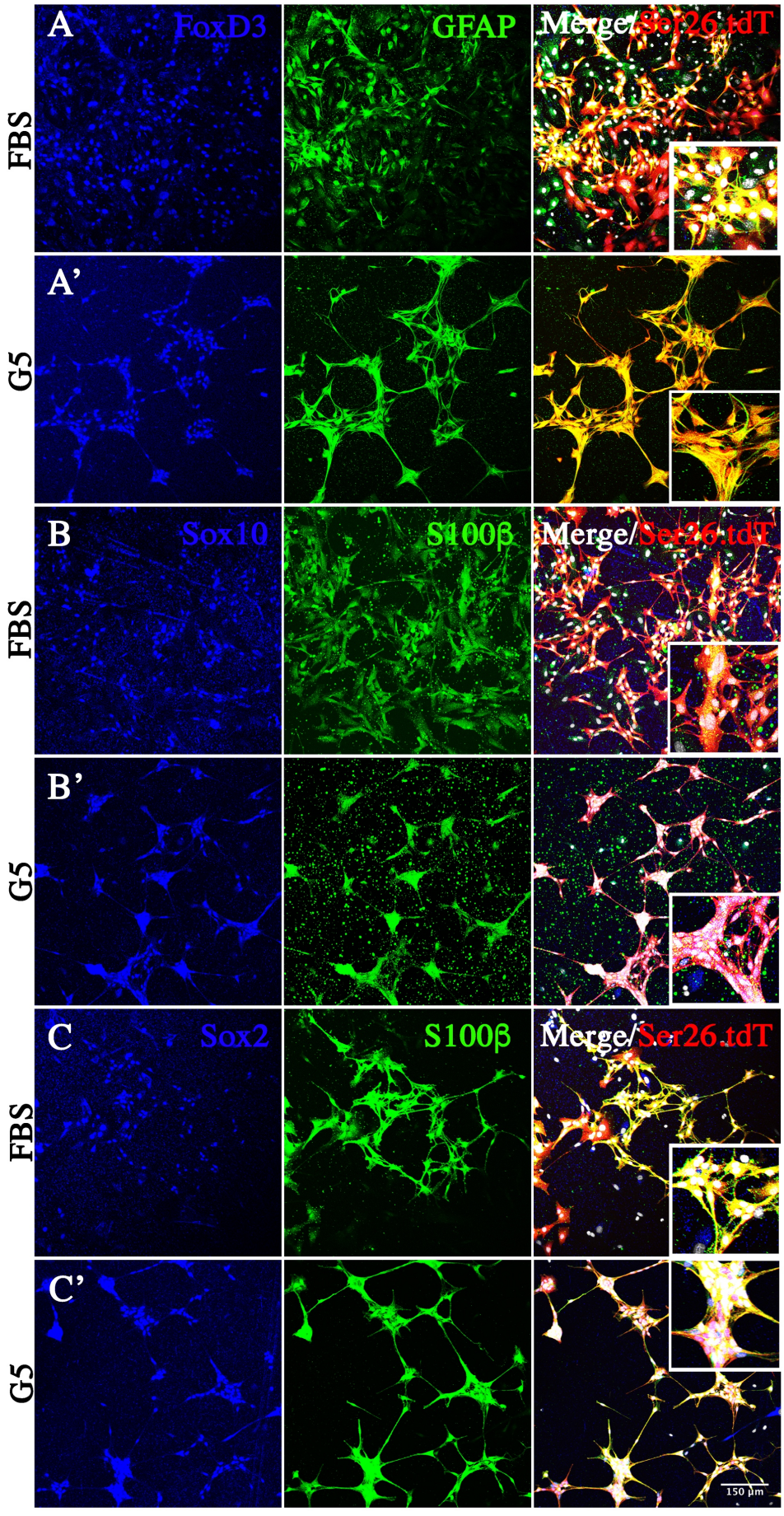

A
FoxD3
GFAP
Merge/Ser26.tdT
FBS
A'
G5
B
Sox10
S100β
Merge/Ser26.tdT
FBS
B'
G5
C
Sox2
S100β
Merge/Ser26.tdT
FBS
C'
G5
150 µm

Figure 3.4. *In vitro* expression of EGC-lineage markers in tdT⁺ EGCs. (A-C') Representative confocal images showing the expression of known EGC-lineage markers at DIV6 by tdT⁺ EGCs (red) cultured in presence of FBS **(A, B and C)** or G5 media **(A', B' and C')**. Immunocytochemistry to detect FoxD3 (blue) and GFAP (green) expression in tdT⁺ EGCs in FBS **(A)** and G5 **(A')** culture conditions. Immunocytochemistry to identify Sox10 (blue) and S100β (green) in cultures of tdT⁺ EGCs (red) in FBS **(B)** and G5 **(B')** media. Immunocytochemistry for the EGC markers Sox2 (blue) and S100β (green) in cultures of tdT⁺ EGCs (red) in FBS **(C)** and G5 **(C')** media. Nuclei were visualised by DAPI staining. Scale bar: 150 μm. Representative of more than three experiments.

3.1.4 Discussion

It has been suggested that EGCs are involved in many aspects of GI physiology by supporting the development and function of enteric neurons (Ruhl, 2005), keeping homeostasis of the epithelial barrier (Bush et al., 1998; Cornet et al., 2001), interacting with the gut microbiota (Kabouridis et al., 2015) and immune system (Ibiza et al., 2016). Moreover, EGCs were reported to have a dual role in the progression and constriction of inflammatory responses (I. A. Brown et al., 2016; Cirillo, Sarnelli, Esposito, et al., 2011). The complexity and redundancy of the participation of EGCs in several GI events *in vivo*, resulting in the lack of clear mechanisms by which they mediate different functions in the gut, prompted us to generate a robust *in vitro* system that would facilitate the direct manipulation of these cells.

To address this matter, we developed a technique that permits the isolation, purification and supports the maintenance of EGCs from the small intestine of adult mice. Our method is based on our expertise for the fast dissection of LMMPs, the use and adaptation of two different media conditions previously reported in independent studies (Boesmans et al., 2015; Cirillo, Sarnelli, Turco, et al., 2011) and the use of the *Ser26.tdT* mouse line which allowed us to follow the expansion of EGCs *in vitro* (Laranjeira et al., 2011).

At first, we opted for using DMEM/F12 supplemented with 10% FBS as this is one of well-established conditions for growing glial cells (Cirillo, Sarnelli, Turco, et al., 2011; Ruhl, Trotter, & Stremmel, 2001). By using FBS media supplementation, we were able to isolate EGC populations that were positive for lineage-specific markers such as Sox10, Sox2, FoxD3, GFAP and S100β. We also observed the formation of small colonies of tdT⁺ cells from DIV2. Our data also showed that in FBS-supplemented cultures, there was an

increased outgrowing of SMA^+ myofibroblasts. The overgrowth of fibroblasts *in vitro* is one of the major complications in long-term cultures and it has been reported in many protocols of primary EGC cultures. To be able to exclude unwanted fibroblast populations, studies have used negative selection methods to isolate these cells from cells of interest. This technique implicates in trypsinisation and resuspension of cells, the use of antibody-coated magnetic beads to detect markers expressed in the surface of fibroblasts (i.e. Thy-1.1), and consequent magnetic separation of cells. This method was demonstrated to be efficient in isolation of EGCs from myofibroblasts (Cirillo, Sarnelli, Turco, et al., 2011; Ruhl, Trotter, et al., 2001). However, it involves an extensive manipulation of cells that we wanted to avoid in our protocol. Besides, published data have shown that FBS-supplemented EGC cultures take about 3-4 weeks to reach confluence (Cirillo, Sarnelli, Turco, et al., 2011), and that is also a problem to be taken into consideration when choosing the most efficient method to grow EGCs *in vitro*.

Alongside the FBS group, our second choice was to supplement our *in vitro* preparations with growth factors that are known for supporting the survival of neural cells (Boesmans, Martens, et al., 2013). We used DMEM/F12 serum-free, supplemented with N2, G5 and NGF (Boesmans, Martens, et al., 2013). By cultivating cells from LMMP preparations in G5 media, we were able to isolate and maintain EGCs that express specific lineage-markers such as FoxD3, GFAP, Sox10, S100β and Sox2. As with the FBS group, we could also observe the formation of small colonies. The morphology of EGCs also differed from the FBS group displaying a triangular cell body with small and short processes, or bipolar with two elongated processes. Moreover, EGCs under G5 condition form compact clusters that resemble the structure of the ENS ganglia, suggesting that perhaps EGCs supplemented with G5 media can keep their physiological property of maintaining the ganglia formation. Surprisingly, the presence of SMA^+ myofibroblasts in this condition was barely detectable, suggesting that G5 media does not favour the outgrowing of myofibroblasts *in vitro*.

Distinct morphologies of EGC colonies observed in our experiments in different media conditions could indicate that perhaps the culture environment favours a subtype-specific selection of EGC populations, suggesting the plasticity of these cells to respond to environmental changes *in vitro*. Available protocols to culture EGCs from different studies have failed to demonstrate a uniform morphological characteristic of these cells *in vitro*, suggesting that perhaps different studies have also selected specific populations of these

cells. It would be an essential contribution to the ENS research, specifically on the understanding of EGCs molecular features, to generate an EGC line to maintain the uniformity and by consequence increase the reliability of studies on this complex cell type. However, taken into consideration the protocol for dissection and digestion of LMMPs, the short-time to obtain lineage-specific expressing EGCs, and the reduced contamination with myofibroblasts with G5 media, together, our data suggest that were able to successfully generate a robust *in vitro* system to isolate and maintain EGCs from the adult gut. Our protocol for growing EGCs *in vitro* has been successfully implemented in our lab to address several questions about the physiological and molecular properties of these cells and their plasticity to respond to different conditions. For these experiments, we have not followed the fate of the cultured EGCs long-term. Given the plasticity of these cells it is likely that they generate other cell types, such as neurons, which does not readily happen *in vivo*. Therefore, one of the uses of these culture systems in our lab is to understand the plasticity of EGCs and study the mechanisms that activate their neurogenic potential. If this happens indeed, and now we have evidence to support that (Chng et al., *manuscript in preparation*) it would be very interesting to understand why EGCs *in vivo* do not rapidly generate neurons as they do in culture. Also, EGCs *in vivo* are quiescent but they quickly divide and increase their numbers in culture. It would be interesting to understand the differences in mechanisms that maintain the quiescent state of these cells *in vivo*, and trigger these cells to enter the cell cycle and undergo neurogenesis *in vitro*.

3.2 AAV-based strategies for the characterisation of adult enteric neurons

3.2.1 Introduction

Enteric neuronal physiology is integrated into GI physiology by regulating vascular function (Vanner & Surprenant, 1991), epithelial secretion and absorption (J. B. Furness, 2000), interaction with the immune system and microbiota (Cardoso et al., 2017; De Vadder et al., 2018; Gabanyi et al., 2016; Klose et al., 2017; Muller et al., 2014), and initiating and propagating gut motility (Costa et al., 2015; Roberts et al., 2007). However, the mechanisms that control the enteric neuronal functions are still poorly elucidated due to the lack of a clear understanding of their molecular properties. Because of the complexity and heterogeneity of the enteric neuronal network within different parts of the GI tract, the manipulation and understanding of the physiology of individual groups of neurons is a significant challenge for intestinal neuroscience.

Enteric neuronal cell bodies are located within the myenteric and submucosal ganglia and can project their fibres in multiple directions, such as orally, anally, centripetally, vertically and horizontally within the gut wall (John Barton Furness, 2006). Neuronal cell bodies in the ganglia are protected by surrounding muscles, EGCs and connective tissue (Gabella, 1972) and send projections over long distances within the intestinal tissue, connecting multiple ganglia and projecting to all gut layers including the outer muscle layers and the inner mucosa. The populations of enteric neurons within the ganglia are very heterogeneous, including about 20 subtypes of neurons that present distinct molecular features resulting in different functions (John Barton Furness, 2006). Furthermore, the length of the GI tract and its cellular and environmental compositions in different areas contribute to the mosaic of enteric neuronal network. All these facts add to the complexity of studying the enteric neurons *in vivo*.

Although the ENS was first described about 150 years ago, there are still few techniques to study this system in adult mice. Progress in revealing the mechanisms that underlie the development of enteric neurons has been made largely because of methods that allow the genetic manipulation of these cells. For instance, inducible or constitutive manipulation of gene expression in mouse lines, in which a gene can be deleted or improved have provided new insights into the physiology of enteric neurons. One example is the manipulation of the *Ret* gene, which plays a pivotal role in the development of the ENS. It has been shown that deletion of *Ret* during development is deleterious to the enteric neuronal

network in mice, resulting in a similar (but more severe) phenotype as observed in patients with Hirschsprung's disease (Schuchardt et al., 1994).

Moreover, the use of transgenic reporter mouse lines, in which a fluorescent protein is inserted into the genome, replacing or fusing into a gene of interest, has allowed the visualisation and tracking of specific genes, such as, for example, those that are expressed by enteric neurons. Some of these tools are currently being used in ENS research, including the *Ret*, *Wnt1* and neuronal subtype-specific reporter lines. However, to study different mutations in association with neuronal labelling, consecutive breeding strategies are necessary in order to generate the genotype of interest. This delays the course and the execution of experiments and increases the number of animals used. Another limiting fact is that the genetic manipulation using these methods mentioned above are not feasible in wildtype adult mice, restricting the use of these techniques in non-genetically modified animals.

Another strategy that has been currently and widely used for gene delivery is based on the use of adeno-associated viral (AAV) vectors. AAV is a non-pathogenic viral vector system that infects both dividing and non-dividing cells, with minimal host immune response. Expression of transgenes delivered by AAVs is robust, and it can be maintained throughout the lifetime of an organism (Gombash, 2015). AAVs have been used to deliver particles to the CNS and have also been applied to deliver drugs in clinical trials (Samulski & Muzyczka, 2014). However, the use of this strategy to target ENS cells is still very limited. It has been described that the efficiency of transduction of ENS by AAVs is dependent on the route of administration and AAV serotype. Beskey et al. reported viral spread into myenteric and submucosal neurons by using local direct injection into the colonic wall of AAV serotypes expressing GFP under the control of hybrid chicken β-actin/cytomegalovirus (CB/CMV) promoter (Benskey et al., 2015). This work suggested that AAV6 and AAV9 showed high levels of tropism to the ENS (Benskey et al., 2015). In addition, Gombash et al. demonstrated that the systemic delivery of AAV9 resulted in transduction of about 25-57% of myenteric neurons in mice. Similarly, AAV8 transduced both enteric neurons and EGCs (Gombash et al., 2014). Transduction of the ENS by AAV8 and AAV9 was also observed in guinea-pig and macaques (Gombash et al., 2014; Gombash et al., 2017). Most of studies have used the CB/CMV promoter to transduce the GI due to its well-known robust expression in this tissue, combined to a fluorescent particle, usually GFP to label the cells (Gombash, 2015). More recently, enriched (PHP.S) packaging of AAV

containing CAG promoter conjugated to a nuclear GFP (AAV-PHP.S:CAG-NSL-GFP) was used to improve the transduction of the CNS more specifically, by using neuron and astrocyte-specific Cre mouse lines. This strategy was also efficient in labelling the ENS (Chan et al., 2017).

Although recent data have demonstrated a novel and efficient methodology to label the ENS network *in vivo,* by using an AAV strategy system to deliver genetic material to neurons, the understanding of their molecular properties is still not well elucidated. Recently, bulk and single-cell RNA sequencing from embryonic reporter mouse lines have been successfully used to characterise the properties of progenitor ENS cells (Lasrado et al., 2017; Memic et al., 2018). However, technical limitations have hampered progress in the adult ENS. As mentioned earlier on, the adult enteric neuronal cell bodies are confined to the outer muscle layers and are surrounded by many other cell types that increase the chances of contamination during cell isolation. Another inconvenience for enteric neuronal isolation is the fact that these cells present long and branched projections that are damaged during dissociation of intestinal tissue, which is detrimental to neuronal survival. Adult enteric neurons are also sensitive to the environment and trypsinisation of these cells can reduce their viability. As a result, robust protocols of enteric neuronal isolation from adult mice are still missing in the ENS research. In summary, the dissection of intestinal neurons itself, followed by enzymatic reactions, relatively lengthy times required to isolate cells from the entire extension of the gut and cell sorting are harmful to enteric neuronal viability. This results in delays in the progression of the adult ENS research and restrains the generation of new data on the molecular characterisation of these cells.

To tackle this problem, I have contributed to the development of a strategy led by Dr Obata in our lab, which uses an AAV9 delivery system to transduce a GFP-KASH hybrid protein (Klarsicht ANC-1 Syne Homology) to the outer membrane of the nuclear envelope of enteric neurons (Starr & Fischer, 2005). This strategy aimed to not only to label enteric neurons but also to isolate enteric neuronal nuclei for further molecular analysis (Obata et al., *manuscript in preparation).*

In this part, we have used an AAV9 delivery system to specifically and efficiently label enteric neurons in the small and large intestines in adult mice. In addition, we have also successfully isolated the nuclei of enteric neurons from the small intestine of adult mice.

3.2.2 Aims

Recent studies on the use of AAV serotypes to deliver genetic material to cells of interest combined with the challenge of isolating enteric neurons in the adulthood, prompted us to test the possibility of applying viral delivered particles to label the nuclei of enteric neurons in adult wildtype mice which would facilitate nuclear isolation from mature enteric neurons.

The specific aims of this part of the chapter were:

1. Characterise the efficiency of neuronal transduction by using AAV9 delivery system using the CaMKII promoter.
2. Confirm the specificity of neuronal transduction by AAV9-CaMKII-KASHeGFP.
3. Isolate the nuclei of enteric neurons from the MP of the small intestine.
4. Confirm the purity of isolated neuronal nuclei.

3.2.3 Results

3.2.3.1 AAV9-CaMKII.Cre efficiently transduces enteric neurons from the myenteric and submucosal plexuses following intravenous injection in the adult mice

Experimental set-up

Based on recent findings in which AAV9 was shown to have a tropism towards the ENS (Gombash et al., 2014; Gombash et al., 2017), we decided to introduce this AAV serotype carrying the neuron-specific promoter of the Ca^{2+}/calmodulin-dependent protein kinase II driving bacterial Cre recombinase (CaMKII.Cre) into *Rosa26Td^{Tomato}* reporter mice. CaMKII is a serine/threonine protein kinase regulated by Ca^{2+}, and it is highly and specifically expressed in neurons. As the route of AAV delivery is important for efficient transduction (Gombash, 2015), AAV9.CaMKII.Cre was injected into the tail vein of 6 weeks old male mice. Four weeks after injection, the GI tract of the *Rosa26Td^{Tomato}* injected with AAV9-CaMKII.Cre mice (section 2.2.4) was collected and the myenteric and submucosal plexuses of the small intestine and colon dissected (section 2.2.2.2) **(Figure 3.5A)**.

AAV9-CaMKII.Cre transduces myenteric and submucosal plexuses in the colon and small intestines of adult Rosa26Td^{Tomato} mice

To examine AAV9 ENS transduction in the myenteric and subcostal plexuses, several layers of the small intestine and colon were analysed by confocal microscopy. To

visualise multiple intestinal layers in this experiment, intestinal tissues were imaged from serosa to the mucosal layers, and all images shown in the y-axis in Figure 3.5 are from the same area of the gut. tdT^{+} neuronal cell bodies were observed within the MP of the small intestine **(Figure 3.5B1)** and colon **(Figure 3.5B2)**, in addition to robust tdT expression in neuronal fibres detected at the same level of the ganglia. Similarly, submucosal neurons and fibres had a strong tdT transduction in the small intestine **(Figure 3.5C1)** and colon **(Figure 3.5C2)**. Interestingly, neuronal fibres within mucosal layers of the small intestine **(Figure 3.5D)** and colon **(Figure 3.5D)** also presented a strong tdT expression, suggesting that AAV9-CaMKII.Cre efficiently transduced enteric neurons in several layers within the intestinal wall.

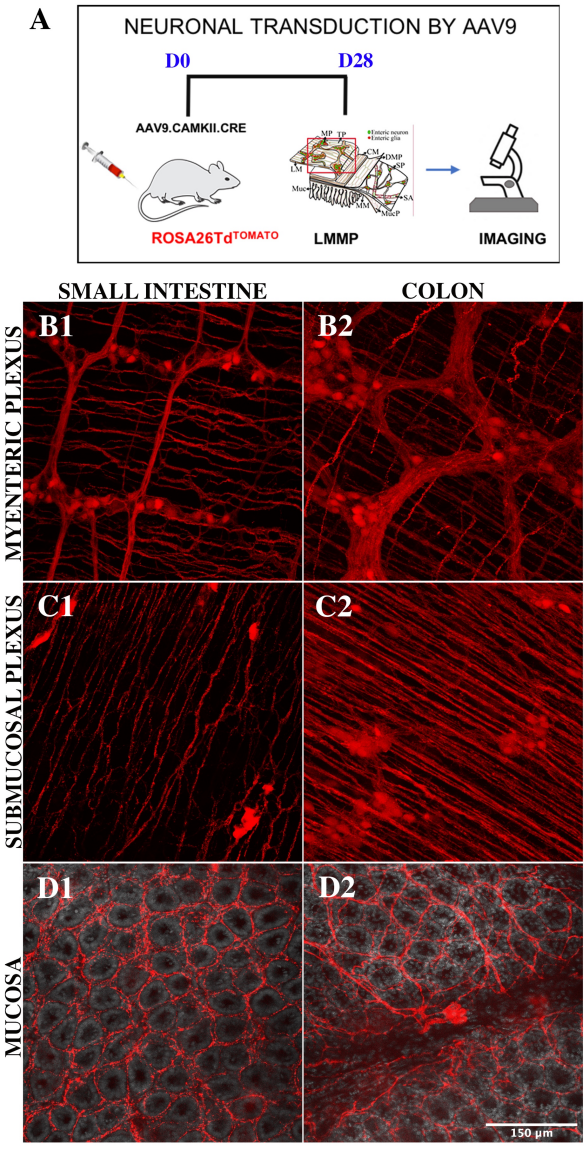


Figure 3.5. tdT expression in the myenteric and submucosal plexuses and mucosa following intravenous injection of AAV9-CaMKII.Cre into the adult mice. (A) Schematic illustrating the protocol for AAV9 injection, tissue collection and imaging. Four weeks after tail vein injection of AAV9-CaMKII.Cre into *Rosa26Td*^{Tomato} adult mice 6 weeks of age, resulted in tdT (red) expression in the MP, SMP and mucosa of the small **(B1, C1 and D1)** and large intestines **(B2, C2 and D2)**, respectively. Nuclei were identified with DAPI (grey). Images were acquired from the serosa to the mucosal layers from the same tissue. Scale bar: 150 µm. Images representative of three experiments.

3.2.3.2 AAV9-KASHeGFP drives expression of GFP protein to the nuclear envelope of neurons from the MP and SMP of adult mouse intestine

Our previous result suggests that AAV9 is an efficient strategy to label enteric neurons in the adult mice. However, the isolation of these cells from adult intestines is still a challenge to be addressed. To approach this, Dr Obata generated a new vector which included the CaMKII promoter and KASH in combination with a fluorescent protein (section 2.2.4). Given the ability of AAV9 to transduce ENS, specifically enteric neurons, CaMKII-KASHeGFP or td^{Tomato} vectors were inserted into this serotype and expected to efficiently result in the expression of eGFP into enteric neurons. Adult male mice, 6 weeks of age were injected systemically via tail vein with AAV9-CAMKII-KASHeGFP/td^{Tomato} (section 2.2.4). Duodenum, jejunum, ileum, proximal, middle and distal colons were collected 4 weeks post-injection.

To determine the efficiency of neuronal transduction, immunohistochemistry to detect GFP and the pan-neuronal marker PGP9.5 was performed in LMMPs from distinct areas of the gut. GFP expression was detected within the nuclear membrane of all regions of the intestinal tissue, including duodenum, jejunum, ileum, proximal, middle and distal colons **(Figure 3.6A-F)**. To analyse the efficiency of enteric neuron transduction, the percentage of cells co-expressing GFP and PGP9.5 was quantified. The average of neuronal transduction ranged from 51% to 91% depending on the area of the intestine analysed. GFP expression was more abundant in the duodenum (90.9% of 1105 PGP9.5$^+$ counted cells), followed by the jejunum (81.4% of 1115 PGP9.5$^+$ cells), ileum (89.2% of 1003 PGP9.5$^+$ cells), and proximal colon (84.8% of 1308 PGP9.5$^+$ cells). Surprisingly, in the middle (51.37% of 1032 PGP9.5$^+$ cells) and distal colons (61% of 754 PGP9.5$^+$ cells), the efficiency of neuronal transduction was decreased **(Figure 3.6G and Table3.1)**. In addition, GFP expression was found in the majority of neurons in the submucosal ganglia from the small intestine **(Figure 3.6G)** and colon **(Appendix 4)**.

In summary, these data suggest that AVV9-KASHeGFP efficiently transduce enteric neurons in all regions of the GI tract. However, transduction of enteric neurons is reduced in middle and distal colons.

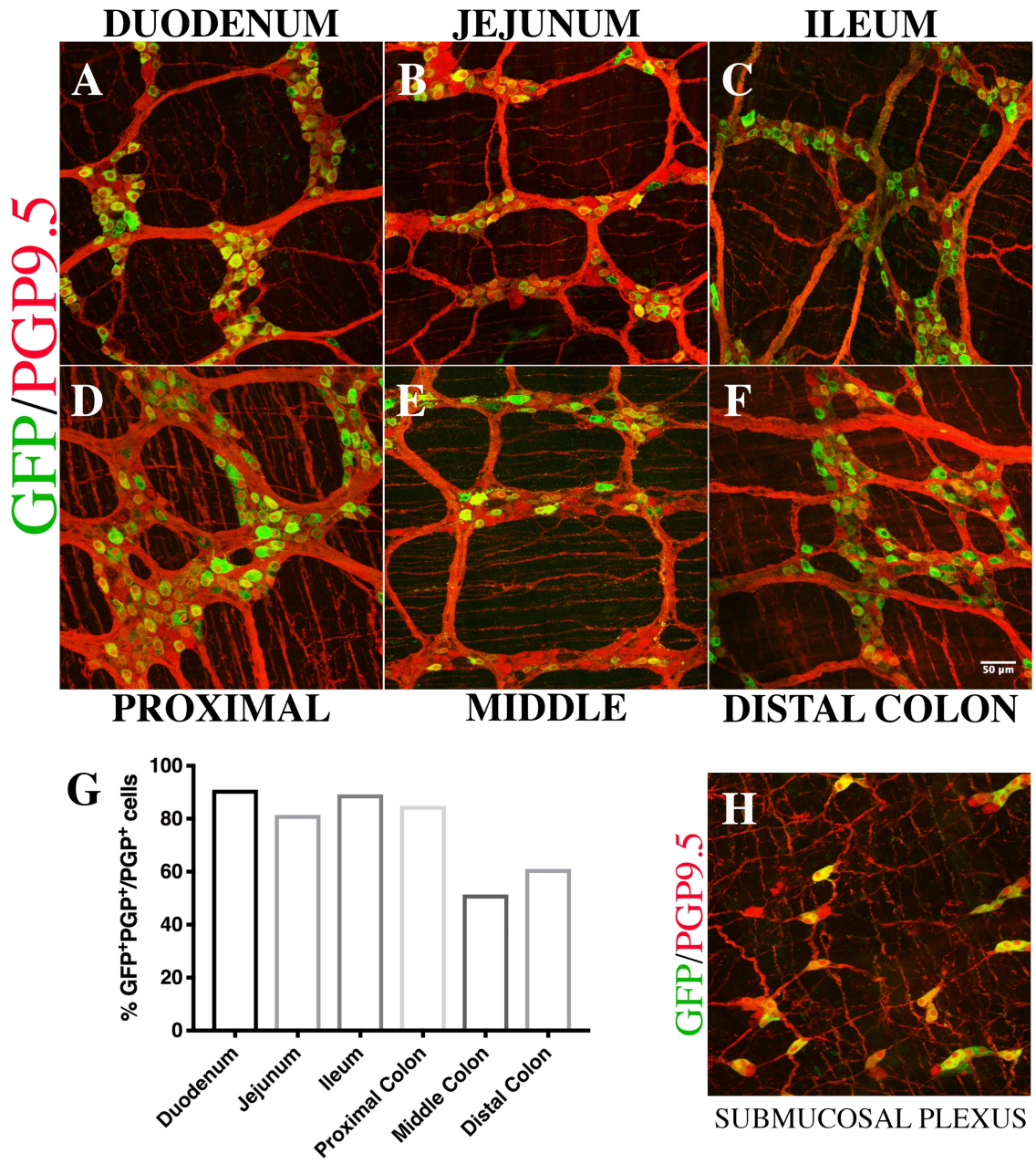


Figure 3.6. GFP expression within the MP following tail vein injection of AAV9-KASHeGFP into adult wildtype mice. Confocal images show the expression of GFP (green) on LMMP preparations immunostained for the neuronal marker PGP9.5 (red) from the duodenum **(A)**, jejunum **(B)**, ileum **(C)**, proximal colon **(D)**, middle colon **(E)** and distal colon **(F)** four weeks after systemic injection of AAV9-KASHeGFP into wildtype mice. **(G)** Quantification of the percentage of $GFP^+PGP9.5^+$ myenteric neurons across different regions of the gut suggests a reduction of neuronal transduction in the middle and distal colons. Results are pooled from two independent experiments (n=2). Because of the nature of this exploratory experiment and the low sample size, statistical analysis was not completed. **(H)** GFP^+ cells (green) were identified in $PGP9.5^+$ neurons within submucosal plexus of the small intestine. All images were acquired using the same magnification. Scale bar: 50 µm.

Table 3.1 Quantification of GFP$^+$ neurons within the MP

Regions	Total PGP9.5$^+$ neurons	Total GFP$^+$ cells	Number of mice
Duodenum	1105	1062	2
Jejunum	1115	1000	2
Ileum	1003	892	2
Proximal Colon	1308	1151	2
Middle Colon	1032	477	2
Distal Colon	754	452	2

Quantification of total transduced and non-transduced myenteric neurons within the MP in different regions of mice injected with AAV9-KASHeGFP (n=2).

3.2.3.3 Chemical coding of AAV9-KASHeGFP transduced neurons in the MP and SMP from the small intestine of adult mice

To determine whether specific neuronal subtypes were excluded or preferentially transduced by AAV9-KASHeGFP, LMMP preparations from the small intestine were labelled by immunohistochemistry to detect most prominent neuronal subtypes. GFP was combined with other neuronal markers and the co-localization of those markers are highlighted in the following images with a white arrowhead. AAV9 mediated the expression of GFP in the nuclear membrane of NOS1$^+$ inhibitory motor neurons **(Figure 3.7A1)** and Calretinin$^+$ excitatory motor neuron **(Figure 3.7A2)**. VIP$^+$ neurons are rare within the MP, but we also found few VIP$^+$ neurons expressing GFP **(Figure 3.7B1)**. ChAT population was efficiently transduced by AAV9 and co-localised with GFP expression **(Figure 3.7B2)**. NPY$^+$ neurons are very few within the MP, and we were not able to confirm the transduction of this neuronal subtype by immunohistochemistry **(Figure 3.7C)**. In the submucosal ganglia, the VIP population seems to be increased, and GFP was detected within these cells **(Figure 3.7D),** as well as in NOS1$^+$ and Calretinin$^+$ neurons **(Figure 3.7E)**.

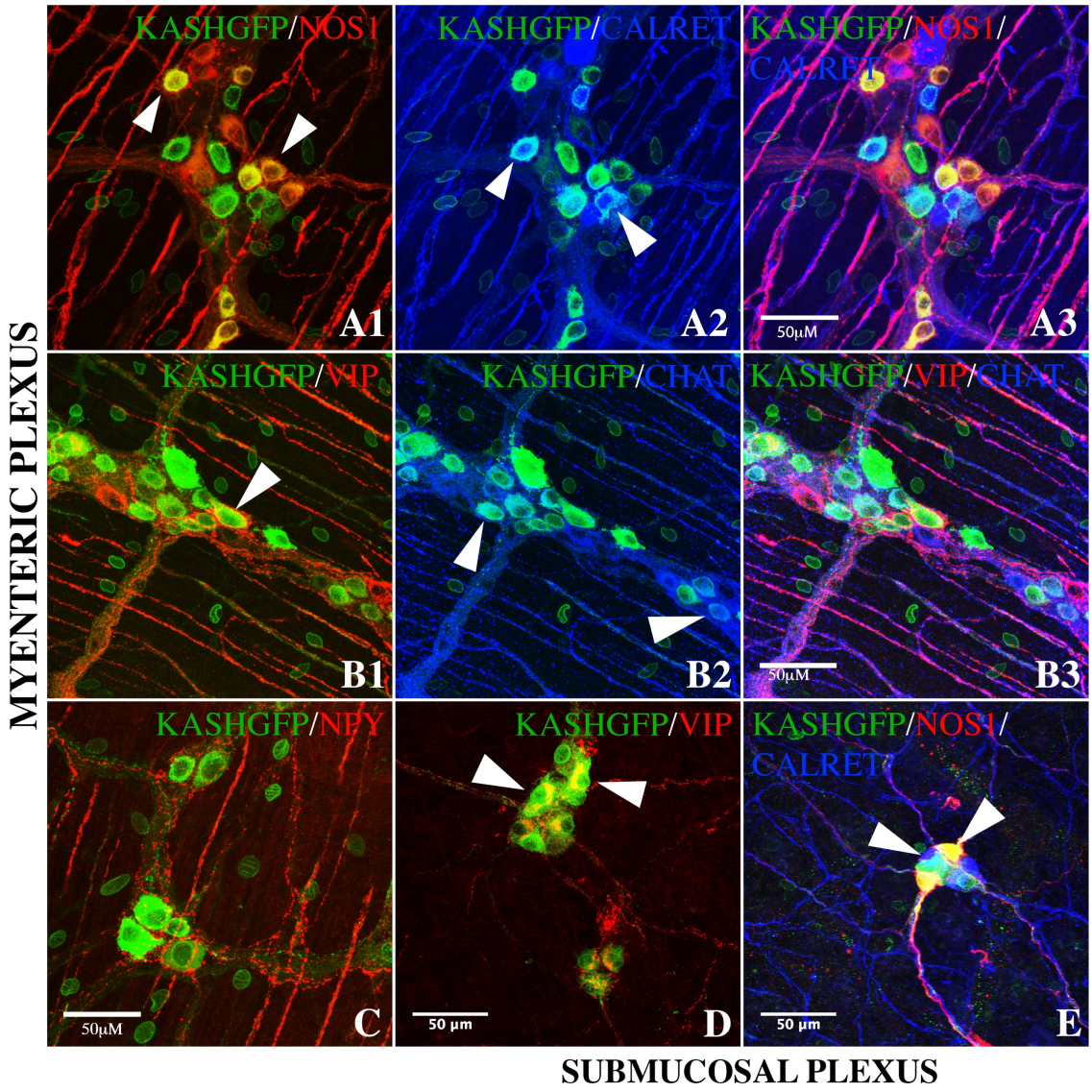


Figure 3.7. Chemical coding of transduced myenteric and submucosal GFP$^+$ neurons from the small intestine after AAV9-KASHeGFP systemic injection. (A-E) Confocal images of the myenteric and submucosal plexuses from the small intestine of wildtype mice injected with AAV9-KASHeGFP. Arrowheads indicate double-positive cells (GFP$^+$/Neuronal subtype$^+$). GFP expression (green) was detected in NOS1$^+$ (red) **(A)**, Calretinin$^+$ (blue) **(A2)**, VIP$^+$ (red) **(B1)**, ChAT$^+$ (blue) **(B2)** neurons within the MP. **(C)** Transduction of NPY$^+$ neurons (red) was not detected. In the SMP, GFP was detected in VIP$^+$(red) **(D)**, Calretinin$^+$ (blue) and NOS1$^+$ (red) **(E)** neurons. Scale bars: 50 µm. Representative images of three independent experiments.

Some populations of GFP$^+$ cells but which were negative for any other neuronal markers were observed outside the MP in the small intestine. This group expressed GFP/tdT at lower levels and presented smaller cell bodies when compared to enteric neurons. To note, neuronal cell bodies are not found outside ganglionic structures. To investigate which non-

neuronal cell population was possibly transduced by AAV9, LMMPs were dissected and immunohistochemistry performed to detect EGCs (Sox10), macrophages (Iba1), T lymphocytes (CD3) and ICCs (c-Kit). Wildtype mice were injected with AAV9-KASHTdT and AAV9-KASHeGFP to transduce the ENS. Yellow arrowheads were placed on figures to identify non-neuronal transduced cells. EGCs Sox10^{+} did not colocalise with tdT^{+} expressing cells **(Figure 3.8A)**. Moreover, neither Iba1^{+} macrophages nor CD3^{+} T cells expressed tdT **(Figure 3.8B)**. Surprisingly, c-KIT^{+} ICCs colocalised with the extraganglionic GFP expressing cells in the small intestine **(Figure 3.8C)**. Interestingly, extraganglionic GFP^{+} cells were undetectable in the colon stained for c-KIT **(Figure 3.8D)**.

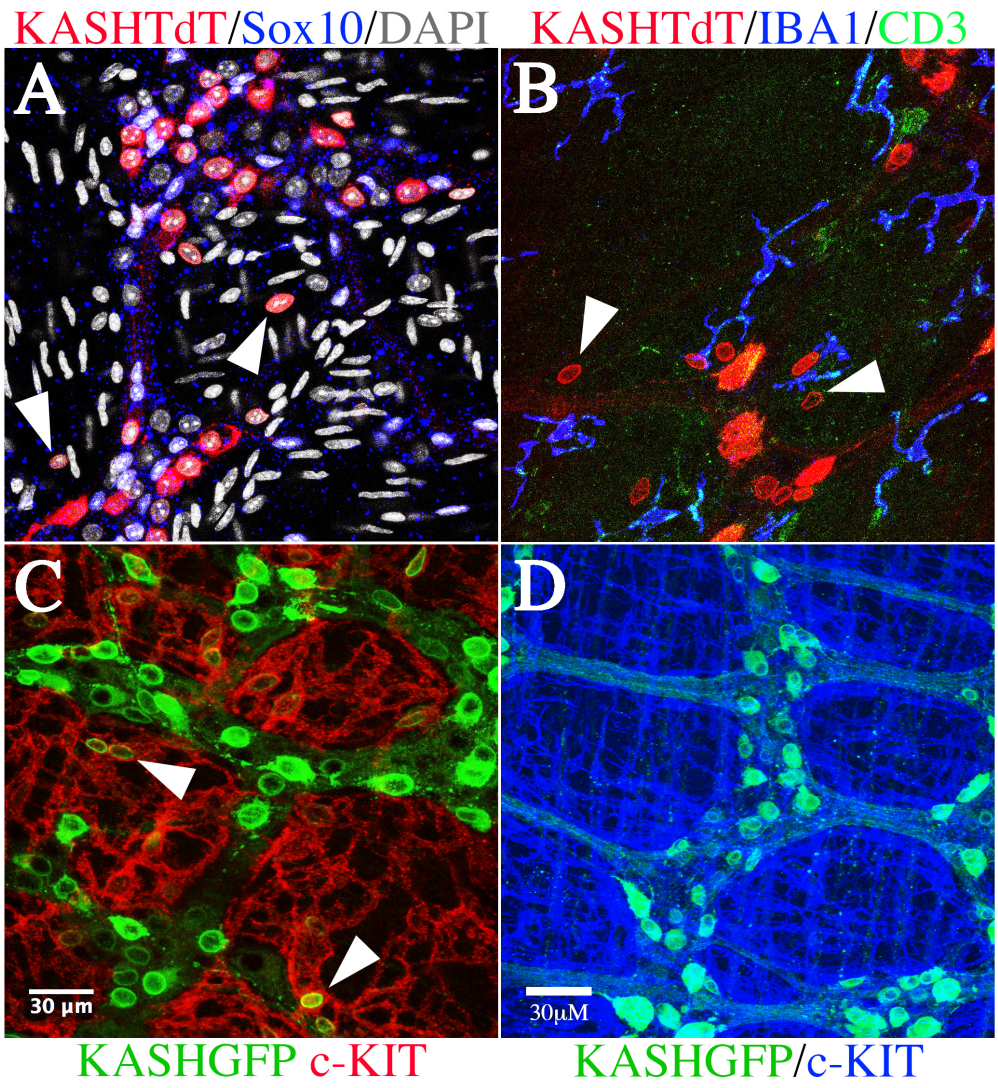


Figure 3.8. Identification of extraganglionic non-neuronal cells in LMMPs of mice transduced with AAV9-KASHtdT and AAV9-KASHeGFP. Confocal images of LMMPs from the small intestine **(A-C)** and

colon **(D)** of mice injected with AAV9-KASHtdT (top panel) **(A and B)** and AAV9-KASHeGFP (bottom panel) **(C and D)**. **(A)** Immunohistochemistry for the EGC marker Sox10 (blue) in mice injected with AAV9-KASHTdT. **(B)** Immunohistochemistry for the macrophage marker Iba1 (blue) and T cell marker CD3 (green) in mice injected with AAV9-KASHtdT. **(C)** Image shows the colocalization of extraganglionic GFP expressing cells with c-KIT$^+$ ICCs in the small intestine. **(D)** Extraganglionic GFP expressing cells were not detected in the colon. White arrowheads highlight the position of extraganglionic transduced cells. Scale bars: 30 µm. Representative images of three independent experiments.

3.2.3.4 Efficient isolation of enteric neuronal nuclei from the MP of mice transduced with AAV9-KASH-eGFP/tdT

Enteric neuronal nuclei isolation

A recently published protocol which describes a successful isolation of post-mortem neurons for single-nRNAseq was adapted for the isolation of enteric neuronal nuclei (Krishnaswami et al., 2016). For enteric neuronal nuclei isolation, at first, young C57Bl/6 wildtype male mice were systemically injected with either AAV9-KASHeGFP or AAV9-KASHtdT following the same strategy described above. Four weeks post-injection, the small intestine was removed and LMMPs isolated on ice (section 2.2.2.2). After dissection, LMMPs were transferred into a 1.5 mL plastic tube and cut into small pieces using fine scissors. Next, samples were transferred into a homogeniser containing a small volume of NIM2 buffer (1.5 M sucrose, 1M KCl, 1 M Tris buffer - pH 8.0, nuclease-free water, 1 mM DTT, 50x protease inhibitor and DAPI) and further triturated. Of note, this buffer contains detergent to lyse the cell membrane and this step is crucial for the acquisition of sufficient nuclei numbers. Following, the suspension already containing single nuclei was filtered into a 50 mL plastic tube, and the remaining tissue held in the strain was passed into a new 1.5 mL plastic tube, and again triturated by using a plastic pestle. The homogenate was transferred into a 50 mL plastic tube and centrifuged at 4ºC for 8 min at 1000 g. Finally, the precipitate was resuspended in NIM2 and submitted for nuclei sorting by FACS **(Figure 3.9A)**.

Although the isolation of enteric neuronal nuclei seems trivial, critical steps need to be followed, including the setting of appropriate FACS parameters. Different from live cell sorting, nuclei homogenates do not include viability markers. Instead, the gating strategy is based on the integrity of nuclei analysed by singlet DAPI$^+$ nuclei **(Figures 3.9B1 and B3)**. P1 includes a population with intact DAPI$^+$ nuclei and devoid cellular debris. Next, FSC-

Height (FSC-H) vs FSC-Area (FSC-A) gate was used to exclude the doublet events, followed by FSC and SSC to double select singlet nuclei **(Figures 3.9B3 and B4)**. Nuclei were then separated by the intensity of the fluorophore, into cells that are positive and negative for the marker of interest. In this case, nuclei isolated from the AAV9.KASHeGFP injection, the separation of $eGFP^+$ and $eGFP^-$ neuronal nuclei was assigned according to cells expressing high levels of eGFP. The gate to select the positive population is very strict as a non-neuronal expressing eGFP population was observed in the previous experiments and wanted to be avoided. As the non-neuronal expressing eGFP cells have lower levels of the fluorescent protein and their nuclei can be excluded by adjusting the gate **(Figure 3.9B5)**. The numbers of nuclei isolated per mice can vary according to the efficiency of transduction, length of the gut, nuclei isolation technique and gating strategy from 15-50K $eGFP^+$ nuclei (observed in n>5 experiments). However, on average, at least about 15.000 nuclei should be isolated from the adult small intestine by using this strategy. AAV9-KASHtdT were also used for pilot experiments, and the FACS profile was similar to the AAV9-KASHeGFP (data not shown).

To confirm the purity of nuclei populations separated by FACS, RNA was isolated from AAV9-KASHeGFP ($eGFP^+$ and $eGFP^-$ nuclei), and AAV9-KASHtdT (tdT^+ and tdT^- nuclei) samples. To test the identity of isolated cells, qRT-PCR was performed by using Taqman probes to amplify specific neuronal and glial markers within the positive and negative populations for eGFP and tdT. Interestingly, well-known pan-neuronal markers *Ret* and *Elavl3* (HuC) were expressed only in eGFP and tdT positive nuclei isolated samples, and not detectable (nd) in the negative nuclei isolated pool **(Figure 3.9C - top panel)**. On the other hand, EGC markers *S100* and *Sox10* were expressed by the negative nuclei isolated cells and not detectable either in the $eGFP^+$ or tdT^+ groups **(Figure 3.9C - bottom panel)**. Together, these data suggest that we have successfully generated and characterised a novel method to label and isolate enteric neurons from the MP of the small intestine of adult mice.

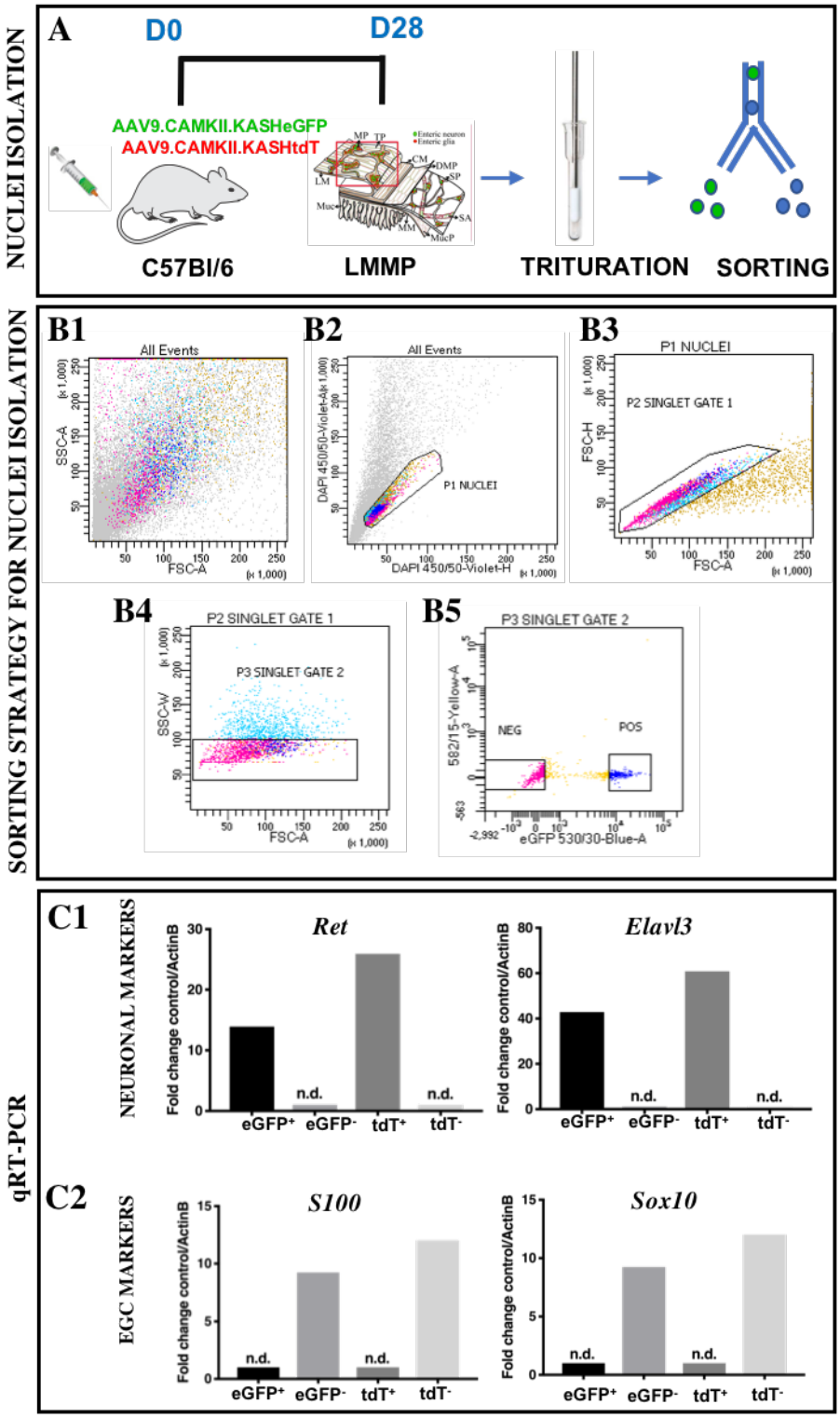


Figure 3.9. GFP$^+$ and tdT$^+$ neuronal nuclei isolation from the MP of the small intestine in mice injected with AAV9-KASHeGFP and AAV9-KASHtdT. (A) Schematic illustrating the procedure for the isolation of neuronal nuclei. FACS gating on eGFP$^+$ neuronal nuclei. **(B1)** The first plot shows all events after loading the samples into the machine. **(B2)** Plot 2 shows the gate on the intact DAPI$^+$ nuclei and elimination of debris. **(B3-B4)** Plot 3 and 4 show the strategy to eliminate doublet and select singlet nuclei. **(B5)** Plot 5 gates on DAPI$^+$ singlet nuclei and separate into eGFP$^+$ and eGFP$^-$ populations. qRT-PCR shows transcript expression

levels of the neuronal markers *Ret* and *Elavl3* (top graphs) **(C1)** and EGC *S100* and *Sox10* (bottom graphs) **(C2)** in FACS isolated $eGFP^+$, $eGFP^-$, tdT^+ and tdT^- samples. The relative expression of each gene was normalised by *Actinb*. Due to low sample size the nature of pilot experiments, statistical analysis was not completed. Graph and FACS plots represent one experiment collected from three independent experiments. More experiments were performed and will be shown in Chapter 5.

3.2.4 Discussion

Enteric neurons are extremely heterogeneous in their molecular properties, morphology and physiology. These cells, along with EGCs participate in many aspects of the GI function and form a mosaic of an intricate network that it is localised in between layers of muscle cells within the intestinal wall (John Barton Furness, 2006). Recently, many strategies have been applied to explore the development of enteric neuronal landscape and function by using genetic cell-fate maps of embryonic and newborn enteric neurons (Lasrado et al., 2017; Memic et al., 2018). The generation of genetic tools to label and manipulate specific genes has improved the understanding of given molecules for neuronal maintenance, and as a consequence, on the development of ENS (Sasselli et al., 2013; Schuchardt et al., 1994). However, studies revealing the molecular mechanisms by which adult enteric neurons respond to the intestinal environment in health and disease are still poorly elucidated. The reason for the lack of information on specific features of adult enteric neurons is because the manipulation of these cells is challenging in adult gut, hampering the progress in adult enteric neuronal research.

To address this, we used a recently generated method to deliver genetic material into cells of interest based on AAV transduction. Our choice of AAV9 serotype was based on publications suggesting that this serotype, among others, has a tropism for cells of the nervous system and efficiently transduce the ENS (Gombash et al., 2014). We confirmed this finding by using the commercially available AAV9.CaMKII.Cre adenovirus introduced systemically into *Rosa26tdT* reporter adult mice. We observed that AAV9 efficiently transduced neuronal cell bodies within the myenteric and submucosal plexuses in the small and large intestines. This model can be useful to explore the anatomical interactions between neurons and other cell types within the intestinal wall. Importantly, it also favours the visualisation of enteric neuronal network, and therefore can be possibly used to study the morphological aspects and alterations of enteric neurons in pathologies that affect the GI function, for example, IBD. One disadvantage of the AAV9.CaMKII.Cre method is the

necessity of using transgenic mice to induce the expression of a fluorescent reporter into cells of interest, which prevents the application of this tool in wildtype conditions. To overcome this limitation, preliminary experiments in our lab have shown that co-injections of AAV9.CaMKII.Cre with a Cre-dependent AAV is feasible and allows specific targeting of enteric neurons in wildtype mice.

In addition, Dr Obata and I have developed a novel strategy to label the nuclei of adult enteric neurons with a fluorescent protein (GFP) under the control of the neuronal promoter CaMKII, and transfected this vector into an AAV9 serotype *(Obata et al. in preparation)*. We characterised the enteric neuronal transduction by AAV9-CaMKII-KASHeGFP in several areas of the intestines, and observed that GFP was expressed in enteric neurons (PGP.9.5$^+$) in the MP from the duodenum, jejunum, ileum, proximal colon, middle and distal colons, as well as in the SMP. Moreover, the efficiency of transduction was about 90% in the small intestine and proximal colon. However, in the middle and distal colons, neuronal transduction was reduced to 50-60%. In the literature, Gombash et al. observed about 25 to 57% neuronal transduction along the intestine by using AAV9.CB/CMV/GFP and did not detect any major differences between distinct parts of the colon (Gombash et al., 2014). In our model, enteric neuronal transduction was more efficient in the small intestine and proximal colon, and the percentage in the middle and distal colons was surprisingly similar between these two studies. Besides, Buckinx et al. observed about less than 30% transduction efficiency in enteric neurons from the MP of the small and large intestines in mice that were injected in the temporal vein at P1 and collected at P35 (Buckinx, Van Remoortel, Gijsbers, Waddington, & Timmermans, 2016). Moreover, by using a local injection of AAV9 into the serosa of adult rat gut, Benskey et al. observed that at 4 weeks post-infection the transduction of myenteric neurons was about 70% (Benskey et al., 2015). By comparison, multiple reasons could explain the differences in efficiency of transduction between these studies, including the promoter, titre and route of injections, age and species of animals, duration of injection, as well as the parameters to count cells. Despite the reduction in efficiency of neuronal transduction in the distal part of the colon, we were able to successfully label the majority of enteric neurons in the intestines.

To determine whether the transduction of AAV9 in our model favoured or excluded any neuronal subsets, we examined the colocalization of neuronal subtype makers with GFP in the MP. We observed GFP expression in the main subtypes of NOS1$^+$, Calretinin$^+$, ChAT$^+$ and VIP$^+$ neurons. VIP$^+$, NOS1$^+$ and Calretinin$^+$ neurons expressing GFP were also

identified within the SMP. However, GFP expression in NPY^+ neurons were be very low or undetectable. Even though different subsets of neurons were transduced by AAV9, we aim to further investigate other subtypes by using our data from nRNAseq.

Although recent studies have reported the use of AAV9 delivery system to transduce adult enteric neurons (Benskey et al., 2015; Buckinx et al., 2016; Gombash et al., 2014; Gombash et al., 2017), the application of this method in understanding neuronal characteristics is still to be explored. One of the reasons why enteric neurons are under-studied is because of the difficulty in isolating intact whole cells. This is due to the complexity of enteric neuronal network and their location within the gut wall. Mechanical and chemical manipulation of enteric neurons can cause considerable damage to those cells. Because of the same reason, a new protocol was generated to isolate the nuclei of neurons from the CNS. Krishnaswami et al. have used single nuclei from CNS neurons for nRNAseq, and claimed that the nuclei expression signature is very similar to those acquired from entire cells (Krishnaswami et al., 2016). By combining AAV9 delivery system with nuclei isolation of neurons from the MP, we were able to isolate intact neuronal nuclei from adult mice. We confirmed this finding by analysing the transcript expression of neuronal specific markers in positive populations sorted by FACS. Interestingly, this population did not express EGC markers, such as *Sox10* and *S100*, but expressed *Ret* and *Elavl3* transcripts.

One disadvantage of the AAV9.CAMKII.KASHeGFP method is that we found a small population of non-neuronal extraganglionic GFP expressing cells in the small intestine only. By immunophenotyping these cells, we found that they were c-KIT^+ ICCs. ICCs are considered the pacemakers of the gut through their ability to electrically stimulate enteric neurons to propagate MMCs. The function of ICCs and their interactions with the ENS are still not clear. By constraining the gate parameters in the FACS machine, we could eliminate these cells from our preparations.

The nuclei isolation is a novel and very useful method that can be applied for bulk RNA sequencing. This technique has already been used to compare the transcriptomes of enteric neurons from the small intestine and colon, in addition to its use in investigating the role of the intestinal microbiota in modulating the enteric neuronal transcriptional landscape (Obata et al., *manuscript in preparation*). We have also applied the isolation of neuronal nRNAseq to investigate the effect of the adaptive immune system on neuronal transcriptome. These data will be further discussed in chapter 5. Modifications of this strategy by using antibodies against nuclear antigens can also be considered for the isolation of nuclei from

intestinal samples. Pilot experiments have been performed in our lab and this method is feasible and needs adaptations. This would allow the isolation of nuclei from biopsies or surgical samples that could be used to analyse the transcriptional profile of human enteric neurons, and perhaps can also be used to study other cell types.

In conclusion, we characterised and suggested a novel strategy that can be successfully explored to study the adult enteric neuronal features, including their molecular and morphological properties. Adeno-associated viral vectors can also be considered in the future to manipulate important genes expressed in the adult enteric neurons.

Chapter 4

Impact of gut states on ENS physiology

4. Chapter 4 | Impact of gut states on ENS physiology

This chapter presents our work on the responses of the ENS to non-physiological or pathological states of the gut, such as the absence of microbiota or inflammation. The microbiota study using GF mice was performed in collaboration with colleagues at the Institute of Food Research (currently part of the Quadram Institute of Bioscience) in Norwich, UK, who provided us with these animals. As described in the introduction, the effects of intestinal microbiota on ENS homeostasis are still under investigation. This project set out to build on a recent publication from our lab, which suggested that the gut microbiota modulates the homeostasis of the mucosal EGCs (Kabouridis et al., 2015), and focus on the effects of commensal microorganisms on the MP. We examined whether the absence of microbiota had an impact on EGCs and neuronal homeostasis and function in the adult mice.

In addition, we investigated the response of the ENS to intestinal inflammation by analysing the $TNF^{\Delta ARE}$ and $CD45RB^{hi}CD4^{+}$ adoptive transfer mouse models, which mimic the pathophysiology of human inflammation. Experiments using the adoptive colitis model were performed in collaboration with Dr Mark Wilson, a former group leader at the National Institute for Medical Research (NIMR), London, UK.

Understanding the changes in organisation and function of the ENS resulting from altered microbiota status or inflammation is likely to provide novel insight into the role of the ENS in gut physiology and disease pathogenesis.

4.1 Introduction

The GI tract is composed of different tissue systems that work in concert to control intestinal homeostasis and function. In the healthy gut, the balanced interaction between microbiota, immune system and enteric nervous system is critical for digestive physiology. However, due to its location at the interface between the internal milieu and external environments of the body, the GI tract encounters multiple challenges that can disturb the integrity of each of these systems resulting in pathological conditions, such as IBDs (Gensollen et al., 2016; Sun, He, Cong, & Liu, 2015), and abnormal GI physiology. It has also been proposed that the intestinal microbiota-immune axis has considerable impact in disorders that affect the CNS, including stress, anxiety, depression, and neurodegenerative pathologies such as Alzheimer and Parkinson's diseases (Fung, Olson, & Hsiao, 2017). Nevertheless, our current understanding of the effects of microbiota on the development and function of the ENS is still limited.

The role of the microbiota on the ENS

Due to its anatomical positioning within the GI wall, the ENS is exposed to an extremely rich environment comprised of a diversity of immune cells and microbial products. Although enteric neuronal cell bodies are confined within ganglionic structures located in between the intestinal muscular layers, these cells project their axons to the lamina propria and can sense microbial products (J. B. Furness, 2000). Unlike enteric neurons, EGCs are also found within the mucosal layer (Boesmans et al., 2015; Gulbransen & Sharkey, 2012) and colonisation of the lamina propria by EGCs depend on postnatal establishment of microbial communities in the gut (Kabouridis et al., 2015). EGCs and neurons express PRR receptors, such as TLR2 (Brun et al., 2013), TLR4 (Anitha et al., 2012) and TLR9 (Burgueno et al., 2016) which sense molecular components derived from the intestinal microbiota, suggesting that these cells can directly receive inputs from gut microbes. In these studies, it has been shown that the depletion or stimulation of TLRs in EGCs and neurons cause alterations in the homeostasis and function of the ENS (Anitha et al., 2012; Brun et al., 2013; Burgueno et al., 2016).

In vivo studies to investigate the role of microbiota in host tissues are generally performed by generating animal models born and reared under sterile GF conditions or colonised with specific and well-characterised groups of bacteria (gnobiotic mice). Despite the non-physiological conditions in which these animals are raised, the GF mouse model has proven very useful in understanding the role of intestinal microbes on the homeostasis of the ENS. Recent studies have shown that GF mice present reduced intestinal transit time (Anitha et al., 2012; De Vadder et al., 2018; Yano et al., 2015). Although it has been suggested that this results from changes in the organisation of the ENS, the role of the microbiota on ENS-dependent intestinal motility patterns in adult mice has not yet been reported. Previous work has also demonstrated that mucosal EGCs in the ileum, neuronal networks of the colon and the population of nitrergic inhibitory motoneurons in the MP are reduced in GF mice (Anitha et al., 2012; De Vadder et al., 2018; Kabouridis et al., 2015). Although exciting progress in the microbiota research has raised the possibility that microbes play a role on ENS homeostasis, these interactions still need to be further explored.

ENS response to intestinal inflammation

IBDs are chronic pathological conditions that alter the physiology of the GI tract of patients, causing symptoms such as diarrhoea, abdominal pain, bleeding and bloating (de

Souza & Fiocchi, 2016). IBDs include UC and CD affecting the colon and the ileum of patients, respectively. IBD is associated with extensive immune cell infiltration, epithelial permeabilisation caused by disruption of mucosal barrier integrity and changes in microbiota composition, including appearance of pathogenic microorganisms (dysbiosis). These changes are characterised by the unbalanced production of inflammatory cytokines, such as TNFα, TGFβ and INFγ, which are likely to contribute to the progression of the disease (de Mattos et al., 2015).

IBD can also promote structural abnormalities in the ENS in addition to the immunological manifestation of the disease (Geboes & Collins, 1998). Patients with CD present subtype-specific neuronal changes in the SMP, but the MP seems to be preserved in the colon. In the ileum, however, immunoreactivity for many neuronal subtypes is increased within the MP (Belai et al., 1997; Boyer et al., 2007; J. Schneider et al., 2001). In UC, in turn, the main ENS phenotype described in patients were in EGCs, which were reported to have increased numbers in the MP, followed by increased mRNA and protein levels for S100β, a characteristic enteric glia marker in humans (and other mammals) (Cirillo et al., 2009; Cirillo, Sarnelli, Esposito, et al., 2011; Villanacci et al., 2008). Nonetheless, studies on the effects of IBD on ENS homeostasis are still scarce due to the difficulties in accessing human tissues for research. To tackle this matter, animal models have been generated to mimic these pathologies and facilitate the understanding of the progression of the disease (described in more detail in chapter 1). Although they reproduce the general pathophysiological aspects of IBDs accurately, all models produce a more prominent phenotype on the ENS. For instance, in the TNBS and DNBS-induced CD and DSS-colitis models, a rapid and significant neuronal cell loss was reported following induction of inflammation (Boyer et al., 2005; Linden et al., 2005; G. X. Liu et al., 2014; Sanovic et al., 1999). Interestingly, neuronal cell death in these models appears to be dependent on EGCs. It has been reported that EGC mediators support the progression of inflammatory processes and neuronal damage suggesting that EGCs have a potential role in the progression of disease by modulating immune responses (I. A. Brown et al., 2016; G. X. Liu et al., 2014).

One animal model that displays a phenotype analogous to the human CD is the $TNF^{\Delta ARE}$ mice. AU-rich elements (ARE) are responsible for the regulation of mRNA stability. In these mice, deletion of ARE, which are located at the 3' untranslated region of TNF mRNA and are responsible for the regulation of its stability, resulted in chronic overproduction of TNF, leading to histological alterations and marked immune cell

infiltration in the distal ileum that resembles the CD histopathology. The advantage of this model compared to others is the spontaneous development of CD-like phenotype, that is more similar to the human disease. Homozygous $TNF^{\Delta ARE/\Delta ARE}$ mice show severe inflammation and increased rates of mortality by the first 2 to 4 weeks after birth. Heterozygous mice ($TNF^{\Delta ARE/+}$) in turn, have a slower progression of disease in which the first histological alterations start by around 8 weeks after birth, when there is a significant increase in $CD11b^+$ myeloid cells and $CD8^+$ T cells (Kontoyiannis et al., 2002; Kontoyiannis et al., 1999). TNF is one of the main cytokines in IBDs and is involved in the progression of this pathology. Indeed, recent clinical trials using anti-TNF antibodies have shown considerable success in controlling the evolution of intestinal symptoms in CD (Lovell et al., 2018). However, the cellular mechanisms by which TNF drives the progression of CD is still not clear. TNF production was observed mainly in hematopoietic and stromal cells, and its signals are transduced by the receptors TNFRI and TNFRII. Macrophages and monocytes are the primary sources of TNF production, but lymphocytes can also make significant amounts of this factor (Papadakis & Targan, 2000).

Another well-characterised model for studying chronic colitis and distal ileitis that more precisely reflects the severity of the disease is the T cell transfer model. The disruption in T cell homeostasis induces inflammation in this model. Adoptive transfer of naïve T cells ($CD45RB^{high}CD4^+$) from healthy wildtype mice into immunodeficient recipients, lacking T and B lymphocytes (*Rag1*$^{-/-}$ or *Rag2*$^{-/-}$) promotes pancolitis and inflammation in the distal part of the small intestine at 5-8 weeks after transfer. Signs of severe inflammation are observed in the accumulation of leukocytes transmurally, epithelial disruption and crypt hyperplasia, followed by drastic weight loss and diarrhoea. As in the $TNF^{\Delta ARE}$ mutant mice, the progression of inflammation in the adoptive transfer model is slow, and the very earliest intestinal alterations can be followed (Powrie, 1995; Powrie et al., 1994).

4.2 Aims

Given the limited information in how intestinal alterations such as the absence of microbiota and inflammation can modulate the ENS response, in the first part of this chapter, we aimed to further investigate the role of the microbiota on ENS homeostasis and function. In the second part, we took advantage of two well-characterised models, the $TNF^{\Delta ARE}$ and the T cell adoptive transfer to study the ENS response in the progression of intestinal inflammation.

The specific aims of this chapter were:

1. Assess the effects of microbiota on the organisation and function of the ENS.
2. Study the response of ENS to intestinal inflammation

4.3 Results

4.3.1 Gut microbiota modulates colonic function and homeostasis

Experimental set-up

In order to investigate the role of intestinal microbiota on ENS organisation and function, 3 SPF and 3 GF adult male mice, 11 weeks of age were used. SPF and GF mice had the same genetic background, and the GF group was born and raised in isolators under GF conditions in the Quadram Institute. These animals were transported in isolators into our Institute and checked for GF status (16S sequencing) immediately upon arrival by the microbiology facility at NIMR. GF mice were healthy and lacked microorganisms. To guarantee sterility in the procedures, animals were collected one by one, and the intestinal contents were double-checked for absence of microorganisms. The entire GI tract was carefully removed from the animal, the small intestine was divided into duodenum, jejunum and ileum and samples were collected for sectioning (section 2.2.2.3). LMMPs were dissected for RNA isolation and immunohistochemistry assays (sections 2.2.2.2, 2.2.15 and 2.2.6). In GF mice the cecum was enlarged, and that is one of the characteristics of this condition **(Figure 4.1)**. The large intestine was immediately removed, and about 1 cm of the proximal colon was dissected to separate the LMMP for RNA isolation and immunohistochemistry. The remaining colon was used for spatiotemporal analyses of colonic motility (section 2.2.13).

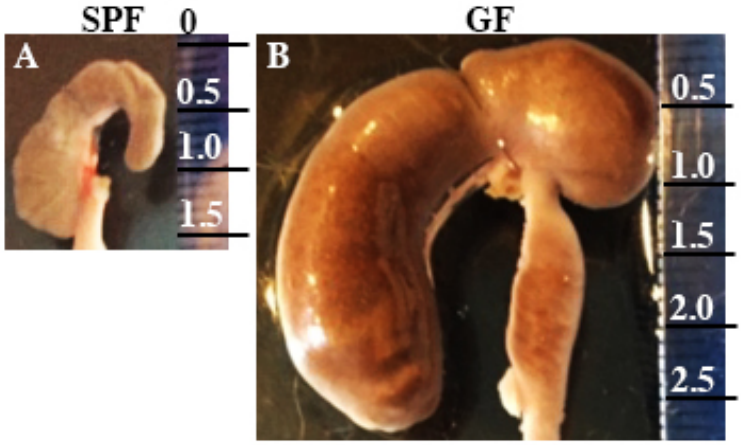


Figure 4.1. Comparison of the size of ceca dissected from SPF (A) and GF mice (B). Ruler on the left corner represents 0.5 cm between each black line.

Since the homeostasis of ENS networks within the mucosa were reported to be determined by microbiota (De Vadder et al., 2018; Kabouridis et al., 2015), we first examined the presence and organisation of EGCs and neuronal projections within the gut wall. To test that, we performed immunohistochemistry for the EGC marker S100β and the neuronal marker Calretinin on 14 μm thick transverse cryosections of segments from the duodenum, jejunum, ileum and proximal colon from SPF and GF mice. S100β is normally expressed in the soma and projections of EGCs within the muscle layers and mucosa, and Calretinin stains the cell body of motoneurons within the ganglia and their projections in the lamina propria. S100β$^+$ EGCs were observed within muscle layers, surrounding crypt areas and within the villi in both SPF and GF mice **(Figures 4.2A-H)**. Moreover, Calretinin$^+$ neurons were found within the ganglia, and their fibres tightly followed EGCs in all intestinal layers in the SPF group **(Figures 4.2A-H)**. In GF intestines, however, we observed Calretinin$^+$ fibres that were not in close association with mucosal EGCs, suggesting that the presence or immunoreactivity of mucosal EGCs for S100β is dependent on microbiota **(Figures 4.2B, D, F and H)**. Furthermore, in the duodenum and colon, immunoreactivity of mucosal EGCs for S100β and neuronal projections for Calretinin appeared to be reduced in GF mice relative to SPF controls **(Figures 4.2E-H)**.

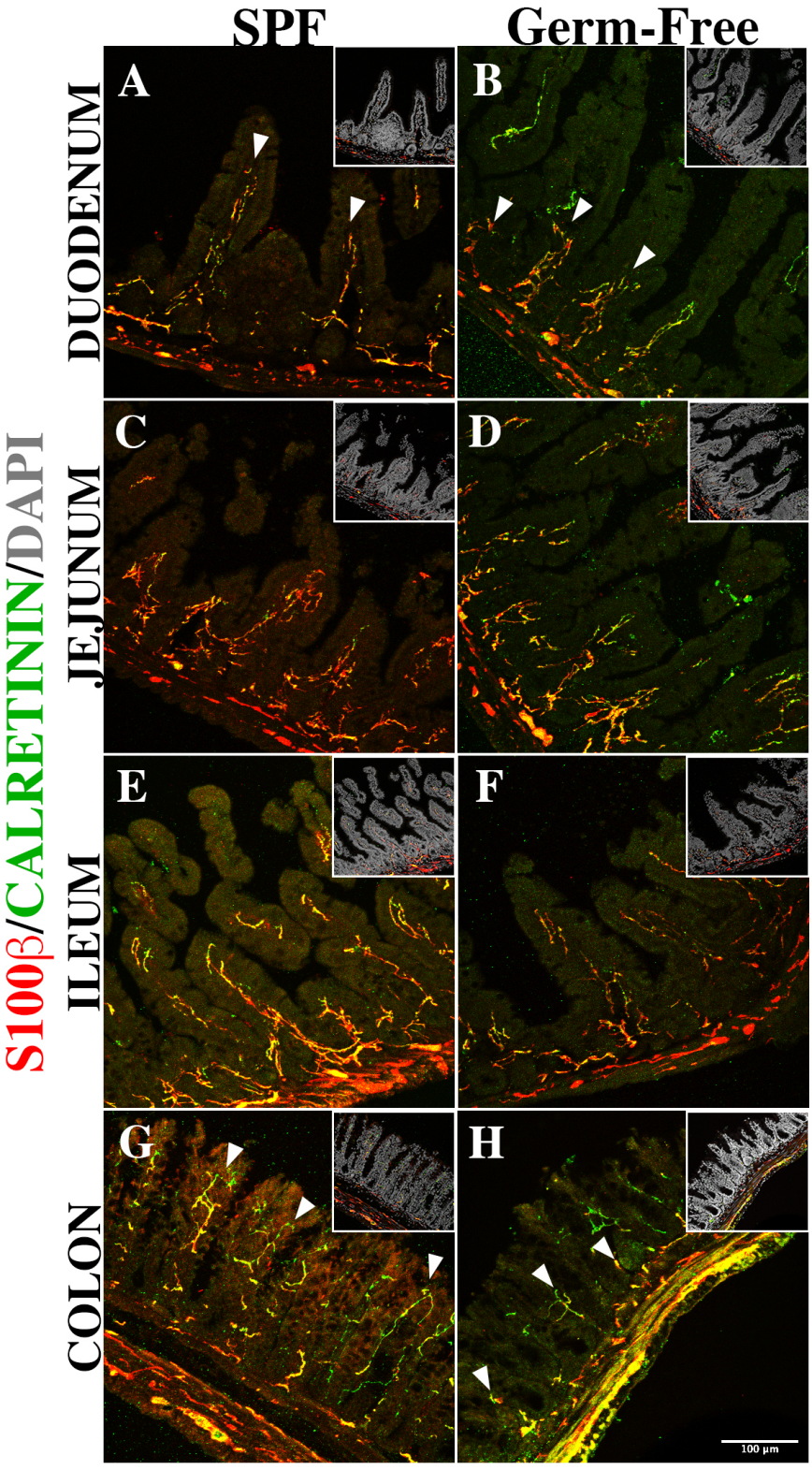


Figure 4.2. Enteric neural network in various segments of intestines of SPF and GF mice. Immunohistochemistry for the EGC marker S100β (red) and the neuronal cell marker Calretinin (green) on cross-sections of duodenum **(A, B)**, jejunum **(C, D)**, ileum **(E, F)** and colon **(G, H)** from SPF **(A, C, E and G)** and GF **(B, D, F and H)** mice. Nuclei were stained with DAPI (grey). Inserts on the top right corner of each

image show the overlay between S100β, Calretinin and DAPI. White arrowheads indicate S100β$^+$ EGCs. Scale bar: 100 μm. Representative images of three experiments (n=3).

Next, we examined the EGC population within the MP of the colon from SFP and GF mice by immunostaining whole-mount preparations of LMMPs with the EGC-specific markers S100β and the transcription factor Sox10. No gross morphological differences were observed in EGCs network in LMMP preparations between these two groups of mice **(Figure 4.3C)**. To compare more accurately EGC populations within the MP of SPF and GF mice, we quantified S100β$^+$ and Sox10$^+$ EGCs in a given area of image (section 2.2.10). We noticed a slight reduction in the numbers of EGCs in the GF group, but no statistically significant difference was observed in the density of either S100β$^+$ (SPF: 83.3 ± 19.18 SD and GF: 68.3 ± 5.7 SD) or Sox10$^+$ EGCs (SPF: 80 ± 19.6 SD and GF: 67.6 ± 5.8 SD) **(Figures 4.3D-E)**. In addition to the colon, we also examined EGC populations in LMMPs from duodenum, jejunum and ileum of SPF and GF mice. For these experiments, LMMPs were immunostained for the EGC markers GFAP, S100β and Sox10 and the percentage of GFAP$^+$Sox10$^+$ and S100β$^+$Sox10$^+$ cells were counted per area of image. We did not observe any differences between GF and SPF mice in the proportions of GFAP$^+$Sox10$^+$ EGCs (duodenum: SPF 29.6 ± 11.8% SD and GF 28.2 ± 11.8% SD *p>0.9999*; jejunum: SPF 22.1 ± 2.7% SD and GF 23 ± 1.09% SD *p>0.9999*; ileum: SPF 21.8 ± 8.9% SD and GF 20.5 ± 8.7% SD *p>0.9999*) **(Figure 4.3F and table 4.1)** or S100β$^+$Sox10$^+$ EGCs in any segments of the small intestine (duodenum: SPF 95.9 ± 2.9% SD and GF 91 ± 6.3% SD *p=0.4000*; jejunum: SPF 93.4 ± 2.6% SD and GF 93.4 ± 4.3% SD *p>0.9999*; ileum: SPF 88.9 ± 11% SD and GF 83.9 ± 13.2% SD *p=0.7000*) **(Figure 4.3G and table 4.1)**.

Next, we carried out comparative characterisation of major enteric neuron subtypes of the colon between SPF and GF mice. Whole-mount immunostaining of colonic LMMPs was performed in order to identify the total population of enteric neurons (HuC/D), the Calretinin-expressing excitatory motoneurons and the NOS1 positive inhibitory motoneurons. No gross morphological differences were detected in the network of calretinergic and nitrergic neurons between the SPF and GF groups **(Figure 4.3H)**. Moreover, quantification of the percentage of Calretinin$^+$HuC/D$^+$ (SPF: 40.64 ± 3.97% and GF: 42.79 ± 3.84% *p=0.2000*) and NOS1$^+$/HuC/D$^+$ (SPF: 39.28 ± 2.47% and GF: 43.47 ± 2.57% *p=0.2286*) neurons within the MP revealed no significant differences between the

SPF and GF groups **(Figures 4.3I-J)**. To assess the neuronal populations within the small intestine, we performed immunohistochemistry for Calretinin and NOS1 in LMMPs from the duodenum, jejunum and ileum of SPF and GF mice. The pan-neuronal marker HuC/D was used in order to identify the total population of enteric neurons. Cells that were positive for HuC/D and either Calretinin or NOS1 were counted and the average of the percentages of Calretinin$^+$HuC/D$^+$ and NOS1$^+$HuC/D$^+$ were plotted in the graphs. Our data indicate that the number and proportions of NOS1$^+$ (duodenum: SPF 25.7 ± 2.2% and GF 27.7 ± 2.7% *p=0.4000*; jejunum: SPF 27.1 ± 2.6% and GF 20.3 ± 0.7% *p>0.9999*; ileum: SPF 29 ± 2.8% and GF 27.2 ± 1.5% *p=0.4000*) **(Figure 4.3L and table 4.2)** and Calretinin$^+$ (duodenum: SPF 40.5 ± 6.5% and GF 40.5 ± 0.7% *p=0.7000*; jejunum: SPF 42.1 ± 4.7% and GF 30.6 ± 4.1% *p=0.8000*; ileum: SPF 42.1 ± 1.6% and GF 39.1 ± 1.3% *p=0.1000*) **(Figure 4.3K and table 4.2)** myenteric neurons were not altered in mice that were born and raised under GF conditions in any segments of the small intestine as well as the neuronal network was not changed. Our data disagree with previous studies that have reported reduced number of enteric neurons and changes in the percentage of nitrergic neurons within the MP in adult GF mice (Anitha et al., 2012).

Table 4.1 Quantification of EGC populations in the small intestine of SPF and GF mice

Duodenum	Total GFAP+	Total S100β+	Total Sox10+	Average % GFAP+Sox10+	Average % GFAP+S100β+	Average % S100β+Sox10+
SPF	519	1681	1753	29.6 ± 11.8% SD	30.1 ± 11.7% SD	95.9 ± 2.9% SD
GF	360	1161	1275	28.2 ± 11.8% SD	31 ± 15.5% SD	91 ± 6.3% SD
Jejunum						
SPF	378	1594	1707	22.1 ± 2.7% SD	23.7 ± 2.3% SD	93.4 ± 2.6% SD
GF	433	1752	1875	23 ± 1.09 %SD	24.7 ± 2.1% SD	93.4 ± 4.3% SD
Ileum						
SPF	281	1145	1288	21.8 ± 8.9% SD	24.5 ± 8.1% SD	88.9 ± 11% SD
GF	376	1538	1832	20.5 ± 8.7% SD	24.4 ± 10.2% SD	83.9 ± 13.2% SD

Quantification of GFAP$^+$Sox10$^+$, GFAP$^+$S100β$^+$ and S100β$^+$Sox10$^+$ EGCs in LMMP preparations of duodenum, jejunum and ileum from SPF and GF mice. N=3/per group.

Table 4.2 Quantification of enteric neurons in the small intestine of SPF and GF mice

Duodenum	Total NOS1+	Total Calretinin+	Total HuC/D+	Average % NOS1+HuC/D+ (SD)	Average % Calretinin+HuC/D+ (SD)
SPF	492	312	1213	25.7 ± 2.2%	40.5 ± 6.5%
GF	322	220	794	27.7 ± 2.7%	40.5 ± 0.7%
Jejunum					
SPF	426	274	1011	27.1 ± 2.6%	42.1 ± 4.7%
GF	301	200	983	20.3 ± 0.7%	30.6 ± 4.1%
Ileum					
SPF	411	284	976	29 ± 2.8%	42.1 ± 1.6%
GF	391	272	1000	27.2 ± 1.5%	39.1 ± 1.3%

Quantification of the percentage of NOS1^{+}HuC/D^{+} and Calretinin^{+}HuC/D^{+} enteric neurons in LMMP preparations of duodenum, jejunum and ileum from SPF and GF mice. N=3/per group.

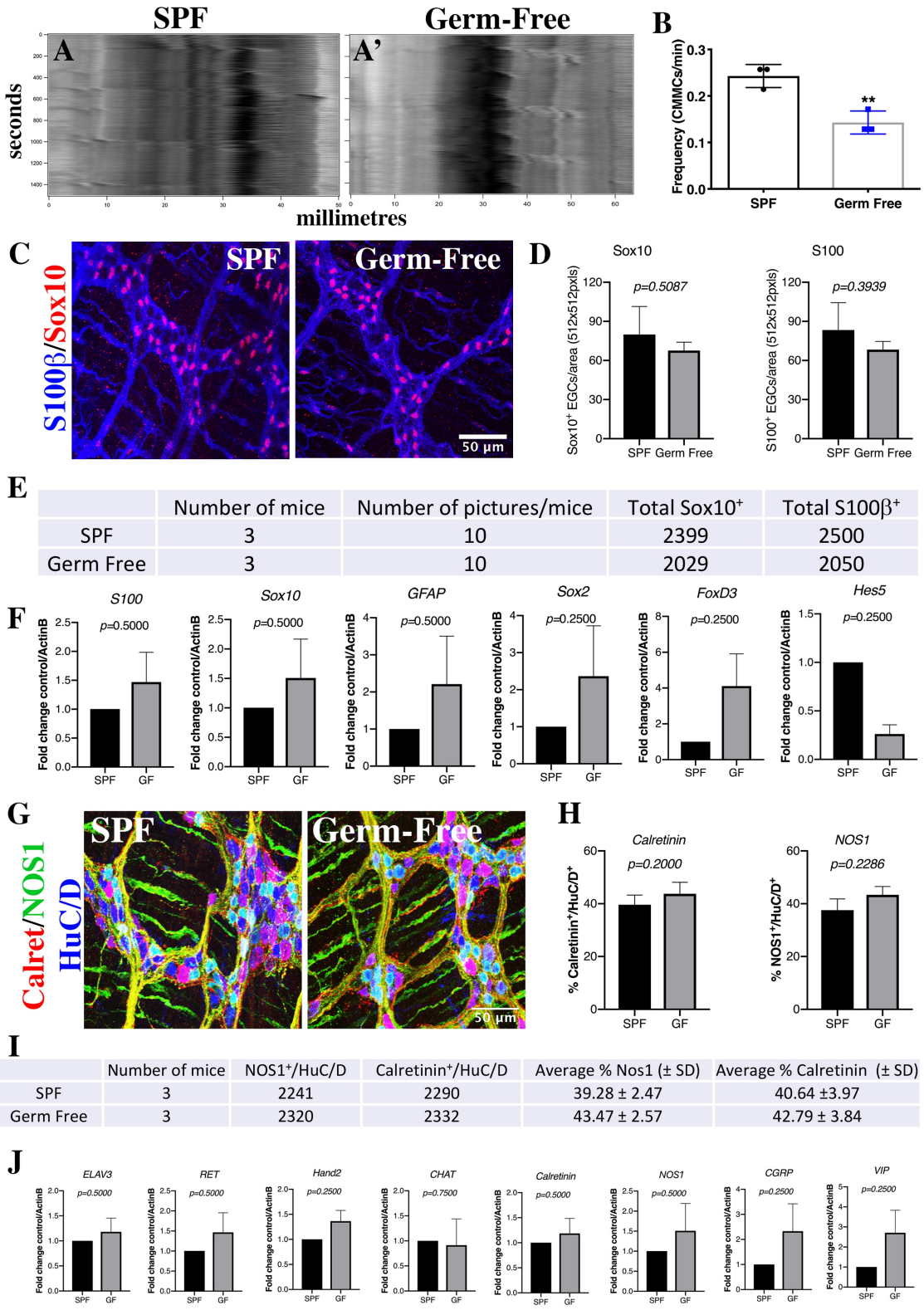
Impact of microbiota on intestinal neurogenic peristalsis

To investigate whether the presence of microbiota is necessary to modulate ENS-derived peristalsis, we video recorded the spontaneous peristaltic activity of isolated colonic segments from SPF and GF mice (Roberts et al., 2007; Sasselli et al., 2013). The video recordings allow us to generate spatiotemporal maps and quantify the frequency and distribution of CMMCs along the organ, which refer to the waves of contractions that propagate from the oral to the anal end of the colon (section 2.2.13) **(Figures 4.3A-A')**. The frequency of CMMCs was quantified by dividing the total number of CMMCs by the total recording time in minutes. Spatiotemporal maps showed that GF mice have a significant reduction in frequency of contractions (0.1 ± 0.48 CMMCs/min ** *p=0.0078,* Unpaired t-test with equal SD) when compared to SPF controls (0.2 ± 0.48 CMMCs/min) **(Figure 4.3B and table4.3)**, indicating the microbiota status influences the neurogenic activity of the gut.

Table 4.3 Quantification of CMMCs in SPF and GF mice

	Number of Mice	Total Time (min)	Average of CMMCs (23min)	Average of CMMCs/min (SD)
SPF	3	23.33	5.6	0.2 ± 0.48 SD
GF	3	23.33	3.3	0.1 ± 0.48 SD

Table represents the quantification of CMMCs in SPF and GF mice. Total time of recordings in minutes=23.33. The average of the number of CMMCs detected was 5.6 in SPF and 3.3 in GF mice. Average of CMMCs/min in the GF group was halved (0.1 CMMCs/min) compared to SPF controls (0.2 CMMCs/min) (n=3/group).



E

	Number of mice	Number of pictures/mice	Total Sox10$^+$	Total S100β$^+$
SPF	3	10	2399	2500
Germ Free	3	10	2029	2050

I

	Number of mice	NOS1$^+$/HuC/D	Calretinin$^+$/HuC/D	Average % Nos1 (± SD)	Average % Calretinin (± SD)
SPF	3	2241	2290	39.28 ± 2.47	40.64 ±3.97
Germ Free	3	2320	2332	43.47 ± 2.57	42.79 ± 3.84

Figure 4.3. Effect of the absence of microbiota on colonic ENS homeostasis and function. Spatiotemporal maps of colonic motility in SPF **(A)** and GF mice **(A')**. Y-axis represents the time in seconds and the X-axis the length of the gut in millimetre (mm). **(B)** Frequency of spontaneous CMMCs represented by the number of colonic contractions in a given time (1400 seconds) comparing SPF and GF groups. Each dot represents one animal. Unpaired student t-test with equal SD, ** $p < 0.01$. **(C)** Immunohistochemistry in colonic LMMPs for

the EGC markers S100β (blue) and Sox10 (red) from SPF and GF mice. Scale bar: 50 μm. **(D)** Quantification of total population of $Sox10^+$ and $S100\beta^+$ EGCs per area (512x512pxls) of the colon. Mann-Whitney test. **(E)** Table shows the total numbers of $Sox10^+$ and $S100\beta^+$ EGCs quantified in 10 pictures per 3 mice. Quantification of EGCs within LMMPs of the duodenum, jejunum and ileum from SPF and GF mice showing the percentage of $GFAP^+Sox10^+$ EGCs **(F)** and $S100\beta^+Sox10^+$ EGC populations **(G)**. **(H)** Immunohistochemistry in colonic LMMPs from SPF and GF mice for the pan-neuronal marker HuC/D (blue) and neuronal subtype-specific makers NOS1, to label inhibitory motoneurons (green) and Calretinin to label excitatory motoneurons (red). Scale bar: 50 μm. **(I)** Quantification of the percentage of $Calretinin^+$ and $NOS1^+$ enteric neurons over total HuC/D^+ neurons per area of image of segments from the duodenum, jejunum and ileum. Mann-Whitney test. **(J)** Table shows the total numbers of counted $NOS1^+HuC/D^+$ and $Calretinin^+HuC/D^+$ enteric neurons quantified in 10 pictures per 3 mice in SPF and GF groups, respectively. The average of the percentage of $NOS1^+HuC/D^+$ and $Calretinin^+HuC/D^+$ enteric neurons in SPF and GF mice are displayed in the table. Quantification of enteric neurons within the MP in duodenum, jejunum and ileum from SPF and GF mice demonstrating the percentage of $Calretinin^+HuC/D^+$ excitatory enteric neurons **(K)** and $NOS1^+HuC/D^+$ inhibitory enteric neurons **(L)**. Mann-Whitney test. N=3/group. Error bars indicate SD.

We further investigated the expression levels of specific EGC marker genes using qRT-PCR in colonic LMMP tissues from SPF and GF mice. We did not observe any significant differences in the transcription levels of *S100b (p=0.7000)*, *Sox10 (p=0.7000)*, *Gfap (p=0.7000)*, *Sox2 (p=0.1000)*, *Foxd3 (p=0.1000)* or *Hes5 (p=0.1000)* between SPF and GF in colonic LMMPs **(Figure 4.4A)**. Moreover, we quantified the levels of neuron-specific transcripts in LMMPs from SPF and GF mice using qRT-PCR. No significant differences were detected in expression levels of pan-neuronal markers such as *Elavl3* (encodes the HuC protein) *(p>0.9999)*, *Ret (p>0.9999)* and *Hand2 (p=0.4000)*, as well as genes expressed in excitatory motoneurons, such as *Chat (p=0.7000)* and *Calb2* (encodes de Calretinin protein) *(p=0.7000)*, or inhibitory motoneurons *as Vip (p=0.4000)* and *Nos1 (p=0.7000)*. No significant differences were observed in sensory neuron-specific expression levels of *Cgrp (p=0.2000)* and *Npy (p=0.1000)* **(Figure 4.4B)**.

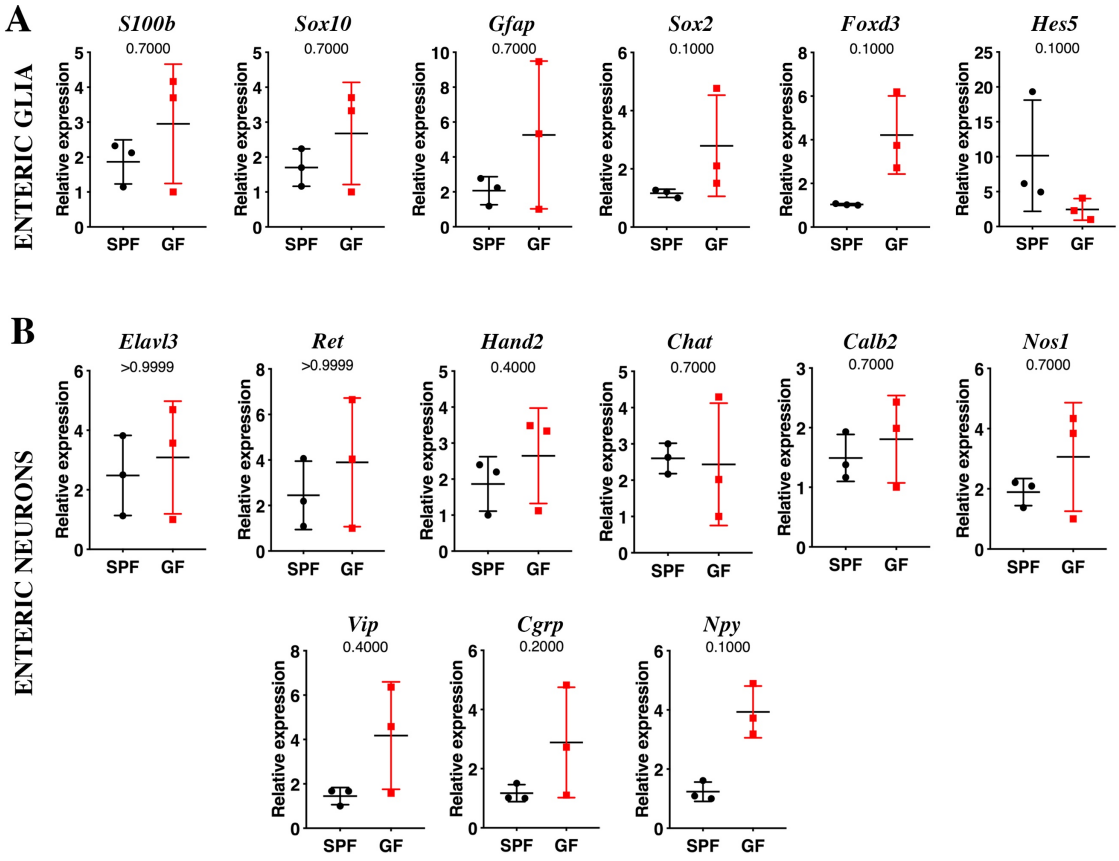


Figure 4.4. Effect of the absence of microbiota on ENS-specific transcript levels within the colon. (A) qRT-PCR on colonic LMMPs for EGC markers *S100b, Sox10*, *Gfap*, *Sox2*, *Foxd3* and *Hes5*. **(B)** qRT-PCR in colonic LMMPs for enteric pan-neuronal markers *Elavl3*, *Ret*, *Hand2*, and subtype-specific markers *Chat, Calb2*, *Nos1*, *Cgrp*, *Vip* and *Npy*. Graphs represent the relative expression values of each transcript normalised to *Actinb*. Mann-Whitney test. All error bars are SD of each animal counted as one biological sample. N=3/group. SPF, specific pathogen-free. GF, germ-free.

In summary, we suggest that the absence of microbiota interferes with expression of S100β immunoreactivity of mucosal EGCs in all segments of the intestines. However, the absence of microbiota did not influence ENS cell populations within LMMPs. We did not observe any significant differences in the numbers of EGC or main populations of neurons in the GF group relative to SPF controls in any segments of the intestines. Although some ENS-specific transcripts were differentially expressed between the two groups, none of the genes investigated was significantly altered. However, we observed a substantial reduction in the frequency of CMMCs, suggesting that microbiota modulate ENS physiology.

4.3.2 The microbiota status of different animal facilities impacts on gut motility

To further assess the effect of changes in microbiota composition on intestinal peristalsis we compared the CMMCs of C57Bl/6 mice, matching age and sex from NIMR and the new Crick Institute, which we knew from 16S-seq provided by the microbiology facility at the Crick, that the balance among different bacteria phyla was different between the two institutes. For instance, a population of SFB, usually present in the murine intestinal lumen was missing in mice from the Crick Institute. To investigate whether alterations in intestinal microbiota influences the colonic motility, we performed *ex-vivo* video recordings of the neurogenic intestinal activity and analysed the frequency of CMMCs. Our data showed that the frequency of CMMCs was significantly reduced in mice from the new Crick animal facility (0.14 ± 0.03 CMMCs/min SD, n=8, * *p=0.0107*) compared to the same inbred strain from the NIMR (0.18 ± 0.01 CMMCs/min SD, n=7) **(Figure 4.5A)**. This corroborates our previous data suggesting the participation of intestinal microbiota in modulating the neurogenic peristalsis of the colon **(Figures 4.5A-B)**.

To examine whether the lack of SFB was responsible for the reduction in the frequency of CMMCs in mice from the Crick facility, we colonised C57Bl/6 mice with SFB by faecal transplantation 3 weeks after birth. These experiments were done in collaboration with Dr Sara Omenetti from the Stockinger lab at the Crick, which confirmed in her experiments that inoculation of mice at this stage with SFB is enough to restore the levels of this bacterium within the intestinal lumen (section 2.2.14). Our experiments did not show any significant difference in the frequency of CMMCs between mice colonised (SFB^+: 0.108 ± 0.02 CMMCs/min SD, n=4, *p=0.5714*) or not with SFB (SFB^-: 0.12 ± 0.01 CMMCs/min SD, n=3) **(Figure 4.5B)**. Since it has been reported that SFB modulates the transcriptional profile of neuropeptides in purified DRG neurons (Yissachar et al., 2017), we next investigated whether SFB participated in regulating the gene expression landscape of ENS cells by performing qRT-PCR in colonic LMMPs in C57Bl/6 mice that were colonised or not with this bacterium. Our data did not show any statistically significant differences between the groups in the levels of *Elavl3 (p=0.6095*) and *Hand2 (p=0.695)* expressed by the majority of enteric neurons, or genes encoding subtype-specific neuronal proteins such as *Nos1 (p=0.7619)*, *Calb2 (p=0.9143)*, *Calb1 (p=0.3524)*, *Cgrp (p=0.7619)*, *Vip (p=0.9143)*, *Npy (p=0.6095)*, *Tac1 (p=0.3524)*, or genes related to the neuronal development *Phox2b (p=0.2571)* and *Ascl1 (p=0.3524)*. The expression of *Ret*, however, was slightly increased *(p=0.0667)*, yet not statistically significant in mice that were

colonised with SFB **(Figure 4.5C)**. We also examined the transcript levels of genes exclusively expressed in EGCs such as *S100b (p=0.9143)*, *Sox10 (p=0.7629)*, *Sox2 (p=0.4762)*, *Gfap (p=0.2571)*, *Hes5 (p>0.9999) and Foxd3 (p=0.3524)* and did not find any significant changes between the two groups **(Figure 4.5D)**. Our results suggest that the microbiota modulates the ENS-dependent colonic activity and this regulation of intestinal motility does not involve the presence of SFB.

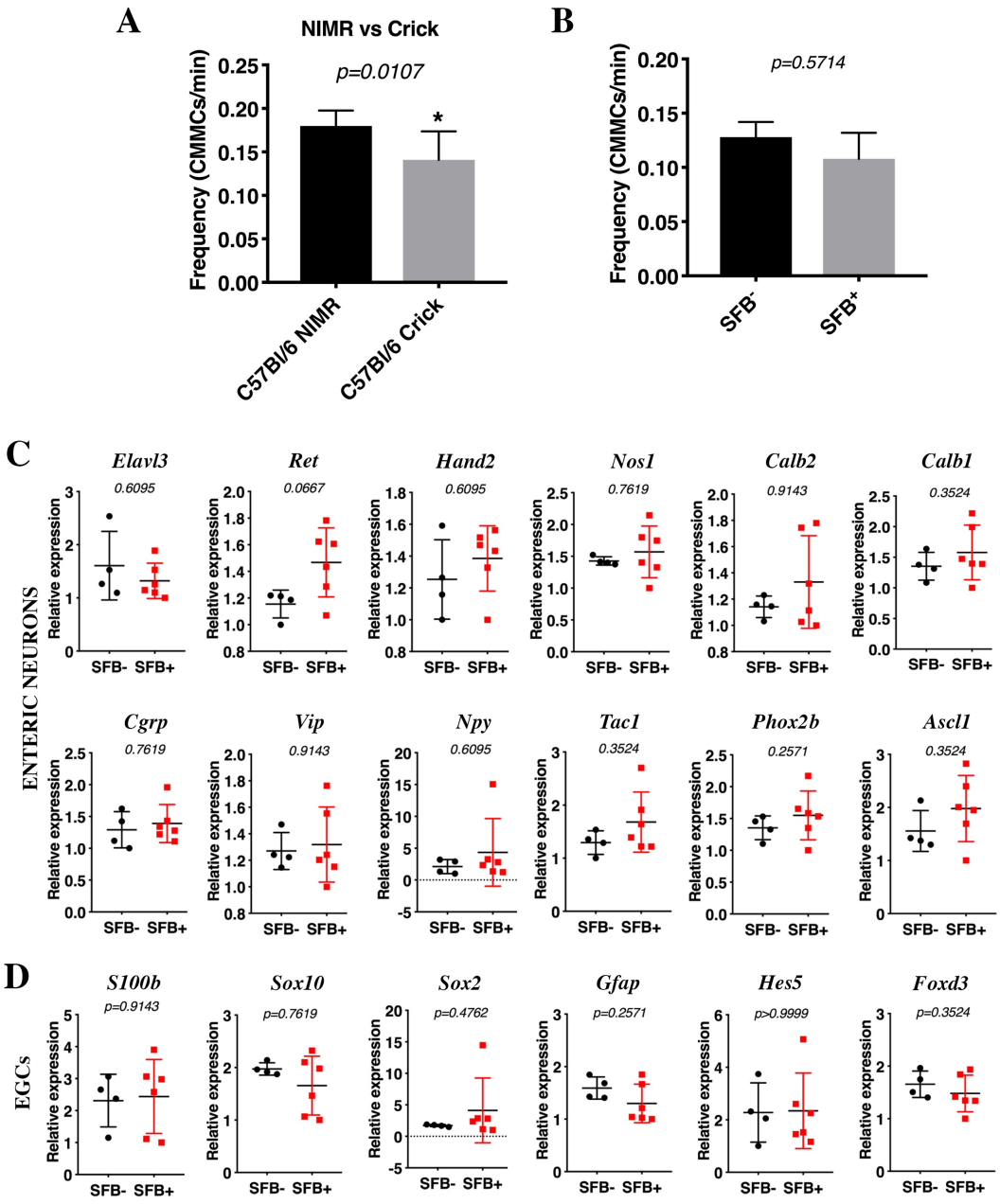


Figure 4.5. Effect of changes in microbiota composition on ENS transcriptional profile and function. (A) Frequency of spontaneous CMMCs represented by the number of colonic contractions per minute of C57BL/6

mice from NIMR and Crick Institutes. NIMR, n=7 and Crick, n=8. Mann-Whitney test, * $p < 0.05$. **(B)** Graph represents the average of frequency of CMMCs per minute of C57BL/6 mice colonised (SFB^+, n=4) or not with SFB (SFB^-, n=3). Mann-Whitney test, *p=0.5714*. **(C)** qRT-PCR of colonic LMMPs for neuron-specific markers, *Elavl3, Ret, Hand2, Nos1, Calb2, Calb1, Cgrp, Vip, Npy, Tac1, Phox2b* and *Ascl1* from SFB^- and SFB^+ C57Bl/6 mice. **(D)** qRT-PCR of colonic LMMPs for EGC-specific markers *S100b, Sox10*, *Sox2*, *Gfap*, *Hes5* and *Foxd3* from SFB^- and SFB^+ C57Bl/6 mice. Graphs represent the relative expression values of transcripts normalised to *Actinb*. All error bars represent SD of each animal counted as one biological sample. SFB^-, n=4 and SFB^+, n=6. Mann-Whitney test.

4.3.3 The ENS response in a model of TNF overexpression induced prior intestinal inflammation

In the first part of this chapter, we suggested that microbiota modulates intestinal motor behaviour, a characteristic physiological output of the ENS. This implies that the gut environment can disturb the equilibrium of ENS function. Moreover, it has been reported that inflammatory conditions have an important impact on ENS homeostasis by altering the structure of neuronal network and modifying the properties of enteric neurons and glia (Belai et al., 1997; Geboes & Collins, 1998). Furthermore, normally quiescent EGCs can enter the cell cycle in response to intestinal insults ((Cirillo, Sarnelli, Turco, et al., 2011; Laranjeira et al., 2011) and Eleni Amaniti, Fränze Progatzky, unpublished observations). Considering these insights, we next investigated the impact of intestinal inflammation on the ENS.

Experimental set-up

We opted for using the heterozygous $TNF^{\Delta ARE/+}$-inducing spontaneous inflammation model for the following reasons: first, TNF has been implicated in IBD progression; second, this experimental tool is "physiological" and mimics human CD; and third, the progression of pathophysiology is relatively slow and can be followed over a reasonable period of time (Kontoyiannis et al., 2002; Kontoyiannis et al., 1999). $TNF^{\Delta ARE/+}$ mouse line was kindly provided by Professor George Kollias at the Fleming Institute (Athens). To maintain $TNF^{\Delta ARE/+}$ heterozygous, $TNF^{\Delta ARE/+}$ (C57Bl/6 background) male mice were bred with wildtype C57Bl/6 females to generate heterozygous (ΔARE/+) and wildtype (+/+) littermates. Wildtype littermates, matching age and sex were used as controls in all experiments described below. Juvenile male mice, 4 weeks of age were chosen for this first set of experiments. At 4 weeks, the heterozygous mice already display

overproduction of TNF in the bloodstream but do not show any signs of intestinal inflammation (Kontoyiannis et al., 2002; Kontoyiannis et al., 1999) **(Schematic in Figure 4.6A)**.

Since the microbiological status can have a dramatic effect on the progression and outcome of IBD, we wished to confirm the $TNF^{\Delta ARE/+}$ phenotype described in the literature with animals bred in our facility. For this, segments of the distal ileum were dissected, fixed and embedded in paraffin for histological analysis. To examine the structure of the distal ileum, H&E staining was performed on 5 μm cross-sections in the wildtype and $TNF^{\Delta ARE/+}$. As expected, at 4 weeks of age, the anatomical structure of the ileum was preserved in the heterozygous mice, with no signs of intestinal inflammation, immune cell infiltration or epithelial damage, in comparison to control animals **(Figure 4.6B)**. In addition, we analysed the gross morphology of the ENS by immunostaining whole-mount LMMP preparations for the EGC marker S100β and the neuronal marker HuC/D to assess the overall architecture of the MP and neuronal networks. No visible differences in the morphology and organisation of the MP were observed between the two groups, suggesting that at this (relatively early) stage the ENS is well-preserved in $TNF^{\Delta ARE/+}$ mice **(Figure 4.6C)**.

To test the effect of TNF overproduction on GI motility *in vivo*, we performed the whole gut transit time assay (Sasselli et al., 2013). In this experiment, animals were orally gavaged with carmine dye red solution. We first analysed the time between the moment we administered the red dye and the time the animals took to expel the red pellet and the average time that the first faecal pellet was extruded was calculated. Our data showed that the whole gut transit time of the mutant mice (170 ± 5.6 min SD n=4) was consistently similar to the control mice (183 ± 17 min SD n=3) at this stage **(Figure 4.6D)**. We also analysed the stool water content by calculating the difference between wet weight and dry weight of the intestinal pellets. We did not observe any difference in the percentage of water in the intestinal pellets between the groups (+/+: 46.5 ± 20.16% and ΔARE/+: 44.5 ± 7.83% *p=0.7922*) **(Figure 4.6D')**. To examine the ENS-dependent intestinal peristalsis in these mice, we next generated spatiotemporal motility maps of the colon. Colonic recordings in the $TNF^{\Delta ARE/+}$ showed a slight increase but not statistically significant in the frequency of CMMCs (0.24 ± 0.01 CMMCs/min SD n=3), relative to the control littermates (0.12 CMMCs/min n=3) **(Figure 4.6E)**.

One of the features of EGCs is the capacity to undergo proliferation in response to intestinal challenges (Cirillo, Sarnelli, Turco, et al., 2011; Laranjeira et al., 2011). To assess whether overexpression of TNF stimulates EGCs to transit from a quiescent into an activated state, we collected LMMPs from the small intestine and performed immunohistochemistry for the EGC marker Sox10 and Ki67, which is expressed by proliferating cells in all phases of the cell cycle (sections 2.2.2.2 and 2.2.6). The percentage of proliferating EGCs was calculated by quantifying $Sox10^{+}$ cells that were co-stained for Ki67. We observed a small but statistically significant increase in the percentage of proliferating $Sox10^{+}$ EGCs in the ileum of $TNF^{\Delta ARE/+}$ mice compared to littermate controls (ΔARE/+: 2 ± 1.7% SD, n=9; +/+: 0.75 ± 0.89% SD n=12. Mann-Whitney test * $p = 0.0488$ **(Figures 4.6F-F' and table 4.4)**, suggesting that the overexpression of TNF triggers EGCs to undergo proliferation within LMMPs of the ileum.

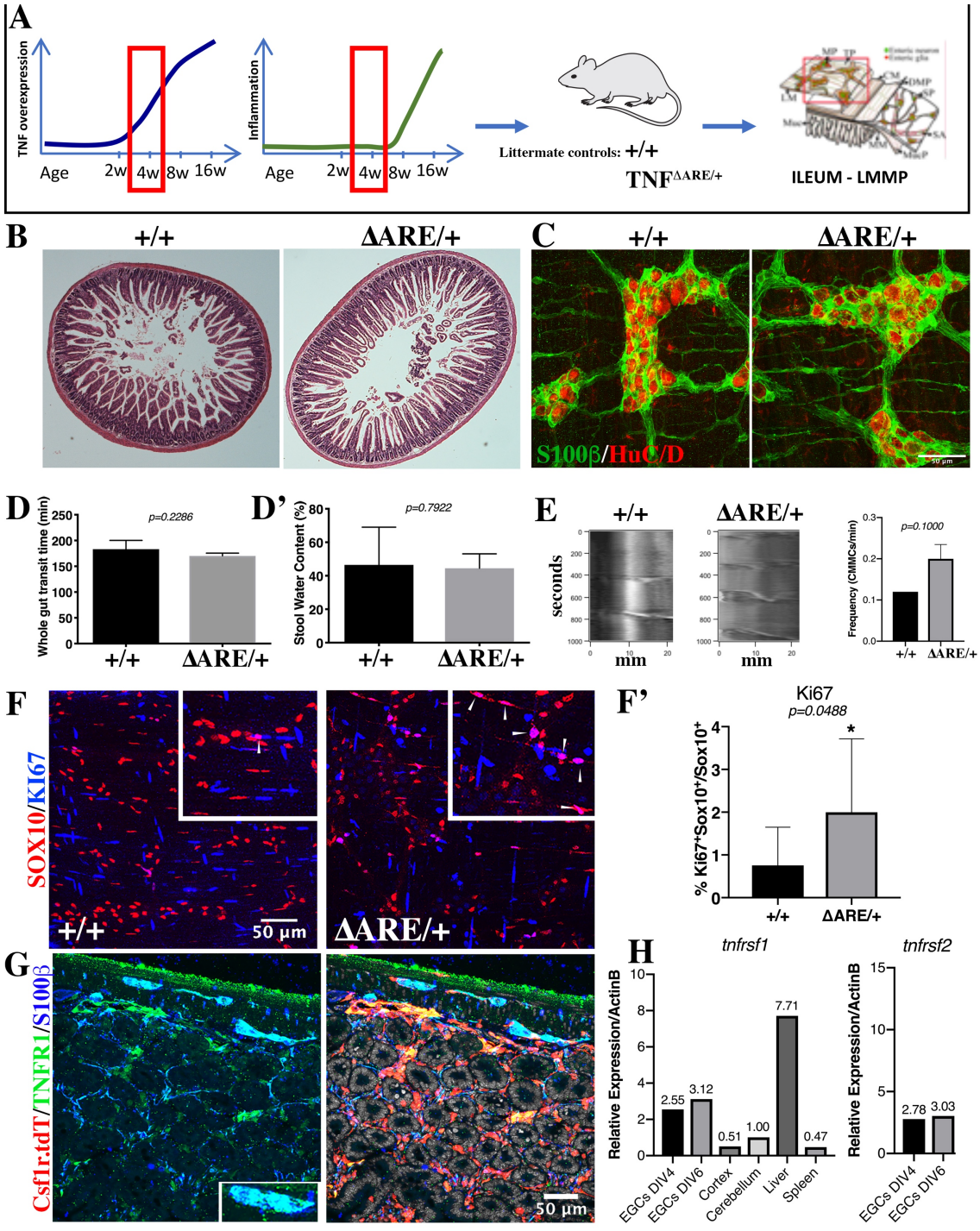


Figure 4.6. Analysis of ENS structure and function in TNF$^{\Delta ARE/+}$ mice at 4 weeks. (A) Schematic representation of mice status at 4 weeks prior inflammation. **(B)** Transversal sections of formalin fixed and paraffin embedded (FFPE) adult ileum from TNF$^{+/+}$ and TNF$^{\Delta ARE/+}$ mice stained with haematoxylin & eosin (H&E) showing the intestinal structure. X4 magnification. **(C)** Whole-mount preparation of LMMPs of the distal ileum immunostained for the EGC marker S100β (green) and the neuronal marker HuC/D (red) from TNF$^{+/+}$ and TNF$^{\Delta ARE/+}$ mice. Representative images of more than three mice. **(D)** Average of whole-gastrointestinal transit time in minutes of TNF$^{+/+}$ (n=3) and TNF$^{\Delta ARE/+}$ mice (n=4). Mann-Whitney test. **(D')** Average of the percentage of stool water content from TNF$^{+/+}$ and TNF$^{\Delta ARE/+}$ mice. Mann-Whitney test. Data

pooled from three experiments. **(E)** Spatiotemporal maps of ENS-derived motility from $TNF^{+/+}$ (n=3) and $TNF^{\Delta ARE/+}$ (n=3) mice. Graph shows the average frequency of CMMCs. Mann-Whitney test. Data pooled from three experiments. **(F)** Immunohistochemistry in LMMPs of distal ileum from the $TNF^{+/+}$ and $TNF^{\Delta ARE/+}$ mice stained for Sox10 (red) and Ki67 (blue). White arrowheads indicate double-positive cells for Sox10 and Ki67. **(F')** Quantification of the percentage of $Ki67^{+}Sox10^{+}$ in LMMP preparations of distal ileum from the $TNF^{+/+}$ (n=12) and $TNF^{\Delta ARE/+}$ (n=9) mice. Mann-Whitney test. Experiment pooled from more than three replicates. **(G)** Immunohistochemistry in the distal ileum from *Csf1r.tdT* mice (red) stained for the TNF receptor TNFRI (green) and the EGC marker S100β (blue). White inset highlights $S100\beta^{+}TNFRI^{+}$ EGCs. Graphs represent the relative expression by qRT-PCR of *Tnfrsf1* (TNFRI) and *Tnfrsf2* (TNFRII) transcripts normalised to *Actinb* in EGC cultures at DIV4 and DIV6. Cerebral cortex, cerebellum, liver and spleen were used as positive controls (Samples kindly provided by Dr Song Hui Chng). Graph represents one experiment and it shows the same trend of three independent experiments. W, weeks. LMMP, longitudinal muscle myenteric plexus. DIV, days *in vitro*. Scale bars in all images: 50 μm. Error bars indicate SD.

Table 4.4 Quantification of $Ki67^{+}Sox10^{+}$ EGCs in the model of TNF overexpression

	Total $Ki67^{+}$	**Total $Sox10^{+}$**	**Average % $Ki67^{+}Sox10^{+}$ ± SD**
$TNF^{+/+}$	85	9799	0.755 ± 0.89% SD
$TNF^{\Delta ARE/+}$	161	7727	2 ± 1.7% SD

Quantification of the average of percentage of $Ki67^{+}Sox10^{+}$ EGCs in LMMP preparations of distal ileum from $TNF^{+/+}$ (n=12) and $TNF^{\Delta ARE/+}$ (n=9) mice.

We next examined whether TNF could directly activate the EGCs by investigating the expression of TNF receptors in these cells. For this, we cultured EGCs and performed qRT-PCR to quantify the expression levels of *tnfrsf1* (TNFRI) and *tnfrsf2* (TNFRII) at DIV4 and DIV6 (**Figure 4.6H**). We used lysates from the cerebral cortex, cerebellum, liver and spleen as positive controls. Interestingly, we observed that cultured EGCs express TNFRI and II. To confirm this observation, we performed immunohistochemistry for TNFRI *in vivo*. Macrophages are the main source of TNF production, especially in a pathological environment, and express the TNFRI and TNFRII under steady-state conditions (Wajant, Pfizenmaier, & Scheurich, 2003). Since macrophages express these receptors, we performed immunohistochemistry on 14 μm thick cross-sections of the small intestine from the *Csf1r.tdT* reporter mice, in which macrophages are genetically engineered to express the red

fluorescent protein tdTomato, allowing them to be used as a positive control. Sections were immunostained for the EGC marker S100β and TNFRI. We observed expression of TNFRI in macrophages and EGCs within the ganglia and lamina propria of the small intestine (**Figure 4.6G)**. These data suggest that EGCs can directly respond to TNF levels within the gut wall via the TNF receptors I and II (**Figures 4.6G-H)**.

Next, we examined the impact of more advanced $TNF^{\Delta ARE}$-induced inflammation on the organisation and function of the ENS. For this, we used animals that were older than 16 weeks of age, when TNF expression was enhanced and intestinal inflammation was more advanced (**Figure 4.7A)** (Kontoyiannis et al., 2002; Kontoyiannis et al., 1999). Since inflammation was at its peak at this stage, we first analysed whether the structure of the ENS was preserved at the level of the MP. To assess that, we isolated the distal ileum and performed whole-mount immunohistochemistry for the EGC markers S100β and Sox10 to highlight the ENS network in $TNF^{\Delta ARE/+}$ and littermate controls. We imaged at least 3 mice per group, and we did not observe any morphological differences between the groups (**Figure 4.7B)**.

To evaluate the GI function in these mice, we next performed the whole gut transit time assay in $TNF^{+/+}$ (n=9) and $TNF^{\Delta ARE/+}$ (n=11). The average of the total transit time in the $TNF^{\Delta ARE/+}$ was significantly reduced (181 ± 61 min SD ** *p=0.0021*) compared to the littermate controls (271 ± 51 min SD), but no differences were observed in the amount of water in the faecal contents in these mice (+/+: 46.7 ± 6.4% and ΔARE/+: 48.4 ± 5.2% *p=0.5142*) (**Figure 4.7C)**. To assess the impact of TNF overexpression on ENS-dependent motility, we recorded the spontaneous colonic activity *ex-vivo* and generated spatiotemporal maps to calculate the frequency of CMMCs in these mice. Although the average of the frequency of CMMCs was augmented in the $TNF^{\Delta ARE/+}$ mice (0.14 ± 0.01 CMMCs/min SD n=3) compared to the $TNF^{+/+}$ controls (0.08 ± 0.01 CMMCs/min SD n=3), the increase was not statistically significant (*p=0.0722*) **(Figure 4.7D)**.

Since we observed a significant reduction in the whole GI transit time, followed by an increase in frequency of CMMCs in the $TNF^{\Delta ARE/+}$group, we next investigated the level of expression of several genes known to be expressed in enteric neurons. In these experiments, we dissected LMMPs from the ileum of $TNF^{+/+}$ (n=8) and $TNF^{\Delta ARE/+}$ (n=8) mice, isolated RNA and performed qRT-PCR. We did not observe any differences in transcript levels of genes implicated in the control of intestinal motility, such as *Chat*

(p=0.3147), *Calb2 (p=0.2670)*, *Calb1 (p=0.2031)*, *Nos1 (p=0.1866)*, *Vip (p=0.4244)* and *Npy (p=0.0673)*, sensing of the gut environment as *Tac1 (p=0.6653)*, as well as genes that are expressed in the majority of enteric neurons such as *Ret (p=0.9043)*, *Elavl3 (p=0.4244)* and *Elavl4 (p=0.6681)*. However, our data showed a significant increase in the expression of calcitonin gene-related peptide (*Cgrp*) (** *p=0.0047*) in the $TNF^{\Delta ARE/+}$ mice **(Figure 4.7E)**. Using the same approach, we also analysed genes expressed exclusively in EGCs (n=6 mice/group). No significant differences were observed in the expression levels of *Sox10 (p=0.3095)*, *Sox2 (p=0.1320)*, *Foxd3 (p=0.8182)*, *S100b (p=0.3939)*, *Hes5 (p=0.1797)*, *Plp1 (p=0.3939)* and *Gfap (p=0.0931)* in $TNF^{\Delta ARE/+}$ mice compared to controls (**Figure 4.7F)**.

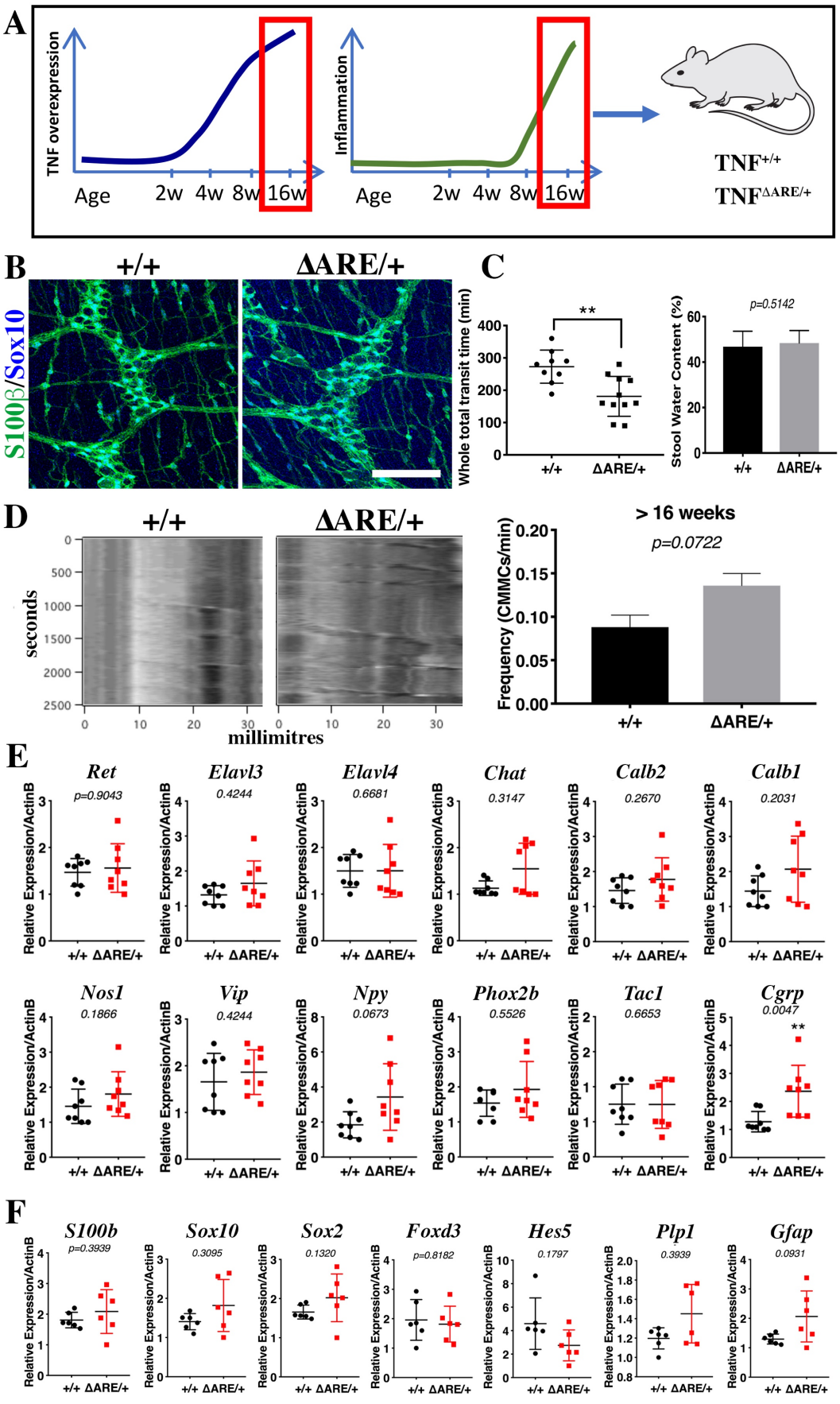

A
TNF overexpression
Age
2w 4w 8w 16w
Inflammation
Age
2w 4w 8w 16w
TNF+/+
TNFΔARE/+
B
+/+
ΔARE/+
S100β/Sox10
C
Whole total transit time (min)
**
+/+
ΔARE/+
Stool Water Content (%)
p=0.5142
+/+
ΔARE/+
D
+/+
ΔARE/+
seconds
millimitres
> 16 weeks
p=0.0722
Frequency (CMMCs/min)
+/+
ΔARE/+
E
Ret
p=0.9043
Elavl3
0.4244
Elavl4
0.6681
Chat
0.3147
Calb2
0.2670
Calb1
0.2031
Nos1
0.1866
Vip
0.4244
Npy
0.0673
Phox2b
0.5526
Tac1
0.6653
Cgrp
0.0047
**
Relative Expression/ActinB
+/+ ΔARE/+
F
S100b
p=0.3939
Sox10
0.3095
Sox2
0.1320
Foxd3
p=0.8182
Hes5
0.1797
Plp1
0.3939
Gfap
0.0931
Relative Expression/ActinB
+/+ ΔARE/+

Figure 4.7. Analysis of ENS structure and function in TNF$^{\Delta ARE/+}$ mice at 16 weeks. **(A)** Schematic representation of TNF overexpression and progression of inflammation at 16 weeks. **(B)** Whole-mount immunohistochemistry for the EGC markers S100β (green) and Sox10 (blue) in LMMPs of the ileum from TNF$^{+/+}$and TNF$^{\Delta ARE/+}$ mice. Scale bar: 100 μm. Representative image of three independent experiments. **(C)** Average of the whole-gastrointestinal transit time in minutes of TNF$^{+/+}$ (n=9) and TNF$^{\Delta ARE/+}$ mice (n=11). Average of the percentage of stool water content of TNF$^{+/+}$ (n=9) and TNF$^{\Delta ARE/+}$ mice (n=11). Graph shows pooled data from more than three experiments. **(D)** Spatiotemporal maps of intestinal neurogenic activity from TNF$^{+/+}$ (n=3) and TNF$^{\Delta ARE/+}$ (n=3) mice. Graph shows the average frequency of CMMCs per minute of three independent experiments. qRT-PCR analysis of genes expressed in enteric neurons such as *Ret*, *Elavl3, Elavl4, Chat, Calb2, Calb1, Nos1, Vip, Npy, Phox2b, Tac1* and *Cgrp* **(E)**, *and EGCs such as S100b, Sox10, Sox2, Foxd3, Hes5, Plp1* and *Gfap* **(F)** *in LMMP preparations from* TNF$^{+/+}$ and TNF$^{\Delta ARE/+}$ mice. Dot plot shows the relative expression values obtained for individual mice pooled from more than 3 experiments (n=8 mice/group for neuronal markers and n=6 mice/group for the EGCs markers) which were normalised to *Actinb*. Mann-Whitney test. $^{**}p < 0.01$. Error bars indicate SD.

4.3.4 EGC response in a model of experimental inflammation induced by a disruption in T cells homeostasis

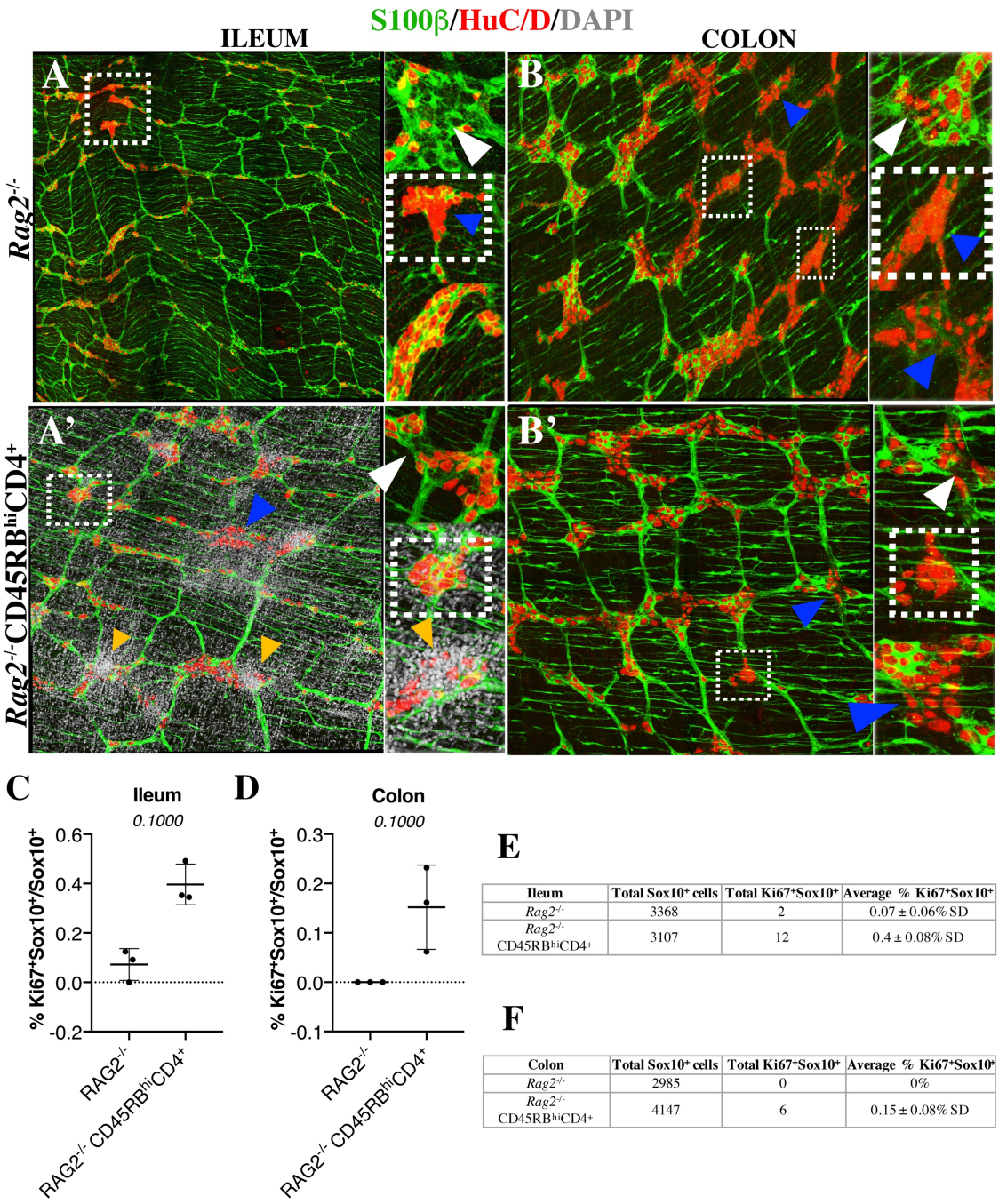
Experimental set-up

In parallel to the TNF overexpression experiments, we also investigated the response of EGCs to inflammation induced by alteration in T cell homeostasis (in collaboration with Dr Mark Wilson at NIMR). In this model, CD45RB^{hi}CD4^{+} naïve T cells isolated from the spleen of immunocompetent mice were injected into *Rag2*$^{-/-}$ immunodeficient male mice that were matched for age and sex. Naïve T cells introduced into immunodeficient mice induce pancolitis and ileitis 5-8 weeks after transfer (Powrie et al., 1994). We collected 3 *Rag2*$^{-/-}$ (used as controls) and 3 *Rag2*$^{-/-}$ mice reconstituted with naïve T cells (*Rag2*$^{-/-}$CD45RB^{hi}CD4^{+}) (experimental colitis) when the animals had lost 20% of their original body weight and presented signs of diarrhoea. For these experiments, the distal ileum and proximal colon were collected and LMMPs isolated and used for immunohistochemistry (sections 2.2.2.2 and 2.2.6).

First, we examined the ENS network by immunohistochemistry to determine whether the inflammation altered the morphology of ENS components in LMMPs. To visualise the enteric network, LMMPs from the distal ileum and colon of naïve (*Rag2*$^{-/-}$) and colitis (*Rag2*$^{-/-}$CD45RB^{hi}CD4^{+}) groups were immunostained for the EGC marker S100β and

the neuronal marker HuC/D. This analysis failed to show any gross morphological differences between the two groups, apart from a transmural infiltration of cells within the myenteric ganglia of mice transferred with T cells **(Figure 4.8A')**. We did not investigate the origin and identity of cell infiltrate within the MP. Interestingly, however, we reproducibly observed that the structure of the ENS was disrupted in more subtle manner in both groups. For example, HuC/D$^+$ neurons were absent in some of the myenteric ganglia of both *Rag2*$^{-/-}$ and *Rag2*$^{-/-}$CD45RB^{hi}CD4$^+$ mice **(Figures 4.8A-B')** while in some myenteric ganglia clusters of HuC/D$^+$ neurons were characterised by the presence of giant cell bodies **(Figures 4.8A-B')**. We also noticed that in areas where EGC immunoreactivity for S100β was weak or absent, the neuronal morphology was also altered **(Figures 4.8A-B')**. All these morphological changes were evident in the ileum and the colon of both groups.

Next, we investigated whether inflammation as indicated by 20% body weight reduction observed in the colitis model triggered proliferation of the EGCs. To address this question, we performed immunohistochemistry in LMMPs from the distal ileum and proximal colon of the naïve and colitis groups for the EGC marker Sox10 and the proliferation marker Ki67. The percentage of Sox10$^+$ EGCs expressing Ki67 was quantified in the distal ileum and proximal colon in the groups. Although there was a small increase in EGCs proliferation in the colitis group in the ileum (0.4 ± 0.08%, 12 Ki67$^+$Sox10$^+$ in 3107 Sox10$^+$ cells) compared to the naïve controls (0.07 ± 0.06%, 2 Ki67$^+$Sox10$^+$ in 3368 Sox10$^+$ cells), the numbers of proliferating EGCs were very low and not statistically significant (**Figures 4.8C and 4.8E)**. In the colon, we did not observe any Ki67$^+$Sox10$^+$ in the naïve group (0 Ki67$^+$Sox10$^+$ total 2985 Sox10$^+$ cells), and only a few cells in the experimental colitis animals (0.15 ± 0.08%, 6 Ki67$^+$Sox10$^+$ in 4147 Sox10$^+$ cells) (**Figure 4.8D and 4.8F**). Altogether, this data indicates that EGCs under chronic inflammation induced by the disruption in T cells homeostasis have the potential to enter the cell cycle and proliferate. However, the numbers of proliferating EGCs are extremely low within the LMMPs in either group.



E

Ileum	Total Sox10⁺ cells	Total Ki67⁺Sox10⁺	Average % Ki67⁺Sox10⁺
Rag2$^{-/-}$	3368	2	0.07 ± 0.06% SD
Rag2$^{-/-}$ CD45RB^{hi}CD4⁺	3107	12	0.4 ± 0.08% SD

F

Colon	Total Sox10⁺ cells	Total Ki67⁺Sox10⁺	Average % Ki67⁺Sox10⁺
Rag2$^{-/-}$	2985	0	0%
Rag2$^{-/-}$ CD45RB^{hi}CD4⁺	4147	6	0.15 ± 0.08% SD

Figure 4.8. T cell transfer model of chronic inflammation and its impact on ENS homeostasis. Immunohistochemistry on whole-mount LMMP preparations from the distal ileum and proximal colon of naïve *Rag2*$^{-/-}$ **(A and B, respectively)** and *Rag2*$^{-/-}$CD45RB^{hi}CD4^{+} colitis mice **(A' and B', respectively)** 9 weeks after transfer. LMMPs were stained for the EGC marker S100β (green), and the neuronal marker HuC/D (red) and DAPI to label cell nuclei (grey). White dotted squares identify clusters of neurons. Yellow arrowheads point to infiltrates of cells within the myenteric ganglia. White arrowheads highlight ganglia with absence of HuC/D^{+} neurons. Blue arrows point to MP with defective EGCs network. Representative graphs of the percentage of Ki67^{+}Sox10^{+} EGCs in LMMPs of the ileum **(C)** and colon **(D)** from naïve *Rag2*$^{-/-}$and *Rag2*$^{-/-}$ CD45RB^{hi}CD4^{+} colitis mice. Total Sox10^{+} and Ki67^{+} counts in the LMMPs from the distal ileum **(E)** and

proximal colon **(F)** of naïve and colitis groups. Data acquired from three independent experiments. N=3 mice/group. Mann-Whitney test. Error bars indicate SD.

4.4 Discussion

The ENS is exposed to a rich tissue and luminal environment, including diverse communities of intestinal microbes and their products, as well as to a highly active immune system. The ENS is expected to participate in the maintenance of GI functions by responding to intestinal cues that challenge the homeostasis of this tissue. In this chapter, we investigated the response of enteric neurons and glial cells to a non-physiological environment that perturbs the function of the GI tract. To dysregulate intestinal homeostasis, we disturbed the gut microbiota (experiments with GF mice) and immune system by promoting chronic intestinal inflammation ($TNF^{\Delta ARE}$ and adoptive T cell transfer models).

First, we employed GF mice to investigate the role of microbiota on ENS function and homeostasis in the adult gut. It has been reported that the intestinal microbiota modulates the homeostasis of mucosal EGCs within the ileum (Kabouridis et al., 2015), as well as the neuronal network within the colonic mucosa in mice (De Vadder et al., 2018). In our experiments, we characterised EGCs and neuronal network within the lamina propria of duodenum, jejunum, ileum and colon from GF and SPF control mice. In all segments and layers of the intestines of SPF mice, $Calretinin^+$ neuronal fibres tightly accompanied $S100\beta^+$ EGCs. In the GF group, however, we found $Calretinin^+$ neuronal fibres that were not associated with mucosal EGCs. In the colon, this phenotype appeared to be more pronounced in GF mice relative to SPF controls. Our data support previous studies suggesting that microbiota modulates the homeostasis of S100β expressing EGCs within the mucosa, and the neuronal-EGCs interface within this layer (De Vadder et al., 2018; Kabouridis et al., 2015). Nonetheless, we could not confirm whether there was a reduction in the population of mucosal EGCs, in S100β expression or whether these cells were differentially arranged within this layer. Moreover, we examined the EGC network, and $Sox10^+$ and $S100\beta^+$ EGC populations within LMMPs in all segments of the intestines. We did not observe any significant differences in network or proportion of EGCs within this layer between GF and SPF mice in our experiments, although the number of $S100\beta^+$ EGCs was slightly reduced in the colon of GF mice. Perhaps, due to a high variability between mice from the same group, the numbers of animals used for these experiments (3) were not sufficient to show any

statistically significant results. Unfortunately, the Norwich GF facility was unable to provide us at the time with additional animals to extend these studies. Currently, we have access to a larger GF facility (Prof. A. Macpherson, University of Bern) and will be in a position to repeat these experiments. Kabouridis et al. did not report any visible alterations in the EGC network within the MP and SMP of GF mice (Kabouridis et al., 2015). On the other hand, de Vadder et al. reported a significant reduction in the total number of S100β$^+$ EGCs within the MP of GF mice relative to conventionally raised animals, with no differences detected in proportion of Sox10$^+$ EGCs (De Vadder et al., 2018). Moreover, Kabouridis et al. took advantage of a genetic reporter mouse line to follow the presence of EGCs within the villi after treatment with antibiotics. It would be interesting to use high resolution genetic fate mapping and lineage tracing methods to investigate the dynamics of EGCs within different layers of the gut, in addition to their response to intestinal microbiota. This will require re-derivation and maintain appropriate transgenic mouse lines under GF conditions, which is currently in progress.

To further investigate the EGCs response to the absence of intestinal microbes, we also analysed the expression levels of genes that are exclusively identified in EGCs in colonic LMMPs. We did not observe any significant differences in expression levels of EGCs transcripts between the groups. Once again, this may be due to the low numbers of animals used for these experiments, and it would be worth increasing the numbers of collected samples. For instance, one of our samples had a substantial variation within the GF group, which could lead to an underestimation of our data.

By using single-cell transcriptome in association with *in vivo* clonal analysis of ENS progenitors in the mouse, Lasrado et al. have suggested that the colonisation of EGCs within the lamina propria occurs along the serosa-mucosa axis (Lasrado et al., 2017). Furthermore, Kabouridis et al. have shown that the presence of EGCs within the villi is dependent on microbiota (Kabouridis et al., 2015), suggesting that the intestinal microbiota triggers the dynamics of the postnatal development of these cells. Although our data did not show any significant differences in numbers of EGCs within the MP, the expression of some of the genes analysed in our experiments such as *S100*, *Sox10*, *Gfap* and *Foxd3* was increased in colonic LMMP preparations in 2 out of 3 mice. A further investigation of ganglionic EGCs by using genetic tools to map, isolate and sequence these cells after microbiota manipulation could bring new insights on the role of gut microbes on the postnatal developmental dynamics of EGCs.

It has been reported that adult GF mice have a slower GI transit time (Anitha et al., 2012; De Vadder et al., 2018; Yano et al., 2015), and reduced enteric neuronal excitability in the jejunum (McVey Neufeld et al., 2013). However, the role of microbiota on ENS-derived motility in the colon has not yet been reported. Our data suggest for the first time that microbiota is essential for the modulation of neurogenic colonic motility. Our conclusion was based on *ex-vivo* analysis of spontaneous colonic activity of GF mice, which display a significant reduction in the frequency of CMMCs, suggesting that the absence of intestinal microbes impairs ENS function. It will be particularly interesting to identify the molecular mechanisms responsible for the altered activity of ENS in GF mice. It is currently unclear whether the mechanisms implicated in the effects of the immune system on ENS physiology (Chapter 5) also mediate the effect of the GF state on gut motility. Interestingly, my colleague Dr Yuuki Obata has applied the strategy we co-developed for the fluorescent marking and isolation of neuronal nuclei (Chapter 3) to compare the transcriptomes of enteric neurons from SPF and GF animals and found that the transcription factor AhR, which is normally expressed in colonic neurons of SPF mice is downregulated in colonic neurons from GF animals. This raises the possibility that AhR, which is known to be activated by microbial and diet metabolites, is a candidate molecule that mediates the effects of microbiota on ENS function. The effect of microbiota on ENS physiology is also supported by our evidence that C57Bl/6 mice originating in different animal facilities (NIMR and Crick), which have different composition of microbiota (Dr Brigitta Stockinger's lab, personal communication), show differences in intestinal peristalsis. Since mice from the new Crick animal facility lacked SFB in the intestinal lumen, we tested whether this bacterium could be involved in the modulation of ENS-dependent colonic activity. SFB has been reported to modulate the development and function of Th17, a subset of T lymphocytes since mice lacking SFB were completely devoid of Th17 T cells (Farkas et al., 2015; Ivanov et al., 2009). SFB have also been implicated in the regulation of expression of neuromodulators in DRG neurons (Yissachar et al., 2017). However, in our experiments SFB did not have any impact in the intestinal motility or modulating the ENS transcriptional profile, although the expression of the neuronal marker *Ret* was slightly upregulated in mice colonised with this bacterium. Although the microbes that are responsible for the GI peristalsis differences between NIMR and Crick C57Bl/6 mice, our findings suggest that the interpretation of physiological data on any organ system of the mouse must consider the microbiological status of investigated animals.

It has been reported that postnatal day 3 GF mice have reduced network density, neuronal numbers in the jejunum and ileum, and increased proportions of nitrergic neurons (Collins et al., 2014). Moreover, it has been demonstrated that the NOS1$^+$ neuronal population in the colon (Anitha et al., 2012), and Calbindin$^+$ neurons in the jejunum (McVey Neufeld et al., 2015) are reduced in adult GF mice. Since the colonic motility was impaired in GF mice, we investigated the neuronal network and the two major populations of excitatory (Calretinin$^+$) and inhibitory (NOS1$^+$) enteric neurons within the MP in all segments of the intestines. We did not observe any significant differences between the groups in any part of the gut. We have also analysed the total number of HuC/D$^+$ neurons per area of the gut, and we did not detect any differences between the groups **(Appendix 5)**. Likewise, De Vadder et al. did not identify any alterations in numbers or network of enteric neurons within the MP in the colon of GF mice (De Vadder et al., 2018). We further investigated the transcript levels of genes expressed in other subsets of enteric neurons by qRT-PCR and no significant differences were detected between GF and SPF mice. Nevertheless, *Npy*, *Cgrp* and *Vip* expression showed a trend towards upregulation in GF mice. Neuropeptides have been implicated as neuromodulators in the CNS where they regulate general internal states and activation levels (van den Pol, 2012; Zelikowsky et al., 2018). In addition, neuropeptides participate in the bidirectional communication between the brain and the gut along the microbiota-gut-brain axis and may be involved in the modulation of ENS function driven by the microbiota (Holzer & Farzi, 2014). Therefore, we suggest that neuropeptides could function as neuromodulators of the general level of ENS activity as revealed by intestinal motility.

Although we did not detect any alterations in the morphology or populations of ENS cells in the GF mice, our data suggest a potential role of microbiota in modulating ENS function in the colon. This implies that the gut environment can disturb the equilibrium of ENS physiology. Thus, we next investigated the effect of inflammation on ENS homeostasis. We opted for using two well-established experimental mouse models of spontaneous inflammation, the TNF$^{\Delta ARE}$ transgenic mice, in which the overproduction of TNF causes intestinal inflammation in the distal ileum (Kontoyiannis et al., 1999), and the adoptive T cell transfer model, that is caused by a disruption in the T cells homeostasis (Powrie et al., 1994). Initially, we determined whether overexpression of TNF prior to inflammation had an impact on ENS physiology. Our results demonstrated that the anatomical structure and organisation of ENS network, as well as the overall GI motility were normal prior to

inflammation in $TNF^{\Delta ARE/+}$ mice. Nevertheless, the frequency of ENS-dependent CMMCs was slightly increased in these animals relative to their littermate controls. To further assess the ENS response to alterations in gut homeostasis, we evaluated the EGC activation within the MP by analysing their proliferation status. Our data showed a small but significant increase in proliferating EGCs within the MP in response to TNF overexpression. EGCs proliferation was also slightly increased in the adoptive transfer colitis model, both in the ileum and in the colon. However, the fraction of proliferating EGCs was very low in both models, less than 1% in the adoptive T cell transfer model. Earlier reports have suggested that EGCs undergo proliferation when exposed to pro-inflammatory signals *in vitro*, such as IFN-γ and LPS (Cirillo, Sarnelli, Turco, et al., 2011), and IL-10 (Ruhl, Franzke, & Stremmel, 2001). It has also been shown that EGCs respond to TNF by increasing the number of $GFAP^{+}$ EGCs *in vitro* (von Boyen et al., 2004). However, it is not clear whether increased levels of GFAP are also associated with enhanced proliferation of cells, rather than increased expression of *Gfap*. Despite the minimal induction of proliferation of EGCs by TNFα, we found that EGCs express the TNFRI and TNFRII receptors *in vitro* and *in vivo* under steady-state conditions, implying that TNF can directly activate these cells to respond to inflammation. It has been reported that enteric neurons also express TNF receptors *in vitro*, and the crosstalk between TNF and the neuropeptide NPY modulates inflammation and colonic motility (Chandrasekharan et al., 2013). We quantified the transcript levels of *Npy* in the $TNF^{\Delta ARE/+}$ mice, and we did not find any differences in the expression of this gene compared to the control group. It has also been described that enteric neurons produce TNFα after stimulation with LPS *in vitro*. However, the same report suggested that EGCs were unable to secrete TNF (Coquenlorge et al., 2014). Given that our *in vitro* preliminary data indicate that TNFα can stimulate EGCs to undergo some level of proliferation, it would be interesting to extend these studies and explore the direct effect of this pro-inflammatory cytokine on EGCs.

In vivo, the capacity of adult EGCs to enter the cell cycle is still under debate. Joseph et al. have demonstrated that less than 3% of EGCs enter the cell-cycle under physiological conditions over a 10-week period and that this figure increases to 36% following localised chemical ablation of the ENS (Joseph et al., 2011). Since the extent of EGC proliferation was very low in our experiments, we question the biological relevance of the proliferative rates of EGCs under the inflammatory conditions we tested and argue that enhanced proliferation does not accompany all inflammatory models. Perhaps, EGC

activation in response to inflammation in some models (such as the ones we have tested) is defined more by changes in gene expression. Unbiased whole genome transcriptomic analysis is likely to reveal such changes and define molecular pathways that characterise the inflammatory responses of enteric glia and their potential roles in modulating local immune responses and/or protecting neuronal networks and circuits from damage.

We also investigated the role of inflammation produced by TNF overexpression on ENS function. We did not observe any structural changes in ENS network between the experimental groups. However, the whole-gastrointestinal transit time was significantly reduced in the $TNF^{\Delta ARE/+}$ group, with no changes in the stool water content. Studies using $TNF^{\Delta ARE/+}$ model did not observe any alterations in the stool water content even after the initiation of inflammation (Roulis et al., 2016). To further test the effect of intestinal inflammation caused by TNF overexpression on colonic function, we recorded the spontaneous ENS-dependent motility and observed an increased frequency of CMMCs, although it was not statistically significant. Since the GI function was altered in the $TNF^{\Delta ARE/+}$ group, we quantified the expression levels of several transcripts expressed by enteric neurons and glial cells in LMMPs by qRT-PCR. Among all the genes analysed, we detected a significant increase in neuronal *Cgrp* expression. CGRP expressing neurons are intrinsic primary afferent neurons (IPAN) and function by sensing the intestinal environment. It is known that some pathological conditions can interfere with levels of CGRP expression, for instance inflammation and nerve damage upregulate the expression of this gene (Makowska & Gonkowski, 2018). Moreover, it has been reported that patients with CD have an increased thickness in $CRGP^{+}$ neuronal fibres (J. Schneider et al., 2001). Nevertheless, the role of these neurons on the pathophysiology of intestinal inflammation is still not clear. Furthermore, we did not detect any statistically significant alterations in transcripts expressed by the EGCs. However, expression level of *Gfap* were moderately increased in the experimental group. GFAP mRNA and protein levels were reported to be upregulated in several inflammatory conditions as a readout of EGCs activation (Delvalle, Fried, et al., 2018; Rosenbaum et al., 2016). However, the physiological role of the upregulation of GFAP levels in EGCs is still unknown.

In the adoptive transfer model, we did not detect any differences in ENS network between naïve and colitis groups. However, in both groups, neuronal and EGCs network were structurally disrupted. We observed a lack of HuC/D^{+} neurons within some myenteric ganglia; other HuC/D^{+} neurons formed clusters of cells with giant cell bodies. Additionally,

the network of EGCs surrounding neurons were also missing in many ganglia, especially in areas in which neurons were clustered together. Moreover, in this model we hardly observed any EGCs proliferation in the naïve group, suggesting that perhaps the absence of lymphocytes impairs the maintenance of ENS network and immune cells are needed to trigger the activation of EGCs to respond to inflammation.

Overall, our data indicate that multiple inflammatory processes of diverse origin and pathogenesis impact on ENS physiology and intestinal motility. Currently, it is not known whether distinct molecular and signalling pathways associated with individual inflammatory conditions in humans and the respective animal models have similar effects on enteric neuroglia function. Alternatively, different pathological and inflammatory processes could converge into a common mechanism which in turn alters ENS function. Distinguishing between these possibilities will require additional experiments. Nevertheless, studying the effect of gut alterations on ENS is a considerable challenge to be addressed. One of the reasons that make it difficult is the cross-talk between the immune system and microbiota. For instance, in our data using the GF model to eliminate the intestinal microbiota, we observed a significant reduction in ENS-derived motility. We could possibly argue that this phenotype is due to the absence of microbiota. However, it is also known that the immune system depends on intestinal microbiota to develop. The cross-talk between immune system and enteric nervous system could also have a major impact on GI function. Moreover, it has been recently shown that in the $TNF^{\Delta ARE}$ inflammation model there is a defective expression of antimicrobial products and increased dysbiosis, and the progression of the pathology is dependent on microbiota (Roulis et al., 2016). Separating the primary and secondary effects of inflammation on ENS is still a hurdle that needs more attention from different areas of research.

Chapter 5

Neuroimmune communication and intestinal function

5. Chapter 5 | Neuroimmune communication and intestinal function

Chapter 5 presents our research on the role of the neuroimmune communication on adult mouse gut function. Despite the increasing realisation of its utmost importance, the physiological contributions and mechanisms of neuroimmune interactions on GI homeostasis is still poorly elucidated. The first part of this work highlights the anatomical positioning of immune cells relative to the ENS as well as their compartmentalisation within the intestinal wall, focusing mainly on adaptive immune cells.

The second part of this chapter converges on the role of the adaptive immune system on ENS maintenance. The hypothesis suggesting that the adaptive immune system plays a role on ENS homeostasis was raised by using immunodeficient mouse models to study intestinal inflammation. We previously suggested (chapter 4) that immunocompromised mice display morphological alterations in the MP. Following on from this evidence, in this chapter we take advantage of new and advanced tools generated in the lab (for more details see chapter 3) to further investigate the intestinal neuroimmune communication in the adulthood.

5.1 Introduction

The GI tract routinely fulfils multiple tasks to maintain its homeostatic functions including epithelial absorption and secretion of nutrients, digestion, mixing peristalsis and defence against pathogens. It is expected that a sophisticated cooperative relationship between distinct tissue systems act in parallel to regulate different challenges that could disturb the normal function of this organ. In the previous chapter, we have suggested that the ENS depends on microbiota to maintain normal intestinal motility. This, together with recent publications reporting that intestinal microbes tune the maturation of EGCs (Kabouridis et al., 2015) and neurons (De Vadder et al., 2018) indicate the involvement of multiple systems in modulating the GI function under homeostatic conditions. Moreover, we have proposed that intestinal challenges such as inflammation caused by the overexpression of TNF regulate the neurogenic intestinal peristalsis. The effect of intestinal inflammation on ENS homeostasis has been extensively reported recently (Boyer et al., 2007; Cirillo et al., 2009; Cirillo, Sarnelli, Esposito, et al., 2011; Villanacci et al., 2008). However, little is known about the mechanisms whereby the ENS interacts with the immune system in order to control intestinal inflammation. More importantly, the interplay between the ENS and the immune system under steady-state conditions has not yet been adequately explored.

To understand the physiological functioning of a system as a whole, it is necessary to acknowledge its interactions with the surrounding tissues. The CNS contains physical protective tissues including the meninges, that protect the brain and spinal cord parenchyma from external insults. Together with a potent immunological surveillance, these barriers are necessary to maintain CNS homeostasis. The CNS is considered an immune-privileged organ and the activation of immune responses is remarkably reduced *in situ*, although this system contains an abundant number of microglial cells (Wraith & Nicholson, 2012). These cells are primed to respond to insults within the brain parenchyma, but they also participate in neural function by pruning debris and remodelling synaptic circuits (Paolicelli et al., 2011; Schafer et al., 2012). Moreover, CNS neurons express molecules that were thought to be present exclusively on immune cells, such as MHC class I, CD3 (Corriveau et al., 1998), TCRβ (Syken & Shatz, 2003) and RAG1 (Chun et al., 1991), albeit the role of these molecules on neural cells is not well understood. On the other hand, it has been shown that immune cells can produce neurotransmitters and express their receptors to enhance immune function (Bergquist et al., 1994; Dionisio et al., 2011; Flierl et al., 2007; Gomariz et al., 1993; Lai et al., 1998, 2002; Mashaghi et al., 2016; Reardon et al., 2013; Reardon et al., 2018; Rinner et al., 1998). Altogether, this evidence supports the presence of a resilient neuroimmune interface in the CNS to sustain its function.

In contrast to the CNS, an extraordinary array of immunological processes take place in the intestinal mucosa, reflecting the diversity of immune cells situated within this layer that need to promptly respond to continuous and severe intestinal challenges. These immune cells are mainly located in inductive sites of organised structures named GALTs, positioned in the lamina propria and submucosa of the gut. Even though the GI tract contains a robust epithelial barrier and an active immune system, microbial and dietary products can penetrate the lamina propria and activate immune responses (Agace & McCoy, 2017; Mowat & Agace, 2014). Also localised into compartments within the intestinal wall, the ENS comprises an intricate network of neurons and EGCs. Although the enteric neuronal cell bodies are compacted within ganglionic structures, their processes along with EGCs are exposed to environmental challenges in the mucosal layers of the gut (John Barton Furness, 2006). Until recently, little was known about the interactions between the immune system of the gut and the ENS. However, the interest on intestinal neuroimmune communications has been enhanced considerably during the past 5 years. It has been reported that besides the lamina propria macrophages (LpMs), which present a pro-inflammatory phenotype, MMs

are located within the muscle layer and display a tissue-protective phenotype. These macrophages are closely associated with enteric neuronal cell bodies and fibres and secrete BMP2 that is crucial for the neuronal differentiation. Enteric neurons, in turn, produce CSF1, a growth factor necessary for the development of macrophages (Gabanyi et al., 2016; Muller et al., 2014). MMs resemble microglial cells from the CNS because of their capacity to engulf neuronal debris (De Schepper et al., 2018; Kulkarni et al., 2017). Furthermore, gMacs have unique transcriptional profiles depending on their location within the gut, and are essential for ENS homeostasis (De Schepper et al., 2018). Enteric neurons also interact with ILC2 to promote type 2 immune responses in the gut via neuronal NMU binding to its receptor in ILC2 (Cardoso et al., 2017; Klose et al., 2017). Moreover, EGCs produce GDNF that activates Ret-expressing ILC3 (Ibiza et al., 2016). Together, these studies support the idea that a continuous interplay between the ENS and the innate immune system is essential for GI homeostasis.

Despite such advances, interactions between the adaptive immune system and the ENS remains unexplored. It has been shown that enteric neurons project their fibres to around and inside the PPs (Chiocchetti et al., 2008; Vulchanova et al., 2007) and neuropeptides modulate lymphocytes maturation within these lymphoid structures (Stanisz et al., 1986). In addition, it has been suggested that lymphocytes respond to neurotransmitters and neuropeptides via expression of their receptors, for instance, VIP and NPY receptors (S. Schneider et al., 2018). Nevertheless, the role of neuroactive substances (such as neurotransmitters and neuropeptides) on lymphocytes is still unclear under homeostatic conditions.

5.2 Aims

Given the limited information in the intestinal neuroimmune interplay and its role in gut function, in the first part of this chapter we aimed to describe the anatomical positioning of immune cells relative to the ENS. In the second part, we have used immune deficient mutant mice lacking the adaptive immune system to characterise the importance of these cells on ENS homeostasis.

The specific aims of this chapter were:

1. Characterisation of the anatomical relationship of immune cell populations relative to ENS cells.
2. Characterisation of immune cell populations from different anatomical compartments within the gut wall.
3. Characterisation of the role of adaptive immune cells for ENS-dependent intestinal motility.
4. Evaluation of the ENS structure in mutant mice lacking the adaptive immune system.
5. Investigation of the transcriptional profile of ENS in mice lacking the adaptive immune system.
6. Provide insight into the role of the adaptive immune system in modulating ENS function.

5.3 Results

5.3.1 Anatomical positioning between the ENS and the immune system

Experimental set-up

To investigate the anatomical positioning between immune and ENS cells in the gut, we took advantage of different animal models and tools, such as transgenic reporter lines and viral vector-based labelling of enteric neural networks combined with immunohistochemistry assays. All animals used in these experiments were between 8-16 weeks of age. Intestines were isolated, luminal contents removed and tissues were prepared either for vibratome sectioning or LMMP dissections for immunohistochemistry (sections 2.2.2.3, 2.2.2.2 and 2.2.6).

To explore the relative positioning between macrophages and the ENS within the lamina propria, we used the *Ser26.tdT* mouse line (*Sox10::CreER^{T2};R26R-CAG-td^{Tomato}*; previously described in chapter 3) that labels the vast majority of EGCs with the fluorescent

reporter tdT. Immunohistochemistry on cross-sections of intestines from this mouse line with Iba1 and PGP9.5 allowed us to identify macrophages and enteric neurons, respectively. Iba1$^+$ cells were found within the lamina propria, surrounding crypt regions as well as in the muscle layers **(Figure 5.1A-Ai)**. In the lamina propria, we observed EGCs and neuronal processes embedded in the pool of macrophages within this layer **(Figure 5.1A and inset Ai)**. Moreover, we have established in the lab a transgenic reporter mouse line, *Csf1r.iCre;R26tdT (Csf1r.tdT),* in which the improved Cre recombinase is under the control of *csf1r*, a gene that encodes the receptor for CSF1, a cytokine critical for the development of monocytes and macrophages (Deng et al., 2010). To confirm the specificity of the Cre recombinase, we compared the expression of the tdT reporter with the Iba1 antibody, specifically expressed by macrophages (Ito et al., 1998). We observed that the majority of Iba1$^+$ macrophages overlapped with the tdT$^+$ cells in different layers of the intestines **(Figure 5.1Bi, shows LMMPs)**. To examine the relative positioning between MMs and ENS cells, we performed whole-mount immunohistochemistry in LMMPs from the *Csf1r.tdT* mouse line for the EGC marker S100β and the neuronal marker HuC/D. MMs are very branched and homogeneously distributed within the longitudinal muscle layer, and in close association with ganglionic EGCs and neurons **(Figure 5.1B)**. Although macrophages reside within the vicinity of the MP, we did not find tdT$^+$ macrophages within ganglionic structures in our experiments **(Figure 5.1B')**. MMs were also found near EGCs and neuronal projections in the extraganglionic space **(Appendix 6)**.

To inspect populations of adaptive immune cells across the gut wall, we performed immunohistochemistry in cross-sections from the *Ser26.tdT* mouse line for the pan-T cell marker CD3ε and the neuronal marker PGP9.5. Compared to macrophages, CD3ε$^+$ T cells are fewer within the lamina propria **(Figure 5.1C)**. However, neuronal fibres and EGC projections were found surrounding CD3ε$^+$ T cells within this layer **(Figure 5.1C and inset Ci)**. To visualise the positioning of T lymphocytes relative to ENS cells in LMMPs, we immunostained the whole-mount preparations of wildtype mice intestines for the T cell marker TCRβ and the EGC marker S100β **(Figure 5.1D, 1D' and 1Di)**. Strikingly, the number of T cells at the level of the MP is very small but at least some of the T cells appear to be close to ENS structures (**Figure 5.1 D'**). As a positive control for the TCRβ antibody, we collected and stained for the same markers the PPs, one of the most important sources of immune cells inside the gut wall. As expected, we observed TCRβ$^+$ cells within this

lymphoid tissue and the PPs were surrounded by EGCs (**Figure 5.1 Di**) and neuronal projections **(Appendix 7)**. However, we did not detect any S100β$^+$ EGCs (**Figure 5.1 Di**) or neuronal projections **(Appendix 7)** within this structure.

To further characterise subpopulations of T cells within the gut wall, we immunostained whole-mount intestinal preparations to detect CD4$^+$ T cells in mice that were injected with AAV9.CaMKII.cre.tdT adenovirus, in which the majority of neurons and their projections are labelled in red **(Figures 5.1E – E")** (see chapter 3 for more details). We observed few CD4$^+$ T lymphocytes within the lamina propria that were closely associated with neuronal fibres (red) **(Figures 5.1E')**. PPs were used as positive controls for the CD4 antibody **(Figure 5.1Ei, asterisk)**. Once again, although CD4$^+$ cells were found inside the PPs, neuronal projections were not detected within this lymphoid structure. Moreover, we did not identify CD4$^+$ cells within the longitudinal muscle layers in our preparations **(Figures 5.1E" – E")**. We also investigated the CD8$^+$ subpopulation of T cells using the same assay, and we did not detect CD8$^+$ T cells within the LMMP preparations **(Appendix 8)**. Since we did not observe any CD4$^+$ T cells within the LMMPs by using antibody labelling of these cells, we took advantage of the *Il17a.Cre;R26R^{eYFP}* reporter mice (kindly provided by the Stockinger lab at the Francis Crick Institute), in which the Cre recombinase is under the control of the *Il17a* promoter. All cells that have once expressed *Il17a* are labelled with the eYFP reporter. This includes the T helper 17 (a subpopulation of CD4$^+$ T cells) and ILC3 (Hirota et al., 2011). We co-stained flat preparations of the gut tissue with the anti-TCRβ antibody to identify the total population of T cells and S100β to identify EGCs **(Figures 5.1F – F")**. We anticipated that with this strategy and our combination of antibodies, T cell populations would be labelled in blue, Th17$^+$ T cells (TCRβ$^+$eYFP$^+$) in turquoise and ILC3 (TCRβ$^-$eYFP$^+$) in green. Flat preparations of the intestines were imaged from the mucosal and the serosal layers. In the mucosal layer, we identified a considerable number of TCRβ$^+$ cells and a small proportion of Th17 and ILC3-expressing *Il17* cells **(Figure 5.1F)**. S100β$^+$ EGCs were found near the pool of these cells in the mucosal layer and submucosal layers **(Figure 5.1F and 5.1F')**. However, consistent with our previous data, we only identified a small number of TCRβ$^+$ T lymphocytes in the level of the MP **(Figure 5.1F")**. Th17 cells were extremely rare or absent in several LMMP preparations **(Figure 5.1F")**. Moreover, the few cells we were able to identify within this layer were not necessarily associated with the ENS cells or fibres **(Figure 5.1F")**.

Furthermore, to expand our analysis, we investigated the distribution of $Foxp3^+$ regulatory T lymphocytes (Tregs) in different layers of the gut by using a reporter line in which a reporter expressing a red fluorescent protein has been knocked into the Foxp3 locus allowing the visualisation of these cells (*Foxp3.mRFP*, provided by the Stockinger lab). Intestinal flat preparations were co-stained for the EGC marker S100β. The majority of RFP^+ Tregs were observed within the mucosal layer **(Figures 5.1G – G')** and we failed to detect RFP^+ Tregs within the LMMPs **(Figures 5.1G")**.

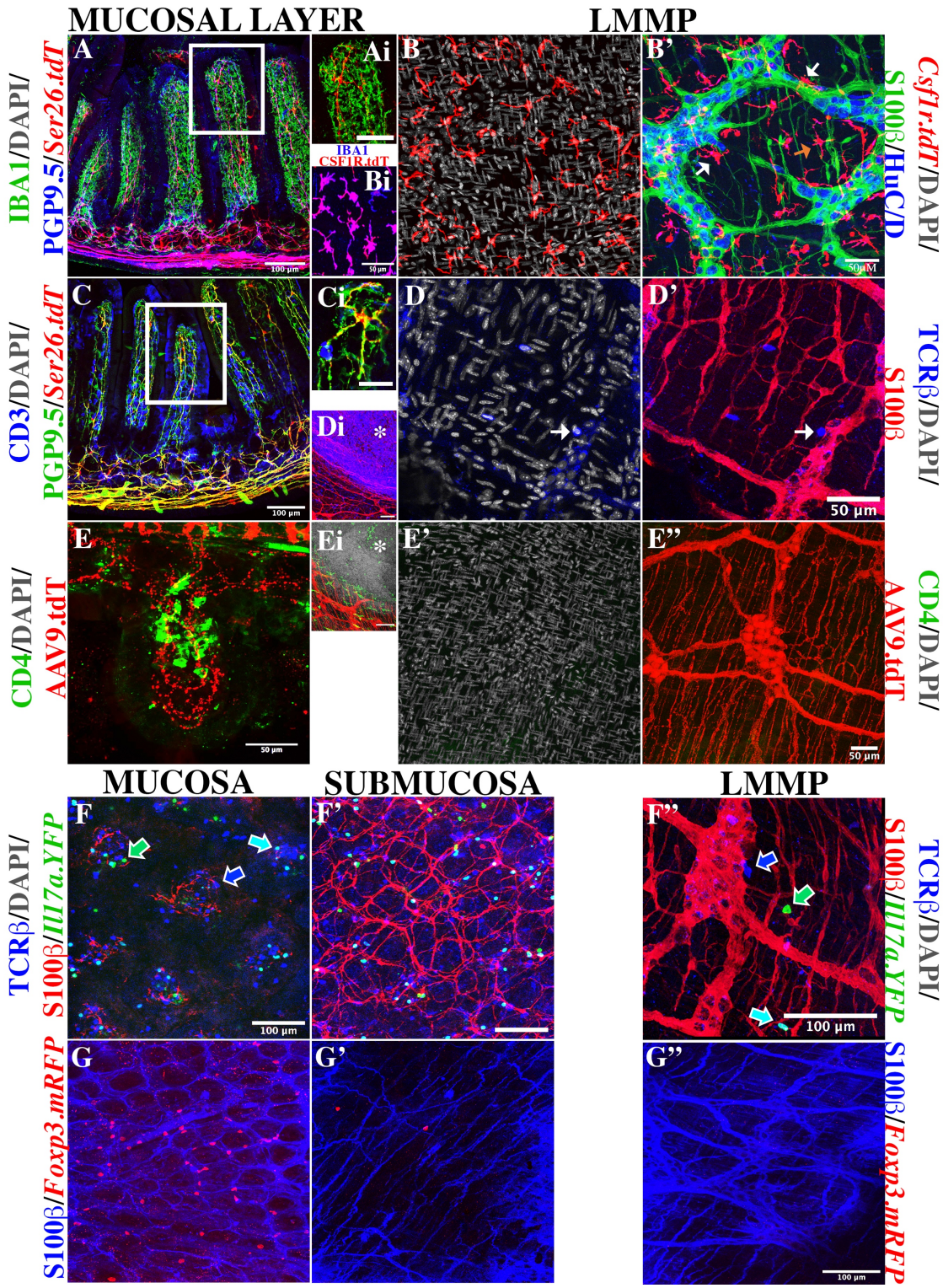


Figure 5.1. Intestinal compartmentalisation of local neuroimmune interactions. Confocal images to detect immune and ENS cells within different layers of the gut. **(A-Ai)** Intestinal cross-section of *Ser26.tdT* mice labelling EGCs in red, co-stained for the macrophage marker Iba1 (green) and the neuronal marker PGP9.5 (blue). Scale bars: 100 µm and 30 µm **(Ai, inset)**. **(B-B')** Immunohistochemistry for the EGC marker S100β (green) and the neuronal marker HuC/D (blue) in whole-mount LMMP preparations of the *Csf1r.tdT* mouse line that labels macrophages in red. White arrow represents MMs closely associated with the MP and orange

arrow with extraganglionic EGCs. **(Bi)** Immunohistochemistry for the macrophage marker Iba1 (blue) in whole-mount LMMP preparations of the *Csf1r.tdT mice*. Scale bar: 50 μm. **(C-Ci)** Cross-section of the intestine from the *Ser26.tdT* mice showing EGCs in red, co-stained for the pan-T cell marker CD3ε (blue) and the neuronal marker PGP9.5 (green). Scale bars: 100 μm **(C)** and 30 μm **(Ci, inset)**. Immunohistochemistry for the EGC marker S100β (red) and the T cell marker TCRβ (white arrows - blue) in whole-mount LMMP preparations **(D-D')** and PPs **(Di)**. Scale bars: 50 μm **(D')** and 100 μm **(Di, inset)**. Immunohistochemistry to detect $CD4^+$ T cell subset (green) in whole-mount LMMP preparations **(E-E")** and PPs **(Ei)** of wildtype mice injected with AAV9.CaMKII.cre.tdT to label the enteric neurons in red. Scale bars: 50 μm **(E")** and 100 μm **(Ei, inset)**. **(F-F")** Immunohistochemistry for the EGC marker S100β (red) and the T cell marker TCRβ (blue) in intestinal whole-mount preparations from the *Il17a.cre.eYFP* mouse line, showing the mucosal, submucosal and LMMP layers. Blue arrows represent $TCR\beta^+$ cells. Turquoise arrows show $TCR\beta^+eYFP^+$ Th17 cells. Green arrows point to $TCR\beta^-eYFP^+$ ILC3. Scale bar: 100 μm. **(G-G")** Immunohistochemistry for the EGC marker S100β (blue) in intestinal whole-mount preparations from the *Foxp3.mRFP* mouse line that labels Tregs in red showing the mucosal, submucosal and LMMP layers. Scale bar: 100 μm. Nuclei were stained with DAPI (grey). LMMP, longitudinal muscle myenteric plexus. All images in this figure are representative of at least three independent experiments.

5.3.2 Regional compartmentalisation of the adaptive immune system

To further analyse the composition and relative abundance of adaptive immune cell populations within LMMPs and mucosal layers of the gut, we immunoprofiled the small intestine and colon of C57Bl/6 mice (n>4) using flow cytometry assays.

Experimental set-up

Single cell suspensions were prepared from intestines of adult wildtype mice and stained with conjugated fluorescent antibodies to detect immune cells (section 2.2.5.1). CD45 antibody was used to identify the total immune cell population while CD19 and CD3ε were used to label B and T cell populations respectively. CD3ε, CD4, Foxp3 (Tregs) and RORγt (Th17) antibodies were used to detect subpopulations of T lymphocytes. Cell suspensions were gated to exclude doublet events based on their size and granularity by using FSC-W (Forward SCatter-Width) versus FSC-H (FSC-Height) **(Figure 5.2A)**, followed by SSC-W (Side SCatter) versus SSC-H **(Figure 5.2A')**. Zombie aqua (L/D) was used to label all dead cells. Second, all single cells were then gated on L/D^-CD45^+ live immune cells **(Figure 5.2A")**. Next, L/D^-CD45^+ cells were separated into $CD3\varepsilon^+$ T

lymphocytes and CD19$^+$ B lymphocytes **(Figure 5.2A''')**. To detect specific subpopulations of T lymphocytes, cells suspensions were then gated on CD4$^+$CD3ε$^+$ (naïve T cells), Foxp3$^+$CD4$^+$ (Tregs) and RORγt$^+$CD4$^+$ (Th17) lymphocytes. MLNs were used for single fluorophore compensation of the antibodies.

Flow cytometry analysis of single cell suspensions prepared from the intestines of adult mice revealed that the proportion of CD19$^+$ B cells is increased in the mucosal layer of the colon (83.5 ± 10.9% SD n=4) and small intestine (77.7 ± 8.3% SD n=3) relative to CD3ε$^+$ T cells (15.9 ± 10.9% n=4 and 20.7 ± 8.3% SD n=3, respectively). In LMMP preparations, the proportion of CD19$^+$ B cells in the colon (56.8 ± 5.1% SD n=4) is slightly augmented relative to CD3ε$^+$ T cells (41.3 ± 5.9% SD n=4). In LMMP cell suspensions from the small intestine, the proportion of CD19$^+$ B cells (43.8 ± 18.1% SD n=3) and CD3ε$^+$ T cells (52.1 ± 17.8% SD n=3) is similar **(Table 5.1)**.

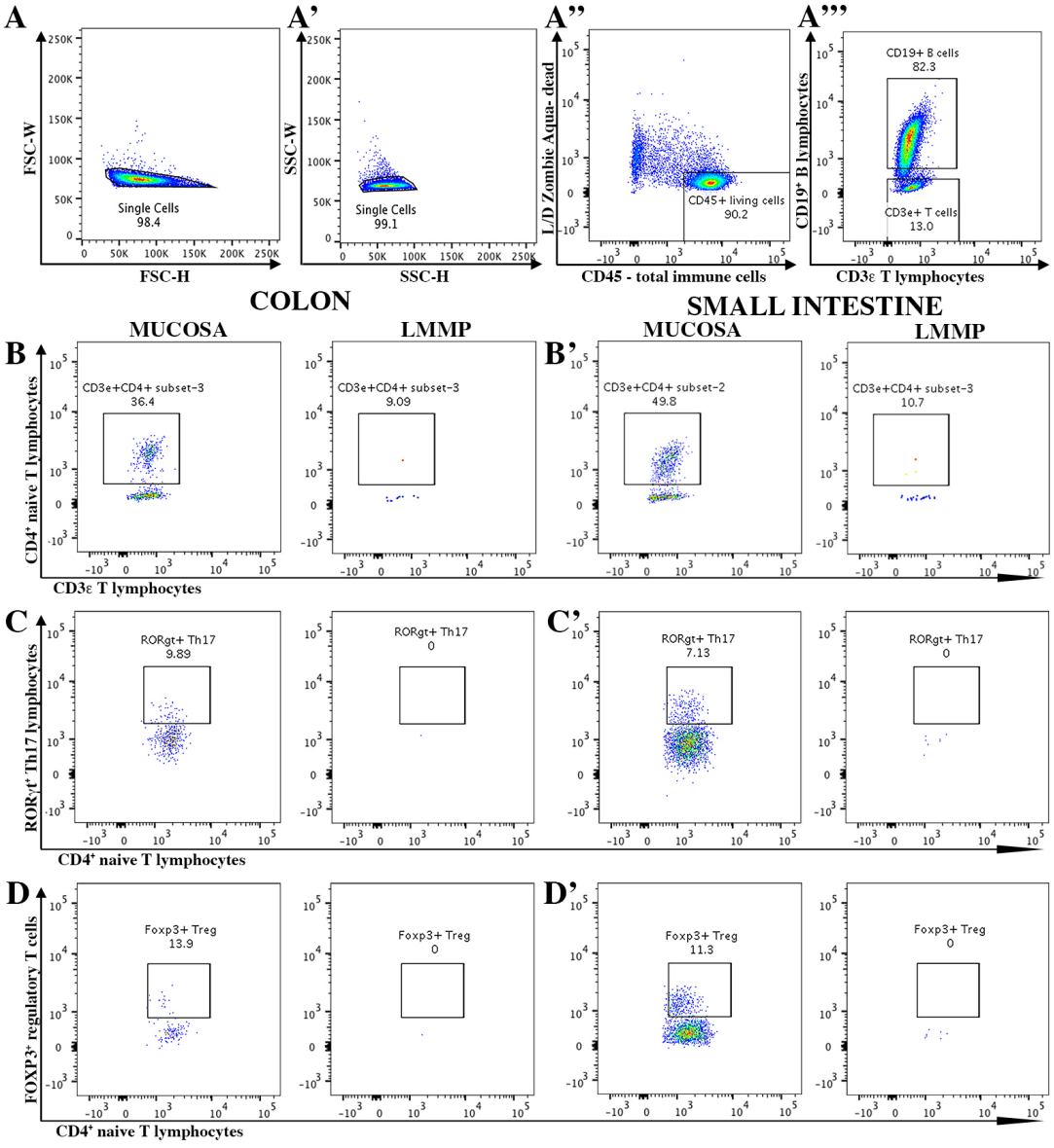
Table 5.1 Proportion of T and B lymphocytes within the mucosal and LMMPs of small intestine and colon

Gated on L/D-CD45+ living cells	% Average Mucosa - Colon	% Average LMMP - Colon	% Average Mucosa - SI	% Average LMMP - SI
CD19+ B lymphocytes	83.5 ± 10.9% SD	56.8 ± 5.1% SD	77.7 ± 8.3% SD	43.8 ± 18.1% SD
CD3ε+ T lymphocytes	15.9 ± 10.9% SD	41.3 ± 5.9% SD	20.7 ± 8.3% SD	52.1 ± 17.8% SD

To support our qualitative data on T cell subsets within different layers of the intestines, cell suspensions containing CD3ε$^+$ T lymphocytes were co-labelled with the CD4 antibody. The proportion of CD4$^+$CD3ε$^+$ cells within the mucosal layer is increased in the colon (39.6 ± 11.3% SD n=4) and small intestine (48.5 ± 12.06% SD n=3) compared to the same population within the LMMPs (12.08 ± 8.7% SD n=4 and 12.6 ± 9.2% SD n=3, respectively) **(Figures 5.2B-B', 5.2E and 5.2F)**. We next investigated the population of Th17 T cells by co-staining cell suspensions with the RORγt antibody. The average of the percentage of RORγt$^+$CD4$^+$ Th17 cells among the total CD3ε$^+$ T cells within the colonic mucosa was around 8.1 ± 4.2% SD and 8.8 ± 4.6% SD in the small intestine and not detectable within the LMMPs from either intestine **(Figures 5.2C-C', 5.2E' and 5.2F)**. Following this, we examined the Foxp3$^+$ Tregs subset of T cells within the mucosa and LMMPs from the small intestine and colon. In the mucosa, the percentage of Foxp3$^+$CD4$^+$

subset was 11.6 ± 5.08% SD in the small intestine and 14 ± 3.1% SD in the colon. Subsets of $Foxp3^{+}CD4^{+}$ Tregs were not detected within the LMMPs of either intestine (**Figures 5.2D-D', 5.2E" and 5.2F**).

Altogether, these data indicate that subsets of the adaptive immune cells within the muscle layer from the small intestine and colon are very rare compared to the same populations within the mucosal layers. Moreover, our immunohistochemistry data has shown that EGCs and neurons are anatomically localised near these cells at the level of the mucosal layer. However, these physical interactions are undetectable or absent within the LMMPs.



F

Gated on CD3ε+CD45+ living cells	% Average (SD) Mucosa - Colon	% Average (SD) LMMP - Colon	% Average (SD) Mucosa - SI	% Average (SD) LMMP - SI
CD4+ T cells	39.6 ± 11.3%	12.08 ± 8.7 %	48.5 ± 12.06%	12.6 ± 9.2%
Gated on CD4+CD3e+CD45+ living cells				
RORγT+ T cells	8.1 ± 4.2%	0%	8.8 ± 4.6%	0%
FOXP3+ T cells	14 ± 3.1%	0%	11.6 ± 5.08%	0%

Figure 5.2. Analysis of T cell subsets within the mucosa and LMMPs of the small intestine and colon from C57Bl/6 mice. Representative flow cytometry plots of immune cells of the intestine showing FSC-W vs

FSC-H **(A)** and SSC-W vs SSC-H profile and gating strategy to exclude doublets **(A')**. **(A")** Representative flow cytometry gating to select live L/D$^-$CD45$^+$ immune cells. **(A"')** Representative flow cytometry gating to separate CD3ε$^+$ T cells from CD19$^+$ B lymphocytes. Flow cytometry plots demonstrating the CD4$^+$ T cell subset within the mucosa and LMMP of the colon **(B)** and small intestine **(B')**. Flow cytometry plots of RORγt$^+$CD4$^+$ Th17 cell subset within the mucosa and LMMP of the colon **(C)** and small intestine **(C')**. Flow cytometry plots of the Foxp3$^+$CD4$^+$ Treg subset within the mucosa and LMMP of the colon **(D)** and small intestine **(D')**. Quantification of the proportion in percentage of CD4$^+$CD3ε$^+$ T cells **(E)**, RORγt$^+$CD4$^+$ Th17 T cells **(E')** and Foxp3$^+$CD4$^+$ Tregs **(E")** in the mucosa and LMMP layers of the small intestine and colon from C57Bl/6 mice. Each dot represents one animal. **(F)** The table represents the average of the percentage of immune cells in different layers of the small intestine and colon. Data pooled from two experiments (n=4). LMMP, longitudinal muscle myenteric plexus. CD, cluster of differentiation. SD, standard deviation. FSC, forward scatter. SSC, side scatter. SI, small intestine.

5.3.3 The ENS network is impaired in absence of the adaptive immune system

To generate an extensive repertoire of antibodies and T cell receptors, lymphocytes undergo somatic DNA rearrangement by recombining the variable (V), diversity (D) and joining (J) segments of genes, a process known as V(D)J recombination. The recombination of V(D)J sequences is crucial for the development of T and B lymphocytes and is performed by recombination activation genes, called *Rag1* and *Rag2*. Expression of these genes is necessary for the maturation of lymphocytes and the development of lymphoid tissues and genetic ablation of one of these genes impairs the development and maturation of T and B lymphocytes (Mombaerts, Iacomini, et al., 1992; Shinkai et al., 1992). In this chapter, we took advantage of *Rag1* and *Rag2* immunodeficient mice, which present very similar phenotypes, to evaluate the contribution of the adaptive immune cells to ENS homeostasis. In addition to *Rag* mutant mice, we have also used the *Tcrα*$^{-/-}$ mutant mice to accurately study the role of T cells on ENS homeostasis. T-cell receptor (TCR) is a molecule in the surface of T lymphocytes that interacts with MHC complexes expressed in the membrane of antigen-presenting cells. There are two types of TCR receptors in the T cell membrane: TCRγδ that is expressed in about 5% of the total T cell population, and TCRαβ that constitutes 95% of the total T cells. TCRαβ receptor is composed of a α chain and a β chain polypeptides. TCRαβ chains associated with a complex of proteins called CD3 form the T cell receptor in the surface of the T lymphocytes. Ablation of one single protein of the TCR

complex results in failure of TCR expression on the T cell surface, leading to impaired development of T cells (Mombaerts, Clarke, et al., 1992).

In this chapter we took advantage of animal models that lack the adaptive immune system such as *Rag1*$^{-/-}$, *Rag2*$^{-/-}$ and *Tcrα*$^{-/-}$ to analyse the ENS function and homeostasis. All mice used in this chapter were males of 8-10 weeks of age of the C57Bl/6 genetic background. Given our observation that immune cells infiltrate are present in the MP of *Rag2*$^{-/-}$ mice (showed in chapter 4), we first examined the presence of potential macroscopic alterations in ENS cell networks and MMs. For this, whole-mount LMMP preparations from C57Bl/6 and *Rag2*$^{-/-}$ mice were immunostained for the EGC marker S100β, the neuronal marker HuC/D and the macrophage marker Iba1. No morphological alterations in Iba1^{+} cells were observed between the two genotypes **(Figures 5.3A1 and A2)**. Despite the absence of morphological alterations in macrophages, we noticed that many HuC/D-expressing neurons were absent from the MP of *Rag2*$^{-/-}$ mice **(Figure 5.3A2)**. The EGC network was also analysed within the intestinal wall by S100β immunohistochemistry. For this, vibratome cross-sections of intestines from C57Bl/6 and *Rag2*$^{-/-}$ mice were immunostained for the EGC markers S100β and Sox10. No obvious qualitative differences were observed between the groups. Sox10^{+}S100β^{+} EGCs were found in various layers of the gut, including the mucosal, submucosal and muscle layers **(Figures 5.3B1 and B2)**. The neuronal network was also assessed by immunohistochemistry for the pan-neuronal markers PGP9.5 and Tuj1 in vibratome transverse intestinal sections. PGP9.5^{+}Tuj1^{+} enteric neurons were identified within the MP and their projections within the lamina propria both in the C57Bl/6 **(Figure 5.3C1)** and *Rag2*$^{-/-}$ **(Figure 5.3C2)** mice. Nonetheless, the organisation of the neuronal network within the muscle layers of the intestine from *Rag2*$^{-/-}$ mice differed structurally from C57Bl/6 controls **(Figures 5.3C1-2)**.

Since the quantification of the neuronal network in intestinal cross-sections is unworkable, and the analysis based on fluorescence intensity of a given marker is not reliable, we opted for using a fluorescent neurotracer dye to evaluate neuronal projections in LMMPs. In these experiments, colonic segments of 2 cm long from C57Bl/6, *Rag2*$^{-/-}$ and *Tcrα*$^{-/-}$ mice were isolated and fixed flat. Tissues were pinned at the edges onto Sylgard-plates, and an additional pin was dipped into DiI tissue-labelling paste and placed in the middle of the tissue **(Figure 5.3D)**. Samples were then incubated at 37ºC for 14 days and

examined using a confocal microscope (section 2.2.7). DiI is a lipophilic neuronal tracer dye that diffuses in the plasma membrane of cells and allows the visualisation of the neuronal network (Sasselli et al., 2013). For our analysis, the percentage of the spreading of the dye per surface was measured and plotted in the graph. Two segments of the colon were analysed per animal in a total of 2 C57Bl/6, 5 *Rag2*$^{-/-}$ and *3 Tcrα*$^{-/-}$ mice. We observed that the percentage of DiI spreading in the *Rag2*$^{-/-}$ (70.43 ± 21.45% SD *p=0.0869*) and *Tcrα*$^{-/-}$ (79.16 ± 9.2% SD *p=0.1588*) mice was marginally decreased when compared with C57Bl/6 controls, yet this decrease was not statistically significant **(Figures 5.3E-F)**. Additionally, we noticed that MPs adjacent to the centre of the dye in the C57Bl/6 control mice **(Figure 5.3G1)** were fulfilled with neuronal projections labelled with DiI, while in the *Rag2*$^{-/-}$ **(Figure 5.3G2)** and *Tcrα*$^{-/-}$ **(Figure 5.3G3)** mice we could only find few labelled neurons. Qualitative analyses of bundles of neuronal projections also suggested that in the *Rag2*$^{-/-}$ and *Tcrα*$^{-/-}$ mice the network of enteric neurons is impaired relative to the C57Bl/6 controls. To confirm the morphological alterations in neuronal network of the MP from immunodeficient mice, immunohistochemistry for the neuronal marker Tuj1 was performed on colonic LMMPs from C57Bl/6, *Rag2*$^{-/-}$ and *Tcrα*$^{-/-}$ mice. We observed that the structure of Tuj1^{+} neuronal fibres within the myenteric ganglia of immunodeficient mice were disorganised, displaying of diffused processes relative to the C57Bl/6 controls **(Figures 5.3H1-3)**.

We further investigated the ENS network within the MP of C57Bl/6 and *Rag2*$^{-/-}$ mice by immunohistochemistry for the EGC markers S100β and Sox10, and the neuronal marker HuC/D on whole-mount colonic LMMP preparations. In the control mice, the majority of the EGCs co-expressed Sox10 and S100β, and these cells tightly surrounded HuC/D^{+} enteric neuronal cell bodies with no apparent gaps between ENS cells **(Figures 5.3I1 and I2)**. However, in *Rag2*$^{-/-}$ mice, gaps between HuC/D^{+} neurons and EGC network were observed within the MP, followed by variable levels of expression of EGC markers between cells **(Figures 5.3J1 and J2)**.

Altogether, these data suggest that the presence of adaptive immune cells is crucial to maintaining the organisation of ENS structures within the MP. However, because the ENS network is extremely complex and heterogeneous and shows no topographic organisation, the methodology for the quantification of important but subtle morphological alterations is frustratingly missing.

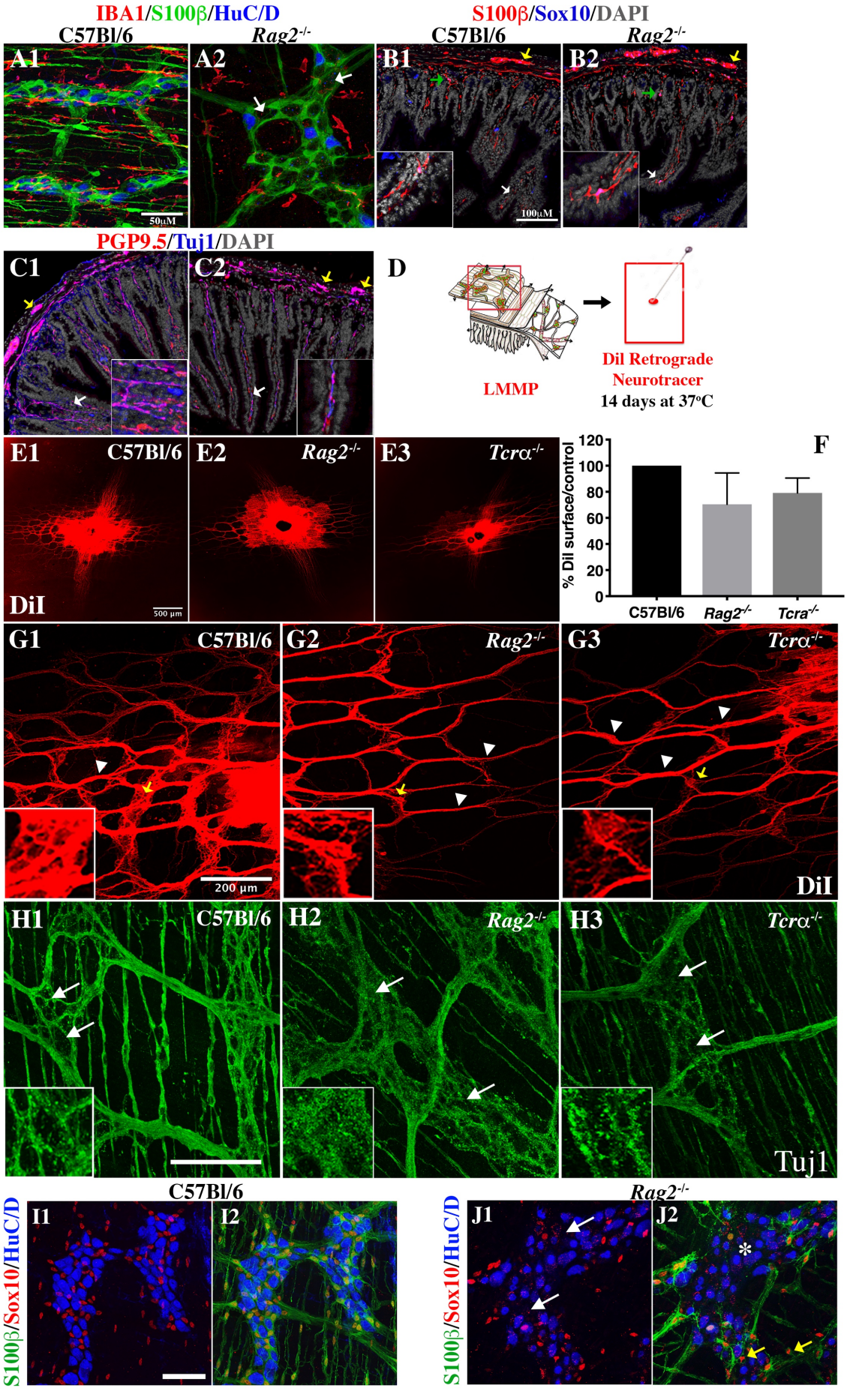

IBA1/S100β/HuC/D
C57Bl/6
Rag2-/-
A1
A2
50μM
S100β/Sox10/DAPI
C57Bl/6
Rag2-/-
B1
B2
100μM
PGP9.5/Tuj1/DAPI
C1
C2
D
LMMP
DiI Retrograde
Neurotracer
14 days at 37°C
E1
C57Bl/6
E2
Rag2-/-
E3
Tcrα-/-
DiI
500 μm
F
% DiI surface/control
120
100
80
60
40
20
0
C57Bl/6
Rag2-/-
Tcra-/-
G1
C57Bl/6
G2
Rag2-/-
G3
Tcrα-/-
200 μm
DiI
H1
C57Bl/6
H2
Rag2-/-
H3
Tcrα-/-
Tuj1
C57Bl/6
Rag2-/-
S100β/Sox10/HuC/D
I1
I2
J1
J2
S100β/Sox10/HuC/D

Figure 5.3. Morphological analyses of the ENS network in mice lacking the adaptive immune system. Immunohistochemistry for the EGC marker S100β (green), pan-neuronal marker HuC/D (blue) and the macrophage marker Iba1 (red) in whole-mount LMMP preparations of C57Bl/6 **(A1)** and *Rag2*$^{-/-}$ **(A2)** mice. White arrow indicates HuC/D^{-} neurons within the MP. Scale bar: 50 μm. Immunohistochemistry for the EGC markers S100β (green) and Sox10 (blue) in intestinal cross-sections of C57Bl/6 **(B1)** and *Rag2*$^{-/-}$ **(B2)** mice. Arrows indicate the EGCs within the mucosal (white), submucosal (green) and muscle (yellow) layers. Scale bar: 100 μm. Immunohistochemistry for the enteric neuronal markers PGP9.5 (red) and Tuj1 (blue) in intestinal cross-sections of C57Bl/6 **(C1)** and *Rag2*$^{-/-}$ **(C2)** mice. Arrows indicate neuronal projections within the mucosal (white) and muscle layers (yellow). Scale bar: 100 μm. Schematic representation of DiI neurotracer procedure **(D)**. DiI tracing in C57Bl/6 **(E1)**, *Rag2*$^{-/-}$ **(E2)** and *Tcrα*$^{-/-}$ **(E3)** mice. Scale bar: 500 μm. **(F)** Quantification of the percentage of DiI spreading in immunodeficient mice relative to C57Bl/6 controls. Kruskal Wallis test. Higher magnification of DiI tracing in C57Bl/6 **(G1)**, *Rag2*$^{-/-}$ **(G2)** and *Tcrα*$^{-/-}$ **(G3)** mice. Arrows show the spreading of DiI in neuronal projections within the MP (white) and the extraganglionic neuronal bundles (yellow). Scale bar: 200 μm. Immunohistochemistry for the neuronal marker Tuj1 (green) in whole-mount LMMP preparations of C57Bl/6 **(H1)**, *Rag2*$^{-/-}$ **(H2)**, and *Tcrα*$^{-/-}$ **(H3)** mice. White arrows highlight structural alterations of neuronal fibres within the MP. Scale bar: 100 μm. Immunohistochemistry for the EGC markers S100β (green) and Sox10 (red), and the pan-neuronal marker HuC/D (blue) in whole-mount LMMP preparations of C57Bl/6 **(I1-I2)** and *Rag2*$^{-/-}$ **(J1-J2)** mice. White arrows indicate HuC/D^{-} neurons within the MP. Asterisk highlights the absence of EGC network within the MP. Yellow arrows point at Sox10^{+}S100β^{-} EGCs within the myenteric ganglia. Scale bar: 50 μm. Nuclei were stained with DAPI. LMMP, longitudinal muscle myenteric plexus. All data in this figure is representative of more than three experiments.

5.3.4 The ENS function is reduced in mice lacking adaptive immune system

To elucidate whether the absence of adaptive immune system had an impact on GI function, we performed the whole transit time assay on *Rag1*$^{-/-}$ and *Rag2*$^{-/-}$ adult (8 weeks old) immunodeficient male mice (section 2.2.11). To minimise the effect of microbiota variation on this assay, mice were co-housed immediately after weaning until used for the experiment. For the total transit time, animals were gavaged with carmine red dye and the total time that took for the first red pellet to be expelled was calculated and expressed in minutes **(Figure 5.4A)**. Despite considerable variability among the groups, we observed a significant increase in the total transit time in *Rag1*$^{-/-}$ mice relative to C57Bl/6 controls (C57Bl/6: 187.2 ± 82.93 min SD n=10; *Rag1*$^{-/-}$: 273.8 ± 51.81 min SD n=6 * *p=0.0419*; *Rag2*$^{-/-}$: 230.5 ± 83.29 min SD n=10 *p=0.3208* ns, Kruskal Wallis test). No statistically significant difference was observed between the *Rag2*$^{-/-}$ group relative to C57Bl/6 controls

(Figure 5.4B). To analyse faecal composition in the experimental groups, we calculated the average of the percentage of water in the stool samples collected immediately after extrusion. No significant differences in water content in the faecal pellets were observed between the groups (C57Bl/6: 52.52 ± 11.43% SD n=10; *Rag1*$^{-/-}$: 64.78 ± 12.39% SD n=6 *p=0.3238* and *Rag2*$^{-/-}$: 51.4 ± 17.54% SD n=10 *p>0.9999* Kruskal Wallis test) **(Figure 5.4C)**. Additionally, we calculated the weight of each pellet and the average value (in mg) was plotted in the graph (section 2.2.12). We did not detect any significant differences between the immunodeficient and control mouse groups (C57Bl/6: 19.51 ± 7.22 mg SD n=6, *Rag1*$^{-/-}$: 27.35 ± 12.34 mg SD n=6 *p=0.8024* and *Rag2*$^{-/-}$: 27.01 ± 12.65 mg SD n=6 *p>0.9999* Kruskal Wallis test) **(Figure 5.4D)**.

To assess whether the absence of the adaptive immune cells influences the motor output of the ENS, we video recorded the spontaneous peristaltic activity of colon preparations maintained in organ culture from C57Bl/6 (control), *Rag1*$^{-/-}$, *Rag2*$^{-/-}$ and *Tcrα*$^{-/-}$ mice (section 2.2.13). The generated spatiotemporal maps represent the CMMCs, which initiate at the proximal end of the colon and normally travel (time in seconds-y axis) along the entire length of the organ (x-axis). All videos were recorded using the same time frame, and the maps were calibrated to the length of the colon **(Figures 5.4E1-E4)**. The number of CMMCs within the total recording time (2500 seconds) was calculated and represented as the average of frequency per minute (CMMCs/min). Our data revealed a significant reduction in the frequency of CMMCs in *Rag1*$^{-/-}$ (0.096 ± 0.03 CMMCs/min SD n=6 **** *p<0.0001*), *Rag2*$^{-/-}$ (0.106 ± 0.02 CMMCs/min SD n=7 *** *p=0.0003*) and *Tcrα*$^{-/-}$ (0.102 ± 0.01 CMMCs/min SD n=4 *** *p=0.0008*) mice compared to C57Bl/6 controls (0.18 ± 0.01 CMMCs/min SD n=7 Kruskal Wallis test) **(Figure 5.4F)**. We also observed that CMMCs in immunodeficient mice were often incomplete and failed to reach the distal end of the colon **(Figures 5.4E1-E4)**. To quantify this observation, we measured the total length of propagated CMMCs (from start point to the end of the wave) and expressed it as a percentage of distance travelled by the wave relative to the total length of the colon. In C57Bl/6 colons, most CMMCs were propagated along the majority of organ length (94.9 ± 11.53%, n>30 CMMCs/6 mice), but the distance of CMMC propagation was highly variable and drastically reduced in *Rag1*$^{-/-}$ (57.3 ± 19.3%, n>30 CMMCs/5 mice ****$p<0.0001$), *Rag2*$^{-/-}$ (49 ± 24.9%, n>20 CMMCs/4 mice ****$p<0.0001$) and *Tcrα*$^{-/-}$ mice (71 ± 22.5%, n>20 CMMCs/4 mice ****$p<0.0001$; Kruskal Wallis test) **(Figure 5.4G)**. In addition, we

quantified the speed of single CMMCs and compared it between the different groups. The speed of CMMCs was calculated by measuring the time it took a single wave to travel over the length of the gut and was expressed in millimetre/second. This analysis showed a substantial reduction in the speed of CMMCs in *Rag1*$^{-/-}$ (0.52 ± 0.33 mm/s, n>30 CMMCs/5 mice ****$p<0.0001$), *Rag2*$^{-/-}$ (0.55 ± 0.46 mm/s, n>20 CMMCs/4 mice ****$p<0.0001$) and *Tcrα*$^{-/-}$ (0.56 ± 0.41 mm/s, n>20 CMMCs/4 mice ****$p<0.0001$) relative to C57Bl/6 controls (1.7 ± 1.5 mm/s, n>30 CMMCs/6 mice; Kruskal Wallis test) **(Figure 5.4H)**. To evaluate whether the absence of B lymphocytes has an effect on the ENS-dependent motility, we quantified the average of frequency of CMMCs in *muMT*$^{-/-}$ mutant mice. Our data did not show any statistically significant differences in the frequency of CMMCs between B cells immunodeficient mice and C57Bl/6 controls (C57Bl/6: 0.138 ± 0.03 CMMCs/min SD n=8 and *muMT*$^{-/-}$: 0.12 ± 0.02 CMMCs/min SD n=4; $p=0.5273$ Mann-Whitney test) **(Figure 5.4I)**.

In summary, our experiments indicate that the absence of the adaptive immune system, more specifically of T lymphocytes impairs the ENS-derived motility, suggesting that the adaptive immune cells contribute to the regulation of neurogenic intestinal function.

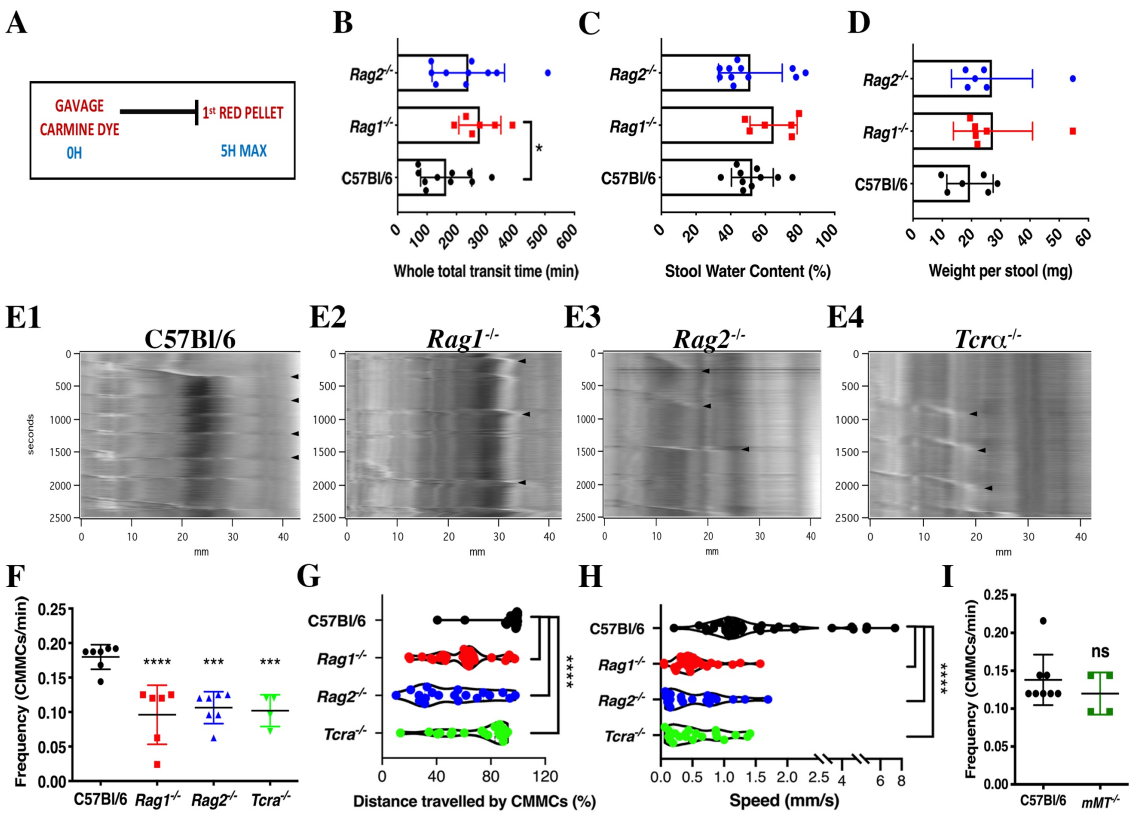


Figure 5.4. Absence of adaptive immune cells impairs the neurogenic intestinal peristalsis. **(A)** Schematic representation of the experimental procedure. **(B)** Quantification of the whole intestinal transit time expressed in minutes in C57Bl/6, *Rag1*$^{-/-}$ and *Rag2*$^{-/-}$ mice. Graphs represent the percentage of the stool water content **(C)** and the weight per stool in milligrams **(D)** in C57Bl/6, *Rag1*$^{-/-}$ and *Rag2*$^{-/-}$ mice. **(B-C)** Each dot represents one animal pooled from at least three experiments. Spatiotemporal maps generated by video recordings of the ENS-derived spontaneous motility of C57Bl/6 **(E1)**, *Rag1*$^{-/-}$ **(E2)**, *Rag2*$^{-/-}$ **(E3)** and *Tcrα*$^{-/-}$ **(E4)** mice colons. Black arrowheads indicate the end of individual CMMCs. **(F)** Quantification of the frequency of CMMCs per minute in the C57Bl/6, *Rag1*$^{-/-}$, *Rag2*$^{-/-}$ and *Tcrα*$^{-/-}$ mice. Each dot represents one animal pooled from more than three experiments. **(G)** Volcano plot shows the measurement of the distance travelled of individual CMMCs expressed by the percentage of total length of the colon in C57Bl/6, *Rag1*$^{-/-}$, *Rag2*$^{-/-}$ and *Tcrα*$^{-/-}$ mice. **(H)** Analysis of the speed of individual CMMCs expressed in millimetres per second in C57Bl/6, *Rag1*$^{-/-}$, *Rag2*$^{-/-}$ and *Tcrα*$^{-/-}$ mice. Kruskal Wallis test. More than 20 CMMCs were quantified and data was pooled from at least three experiments. **(I)** Quantification of the frequency of CMMCs per minute in the C57Bl/6 and *muMT*$^{-/-}$ B cells immunodeficient mice. Each dot represents one animal. Mann-Whitney test. Bars represent standard deviation in all graphs.

5.3.5 Adoptive transfer of T lymphocytes into immunodeficient mice rescues ENS-dependent motility

Our experiments so far have demonstrated that the absence of T lymphocytes impacts on ENS-dependent intestinal motility. To further establish the role of lymphocytes on ENS function, we investigated intestinal motility in immunodeficient mice that were recolonised with the missing lymphocyte populations (adoptive transfer assay of T lymphocytes). Specifically, we analysed and compared in parallel the total transit time and spatiotemporal maps of C57Bl/6, *Tcrα*$^{-/-}$ and *Tcrα*$^{-/-}$ mice that had received Tregs and T naïve lymphocytes from age- and sex-matched C57Bl/6 donors.

Experimental set-up for the adoptive cell transfer experiments

All mice used in these experiments were male and matched for age. For lymphocyte isolation, MLNs and spleens from 7-week-old male C57Bl/6 mice were dissected, dissociated, immunostained for subtype markers (L/D Zombie Aqua to exclude dead cells; CD45Alexa Fluor 700 to detect the total immune cell population; CD3 PerCP-Cy5.5 to identify the total population of T lymphocytes; CD4 APC to detect naïve T cells and CD25 Alexa Fluor 488 to detect Tregs) and subjected to FACS analysis (section 2.5.3). Cell suspensions were gated to exclude double events using FSC-H vs FSC-A and SSC-W vs

SSC-A. Live single cells (L/D^-) were then selected and $CD3^+CD45^+$ T lymphocytes were next separated into $CD25^+CD4^+$ Tregs and $CD25^-CD4^+$ naïve T cells. 3 x 10^6 $CD25^+CD4^+$ Tregs or $CD25^-CD4^+$ naïve T cells were sorted from MLN and spleen from 8 C57Bl/6 mice. 6 x 10^5 $CD25^+CD4^+$ Tregs or 6 x 10^5 $CD25^-CD4^+$ naïve T cells were intravenously injected into *Tcrα*$^{-/-}$ mice and recipient mice were analysed 10 weeks after the transfer together with C57Bl/6 and *Tcrα*$^{-/-}$ controls **(Figure 5.5A)**.

To confirm the efficiency of adoptive transfer, we isolated the spleen **(Appendix 9)** and MLNs of individual mice from each group and performed flow cytometry analysis to identify the adaptive immune cells **(Figures 5.5B-E)**. The gating strategy to analyse the presence of naïve and Treg T cells in these lymphoid tissues was established as shown in the representative cytometry plots of C57Bl/6 mice: Cell suspensions were gated on singlet (SSC-A vs FSC-A and FSC-W vs FSC-H) **(Figure 5.5B)** live (L/D^-) immune cells ($CD45^+$) **(Figure 5.5B1)** and separated into T lymphocytes ($TCR\beta^+$) and B lymphocytes ($CD19^+$) **(Figure 5.5B2)**. Treg cells ($Foxp3^+TCR\beta^+$) were detected by immunostaining in cell suspensions for Foxp3 **(Figure 5.5B3)**. *Tcrα*$^{-/-}$ mice did not display any $TCR\beta^+$ cells although $CD19^+$ B lymphocytes were present as expected **(Figure 5.5C)**. Moreover, the transfer of naïve T lymphocytes into *Tcrα*$^{-/-}$ mice effectively rescued this population within lymphoid tissues **(Figure 5.5D)**. Likewise, adoptive transfer of $Foxp3^+$ Tregs efficiently replaced this population within lymphoid tissues **(Figure 5.5E)**.

To assess whether the adoptive transfer of naïve T cells or Tregs could rescue the phenotype of GI motility, we first performed the total transit time assay as described above. We observed a significant reduction in the total transit time in *Tcrα*$^{-/-}$ mice that received Tregs (90 ± 20.9 min, n=5 ** $p = 0.0025$) and naïve T cells (110 ± 7.3 min, n=5 * $p = 0.0135$) relative to *Tcrα*$^{-/-}$ controls (182.8 ± 42.6 min, n=10 Kruskal-Wallis test) **(Figure 5.5F)**. To analyse the faecal composition between the experimental groups, we examined the stool water content in these mice and found that the stool water content was similar across all groups (C57Bl/6, 42.9 ± 4.3% SD n=8; *Rag2*$^{-/-}$, 37.7 ± 3.4% SD n=5; *Tcrα*$^{-/-}$, 35.7 ± 7.9% SD n=10; *Tcrα*$^{-/-}$ + Tregs, 35.2 ± 3.9% SD n=5; *Tcrα*$^{-/-}$ + naïve T cells, 35.5 ± 7.5% SD n=5) **(Figure 5.5F')**. Together these findings suggest that the reduced total transit time following adoptive transfer was not related to the development of intestinal inflammation.

To directly test whether the adoptive transfer of lymphocytes restores ENS function, we generate spatiotemporal maps and compared the frequency of CMMCs (an ENS-dependent motility pattern) between C57Bl/6, *Tcrα*$^{-/-}$, *Tcrα*$^{-/-}$ + naïve T cells and *Tcrα*$^{-/-}$ + Tregs **(Figure 5.6H-H'")**. The number of CMMCs within the total recording time (2500 seconds) was analysed and represented as the average of frequency per minute. Consistent with our previous experiments **(Figure 5.4F)**, *Tcrα*$^{-/-}$ (0.091 ± 0.07 CMMCs/min SD n=5 *** *p = 0.0007*) displays a significant reduction in the frequency of CMMCs when compared to C57Bl/6 controls (0.234 ± 0.02 CMMCs/min SD n=4) **(C57Bl/6 vs *Tcrα*$^{-/-}$, Figure 5.5G)**. To examine whether the adoptive transfer rescued this phenotype, we first compared the average of the frequency of CMMCs between the *Tcrα*$^{-/-}$ and *Tcrα*$^{-/-}$ + Tregs group. Interestingly, our data demonstrate that the adoptive transfer of Tregs into *Tcrα*$^{-/-}$ mice partially rescued the ENS-derived motility (0.197 ± 0.01 CMMCs/min SD n=5 * *p = 0.0346*) when compared to the *Tcrα*$^{-/-}$ group **(*Tcrα*$^{-/-}$ vs *Tcrα*$^{-/-}$+ Tregs, Figure 5.5G)**. Moreover, no significant differences were observed when we compared the *Tcrα*$^{-/-}$ + Tregs with the C57Bl/6 controls (*p=0.5678*), further suggesting that Tregs interact with the ENS to modulate intestinal motility **(C57Bl/6 vs *Tcrα*$^{-/-}$+ Tregs, Figure 5.5G)**. However, the transfer of naïve T cells into the *Tcrα*$^{-/-}$ was not sufficient to rescue the frequency of CMMCs (0.173 ± 0.01 CMMCs/min SD n=5 *p = 0.5599*) relative to *Tcrα*$^{-/-}$ mice **(*Tcrα*$^{-/-}$ vs *Tcrα*$^{-/-}$+ naïve T cells, Figure 5.5G)**. To further support that, we compared the *Tcrα*$^{-/-}$ + naïve T cells group with the C57Bl/6 controls, and we found a significant difference in the frequency of the CMMCs (*p= 0.0429* Kruskal-Wallis test), suggesting that the adoptive transfer of naïve T lymphocytes into *Tcrα*$^{-/-}$ is not enough to restore the ENS-derived intestinal motility **(C57Bl/6 vs *Tcrα*$^{-/-}$+ naïve T cells, Figure 5.5G)**. We additionally evaluated whether the adoptive transfer of T and B cells would restore the motility defects in *Rag2*$^{-/-}$ immunodeficient mice. Although we observed a slight increase in the frequency of the CMMCs after transfer with T and T and B cells, this increase was not statistically significant (n ≥ 5 mice/group – **Appendix 10**).

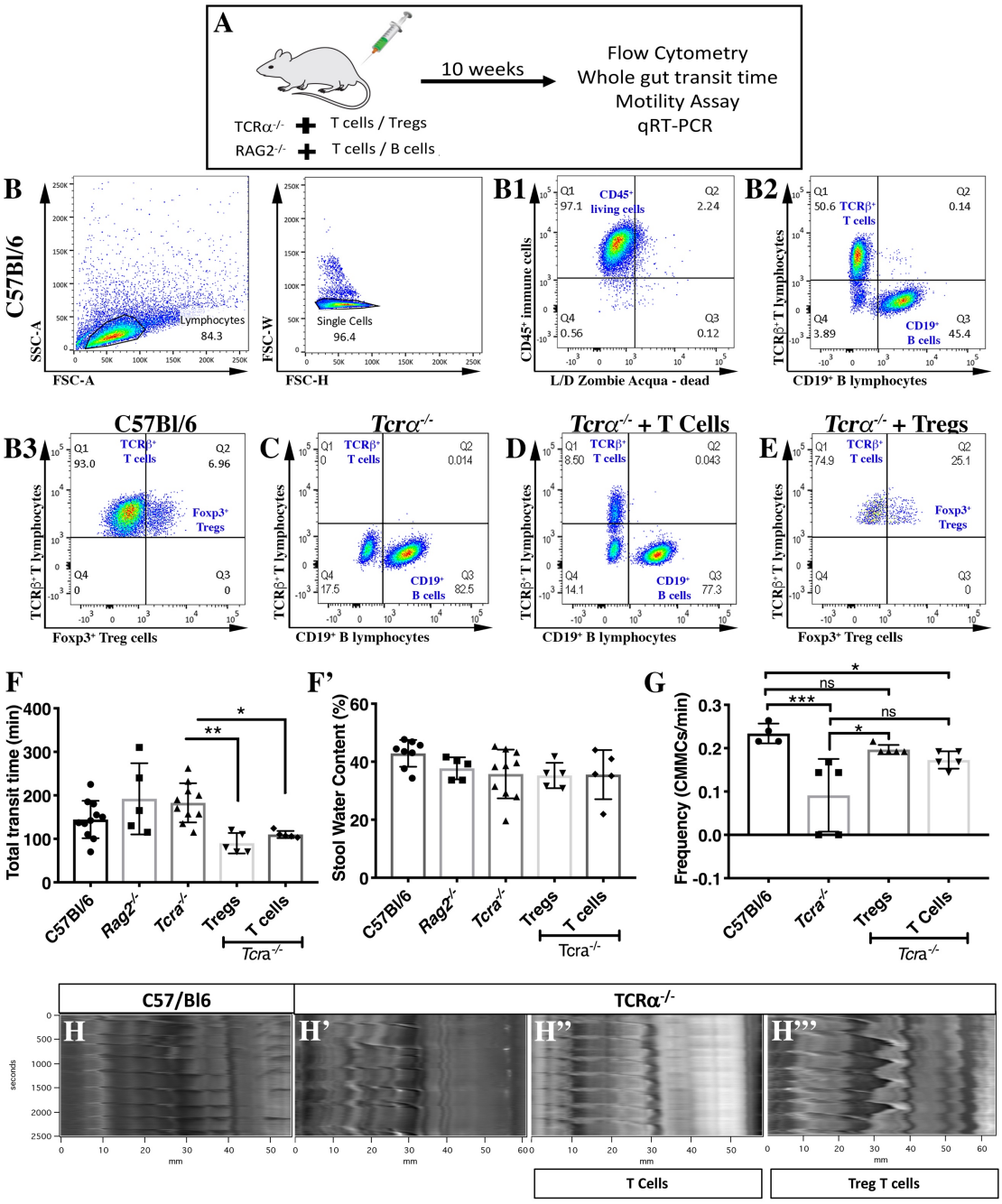


Figure 5.5. Regulatory T cells modulate the ENS-dependent colonic motility. (A) Schematic representing the experimental procedure of the adoptive transfer. **(B)** Representative flow cytometry plots of cell suspensions from the MLN in C57Bl/6 mice showing SSC-A vs FSC-A and FSC-W vs FSC-H gating strategy to exclude doublets. **(B1)** Representative gating to select live CD45$^+$ immune cells (top left quadrant). **(B2)** Flow cytometry gating to separate TCRβ$^+$ T cells (top left quadrant) and CD19$^+$ B lymphocyte (bottom right quadrant) populations. **(B3)** Representative plot to identify Foxp3$^+$TCRβ$^+$ Tregs (top right quadrant). **(C)** Flow cytometry plot of MLN from the *Tcrα*$^{-/-}$ controls showing the absence of TCRβ$^+$ T cells (top left quadrant) and the presence of CD19$^+$ B lymphocytes (bottom right quadrant). **(D)** Flow cytometry plot of MLN from the *Tcrα*$^{-/-}$ transferred with naïve T cells showing TCRβ$^+$ T lymphocytes (top left quadrant) and CD19$^+$ B lymphocytes (bottom right quadrant). **(E)** Flow cytometry plot of MLN from the *Tcrα*$^{-/-}$ transferred with

regulatory T cells showing Foxp3$^+$TCRβ$^+$ Tregs (top right quadrant). **(F)** Quantification of the whole intestinal transit time expressed in minutes in C57Bl/6, *Rag2*$^{-/-}$, *Tcrα*$^{-/-}$, *Tcrα*$^{-/-}$ + Tregs, *Tcrα*$^{-/-}$ + naïve T cells mice. Kruskal-Wallis test. * $p < 0.05$, ** $p < 0.01$ n ≥ 5 mice/group. **(F')** Graphs represent the percentage of the stool water content in mg in C57Bl/6, *Rag2*$^{-/-}$, *Tcrα*$^{-/-}$, *Tcrα*$^{-/-}$ + Tregs, *Tcrα*$^{-/-}$ + naïve T cells mice. Kruskal-Wallis test. Each dot represents one animal n ≥ 5 mice/group. **(G)** Quantification of the frequency of CMMCs per minute in C57Bl/6, *Tcrα*$^{-/-}$, *Tcrα*$^{-/-}$ + Tregs, *Tcrα*$^{-/-}$ + naïve T cells mice. Kruskal-Wallis test multiple comparisons. n ≥ 4 mice/group * $p < 0.05$, ** $p < 0.01$. All bars represent SD. Spatiotemporal maps generated by video recordings of the ENS-derived spontaneous motility of C57Bl/6 **(H)**, *Tcrα*$^{-/-}$ **(H1)**, *Tcrα*$^{-/-}$ + naïve T cells **(H2)** and *Tcrα*$^{-/-}$ + Tregs **(H3)** mice. All data in this figure was pooled from two independent experiments with n≥5

5.3.6 Absence of the adaptive immune system alters the ENS transcriptome

The coordination of ENS-dependent motility is due to an orchestrated activity of several subsets of neurons located within ganglionic structures. Since our data have suggested that intestinal motility is impaired in mice lacking the adaptive immune system, we next investigated the two main populations of enteric neurons that have key roles in peristalsis. Specifically, we performed immunohistochemistry in whole-mount preparations of colonic LMMPs from C57Bl/6, *Tcrα*$^{-/-}$ and *Rag2*$^{-/-}$ mice for the pan-neuronal marker HuC/D, Calretinin, which identifies excitatory motoneurons and nNos, which is expressed by a population of inhibitory motoneurons **(Figures 5.6A1-A3)**. The population of nNos$^+$ neurons was quantified per image in these groups and expressed as an average of the percentage of nNos$^+$HuC/D$^+$ neurons. Our data show that the population of nitrergic neurons is significantly reduced in LMMPs from the *Tcrα*$^{-/-}$ (11.9 ± 6.8% SD n=3 ***p=0.0042*) and *Rag2*$^{-/-}$ (13.6 ± 8.2% SD n=3 **p=0.0141*) immunodeficient mice relative to C57Bl/6 controls (26.9 ± 7.9% SD n=3 Kruskal Wallis test) **(Figure 5.6B1)**. In parallel, the population of Calretinin$^+$ neurons within the MP was quantified and expressed as an average of the percentage of Calretinin$^+$HuC/D$^+$ neurons. We observed a significant decrease in the percentage of these cells within the MP of *Tcrα*$^{-/-}$ (11.6 ± 5.7% SD n=3 ***p=0.0029*) and *Rag2*$^{-/-}$ (11.9 ± 7.4% SD n=3 **p=0.0018* mice compared to the C57Bl/6 mice (26.3 ± 5% SD n=3 Kruskal Wallis test) **(Figure 5.6B2)**.

To further characterise the molecular profile of enteric neuron and glial cells in immunodeficient mice, we evaluated the expression of neuron- and glia-specific genes in

colonic LMMPs isolated from *Rag2*$^{-/-}$ mice relative to C57Bl/6 controls by qRT-PCR. In *Rag2*$^{-/-}$ mice we observed a significant downregulation of genes that are normally expressed by the majority of enteric neurons, such as *Elavl3 (** p=0.0010)*, *Elavl4 (* p=0.0286)* and *Ret (** p=0.0011)*, and genes expressed by motoneurons, such as *Chat (** p=0.0079)*, *Nos1 (* p=0.0126)* and *Calb2 (* p=0.0103)* (each dot in the plots represents one animal. Mann-Whitney test). However, no statistically significant differences were observed between mutant and control groups in the expression of developmental genes [*Hand2 (p=0.0693)*, *Phox2b (p=0.6905)* and *Ascl1 (p=0.4127)*] or genes encoding neuron-specific proteins and neuropeptides [*Calb1 (p=0.4127)*, *Cgrp (p=0.1453)*, *Vip (p=0.1866)*, *Npy (p=0.5526)*, *Tac1 (p>0.9999)* and *Tph2 (p=0.3095)*] **(Figure 5.6C)**. We also quantified the transcript levels of genes exclusively expressed by EGCs and observed a significant downregulation of *S100 (* p=0.0499)* and *Sox2 (** p=0.0068)*, although *Sox10 (p=0.2168)*, *Gfap (p=0.1648)*, *Foxd3 (p=0.1121)*, *Hes5 (p=0.9725)*, *Gdnf (p=0.1218)* and *Erbb3 (p=0.3013)* were not altered in *Rag2*$^{-/-}$ mice (Mann-Whitney test) **(Figure 5.6D)**. Finally, we examined the expression levels of *Ret (** p=0.0023)* and *Elavl3 (*** p=0.0006)* in muscularis externa of *Tcr*$\alpha^{-/-}$ mice and observed a significant reduction in the expression of these markers when compared to the C57Bl/6 controls (n=7/group Mann-Whitney test) **(Figure 5.6E)**.

Since our previous data have suggested by qRT-PCR that some important genes expressed in enteric neurons are downregulated in mice lacking the adaptive immune system, we next assessed whether the adoptive transfer of T cells could modulate the transcriptional profile of enteric neurons. To test that, we quantified the transcript levels of *Elavl3* in several groups of immunodeficient mice that were reconstituted with various combinations of immune cells. The groups analysed were C57Bl/6, *Tcr*$\alpha^{-/-}$, *Tcr*$\alpha^{-/-}$ + naïve T cells, *Tcr*$\alpha^{-/-}$ + Treg cells, *Rag2*$^{-/-}$, *Rag2*$^{-/-}$ + T cells and *Rag2*$^{-/-}$ + B cells. Although we observed a significant reduction in the level of expression of *Elavl3* in all groups relative to the C57Bl/6 as previously shown here, the adoptive transfer in any condition did not restore the transcriptional profile of *Elavl3* in the immunodeficient mice (n=4mice/group Kruskal-Wallis Multiple comparisons test * $p < 0.05$) **(Figure 5.6F)**.

Taken together, these experiments suggest that the ENS of immunodeficient mice is characterised by specific changes in neuronal and glial gene expression, and the reconstitution of adaptive immune populations is not enough to restore the transcriptional profile of enteric neurons.

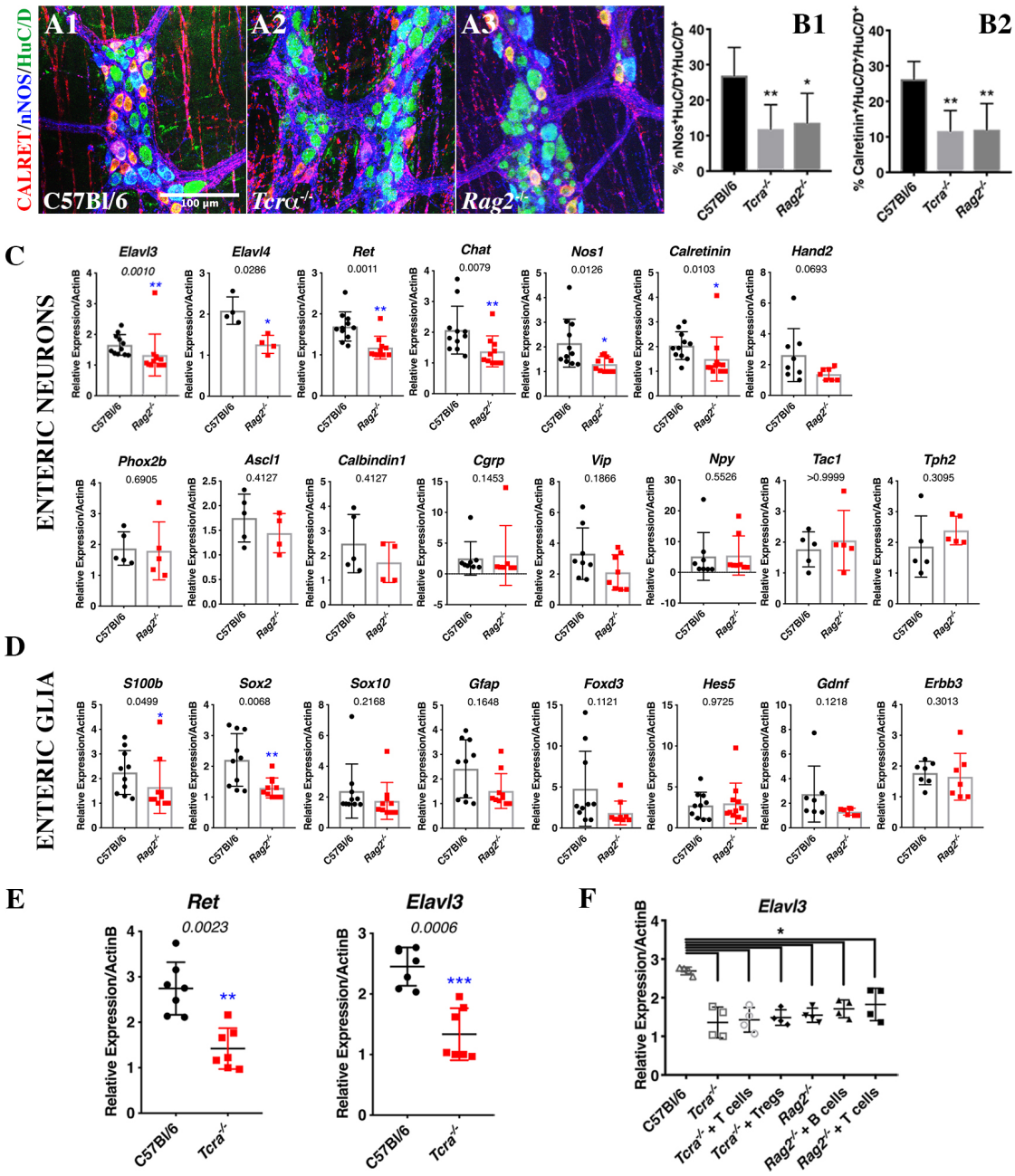


Figure 5.6. Effect of the absence of the adaptive immune system on ENS-specific transcript levels within the colon. Immunohistochemistry for the neuronal marker HuC/D (green), Calretinin (red) and nNos (blue) in whole-mount LMMP preparations of the colon from C57Bl/6 **(A)**, *Tcrα*$^{-/-}$ **(A2)** and *Rag2*$^{-/-}$ **(A3)**. Scale bar: 100 µm. **(B1)** Quantification of the average of the percentage of nNos^{+}HuC/D^{+} enteric neurons within the MP from C57Bl/6, *Tcrα*$^{-/-}$ and *Rag2*$^{-/-}$ mice. **(B2)** Quantification of the average of the percentage of Calretinin^{+}HuC/D^{+} enteric neurons within the MP from C57Bl/6, *Tcrα*$^{-/-}$ and *Rag2*$^{-/-}$ mice. Kruskal-Wallis test. Results were pooled from three independent experiments. **(C)** qRT-PCR analysis of neuronal molecular markers such as *Elavl3*, *Elavl4*, *Ret*, *Chat*, *Nos1*, *Calb2*, *Hand2*, *Phox2b*, *Ascl1*, *Calb1*, *Cgrp*, *Vip*, *Npy*, *Tac1* and *Tph2* transcript levels in C57Bl/6 and *Rag2*$^{-/-}$ mice. **(D)** qRT-PCR analysis of enteric glia molecular

markers such as *S100b*, *Sox2, Sox10*, *Gfap*, *Foxd3*, *Hes5, Gdnf* and *Erbb3* transcript levels in C57Bl/6 and *Rag2*$^{-/-}$ mice. **(E)** qRT-PCR analysis of *Elavl3* and *Ret* transcript levels in C57Bl/6 and *Tcrα*$^{-/-}$ mice. Dot plots show the relative expression values obtained from an individual mouse (n>4/group) which were normalised to *Actinb*. * $p < 0.05$, ** $p < 0.01$, *** $p < 0.001$. Mann-Whitney test. **(F)** qRT-PCR analysis of *Elavl3* transcript levels in C57Bl/6, *Tcrα*$^{-/-}$, *Tcrα*$^{-/-}$ + Tregs, *Tcrα*$^{-/-}$ + naïve T cells, *Rag2*$^{-/-}$, *Rag2*$^{-/-}$ + B cells and *Rag2*$^{-/-}$ + T cells mice. Dot plots show the relative expression values obtained from an individual mouse which were normalised to *Actinb* (All data was pooled from more than three independent replicates, n≥4 mice/group Kruskal-Wallis multiple comparisons test * $p < 0.05$). All bars represent SD.

Since our gene expression analysis by qRT-PCR was carried out in tissue segments (colonic LMMPs) containing non-ENS cell types and targeted to a restricted set of genes, we expanded the characterisation of the transcriptional profile of enteric neurons using bulk nRNAseq. As mentioned in Chapter 3, the isolation of enteric neurons is challenging due to their location within the intestinal wall, the complexity of neuronal network and extensive branching and sensitivity of these cells to mechanical manipulations. Dr Obata from our lab has developed an efficient strategy to target neuronal nuclei which uses AAV vectors to transduce nuclear localised fluorescent reporters in enteric neurons. I have contributed to the development of this strategy by characterising the efficiency of neuronal transduction in wildtype mice, and applied this technique to label and isolate the neuronal nuclei of immunodeficient mice for bulk nRNAseq **(Figure 5.7A)**. First, to assess the efficiency of neuronal transduction in immunodeficient mice, AAV9-CAMKII-KASHeGFP was injected into the tail vein of *Rag2*$^{-/-}$ mice and C57Bl/6. Four weeks after the injections, the intestines of injected mice were harvested and the percentage of eGFP^{+} enteric neurons was determined in both mutant and control mice following HuC/D immunostaining. No significant differences were observed in the percentage of transduced colonic myenteric neurons between *Rag2*$^{-/-}$ (81.9 ± 4.9% SD) and C57Bl/6 mice (84.7 ± 2.6% SD) **(Figures 5.7A1-A3)**. This experiment, indicating that genetic ablation of adaptive immune cells does not impact on enteric neuron transduction by AAV vectors, allowed us to proceed with our experimental strategy to target enteric neuron nuclei with fluorescent reporters and isolate them for bulk nRNAseq.

We chose to perform nRNAseq of enteric neurons isolated from *Tcrα*$^{-/-}$ mice, since all ENS related phenotypes in these mutant mice (both histological and functional) were very similar to the *Rag1*$^{-/-}$ and *Rag2*$^{-/-}$ immunodeficient mice **(Figures 5.3 and 5.4)**. Moreover,

our motility assay did not show any significant difference in the frequency of CMMCs in mice lacking B lymphocytes **(Figure 5.4I)**, suggesting that perhaps the absence of T, but not B cells have an impact on the ENS-dependent motility.

Experimental set-up

For enteric neuron nuclear isolation, 4 C57Bl/6 and 4 *Tcrα*$^{-/-}$ male 6-week old mice were injected systemically via tail vein with the AAV9-CAMKII-KASHeGFP vector. LMMPs from the entire colon were isolated from control and mutant mice 4 weeks post-injection. Detailed protocols for tissue dissections, nuclear isolation and gating strategy are presented in Chapter 3 and section 2.2.5.5. The total numbers of nuclei isolated from each animal and sample are shown in **Table5.2**.

Table 5.2 Total numbers of isolated nuclei from C57Bl/6 and *Tcrα*$^{-/-}$ colonic LMMPs

	eGFP^{+}	**eGFP^{-}**
C57Bl/6-1	21037	40967
C57Bl/6-2	22161	35238
C57Bl/6-3	50000	50000
C57Bl/6-4	33440	50000
***Tcrα*$^{-/-}$-1**	18694	30119
***Tcrα*$^{-/-}$-2**	15701	36284
***Tcrα*$^{-/-}$-3**	21434	50000
***Tcrα*$^{-/-}$-4**	>30000	50000

RNA from each sample was prepared using TRIzoL and Invitrogen PureLink column, reagents optimised for small amounts of RNA, and total RNA isolated from each sample was submitted to the Advanced Sequencing Facility of the Francis Crick Institute. All samples were reviewed and tested for quality control by using MultiQC. Bioinformatics analyses were carried out by Dr Stefan Boeing at the Bioinformatics and Biostatistics Science Technology Platform of the Crick Institute (sections 2.2.2.2, 2.2.4, 2.2.5 and 2.2.15.3).

Dimensionality reduction algorithms, such as principal component analysis (PCA) were used initially to cluster samples with similar transcriptional profile. With each dot in the PCA plot of **Figure 5.7B** representing the transcriptional profile of a group of nuclei isolated from an individual animal, it is evident that the nuclear transcriptomes of enteric

neurons from C57Bl/6 and *Tcrα*$^{-/-}$ mice clustered together. Likewise, the nuclear transcriptomes of non-neuronal cells isolated from C57Bl/6 and *Tcrα*$^{-/-}$ mice generally clustered together. These observations suggest that the *Tcrα* mutation does not have a dramatic impact on the transcriptional profile of colonic enteric neurons **(Figure 5.7B)**. As an additional quality control of our experiment, we overlapped our differentially expressed gene set between C57Bl/6 neuronal and non-neuronal nuclei, with the data set acquired independently in the lab by Dr Obata using the same technique from the colon of wildtype (C57Bl/6) mice (Obata et al, 2019 *in preparation*). We observed a complete overlap in the neuronal transcripts between our and Dr Obata's samples **(Figure 5.7C)**. Among the genes identified as neuron-specific were *Elavl3*, *Elavl4* and *Ret*, established markers of enteric neurons **(Figure 5.7C)**. We also compared our data with Dr Obata's most highly expressed neuronal genes. As shown in the heat map of **Figure 5.7D**, we observed that the transcripts of a characteristic set of neuronal marker genes (*Camk2, Elavl4, Nos1, Ret, Elavl3, Tubb3* and *Chat*) identified in Obata's data are similarly distributed in the positive (neuronal) and negative (non-neuronal) populations of nuclei isolated from the colon of C57Bl/6 and *Tcrα*$^{-/-}$ mice. Taken together, our analysis suggests that the protocol for nuclear transcriptome analysis we have employed here is highly reproducible and robust.

Next, we used gene set enrichment analysis to identify differentially expressed genes between colonic neurons from C57Bl/6 and the *Tcrα*$^{-/-}$ mice. Surprisingly, no differentially expressed genes were identified, except for *Rb1*, which was significantly reduced in enteric neurons from *Tcrα*$^{-/-}$ mice **(Figures 5.7E and 7F)**. Therefore, our nRNAseq analysis challenges our earlier qRT-PCR analysis **(Figure 5.6C)** which revealed that several neuron-specific genes were downregulated in mutants. Nevertheless, it has identified *Rb1* as specifically downregulated in colonic neurons of *Tcrα*$^{-/-}$ mutants, suggesting that this transcriptional regulator supports the fitness of intestinal neural networks in response to neuroimmune interactions within the gastrointestinal tract.

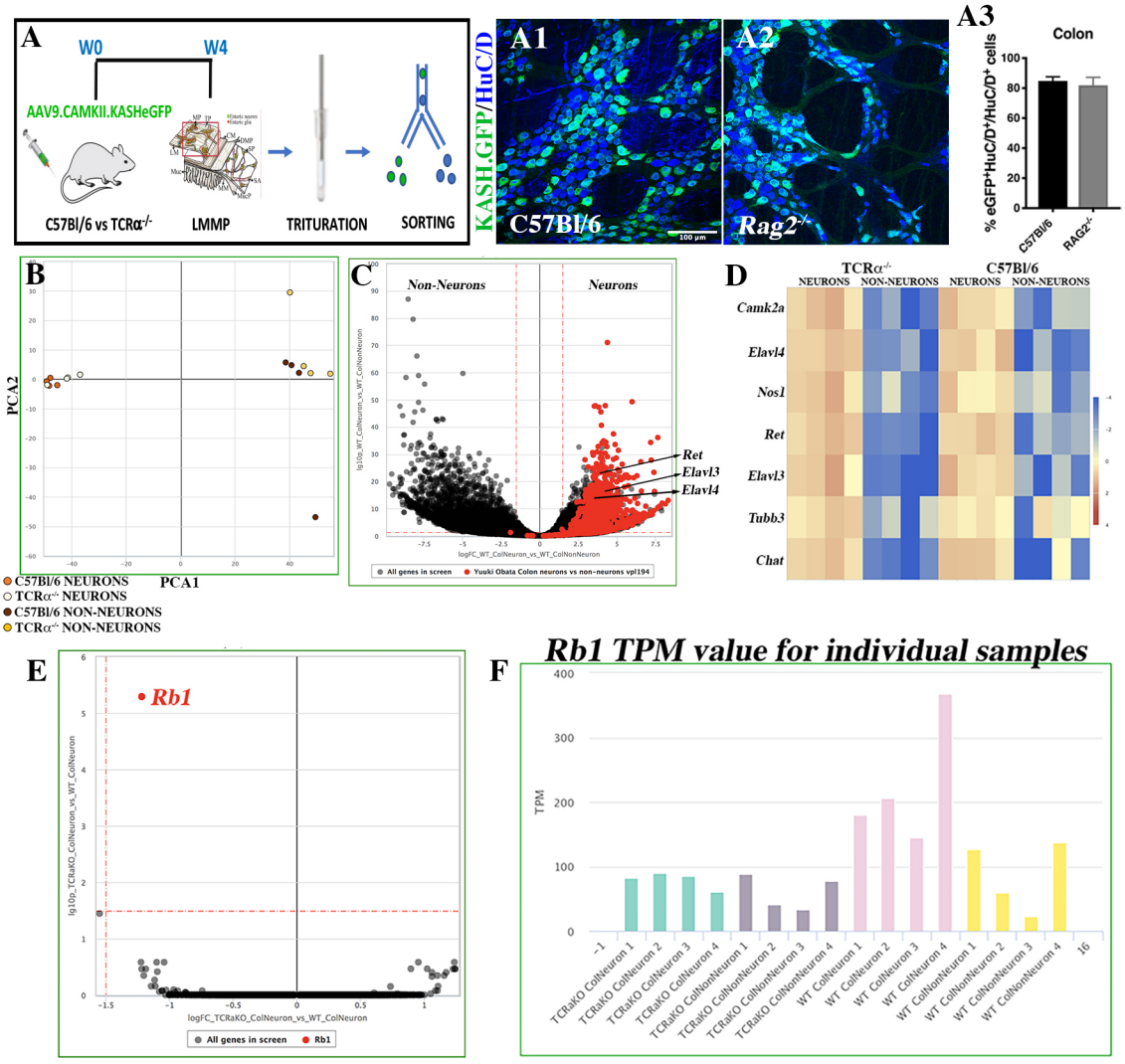


Figure 5.7. Impact of the absence of T lymphocytes on the transcriptional profile of enteric neurons. (A) Schematic representation of the nuclei isolation procedure. Immunohistochemistry to detect HuC/D^{+} (blue) neurons in whole-mount colonic LMMP preparations of C57Bl/6 **(A1)** and *Rag2*$^{-/-}$ **(A2)** injected with AAV9.KASHeGFP (green). Scale bar: 100 µm. **(A3)** Quantification of the percentage of eGFP^{+}HuC/D^{+} myenteric neurons in C57Bl/6 and *Rag2*$^{-/-}$. Mann-Whitney test. Error bars represent SD. **(B)** PCA plots of clusters of eGFP^{+} neurons from C57Bl/6 (orange dots), *Tcrα*$^{-/-}$ (white dots) and eGFP^{-} populations from C57Bl/6 (brown dots) and *Tcrα*$^{-/-}$ (yellow dots). Each dot represents clusters of the transcriptional profile of groups of cells from one individual animal (n=4/group). **(C)** Volcano plot of differentially expressed genes between the eGFP^{+} (neuronal) and eGFP^{-} (non-neuronal) populations of the C57Bl/6 mice (black dots) overlapped with neuronal genes identified in Dr Obata's nRNAseq experiments (red). Back arrows highlight well-known neuronal genes *Ret*, *Elavl3* and *Elavl4*. **(D)** Heat map of gene expression of most highly expressed neuronal-specific genes identified in Dr Obata's nRNAseq data in the eGFP^{+} and eGFP^{-} populations from the C57Bl/6 and *Tcrα*$^{-/-}$ mice. Gradient of colours represents the level of expression of a single gene (red, highly and blue, lower expressed genes). **(E)** Volcano plot of highly differentially expressed neuronal genes between the C57Bl/6 and the *Tcrα*$^{-/-}$ mice highlighting *Rb1* in red. **(F)** TPM values for *Rb1* gene expression in individual

samples of eGFP$^+$ neurons and eGFP$^-$ cells from the C57Bl/6 (pink bars and yellow bars, respectively) and *Tcrα*$^{-/-}$ (green bars and purple bars, respectively). N=4 mice/group from one experiment.

5.4 Discussion

Little is known about the mechanisms whereby the ENS communicates with adjacent tissue systems to promote intestinal health. Understanding these interactions under homeostatic conditions is essential in order to unravel the response of this system to environmental and pathological challenges which could affect the normal function of the intestine. In this chapter, we investigated the role of neuroimmune communications in the homeostatic maintenance of the ENS. Our findings demonstrate for the first time that, similar to the innate immune system, the adaptive immune system of the gut makes important contributions to in modulating ENS organisation and function.

Research investigating intestinal neuroimmune communication has advanced considerably of the past several years. However, most studies have focused so far on the interactions between MMs and enteric neurons. Specifically, it has been proposed that MM*s* are closely associated with enteric neurons at the level of the MP, residing at the periphery of the ganglia (Gabanyi et al., 2016; Muller et al., 2014; Phillips & Powley, 2012). These earlier studies did not report any MMs within the ganglia of the plexi. However, a new population of intraganglionic macrophages has been identified recently within the myenteric ganglia (Dora et al., 2018). By employing several immunolabelling and genetic tools to label intestinal macrophages, we have confirmed that MMs outline the perimeter of the myenteric ganglia juxtaposed to the outer cells and the interganglionic bundles of neuronal fibres and associated glial cells. Nevertheless, we did not identify macrophages within the MP. The reason for this disparity between our findings and those of Dora et al. is currently unclear and may relate to different analytical tools employed or divergent health and microbiota status of the animal facilities. We have also shown that LpMs are closely associated with EGCs and neuronal fibres within the mucosal layers. The close anatomical positioning of macrophages relative to the ENS reflects in a functional interaction between these cellular systems, which is highlighted by evidence indicating that MMs present a neuroprotective phenotype and secrete BMP2 that influences the development of enteric neurons (Gabanyi et al., 2016; Muller et al., 2014). Despite considerable progress in unveiling the neuroimmune communications between the innate immune system and the ENS, little is

known about the interplay between enteric neuroglia networks and intestinal adaptive immune cells.

To further investigate the crosstalk between neuroectodermal cells within the intestine (ENS) and the immune system, we analysed the relative positioning of several populations of adaptive immune cells and ENS cell types in different layers of the small intestine and colon, using immunohistochemistry, transgenic reporter lines and flow cytometry assays. As expected, we identified a large number of lymphocytes, including subsets of $CD4^+$, Th17 expressing *Il17* and $Foxp3^+$ T regulatory lymphocytes, within the mucosal and submucosal layers of the intestines that are anatomically positioned in the immediate vicinity of ENS cells. It is unclear at the moment whether the close apposition between ENS cells and lymphocytes indicates a special affinity between these cell types or results from their large number which inescapably brings them close together. In contrast to the mucosal and submucosal regions, the presence of adaptive immune cells within the outer muscle layers which harbour the MP was very rare or absent in our experimental animals. This is characteristically different from the myeloid cells (macrophages) which are very abundant in the muscularis externa and raises the possibility that lymphoid cells do not require a physical contact to interact with the ENS at the level of the MP under a homeostatic environment. Alternatively, even a brief contact of the rare and highly motile lymphocytes in muscularis externa with enteric neurons and glia at this level is sufficient to exert an effect of these cells on ENS networks.

We also investigated the anatomical relationship of enteric neurons within gut lymphoid organs. Earlier studies have proposed that enteric neurons project inside PPs (Chiocchetti et al., 2008; Vulchanova et al., 2007), one of the most important sources of lymphoid cells within the intestinal wall. Using antibody labelling and AAV-mediated transduction of enteric neurons, we observed a pronounced network of neuronal projections around the PPs. However, we did not detect any neuronal fibres inside these structures. In addition, using reporter mouse lines that label the majority of the EGCs, we did not observe any EGCs within the PPs; a prominent EGC network was nevertheless visible around these lymphoid tissues.

Despite the absence of a close anatomical relationship between the adaptive immune system and ENS cells at the level of the MP, we observed remarkable morphological alterations of ENS network within this layer in *Rag2*$^{-/-}$ immunodeficient mice, which lack the adaptive immune system. Given the evidence that absence of the adaptive immune cells

impairs the ENS networks, we wished to examine whether the crosstalk between the adaptive immune system and the nervous system of the gut was necessary to support ENS homeostasis. For this, we used immunodeficient mouse lines that lack T and B lymphocytes (*Rag1*$^{-/-}$ and *Rag2*$^{-/-}$) or T lymphocytes only (*Tcrα*$^{-/-}$) and investigated ENS morphology in these mutant animals. Our morphological analyses in cross-sections of the intestines have not identified any apparent alterations in EGCs and neuronal projections within the mucosal or submucosal layers, although we have not quantified any specific morphological parameters. In LMMPs, our analysis confirmed previous findings reported in chapter 4. Using DiI neurotracer to label the neuronal network within this layer, we found that the surface area of DiI spreading was marginally reduced in immunodeficient mice relative to controls, although this did not pass a strict statistical test. Also, the morphology of neuronal projections in the MP was apparently disorganised in mice lacking the adaptive immune system. Furthermore, the EGCs networks also displayed morphological alterations within the myenteric ganglia. As presented in chapter 4, HuC/D^{+} neurons were missing from some ganglia, while in other ganglia we observed unusually large clusters of HuC/D^{+} neurons.

Quantitative and morphological analysis of neuronal projections within the mucosal layer remains a challenge to be addressed in ENS research. Some studies have quantified the intensity of fluorescence of a relevant marker in the tissue region (De Vadder et al., 2018). However, the mucosal layer of the gut exhibits strong autofluorescence and contains a dense neuronal network resulting in poor data quality and preventing accurate measurements. On the other hand, the neuronal network in LMMPs is very heterogeneous and neuronal fibres in the interganglionic space are extremely compact. Additionally, antibodies that label the total population of enteric neurons in adult mice have some limitations. HuC/D is the most commonly used antibody which allows the quantification of enteric neurons. However, it has been shown that this protein is highly degradable in conditions that affect neuronal homeostasis limiting its value as an assay of enteric neuron number and morphology in several pathological situations (Cirillo et al., 2015; Desmet, Cirillo, & Vanden Berghe, 2014). Here, we were unable to show how the absence of lymphocytes impacts on the modulation of HuC/D protein in enteric neurons but our qualitative morphological analyses have accrued several pieces of evidence to suggest that absence of the adaptive immune system impacts on the homeostasis of ENS network.

A common theme in our analysis of the effects of the immune system on ENS organisation has been our inability to apply strict quantitative assays on the morphological

features of this part of the peripheral nervous system. This is very likely to result from the anatomical features of the ENS, such as the "salt and pepper" arrangement of neurons and glial cells and the absence of clear patterns of neuronal projections in the 3-dimentional space of the gut wall. These limitations highlight the need for the development of new tools for the high resolution morphological and quantitative analysis of the ENS. We propose that the development and use of viral and transgenic tools that can target a small number or individual enteric neurons or glia together with imaging strategies that can visualise the ENS across large areas of the gut will be necessary for proper quantitative analysis of the ENS in pathological conditions and in mutant mouse strains.

One of the most important functions of the ENS is to promote intestinal peristalsis by orchestrating an organised activity involving several subsets of enteric neurons to propel luminal contents along the GI tract (Fida et al., 1997; J. B. Furness, 2000). Our data demonstrate that mice lacking adaptive immune cells have an increased total transit time and a significantly decreased frequency of CMMCs. Moreover, the speed and length of propagation of CMMCs were dramatically reduced in mice lacking lymphocytes relative to immunocompetent controls. To further examine whether the adaptive immune system modulates ENS function, we transferred naïve T cells and Tregs into mice lacking T lymphocytes. Interestingly, the transfer of naïve T cells and Treg lymphocytes significantly rescued the intestinal transit time in *Tcrα*$^{-/-}$ mice. Moreover, addition of Tregs into *Tcrα*$^{-/-}$ mice was sufficient to restore to a large extent the frequency of CMMCs in these mice. Based on these observations, we propose for the first time that the adaptive immune system modulates the function of the ENS. However, the mechanisms by which the adaptive immune cells support the homeostasis of ENS function remain unclear.

Impaired ability of enteric neurons to execute and control intestinal motility has been described in animal models in which neuronal fibres within the MP were aberrant (Sasselli et al., 2013) or populations of motoneurons reduced (Anitha et al., 2012; Collins et al., 2014). Our data have shown that the percentage of Calretinin^{+} and nNos1^{+} neurons, two important populations of motoneurons within the MP, were significantly reduced in colons of immunodeficient mice. This data implies that perhaps the absence of adaptive immune system interferes with the development or maintenance of motoneurons within the MP, resulting in changes in intestinal motility in these mice. Our data also suggest that absence of the adaptive immune system affects the overall level of expression of neuronal and glia markers. Among all the transcripts we have analysed, genes that are expressed by the

majority of enteric neurons, such as *Elavl3*, *Elavl4* and *Ret* were significantly downregulated in *Rag2*$^{-/-}$ and *Tcrα*$^{-/-}$ mice, as well as genes expressed in motoneurons such as *Chat*, *Nos1* and *Calretinin*. However, we did not observe any statistically significant differences in levels of markers expressed in populations of sensory neurons. This might suggest that perhaps, the adaptive neuroimmune communication is selective to a specific subtype of enteric neurons. Interestingly, adoptive transfer of different types of adaptive immune cells into *Tcrα*$^{-/-}$ and *Rag2*$^{-/-}$ mice was not enough to restore the transcriptional profile of *Elavl3* in immunodeficient mice. *Elavl3* and *Elavl4* genes encode the HuC/D protein which is widely used as a pan-neuronal marker. The lower expression of these genes in mice lacking adaptive immune system could explain alterations observed in the pattern of expression of HuC/D mentioned above. Moreover, not only genes expressed in neurons were affected in our model, but also *S100* and *Sox2* expressed in EGCs. In our morphological qualitative analyses, the network of S100β^{+} EGCs within the MP was altered and a group of Sox10^{+} EGCs were not positive for S100β, suggesting that the lack of adaptive immune cells influences the expression of S100 in EGCs. Therefore, due to a limited availability of techniques to study these cells in our model, we were not able to investigate in detail the role of the adaptive immune system on EGCs maintenance within the gut. This highlights again the need to develop novel experimental strategies for high resolution studies and genetic manipulation of enteric glia. In addition, it would be important to interrogate the intracellular proteins of enteric neurons and glial cells in mice lacking adaptive immune system by performing unbiased proteomics-based assays.

To expand our analyses into the transcriptional profile of enteric neurons, we performed bulk nRNAseq of neuronal nuclei isolated from colonic LMMPs of C57Bl/6 and *Tcrα*$^{-/-}$ mice. Our development of AAV-based strategies (AAV9.KASH.eGFP) to label and isolate the nuclei of enteric neurons allowed us to study the transcriptional profile of colonic neuronal nuclei of mice lacking T lymphocytes relative to the same population from wildtype C57Bl/6 mice. We did not observe any significant differences in the percentage of transduced myenteric neurons between the control and the immunodeficient mice, although the number of sorted cells per animal was slightly reduced in the *Tcrα*$^{-/-}$ mice and observation which may relate to the reduction of enteric neurons observed in these animals by immunohistological assays. As expected, our transcriptome data of C57Bl/6 neuronal nuclei largely overlapped with Dr Obata's data of the same population isolated from the colon of

wild-type mice from an independent experiment (Obata et al. *in preparation*). In our preparations, we identified transcripts that are exclusively expressed in enteric neurons, such as *Ret*, *Elavl3* and *Elavl4* suggesting robustness and high reproducibility of our technique. The nuclei of neuronal populations from C57Bl/6 and *Tcrα*$^{-/-}$ mice were analysed, and the most highly differentially expressed genes were identified. To our surprise, we found a single gene, *Rb1* that was differentially expressed in the *Tcrα*$^{-/-}$ mice and passed all statistical tests.

Recently, nRNAseq has been a widely emerging strategy for the isolation and profiling of the molecular signature of cells that cannot be readily dissociated and suffer from mechanical manipulation, as is the case for enteric neurons. This technology has been successfully applied for the study of cell types and identification of gene profiles in different systems, and benefits from the fact that isolation of nuclei is relatively easier and more rapid compared to whole cells. Moreover, nRNAseq data represents high coverage of transcripts and excellent technical reproducibility (Krishnaswami et al., 2016). This assay has the added benefit of allowing focused study of the regulatory mechanisms that take place within the nuclei. It has been previously reported that most of the transcriptional profile in the nuclei is very similar to that in entire cells, with only about 3.5% of the transcriptions exhibiting differential expression (Grindberg et al., 2013). However, these experiments were performed by comparing nuclear versus cytoplasmic transcripts from different single cells. Recently, by using single-cell RNAseq from the nucleus and cytoplasm of the same cell, Abdelmoez et al. have suggested that the analysis of the transcriptional profile of subcellular compartments is valid when other methods are not available, but it has some limitations (Abdelmoez et al., 2018). Some of the main limitations are: 1) use of nRNAseq might result in loss of a range of information contained within cytoplasmic mRNA; 2) small noncoding transcripts and other short sequence mRNAs lacking polyA tails are not detectable using nRNAseq (Abdelmoez et al., 2018; Krishnaswami et al., 2016); 3) low abundance of transcripts in the nucleus could also impact in the detection of some RNAs (Piper & Holt, 2004).

The small number of transcripts that showed statistically significant alterations in the nuclei of neurons between control and *Tcrα*$^{-/-}$ mutants, despite dramatic morphological, functional and transcriptional (by qRT-PCR) phenotypes in these neurons may reflect some technical limitations. Currently whole cell RNAseq is not possible for isolated adult enteric neurons, but would provide more information regarding the downstream biological

landscape and function of these cells. One major reason is that mRNA concentrations within the cytoplasm are rate limiting for protein synthesis, and offer a more sensitive readout of regulated processes. Additionally, it has been proposed that neurons have the ability to translate RNA within the axons. The axonal translation of RNAs provides distinct advantages to these cells, allowing rapid and local protein synthesis, less energy cost and spatial responsiveness to external stimuli that might be functionally relevant to neurons in diseases and insults that affect the intestinal homeostasis (Piper & Holt, 2004).

The scope for significant axonal RNA translation is also likely to be relevant for ENS neurons in particular, especially since the projection of axons in ENS neurons cells can range from several millimetres to several centimetres in length. Our morphological, histochemical and transcriptional analyses (by qRT-PCR using whole LMMP preparations) have suggested that the neuronal homeostasis is impaired in mice lacking the adaptive immune cells. Perhaps additional alterations in the enteric neurons would be detectable if analysing the axonal translation of RNA was possible. However, due to experimental technicalities, such as the complexity of the enteric neuronal network, purification of axonal bundles and contamination with other cell debris the analysis of axonal translation is so far unavailable in the field.

Although we could not detect any other transcriptional alterations in mice lacking T lymphocytes by using nRNAseq analysis, we found that *Rb1* was significantly downregulated in neurons from the *Tcrα*$^{-/-}$ mice. The tumour suppressor retinoblastoma 1 (*Rb1*) participate in the modulation of cell-cycle as a negative regulator of cell proliferation, and it is downregulated in human cancer (Dyson, 2016). Defects in *Rb1* result in the childhood cancer retinoblastoma, bladder and lung cancers (Burkhart & Sage, 2008). *Rb1* expression in nitrergic and cholinergic enteric neurons has recently been reported in single-cell RNA-sequencing data from juvenile mice (Linnarsson lab, Mouse Atlas). Moreover, it has been shown that depletion of *Rb1* from ENS cells led to morphological alterations in the nitrergic subset of enteric neurons. Specifically, Nos1^{+} neurons developed giant nuclei in addition to abnormalities in colonic motility, suggesting that *Rb1* specifically target a population of inhibitory nitrergic enteric neurons that are involved in controlling colonic motility (Fu et al., 2013). Furthermore, studies using human samples from patients with Hirschsprung's disease have shown a downregulation in Rb1 protein expression in aganglionic tissues (O'Donnell, Coyle, & Puri, 2016). Hirschsprung's disease is a well-known congenital condition characterised by the deficit in colonisation of the distal segment

of the colon by enteric neurons (Heanue & Pachnis, 2007; McKeown, Stamp, Hao, & Young, 2013). Altogether, these studies implicate *Rb1* in maintenance of the cellular morphology and function of enteric neurons.

Our analysis of expression levels *Nos1* and *Chat* expressed in enteric motoneurons showed that these transcripts are significantly downregulated in immunodeficient mice. Moreover, we have observed morphological alterations in myenteric neurons of mice lacking adaptive immune system. Also, these mice present impaired intestinal motility and a significant downregulation of *Rb1*. Perhaps, the presence of T lymphocytes is essential for the modulation of *Rb1* in enteric neurons, and the absence of these cells leads to abnormalities on ENS homeostasis and function via downregulation of *Rb1*. Although we have not yet been able to test the role of *Rb1* on the crosstalk between the adaptive immune system and the ENS, our data strongly suggest the exciting possibility that this molecule is implicated in intestinal neuroimmune communications. Understanding the molecular mechanisms that mediate the effect of intestinal immune cells on neuronal *Rb1* expression will advance our understanding of how the immune system impacts on the organisation, maintenance and function of the nervous system.

Chapter 6

Concluding remarks

6. Chapter 6 | Concluding remarks

6.1 Impact of the subject and main findings

The remarkable organisation of the ENS into ganglionic structures that occupy specific regions of the gut wall has been recognised for over a century (John Barton Furness, 2006), but the functional contributions of EGCs and enteric neuron subsets, as well as their interactions with the surrounding tissue systems, are only partly elucidated. The last decades, studies on the molecular mechanisms that control the development of enteric neurons and glial cells and their assembly into spatially organised neuroglia networks, have provided some insight into the contributions of ENS lineages to intestinal physiology (de Graaff et al., 2001; Hao, Anderson, Kobayashi, Whitington, & Young, 2009; Hao et al., 2011; Hao et al., 2013; Hao et al., 2016; Hao et al., 2012; Hao et al., 2010; Hao & Young, 2009; Lasrado et al., 2017; Memic et al., 2018; Young et al., 2014). However, the unpatterned and complex organisation of ENS lineages, the multitude of external challenges (from other gut tissues and the lumen) that influence their homeostasis and function, and the limitations of available methods to study the ENS at the cellular, physiological and molecular level, have slowed progress in understanding the contributions of this system to GI physiology. In this thesis, we have studied the effect of experimental manipulations of the intestinal environment (both tissue and lumen) on the homeostasis and functional output of the ENS in adult animals.

One significant contribution of this thesis was to generate and characterise two different experimental methods to evaluate adult EGCs *in vitro* and enteric neurons *in vivo*. Together with Dr Chng, we developed a robust protocol which allowed us to isolate, purify and trace EGC populations from adult intestines in culture and study their response to experimental manipulations and signalling cues (Chng et al., *manuscript in preparation)*. In parallel, together with Dr Obata, we generated an AAV-based method to *in vivo* label and isolate nuclei of enteric neurons from adult mouse intestines for analysis of their transcriptional profile (Obata et al., *manuscript in preparation)*. The opportunities offered by this method to manipulate enteric neurons *in vivo* using viral vectors, promises to advance the molecular, morphological and physiological understanding of enteric neurons in the adult GI tract. These two novel experimental methods will be important for diverse studies in the field of enteric neuroscience.

Considering that normal GI function depends on the balanced interaction between the ENS, the immune system and the microbiota, we investigated whether alterations in the

microbiota-immune system axis impacts on the physiology of intestinal neuroglia networks. This work led to a second significant finding in this thesis, namely that alterations in the intestinal environment, such as the absence of intestinal microbiota, intestinal inflammation and depletion of adaptive immune cells have a remarkable effect on the function and homeostasis of the ENS. Furthermore, for the first time, we demonstrated the impact of the adaptive immune system on the physiology and molecular features of the ENS by using advanced technology to study the adult nervous system.

6.2 Outlook

Future perspectives: Development of new methods to study the ENS

The complexity of the adult ENS network and the limitation in availability of specific markers to label these cells have represented a significant obstacle in developing useful tools to study the morphology and molecular profile of individual groups of cells within the adult ENS. Genetic cell fate mapping of neuroectodermal cell networks of the intestine, such as EGCs, has provided indubitable evidence that fluorescent lineage markers can be used to precisely and permanently identify these cells within the ENS (Boesmans et al., 2015; Laranjeira et al., 2011; Lasrado et al., 2017). However, the lack of robust experimental models that allow us to isolate and manipulate EGCs from the adult gut has prevented the detailed study of their molecular properties. To fill this gap in ENS research, we have successfully developed a robust *in vitro* system to study EGC and their properties from the adult gut. In our method, we took advantage of a mouse line generated in our lab to label the vast majority of adult EGCs with a fluorescent reporter, combined with the expertise of fast dissection of intestinal segments containing these cells. With our protocol, we were able to purify EGC populations with minimal manipulation, fewer contaminants and further maintain the molecular and morphological properties of these cells *in vitro*. This method is currently being used in our lab to investigate the transcriptional landscape of EGCs and their ability to generate functionally active neuronal subpopulations *in vitro (*collaboration with Dr Chng et al., *manuscript in preparation)*. The generation of an efficient method to study the adult EGCs not only allows the in-depth study of EGC properties *in vitro* but can also be used as a potential therapy for diseases that affect the homeostasis of the ENS in humans.

Although the generation of genetic tools to label and manipulate enteric neurons throughout the ENS development has unquestionably provided insights in the understanding

of the physiological features of these cells, unravelling the complex features of adult neuronal networks remains a challenge. The reason for this is the lack of markers to label and methods to isolate these cells in the adult gut. The adult neuronal network is complex, and cells are extremely sensitive to chemical and mechanical manipulations. To address these limitations, we have effectively generated a strategy to label and isolate intact nuclear material of enteric neurons for RNA sequencing. In our approach, we used adenovirus-associated viral (AAV) vectors to specifically transduce the outer nuclear membrane of enteric neurons with a fluorescent reporter. This strategy allowed us not only to target the majority of enteric neurons within the MP and SMP from the small intestine and colon but also to isolate these cells for molecular studies such as nRNAseq. This technique was used in this thesis to investigate the effect of the absence of immune cells on the enteric neuronal transcriptome. In addition, this method is currently used in the lab to analyse the role of the intestinal microbiota and microbial products on the neuronal molecular profile (collaboration with Obata at al., *manuscript in preparation*). This novel experimental tool provides a substantial contribution to ENS research since for the first time it allows the use of an advanced strategy to reveal the molecular properties of adult enteric neurons in different environments.

AAV- delivery of genetic material was also efficiently used in this thesis to label the enteric neuronal network. This strategy will improve the understanding of the topography of enteric neuronal network within different intestinal segments. However, due to the heterogeneity of the organisation and composition of ENS, quantification and analysis of the ENS network has not been further explored. We suggest that by using multi-colouring AAV transduction of subsets of enteric neurons (brainbow AAV) combined with sparse labelling of these cells would provide new insights into their morphological and molecular properties within different regions of the intestinal wall. More specifically, we aim to unveil the morphological alterations in neuronal network observed in mice lacking adaptive immune cells by using this strategy. A downside of this method is that it does not include the analysis of EGCs. The AAV delivery system, however, can be modified in order to pursue studies on EGCs. Experiments towards this are currently ongoing in the lab by using AAV vectors carrying a glial-specific Cre, Sox10, to label EGCs. The AAV strategy, in combination with transgenic mouse lines, has been used in the lab to analyse the morphology, dynamics and molecular landscape of these cells in health and disease. It is of great interest to pursue the understanding of the transcriptional signature and dynamics of these cells in response to

alterations in the gut environment, such as in the absence of T lymphocytes and inflammation, and we believe this will shed light on the complexity and plasticity of EGCs.

The generation and implementation of advanced technologies are necessary for enteric neuroscience to better comprehend how the ENS develops, functions and integrates with the intricate network of other complex systems to maintain gut function, and further understand its role in health and disease. The ENS participates in controlling many aspects of the GI function. Thus, it is plausible that any alterations in the intestinal environment could result in drastic consequences on the ENS development, homeostasis and function. A wide range of GI pathologies have been reported for affecting the ENS homeostasis, such as HSCR disease, IBD, diabetes, Alzheimer's and Parkinson's disease, although the aetiology, as well as the molecular mechanisms that underlie changes on the ENS equilibrium, remain still elusive (Burns et al., 2016; Chalazonitis & Rao, 2018; Fasano et al., 2015). These enteric neuropathies present to some extent, moderate (chronic constipation) or severe (HSCR) impact on ENS circuitry and motor activity, due to loss, degeneration, and functional impairment of enteric neurons (Burns et al., 2016; Parisi, 1993). However, ENS phenotypes are variable and differ among patients. Although the technique has its limitations, we believe it would be a possible, valuable and relevant contribution for clinical studies to use the strategy of isolation of neuronal nuclei to demystify the intricacy of transcriptional profiles of neuronal and EGCs in distinct pathologies that affect GI function.

Future perspectives: Impact of gut tissue and luminal environment status on ENS physiology

Interest in the contribution of intestinal microbiota on host homeostasis has increased over the past few years. It has been proposed that intestinal microbes modulate the physiology of many tissues, and have a crucial role in the gut-brain communication axis (El Aidy, Dinan, & Cryan, 2015). Moreover, the gut microbiota is thought to regulate the postnatal development and composition of the ENS network (Anitha et al., 2012; Collins et al., 2014; De Vadder et al., 2018; Kabouridis et al., 2015; Yano et al., 2015). Although recent studies have suggested that microbiota tune ENS homeostasis, the role of microbiota on ENS composition and function in different areas of the GI tract was further investigated in this thesis. Our data did not show any statistically significant differences between GF and SPF control mice either in the composition of EGCs and neurons within LMMPs of small intestine and colon or in the level of expression of ENS-specific genes. Our results diverge from previously published data showing that in GF mice the number of neurons within

colonic MP, and particularly nitrergic neurons, is reduced. However, our results provide support to the idea that the absence of microbiota influences the molecular profile of genes expressed by ENS cells. Unfortunately, for practical reasons of animal supply from our collaborators in the Norwich animal facility, the number of mice analysed in these experiments was limited, and variation between mice from the same group was high, thus preventing our findings reaching statistical significance. In support to our data, however, Obata et al., (*manuscript in preparation*) have used GF mice from a different research institute (Prof. Andrew Macpherson, University of Bern) and failed to detect morphological alterations in the neuronal network or changes in neuronal subtype composition of myenteric or submucosal ganglia. Advanced methods, such as the use of AAV particles to transduce neurons and EGCs, could be an effective strategy to examine in more detail the effect of intestinal microbes on the molecular profile and network of ENS. Studies on ENS cell composition are missing for the SMP of GF mice, and morphological and molecular studies of SMP neurons and EGCs within this layer are null. It would be interesting to use the approaches described in this thesis to investigate further these populations localised within the submucosal layer, as they are positioned closer to and therefore are likely to be more exposed to luminal contents. For instance, IPAN neurons, localised within the SMP, project to the mucosa sensing mechanical and environmental stimuli. These neurons secrete neurotransmitters that will activate motoneurons within the MP to orchestrate intestinal peristalsis (John Barton Furness, 2006; J. B. Furness, Rivera, Cho, Bravo, & Callaghan, 2013). Although we did not detect any major alterations on the neuronal network within the MP, it is reasonable to conceive that IPAN neurons would respond to subtle luminal alterations in microbial status.

Notwithstanding the effects of microbiota on morphology and composition of the ENS, our data have strongly suggested that intestinal microbes modulate ENS physiology. Using experimental approaches to evaluate the neurogenic colonic activity, we found that GF mice have a significant reduction in the frequency of CMMCs. Furthermore, our data showed a significant difference in ENS-dependent colonic motility in C57Bl/6 mice from NIMR and Crick institutes. The representation of bacterial phyla diverged between the two Institutes, including the absence of SFB from the lumen of mice from the Crick facility. Since SFB was missing from the new Institute, we assessed whether the absence of this bacterial strain influenced the reduced neurogenic motility in mice from this facility. However, re-introduction of this bacterium into Crick mice was not sufficient to restore the

ENS-dependent motility in C57Bl/6 mice, suggesting that other microbiota-related mechanism(s) independently of SFB modulate the neurogenic activity of the gut in these animals. Once again, investigating specific populations of sensory neurons within the SMP would bring new insights on the role of microbiota on the ENS function. Alterations in bacterial composition also have a critical impact on immune cell homeostasis. GF mice display morphological alterations in lymphoid compartments and reduced populations of immune cells, which translates into decreased immune responses and reduced production of pro-inflammatory cytokines (Gensollen et al., 2016; Luczynski et al., 2016; Rooks & Garrett, 2016). Moreover, it is well-established that the absence of certain bacteria, such as SFB, influences the development of Th17 lymphocytes. Experiments comparing mice from Jacksons Laboratories (JAX) and Taconic Biosciences (TAC) have shown that JAX mice lacked SFB leading to an absence of Th17 cells. Later, it was shown that the presence or absence of SFB was dependent on the particular barrier location at each company and variable within different parts of the same company (Farkas et al., 2015; Ivanov et al., 2009). Our data advocates the importance of subtle changes in bacteria composition on the physiology of the ENS and highlight the need for the microbiota status of different animal facilities to be taken into consideration when designing experiments and interpreting experimental findings.

In this thesis, we have also examined the ENS response to the progression of intestinal inflammation. We observed that inflammation promotes ENS-dependent peristaltic activity, and we found that the neuronal transcript *Cgrp* is upregulated in a mouse model of TNF overexpression. We have also found that EGCs enter the cell cycle in response to intestinal inflammation, conferring the EGCs an immunological role in the GI tract. Analysis of ENS responses to inflammation is challenging due to a diversity of events that simultaneously take part during this process that could influence the response of the system. Inflammation usually leads to the disruption of epithelial barriers, triggering the penetration of microbes and microbial products within the intestinal tissue that causes a strong immune response. We have used neurogenic intestinal activity as a readout for the ENS response to microbiota and inflammation and found that luminal microbes and immunological status of the GI tract dictate ENS motility patterns. The motor behaviour of the gut as controlled by the ENS could be a mechanism for bacterial expulsion and clearance of inflammation. Consistent with this idea, mice in which the microbiota is low or absent, and the immune

system reduced, display reduced intestinal motility, whereas, in mice with transmural penetration of bacteria and an overactive immune system, the neurogenic intestinal motility, and perhaps other activities, such as secretion, are elevated. The use of advanced strategies to evaluate the biological and molecular status of the ENS, immune cells and microbiota in combination would bring new insights on how inflammation interferes with the homeostasis of the GI. Antibiotics to defeat bacterial infection is crucial for human care, and it has been currently used for treatment of IBS, improving symptoms of IBS (Kane & Ford, 2016). It has also been shown that antibiotics ameliorate the symptoms of PD (Lombardi et al., 2018). However, its overuse could promote drastic alterations in microbial diversity (Palleja et al., 2018), having a major effect on the homeostasis of immune cells (Blaser, 2016; Gensollen et al., 2016) and on ENS function, suggested here in this thesis and in Obata et al. *(in preparation)*.

Future perspectives: Neuroimmune communication within the gut

Recently, studies have provided new evidence about the interplay between the innate immune system and the ENS to maintain intestinal homeostasis (Cardoso et al., 2017; De Schepper et al., 2018; Gabanyi et al., 2016; Ibiza et al., 2016; Klose et al., 2017; Muller et al., 2014). Despite progress in unravelling the spatial and physiological role of macrophages and ILCs on ENS function, the contribution the adaptive immune system makes to ENS homeostasis remains unclear. Here, we have examined the anatomical positioning between the adaptive immune and ENS cells in different compartments within the intestinal wall. We found that T lymphocytes and ENS cells and their processes are in close proximity with the intestinal mucosal layers. However, in LMMPs the proportion of these cells is particularly low compared to innate immune cells within the same layer. The ENS is considered as the second brain because its cellular composition, molecular features and physiological characteristics are very similar to the CNS (John Barton Furness, 2006; Michael D. Gershon, 1998). Here we propose that perhaps the compartmentalisation of ENS structures relative to immune cells could also be another feature that resembles the CNS. As is the case for the CNS, the ENS is also restricted to specific compartments (in this case within the intestinal wall), in which neurons and EGCs are located and "protected" within ganglionic structures situated between muscle layers. However, neuronal projections and EGCs are found within the lamina propria of the intestines where most of the immune responses take place. LMMPs containing neuronal cell bodies and EGCs are in close

association with specialised macrophages that present a neuroprotective phenotype and display similar features as microglia from the brain (De Schepper et al., 2018; Gabanyi et al., 2016; Kulkarni et al., 2017; Muller et al., 2014), and these structures have a limited supply of adaptive immune cells, unless the tissue homeostasis is broken. Perhaps, intestinal mucosal layers resemble the peripheral nervous system, in which EGCs tightly follow neuronal projections and are exposed to a highly active immune system and extremely diverse microbiota.

To further evaluate the participation of the adaptive immune cells in ENS homeostasis and function, we analysed several animal models that lack populations of lymphocytes. Our data have shown that the absence of lymphocytes impairs the morphology, molecular profile and function of ENS components within the colonic MP. Additionally, we found that restoring Treg subsets in mice lacking T cells rescued the defective neurogenic colonic activity. Interestingly, all phenotypes observed in the ENS in mice lacking the adaptive immune system were detected within the MP, where neurons that orchestrate the intestinal motility are placed. However, the presence of adaptive immune cells within this layer is rare. Nevertheless, further studies will be necessary to address whether the crosstalk between ENS and the adaptive immune system requires physical contact between these cells within the mucosal layer, or whether those interactions involve the participation of other cell types. To investigate that further, we intend to explore whether other cell types such as macrophages and EGCs, are abundant and dynamic within intestinal layers, could serve as mediators between lymphocytes and enteric neurons. Another possibility is that molecules secreted by the adaptive immune cells within the mucosal layer or lymphoid tissues travel long distances along neuronal fibres to coordinate the homeostasis of the ENS within the MP.

Based on our observations, it would be interesting to evaluate whether changes in the dynamics of the adaptive immune system are aetiological factors for gut dysmotility syndromes and whether adoptive transfer of immune cells could be a possible therapy for patients with severe cases of these conditions, for instance in chronic constipation. It is well-established that immune cells actively participate in inflammatory processes that take part in enteric neuropathies such as IBD (de Mattos et al., 2015). However, the contribution or fitness of immune cell compartments, such as the adaptive immune cells, in patients with other neuropathies remains unclear. In HSCR disease, patients suffer from chronic constipation due to the absence of ENS network within intestinal layers. *Ret* is one of the

essential genes implicated in the genesis of HSCR disease (Burns et al., 2016). This gene is also expressed in ILC3s and has an important role in PPs organogenesis (Ibiza et al., 2016; Veiga-Fernandes et al., 2007). However, it is not known whether immune cells contribute to the aggravation of HSCR phenotype. We have shown that Ret is significantly downregulated in mice lacking T lymphocytes, and these mice display abnormal neuronal networks and reduced intestinal motility. It would be interesting to investigate whether T cells or *Ret* expressing ILC3s participate in the pathophysiology of HSCR disease.

Transcriptional profiling of enteric neurons isolated from the MP using bulk nRNAseq demonstrated that *Rb1* is significantly downregulated in mice lacking T lymphocytes. *Rb1* is expressed in nitrergic and cholinergic neurons, both implicated in intestinal motility. This molecule has been reported to be involved in morphological abnormalities in nitrergic enteric neurons, as well as pathologies that affect the development of the ENS, such as HSCR (Fu et al., 2013; O'Donnell et al., 2016). It will be of our great interest to explore further the role of *Rb1* in the interface between ENS and the adaptive immune system. More specifically, we would like to validate *Rb1* expression in our models and investigate whether T lymphocytes modulate *Rb1* expression in enteric neurons after adoptive transfer of these cells. It is also of interest to examine whether the delivery of *Rb1* by neuronal specific AAV transduction is sufficient to re-establish the neurogenic activity of the colon in mice lacking T cells. Moreover, it will be essential to understand the signalling and molecular mechanisms whereby T cells regulate the expression of *Rb1* in enteric neurons and the role of this transcriptional regulator in these cells. For example, to assess the role of T cells-derived cytokines on the regulation of *Rb1*. For such experiments, we intend to evaluate cytokine receptor expression on neurons and examine which T cell derived cytokines are released in the muscularis externa of the gut. Our first hypothesis, based on our experiments that showed that Tregs could restore the neurogenic motility in mice lacking T cells, would lead us to investigate the expression of receptors for Treg-derived cytokines, such as IL-10R and TGFβR on enteric neurons. Because *Rb1* seems to be involved in the modulation of the ENS neurogenic activity, and in the maintenance of neuronal homeostasis suggested here and in other studies (Fu et al., 2013), we question whether *Rb1* has other important roles on pathologies that affect the fitness of the ENS, such as HSCR disease and IBD.

To summarise, in this thesis, we have developed a holistic and advanced approach to study the ENS homeostasis by combining the influence of the intestinal environment, such as microbiota and immune system on ENS transcriptome, morphology and physiology. Our data and concept development can lead to a better understanding of the adult ENS. We argue that progress in any single tissue system of the gut, as valuable as it may be, represents only part of the gut "story" and that full understanding of gut biology and gastrointestinal diseases will require integrative approaches that take into account the dynamic interactions between all intestinal tissues and the luminal microenvironment.

Chapter 7

Bibliography

7. Bibliography

Abdelmoez, M. N., Iida, K., Oguchi, Y., Nishikii, H., Yokokawa, R., Kotera, H., . . . Shintaku, H. (2018). SINC-seq: correlation of transient gene expressions between nucleus and cytoplasm reflects single-cell physiology. *Genome Biol, 19*(66). doi:10.1186/s13059-018-1446-9

Agace, W. W., & McCoy, K. D. (2017). Regionalized Development and Maintenance of the Intestinal Adaptive Immune Landscape. *Immunity, 46*(4), 532-548. doi:10.1016/j.immuni.2017.04.004

Allendoerfer, K. L., Cabelli, R. J., Escandon, E., Kaplan, D. R., Nikolics, K., & Shatz, C. J. (1994). Regulation of neurotrophin receptors during the maturation of the mammalian visual system. *J Neurosci, 14*(3 Pt 2), 1795-1811.

Almeida, A. R., Arroz-Madeira, S., Fonseca-Pereira, D., Ribeiro, H., Lasrado, R., Pachnis, V., & Veiga-Fernandes, H. (2012). RET/GFRalpha signals are dispensable for thymic T cell development in vivo. *PLoS One, 7*(12), e52949. doi:10.1371/journal.pone.0052949

Amiel, J., Sproat-Emison, E., Garcia-Barcelo, M., Lantieri, F., Burzynski, G., Borrego, S., . . . Hirschsprung Disease, C. (2008). Hirschsprung disease, associated syndromes and genetics: a review. *J Med Genet, 45*(1), 1-14. doi:10.1136/jmg.2007.053959

Andreas, N. J., Kampmann, B., & Mehring Le-Doare, K. (2015). Human breast milk: A review on its composition and bioactivity. *Early Hum Dev, 91*(11), 629-635. doi:10.1016/j.earlhumdev.2015.08.013

Anitha, M., Vijay-Kumar, M., Sitaraman, S. V., Gewirtz, A. T., & Srinivasan, S. (2012). Gut microbial products regulate murine gastrointestinal motility via Toll-like receptor 4 signaling. *Gastroenterology, 143*(4), 1006-1016 e1004. doi:10.1053/j.gastro.2012.06.034

Annese, V., Lombardi, G., Perri, F., D'Inca, R., Ardizzone, S., Riegler, G., . . . Andriulli, A. (2005). Variants of CARD15 are associated with an aggressive clinical course of Crohn's disease--an IG-IBD study. *Am J Gastroenterol, 100*(1), 84-92. doi:10.1111/j.1572-0241.2005.40705.x

Aube, A. C., Cabarrocas, J., Bauer, J., Philippe, D., Aubert, P., Doulay, F., . . . Neunlist, M. (2006). Changes in enteric neurone phenotype and intestinal functions in a transgenic mouse model of enteric glia disruption. *Gut, 55*(5), 630-637. doi:10.1136/gut.2005.067595

Avetisyan, M., Rood, J. E., Huerta Lopez, S., Sengupta, R., Wright-Jin, E., Dougherty, J. D., . . . Heuckeroth, R. O. (2018). Muscularis macrophage development in the absence of an enteric nervous system. *Proc Natl Acad Sci U S A, 115*(18), 4696-4701. doi:10.1073/pnas.1802490115

Badner, J. A., Sieber, W. K., Garver, K. L., & Chakravarti, A. (1990). A genetic study of Hirschsprung disease. *Am J Hum Genet, 46*(3), 568-580.

Bain, C. C., Bravo-Blas, A., Scott, C. L., Gomez Perdiguero, E., Geissmann, F., Henri, S., . . . Mowat, A. M. (2014). Constant replenishment from circulating monocytes maintains the macrophage pool in the intestine of adult mice. *Nat Immunol, 15*(10), 929-937. doi:10.1038/ni.2967

Bayguinov, P. O., Hennig, G. W., & Smith, T. K. (2010). Calcium activity in different classes of myenteric neurons underlying the migrating motor complex in the murine colon. *J Physiol, 588*(Pt 3), 399-421. doi:10.1113/jphysiol.2009.181172

Bayliss, W. M., & Starling, E. H. (1899). The movements and innervation of the small intestine. *J Physiol, 24*(2), 99-143.

Beck, J. A., Lloyd, S., Hafezparast, M., Lennon-Pierce, M., Eppig, J. T., Festing, M. F., & Fisher, E. M. (2000). Genealogies of mouse inbred strains. *Nat Genet, 24*(1), 23-25. doi:10.1038/71641

Belai, A., Boulos, P. B., Robson, T., & Burnstock, G. (1997). Neurochemical coding in the small intestine of patients with Crohn's disease. *Gut, 40*(6), 767-774.

Belkaid, Y., & Harrison, O. J. (2017). Homeostatic Immunity and the Microbiota. *Immunity, 46*(4), 562-576. doi:10.1016/j.immuni.2017.04.008

Belkind-Gerson, J., Graham, H. K., Reynolds, J., Hotta, R., Nagy, N., Cheng, L., . . . Goldstein, A. M. (2017). Colitis promotes neuronal differentiation of Sox2+ and PLP1+ enteric cells. *Sci Rep, 7*(1), 2525. doi:10.1038/s41598-017-02890-y

Benskey, M. J., Kuhn, N. C., Galligan, J. J., Garcia, J., Boye, S. E., Hauswirth, W. W., . . . Manfredsson, F. P. (2015). Targeted gene delivery to the enteric nervous system using AAV: a comparison across serotypes and capsid mutants. *Mol Ther, 23*(3), 488-500. doi:10.1038/mt.2015.7

Bergquist, J., Tarkowski, A., Ekman, R., & Ewing, A. (1994). Discovery of endogenous catecholamines in lymphocytes and evidence for catecholamine regulation of lymphocyte function via an autocrine loop. *Proc Natl Acad Sci U S A, 91*(26), 12912-12916.

Bertrand, P. P., Kunze, W. A., Bornstein, J. C., Furness, J. B., & Smith, M. L. (1997). Analysis of the responses of myenteric neurons in the small intestine to chemical stimulation of the mucosa. *Am J Physiol, 273*(2 Pt 1), G422-435.

Bhat, M., Nguyen, G. C., Pare, P., Lahaie, R., Deslandres, C., Bernard, E. J., . . . Bitton, A. (2009). Phenotypic and genotypic characteristics of inflammatory bowel disease in French Canadians: comparison with a large North American repository. *Am J Gastroenterol, 104*(9), 2233-2240. doi:10.1038/ajg.2009.267

Blander, J. M., Longman, R. S., Iliev, I. D., Sonnenberg, G. F., & Artis, D. (2017). Regulation of inflammation by microbiota interactions with the host. *Nat Immunol, 18*(8), 851-860. doi:10.1038/ni.3780

Blaser, M. J. (2016). Antibiotic use and its consequences for the normal microbiome. *Science, 352*(6285), 544-545. doi:10.1126/science.aad9358

Bluestone, J. A., Mackay, C. R., O'Shea, J. J., & Stockinger, B. (2009). The functional plasticity of T cell subsets. *Nat Rev Immunol, 9*(11), 811-816. doi:10.1038/nri2654

Boesmans, W., Cirillo, C., Van den Abbeel, V., Van den Haute, C., Depoortere, I., Tack, J., & Vanden Berghe, P. (2013). Neurotransmitters involved in fast excitatory neurotransmission directly activate enteric glial cells. *Neurogastroenterol Motil, 25*(2), e151-160. doi:10.1111/nmo.12065

Boesmans, W., Hao, M. M., & Vanden Berghe, P. (2018). Optogenetic and chemogenetic techniques for neurogastroenterology. *Nat Rev Gastroenterol Hepatol, 15*(1), 21-38. doi:10.1038/nrgastro.2017.151

Boesmans, W., Lasrado, R., Vanden Berghe, P., & Pachnis, V. (2015). Heterogeneity and phenotypic plasticity of glial cells in the mammalian enteric nervous system. *Glia, 63*(2), 229-241. doi:10.1002/glia.22746

Boesmans, W., Martens, M. A., Weltens, N., Hao, M. M., Tack, J., Cirillo, C., & Vanden Berghe, P. (2013). Imaging neuron-glia interactions in the enteric nervous system. *Front Cell Neurosci, 7*, 183. doi:10.3389/fncel.2013.00183

Boyer, L., Ghoreishi, M., Templeman, V., Vallance, B. A., Buchan, A. M., Jevon, G., & Jacobson, K. (2005). Myenteric plexus injury and apoptosis in experimental colitis. *Auton Neurosci, 117*(1), 41-53. doi:10.1016/j.autneu.2004.10.006

Boyer, L., Sidpra, D., Jevon, G., Buchan, A. M., & Jacobson, K. (2007). Differential responses of VIPergic and nitrergic neurons in paediatric patients with Crohn's disease. *Auton Neurosci, 134*(1-2), 106-114. doi:10.1016/j.autneu.2007.03.001

Braun, N., Sevigny, J., Robson, S. C., Hammer, K., Hanani, M., & Zimmermann, H. (2004). Association of the ecto-ATPase NTPDase2 with glial cells of the peripheral nervous system. *Glia, 45*(2), 124-132. doi:10.1002/glia.10309

Brehmer, A., Schrodl, F., & Neuhuber, W. (1999). Morphological classifications of enteric neurons--100 years after Dogiel. *Anat Embryol (Berl), 200*(2), 125-135.

Brierley, S. M., Nichols, K., Grasby, D. J., & Waterman, S. A. (2001). Neural mechanisms underlying migrating motor complex formation in mouse isolated colon. *Br J Pharmacol, 132*(2), 507-517. doi:10.1038/sj.bjp.0703814

Broadhead, M. J., Bayguinov, P. O., Okamoto, T., Heredia, D. J., & Smith, T. K. (2012). Ca2+ transients in myenteric glial cells during the colonic migrating motor complex in the isolated murine large intestine. *J Physiol, 590*(2), 335-350. doi:10.1113/jphysiol.2011.219519

Brookes, S. J. (2001). Classes of enteric nerve cells in the guinea-pig small intestine. *Anat Rec, 262*(1), 58-70.

Brown, I. A., McClain, J. L., Watson, R. E., Patel, B. A., & Gulbransen, B. D. (2016). Enteric glia mediate neuron death in colitis through purinergic pathways that require connexin-43 and nitric oxide. *Cell Mol Gastroenterol Hepatol, 2*(1), 77-91. doi:10.1016/j.jcmgh.2015.08.007

Brown, I. A. M., McClain, J. L., Watson, R. E., Patel, B. A., & Gulbransen, B. D. (2015). *Enteric Glia Mediate Neuron Death in Colitis Through Purinergic Pathways That Require Connexin-43 and Nitric Oxide*. Cellular and Molecular Gastroenterology and Hepatology.

Brun, P., Giron, M. C., Qesari, M., Porzionato, A., Caputi, V., Zoppellaro, C., . . . Castagliuolo, I. (2013). Toll-like receptor 2 regulates intestinal inflammation by controlling integrity of the enteric nervous system. *Gastroenterology, 145*(6), 1323-1333. doi:10.1053/j.gastro.2013.08.047

Buckinx, R., Van Remoortel, S., Gijsbers, R., Waddington, S. N., & Timmermans, J. P. (2016). Proof-of-concept: neonatal intravenous injection of adeno-associated virus vectors results in successful transduction of myenteric and submucosal neurons in the mouse small and large intestine. *Neurogastroenterol Motil, 28*(2), 299-305. doi:10.1111/nmo.12724

Burgueno, J. F., Barba, A., Eyre, E., Romero, C., Neunlist, M., & Fernandez, E. (2016). TLR2 and TLR9 modulate enteric nervous system inflammatory responses to lipopolysaccharide. *J Neuroinflammation, 13*(1), 187. doi:10.1186/s12974-016-0653-0

Burkhart, D. L., & Sage, J. (2008). Cellular mechanisms of tumour suppression by the retinoblastoma gene. *Nat Rev Cancer, 8*(9), 671-682. doi:10.1038/nrc2399

Burns, A. J., & Douarin, N. M. (1998). The sacral neural crest contributes neurons and glia to the post-umbilical gut: spatiotemporal analysis of the development of the enteric nervous system. *Development, 125*(21), 4335-4347.

Burns, A. J., Goldstein, A. M., Newgreen, D. F., Stamp, L., Schafer, K. H., Metzger, M., . . . Vanden Berghe, P. (2016). White paper on guidelines concerning enteric nervous system stem cell therapy for enteric neuropathies. *Dev Biol, 417*(2), 229-251. doi:10.1016/j.ydbio.2016.04.001

Bush, T. G., Savidge, T. C., Freeman, T. C., Cox, H. J., Campbell, E. A., Mucke, L., . . . Sofroniew, M. V. (1998). Fulminant jejuno-ileitis following ablation of enteric glia in adult transgenic mice. *Cell, 93*(2), 189-201.

Butler Tjaden, N. E., & Trainor, P. A. (2013). The developmental etiology and pathogenesis of Hirschsprung disease. *Transl Res, 162*(1), 1-15. doi:10.1016/j.trsl.2013.03.001

Cardoso, V., Chesne, J., Ribeiro, H., Garcia-Cassani, B., Carvalho, T., Bouchery, T., . . . Veiga-Fernandes, H. (2017). Neuronal regulation of type 2 innate lymphoid cells via neuromedin U. *Nature, 549*(7671), 277-281. doi:10.1038/nature23469

Castro-Perez, E., Soto-Soto, E., Perez-Carambot, M., Dionisio-Santos, D., Saied-Santiago, K., Ortiz-Zuazaga, H. G., & Pena de Ortiz, S. (2016). Identification and Characterization of the V(D)J Recombination Activating Gene 1 in Long-Term Memory of Context Fear Conditioning. *Neural Plast, 2016*, 1752176. doi:10.1155/2016/1752176

Chalazonitis, A., Pham, T. D., Li, Z., Roman, D., Guha, U., Gomes, W., . . . Gershon, M. D. (2008). Bone morphogenetic protein regulation of enteric neuronal phenotypic diversity: relationship to timing of cell cycle exit. *J Comp Neurol, 509*(5), 474-492. doi:10.1002/cne.21770

Chalazonitis, A., & Rao, M. (2018). Enteric nervous system manifestations of neurodegenerative disease. *Brain Res, 1693*(Pt B), 207-213. doi:10.1016/j.brainres.2018.01.011

Chan, K. Y., Jang, M. J., Yoo, B. B., Greenbaum, A., Ravi, N., Wu, W. L., . . . Gradinaru, V. (2017). Engineered AAVs for efficient noninvasive gene delivery to the central and peripheral nervous systems. *Nat Neurosci, 20*(8), 1172-1179. doi:10.1038/nn.4593

Chandrasekharan, B., Jeppsson, S., Pienkowski, S., Belsham, D. D., Sitaraman, S. V., Merlin, D., . . . Srinivasan, S. (2013). Tumor necrosis factor-neuropeptide Y cross talk regulates inflammation, epithelial barrier functions, and colonic motility. *Inflamm Bowel Dis, 19*(12), 2535-2546. doi:10.1097/01.MIB.0000437042.59208.9f

Chen, Q. Q., Haikal, C., Li, W., Li, M. T., Wang, Z. Y., & Li, J. Y. (2018). Age-dependent alpha-synuclein accumulation and aggregation in the colon of a transgenic mouse model of Parkinson's disease. *Transl Neurodegener, 7*, 13. doi:10.1186/s40035-018-0118-8

Chiocchetti, R., Mazzuoli, G., Albanese, V., Mazzoni, M., Clavenzani, P., Lalatta-Costerbosa, G., . . . Furness, J. B. (2008). Anatomical evidence for ileal Peyer's patches innervation by enteric nervous system: a potential route for prion neuroinvasion? *Cell Tissue Res, 332*(2), 185-194. doi:10.1007/s00441-008-0583-y

Chow, A. K., & Gulbransen, B. D. (2017). Potential roles of enteric glia in bridging neuroimmune communication in the gut. *Am J Physiol Gastrointest Liver Physiol, 312*(2), G145-G152. doi:10.1152/ajpgi.00384.2016

Christensen, J., & Rick, G. A. (1985). Nerve cell density in submucous plexus throughout the gut of cat and opossum. *Gastroenterology, 89*(5), 1064-1069.

Chun, J. J., Schatz, D. G., Oettinger, M. A., Jaenisch, R., & Baltimore, D. (1991). The recombination activating gene-1 (RAG-1) transcript is present in the murine central nervous system. *Cell, 64*(1), 189-200.

Cirillo, C., Bessissow, T., Desmet, A. S., Vanheel, H., Tack, J., & Vanden Berghe, P. (2015). Evidence for neuronal and structural changes in submucous ganglia of patients with functional dyspepsia. *Am J Gastroenterol, 110*(8), 1205-1215. doi:10.1038/ajg.2015.158

Cirillo, C., Sarnelli, G., Esposito, G., Grosso, M., Petruzzelli, R., Izzo, P., . . . Cuomo, R. (2009). Increased mucosal nitric oxide production in ulcerative colitis is mediated in part by the enteroglial-derived S100B protein. *Neurogastroenterol Motil, 21*(11), 1209-e1112. doi:10.1111/j.1365-2982.2009.01346.x

Cirillo, C., Sarnelli, G., Esposito, G., Turco, F., Steardo, L., & Cuomo, R. (2011). S100B protein in the gut: the evidence for enteroglial-sustained intestinal inflammation. *World J Gastroenterol, 17*(10), 1261-1266. doi:10.3748/wjg.v17.i10.1261

Cirillo, C., Sarnelli, G., Turco, F., Mango, A., Grosso, M., Aprea, G., . . . Cuomo, R. (2011). Proinflammatory stimuli activates human-derived enteroglial cells and induces autocrine nitric oxide production. *Neurogastroenterol Motil, 23*(9), e372-382. doi:10.1111/j.1365-2982.2011.01748.x

Collins, J., Borojevic, R., Verdu, E. F., Huizinga, J. D., & Ratcliffe, E. M. (2014). Intestinal microbiota influence the early postnatal development of the enteric nervous system. *Neurogastroenterol Motil, 26*(1), 98-107. doi:10.1111/nmo.12236

Coquenlorge, S., Duchalais, E., Chevalier, J., Cossais, F., Rolli-Derkinderen, M., & Neunlist, M. (2014). Modulation of lipopolysaccharide-induced neuronal response by activation of the enteric nervous system. *J Neuroinflammation, 11*, 202. doi:10.1186/s12974-014-0202-7

Cornet, A., Savidge, T. C., Cabarrocas, J., Deng, W. L., Colombel, J. F., Lassmann, H., . . . Liblau, R. S. (2001). Enterocolitis induced by autoimmune targeting of enteric glial cells: a possible mechanism in Crohn's disease? *Proc Natl Acad Sci U S A, 98*(23), 13306-13311. doi:10.1073/pnas.231474098

Corriveau, R. A., Huh, G. S., & Shatz, C. J. (1998). Regulation of class I MHC gene expression in the developing and mature CNS by neural activity. *Neuron, 21*(3), 505-520.

Cossais, F., Durand, T., Chevalier, J., Boudaud, M., Kermarrec, L., Aubert, P., . . . Neunlist, M. (2016). Postnatal development of the myenteric glial network and its modulation by butyrate. *Am J Physiol Gastrointest Liver Physiol, 310*(11), G941-951. doi:10.1152/ajpgi.00232.2015

Costa, M., Wiklendt, L., Simpson, P., Spencer, N. J., Brookes, S. J., & Dinning, P. G. (2015). Neuromechanical factors involved in the formation and propulsion of fecal pellets in the guinea-pig colon. *Neurogastroenterol Motil, 27*(10), 1466-1477. doi:10.1111/nmo.12646

Costea, P. I., Hildebrand, F., Arumugam, M., Backhed, F., Blaser, M. J., Bushman, F. D., . . . Bork, P. (2018). Enterotypes in the landscape of gut microbial community composition. *Nat Microbiol, 3*(1), 8-16. doi:10.1038/s41564-017-0072-8

de Fontgalland, D., Brookes, S. J., Gibbins, I., Sia, T. C., & Wattchow, D. A. (2014). The neurochemical changes in the innervation of human colonic mesenteric and submucosal blood vessels in ulcerative colitis and Crohn's disease. *Neurogastroenterol Motil, 26*(5), 731-744. doi:10.1111/nmo.12327

de Graaff, E., Srinivas, S., Kilkenny, C., D'Agati, V., Mankoo, B. S., Costantini, F., & Pachnis, V. (2001). Differential activities of the RET tyrosine kinase receptor isoforms during mammalian embryogenesis. *Genes Dev, 15*(18), 2433-2444. doi:10.1101/gad.205001

de Mattos, B. R., Garcia, M. P., Nogueira, J. B., Paiatto, L. N., Albuquerque, C. G., Souza, C. L., . . . Simioni, P. U. (2015). Inflammatory Bowel Disease: An Overview of Immune Mechanisms and Biological Treatments. *Mediators Inflamm, 2015*, 493012. doi:10.1155/2015/493012

De Schepper, S., Verheijden, S., Aguilera-Lizarraga, J., Viola, M. F., Boesmans, W., Stakenborg, N., . . . Boeckxstaens, G. (2018). Self-Maintaining Gut Macrophages Are Essential for Intestinal Homeostasis. *Cell, 175*(2), 400-415 e413. doi:10.1016/j.cell.2018.07.048

de Souza, H. S., & Fiocchi, C. (2016). Immunopathogenesis of IBD: current state of the art. *Nat Rev Gastroenterol Hepatol, 13*(1), 13-27. doi:10.1038/nrgastro.2015.186

De Vadder, F., Grasset, E., Manneras Holm, L., Karsenty, G., Macpherson, A. J., Olofsson, L. E., & Backhed, F. (2018). Gut microbiota regulates maturation of the adult enteric nervous system via enteric serotonin networks. *Proc Natl Acad Sci U S A, 115*(25), 6458-6463. doi:10.1073/pnas.1720017115

Debock, I., & Flamand, V. (2014). Unbalanced Neonatal CD4(+) T-Cell Immunity. *Front Immunol, 5*, 393. doi:10.3389/fimmu.2014.00393

DeLuca, D. S., Levin, J. Z., Sivachenko, A., Fennell, T., Nazaire, M. D., Williams, C., . . . Getz, G. (2012). RNA-SeQC: RNA-seq metrics for quality control and process optimization. *Bioinformatics, 28*(11), 1530-1532. doi:10.1093/bioinformatics/bts196

Delvalle, N. M., Dharshika, C., Morales-Soto, W., Fried, D. E., Gaudette, L., & Gulbransen, B. D. (2018). Communication Between Enteric Neurons, Glia, and Nociceptors Underlies the Effects of Tachykinins on Neuroinflammation. *Cell Mol Gastroenterol Hepatol, 6*(3), 321-344. doi:10.1016/j.jcmgh.2018.05.009

Delvalle, N. M., Fried, D. E., Rivera-Lopez, G., Gaudette, L., & Gulbransen, B. D. (2018). Cholinergic activation of enteric glia is a physiological mechanism that contributes to the regulation of gastrointestinal motility. *Am J Physiol Gastrointest Liver Physiol, 315*(4), G473-G483. doi:10.1152/ajpgi.00155.2018

Deng, L., Zhou, J. F., Sellers, R. S., Li, J. F., Nguyen, A. V., Wang, Y., . . . Lin, E. Y. (2010). A novel mouse model of inflammatory bowel disease links mammalian target of rapamycin-dependent hyperproliferation of colonic epithelium to inflammation-associated tumorigenesis. *Am J Pathol, 176*(2), 952-967. doi:10.2353/ajpath.2010.090622

Denning, T. L., Norris, B. A., Medina-Contreras, O., Manicassamy, S., Geem, D., Madan, R., . . . Pulendran, B. (2011). Functional specializations of intestinal dendritic cell and macrophage subsets that control Th17 and regulatory T cell responses are dependent on the T cell/APC ratio, source of mouse strain, and regional localization. *J Immunol, 187*(2), 733-747. doi:10.4049/jimmunol.1002701

Desmet, A. S., Cirillo, C., Tack, J., Vandenberghe, W., & Vanden Berghe, P. (2017). Live calcium and mitochondrial imaging in the enteric nervous system of Parkinson patients and controls. *Elife, 6*. doi:10.7554/eLife.26850

Desmet, A. S., Cirillo, C., & Vanden Berghe, P. (2014). Distinct subcellular localization of the neuronal marker HuC/D reveals hypoxia-induced damage in enteric neurons. *Neurogastroenterol Motil, 26*(8), 1131-1143. doi:10.1111/nmo.12371

Devos, D., Lebouvier, T., Lardeux, B., Biraud, M., Rouaud, T., Pouclet, H., . . . Derkinderen, P. (2013). Colonic inflammation in Parkinson's disease. *Neurobiol Dis, 50*, 42-48. doi:10.1016/j.nbd.2012.09.007

di Giancamillo, A., Vitari, F., Bosi, G., Savoini, G., & Domeneghini, C. (2010). The chemical code of porcine enteric neurons and the number of enteric glial cells are altered by dietary probiotics. *Neurogastroenterol Motil, 22*(9), e271-278. doi:10.1111/j.1365-2982.2010.01529.x

Dionisio, L., Jose De Rosa, M., Bouzat, C., & Esandi Mdel, C. (2011). An intrinsic GABAergic system in human lymphocytes. *Neuropharmacology, 60*(2-3), 513-519. doi:10.1016/j.neuropharm.2010.11.007

Dobin, A., Davis, C. A., Schlesinger, F., Drenkow, J., Zaleski, C., Jha, S., . . . Gingeras, T. R. (2013). STAR: ultrafast universal RNA-seq aligner. *Bioinformatics, 29*(1), 15-21. doi:10.1093/bioinformatics/bts635

Doe, W. F. (1989). The intestinal immune system. *Gut, 30*(12), 1679-1685.

Dominguez-Bello, M. G., De Jesus-Laboy, K. M., Shen, N., Cox, L. M., Amir, A., Gonzalez, A., . . . Clemente, J. C. (2016). Partial restoration of the microbiota of cesarean-born infants via vaginal microbial transfer. *Nat Med, 22*(3), 250-253. doi:10.1038/nm.4039

Dora, D., Arciero, E., Hotta, R., Barad, C., Bhave, S., Kovacs, T., . . . Nagy, N. (2018). Intraganglionic macrophages: a new population of cells in the enteric ganglia. *J Anat, 233*(4), 401-410. doi:10.1111/joa.12863

Dou, D., Chen, L., Di, H., Song, Z., Li, S., Bu, X., . . . Jing, H. (2018). Vasopressin augments TNBS-induced colitis through enteric neuronal V1a receptor-mediated COX-2-dependent prostaglandin release from mast cells in mice. *Neurogastroenterol Motil*, e13493. doi:10.1111/nmo.13493

Dupont, J. R., Jervis, H. R., & Sprinz, H. (1965). Auerbach's plexus of the rat cecum in relation to the germfree state. *J Comp Neurol, 125*(1), 11-18.

Dyson, N. J. (2016). RB1: a prototype tumor suppressor and an enigma. *Genes Dev, 30*(13), 1492-1502. doi:10.1101/gad.282145.116

Eaker, E. Y., & Sallustio, J. E. (1994). The distribution of novel intermediate filament proteins defines subpopulations of myenteric neurons in rat intestine. *Gastroenterology, 107*(3), 666-674.

El Aidy, S., Dinan, T. G., & Cryan, J. F. (2015). Gut Microbiota: The Conductor in the Orchestra of Immune-Neuroendocrine Communication. *Clin Ther, 37*(5), 954-967. doi:10.1016/j.clinthera.2015.03.002

Engelhardt, B., & Ransohoff, R. M. (2005). The ins and outs of T-lymphocyte trafficking to the CNS: anatomical sites and molecular mechanisms. *Trends Immunol, 26*(9), 485-495. doi:10.1016/j.it.2005.07.004

Farina, C., Aloisi, F., & Meinl, E. (2007). Astrocytes are active players in cerebral innate immunity. *Trends Immunol, 28*(3), 138-145. doi:10.1016/j.it.2007.01.005

Farkas, A. M., Panea, C., Goto, Y., Nakato, G., Galan-Diez, M., Narushima, S., . . . Ivanov, II. (2015). Induction of Th17 cells by segmented filamentous bacteria in the murine intestine. *J Immunol Methods, 421*, 104-111. doi:10.1016/j.jim.2015.03.020

Fasano, A., Visanji, N. P., Liu, L. W., Lang, A. E., & Pfeiffer, R. F. (2015). Gastrointestinal dysfunction in Parkinson's disease. *Lancet Neurol, 14*(6), 625-639. doi:10.1016/S1474-4422(15)00007-1

Feng, B., Bulchand, S., Yaksi, E., Friedrich, R. W., & Jesuthasan, S. (2005). The recombination activation gene 1 (Rag1) is expressed in a subset of zebrafish olfactory neurons but is not essential for axon targeting or amino acid detection. *BMC Neurosci, 6*, 46. doi:10.1186/1471-2202-6-46

Fernandez-Blanco, J. A., Barbosa, S., Sanchez de Medina, F., Martinez, V., & Vergara, P. (2011). Persistent epithelial barrier alterations in a rat model of postinfectious gut dysfunction. *Neurogastroenterol Motil, 23*(11), e523-533. doi:10.1111/j.1365-2982.2011.01777.x

Ferrante, M., de Hertogh, G., Hlavaty, T., D'Haens, G., Penninckx, F., D'Hoore, A., . . . van Assche, G. (2006). The value of myenteric plexitis to predict early postoperative Crohn's disease recurrence. *Gastroenterology, 130*(6), 1595-1606. doi:10.1053/j.gastro.2006.02.025

Ferri, G., Probert, L., Cocchia, D., Michetti, F., Marangos, P., & Polak, J. (1982). Evidence for the presence of S-100 protein in the glial component of the human enteric nervous system. *Nature, 297*(5865), 409-410.

Festing, M. F. (2010). Inbred strains should replace outbred stocks in toxicology, safety testing, and drug development. *Toxicol Pathol, 38*(5), 681-690. doi:10.1177/0192623310373776

Fida, R., Lyster, D. J., Bywater, R. A., & Taylor, G. S. (1997). Colonic migrating motor complexes (CMMCs) in the isolated mouse colon. *Neurogastroenterol Motil, 9*(2), 99-107.

Fletcher, E. L., Clark, M. J., & Furness, J. B. (2002). Neuronal and glial localization of GABA transporter immunoreactivity in the myenteric plexus. *Cell Tissue Res, 308*(3), 339-346. doi:10.1007/s00441-002-0566-3

Flierl, M. A., Rittirsch, D., Nadeau, B. A., Chen, A. J., Sarma, J. V., Zetoune, F. S., . . . Ward, P. A. (2007). Phagocyte-derived catecholamines enhance acute inflammatory injury. *Nature, 449*(7163), 721-725. doi:10.1038/nature06185

Francino, M. P. (2018). Birth Mode-Related Differences in Gut Microbiota Colonization and Immune System Development. *Ann Nutr Metab, 73 Suppl 3*, 12-16. doi:10.1159/000490842

Frykman, P. K., & Short, S. S. (2012). Hirschsprung-associated enterocolitis: prevention and therapy. *Semin Pediatr Surg, 21*(4), 328-335. doi:10.1053/j.sempedsurg.2012.07.007

Fu, M., Landreville, S., Agapova, O. A., Wiley, L. A., Shoykhet, M., Harbour, J. W., & Heuckeroth, R. O. (2013). Retinoblastoma protein prevents enteric nervous system defects and intestinal pseudo-obstruction. *J Clin Invest, 123*(12), 5152-5164. doi:10.1172/JCI67653

Fung, T. C., Olson, C. A., & Hsiao, E. Y. (2017). Interactions between the microbiota, immune and nervous systems in health and disease. *Nat Neurosci, 20*(2), 145-155. doi:10.1038/nn.4476

Furness, J. B. (2000). Types of neurons in the enteric nervous system. *J Auton Nerv Syst, 81*(1-3), 87-96.

Furness, J. B. (2006). *The Enteric Nervous System*: Wiley-Blackwell.

Furness, J. B. (2012). The enteric nervous system and neurogastroenterology. *Nat Rev Gastroenterol Hepatol, 9*(5), 286-294. doi:10.1038/nrgastro.2012.32

Furness, J. B., & Costa, M. (1980). Types of nerves in the enteric nervous system. *Neuroscience, 5*(1), 1-20.

Furness, J. B., Rivera, L. R., Cho, H. J., Bravo, D. M., & Callaghan, B. (2013). The gut as a sensory organ. *Nat Rev Gastroenterol Hepatol, 10*(12), 729-740. doi:10.1038/nrgastro.2013.180

Gabanyi, I., Muller, P. A., Feighery, L., Oliveira, T. Y., Costa-Pinto, F. A., & Mucida, D. (2016). Neuro-immune Interactions Drive Tissue Programming in Intestinal Macrophages. *Cell, 164*(3), 378-391. doi:10.1016/j.cell.2015.12.023

Gabella, G. (1970). [Presence of gliofilaments in the glial cells of the myenteric plexus]. *Boll Soc Ital Biol Sper, 46*(5), 213-215.

Gabella, G. (1971). Glial cells in the myenteric plexus. *Z Naturforsch B, 26*(3), 244-245.

Gabella, G. (1972). Fine structure of the myenteric plexus in the guinea-pig ileum. *J Anat, 111*(Pt 1), 69-97.

Gabella, G. (1981). Ultrastructure of the nerve plexuses of the mammalian intestine: the enteric glial cells. *Neuroscience, 6*(3), 425-436.

Gabella, G. (1987). The number of neurons in the small intestine of mice, guinea-pigs and sheep. *Neuroscience, 22*(2), 737-752.

Gabella, G., & Trigg, P. (1984). Size of neurons and glial cells in the enteric ganglia of mice, guinea-pigs, rabbits and sheep. *J Neurocytol, 13*(1), 49-71.

Gagliani, N., Magnani, C. F., Huber, S., Gianolini, M. E., Pala, M., Licona-Limon, P., . . . Roncarolo, M. G. (2013). Coexpression of CD49b and LAG-3 identifies human and mouse T regulatory type 1 cells. *Nat Med, 19*(6), 739-746. doi:10.1038/nm.3179

Geboes, K., & Collins, S. (1998). Structural abnormalities of the nervous system in Crohn's disease and ulcerative colitis. *Neurogastroenterol Motil, 10*(3), 189-202.

Geboes, K., Rutgeerts, P., Ectors, N., Mebis, J., Penninckx, F., Vantrappen, G., & Desmet, V. J. (1992). Major histocompatibility class II expression on the small intestinal nervous system in Crohn's disease. *Gastroenterology, 103*(2), 439-447.

Gensollen, T., Iyer, S. S., Kasper, D. L., & Blumberg, R. S. (2016). How colonization by microbiota in early life shapes the immune system. *Science, 352*(6285), 539-544. doi:10.1126/science.aad9378

Genton, L., & Kudsk, K. A. (2003). Interactions between the enteric nervous system and the immune system: role of neuropeptides and nutrition. *Am J Surg, 186*(3), 253-258.

Gershon, M. D. (1998). *The Second Brain*. New York: HarperCollins Publishers Inc.

Gershon, M. D., & Erde, S. M. (1981). The nervous system of the gut. *Gastroenterology, 80*(6), 1571-1594.

Gershon, M. D., & Rothman, T. P. (1991). Enteric glia. *Glia, 4*(2), 195-204. doi:10.1002/glia.440040211

Geuking, M. B., Koller, Y., Rupp, S., & McCoy, K. D. (2014). The interplay between the gut microbiota and the immune system. *Gut Microbes, 5*(3), 411-418. doi:10.4161/gmic.29330

Giancola, F., Torresan, F., Repossi, R., Bianco, F., Latorre, R., Ioannou, A., . . . De Giorgio, R. (2017). Downregulation of neuronal vasoactive intestinal polypeptide in Parkinson's disease and chronic constipation. *Neurogastroenterol Motil, 29*(5). doi:10.1111/nmo.12995

Goddard, C. A., Butts, D. A., & Shatz, C. J. (2007). Regulation of CNS synapses by neuronal MHC class I. *Proc Natl Acad Sci U S A, 104*(16), 6828-6833. doi:10.1073/pnas.0702023104

Goldstein, A. M., & Nagy, N. (2008). A bird's eye view of enteric nervous system development: lessons from the avian embryo. *Pediatr Res, 64*(4), 326-333. doi:10.1203/PDR.0b013e31818535e8

Gomariz, R. P., Delgado, M., Naranjo, J. R., Mellstrom, B., Tormo, A., Mata, F., & Leceta, J. (1993). VIP gene expression in rat thymus and spleen. *Brain Behav Immun, 7*(4), 271-278. doi:10.1006/brbi.1993.1027

Gombash, S. E. (2015). Adeno-Associated Viral Vector Delivery to the Enteric Nervous System: A Review. *Postdoc J, 3*(8), 1-12.

Gombash, S. E., Cowley, C. J., Fitzgerald, J. A., Hall, J. C., Mueller, C., Christofi, F. L., & Foust, K. D. (2014). Intravenous AAV9 efficiently transduces myenteric neurons in neonate and juvenile mice. *Front Mol Neurosci, 7*, 81. doi:10.3389/fnmol.2014.00081

Gombash, S. E., Cowley, C. J., Fitzgerald, J. A., Lepak, C. A., Neides, M. G., Hook, K., . . . Foust, K. D. (2017). Systemic gene delivery transduces the enteric nervous system of guinea pigs and cynomolgus macaques. *Gene Ther, 24*(10), 640-648. doi:10.1038/gt.2017.72

Gosain, A. (2016). Established and emerging concepts in Hirschsprung's-associated enterocolitis. *Pediatr Surg Int, 32*(4), 313-320. doi:10.1007/s00383-016-3862-9

Goyal, R. K., & Hirano, I. (1996). The enteric nervous system. *N Engl J Med, 334*(17), 1106-1115. doi:10.1056/NEJM199604253341707

Green, C. L., Ho, W., Sharkey, K. A., & McKay, D. M. (2004). Dextran sodium sulfate-induced colitis reveals nicotinic modulation of ion transport via iNOS-derived NO. *Am J Physiol Gastrointest Liver Physiol, 287*(3), G706-714. doi:10.1152/ajpgi.00076.2004

Grindberg, R. V., Yee-Greenbaum, J. L., McConnell, M. J., Novotny, M., O'Shaughnessy, A. L., Lambert, G. M., . . . Lasken, R. S. (2013). RNA-sequencing from single nuclei. *Proc Natl Acad Sci U S A, 110*(49), 19802-19807. doi:10.1073/pnas.1319700110

Gulbransen, B. D., Bains, J. S., & Sharkey, K. A. (2010). Enteric glia are targets of the sympathetic innervation of the myenteric plexus in the guinea pig distal colon. *J Neurosci, 30*(19), 6801-6809. doi:10.1523/JNEUROSCI.0603-10.2010

Gulbransen, B. D., & Sharkey, K. A. (2009). Purinergic neuron-to-glia signaling in the enteric nervous system. *Gastroenterology, 136*(4), 1349-1358. doi:10.1053/j.gastro.2008.12.058

Gulbransen, B. D., & Sharkey, K. A. (2012). Novel functional roles for enteric glia in the gastrointestinal tract. *Nat Rev Gastroenterol Hepatol, 9*(11), 625-632. doi:10.1038/nrgastro.2012.138

Guryev, V., Koudijs, M. J., Berezikov, E., Johnson, S. L., Plasterk, R. H., van Eeden, F. J., & Cuppen, E. (2006). Genetic variation in the zebrafish. *Genome Res, 16*(4), 491-497. doi:10.1101/gr.4791006

Halliez, M. C., & Buret, A. G. (2015). Gastrointestinal Parasites and the Neural Control of Gut Functions. *Front Cell Neurosci, 9*, 452. doi:10.3389/fncel.2015.00452

Han, X., Tang, S., Dong, L., Song, L., Dong, Y., Wang, Y., & Du, Y. (2017). Loss of nitrergic and cholinergic neurons in the enteric nervous system of APP/PS1 transgenic mouse model. *Neurosci Lett, 642*, 59-65. doi:10.1016/j.neulet.2017.01.061

Hanani, M., & Reichenbach, A. (1994). Morphology of horseradish peroxidase (HRP)-injected glial cells in the myenteric plexus of the guinea-pig. *Cell Tissue Res, 278*(1), 153-160.

Hao, M. M., Anderson, R. B., Kobayashi, K., Whitington, P. M., & Young, H. M. (2009). The migratory behavior of immature enteric neurons. *Dev Neurobiol, 69*(1), 22-35. doi:10.1002/dneu.20683

Hao, M. M., Boesmans, W., Van den Abbeel, V., Jennings, E. A., Bornstein, J. C., Young, H. M., & Vanden Berghe, P. (2011). Early emergence of neural activity in the developing mouse enteric nervous system. *J Neurosci, 31*(43), 15352-15361. doi:10.1523/JNEUROSCI.3053-11.2011

Hao, M. M., Bornstein, J. C., Vanden Berghe, P., Lomax, A. E., Young, H. M., & Foong, J. P. (2013). The emergence of neural activity and its role in the development of the enteric nervous system. *Dev Biol, 382*(1), 365-374. doi:10.1016/j.ydbio.2012.12.006

Hao, M. M., Foong, J. P., Bornstein, J. C., Li, Z. L., Vanden Berghe, P., & Boesmans, W. (2016). Enteric nervous system assembly: Functional integration within the developing gut. *Dev Biol, 417*(2), 168-181. doi:10.1016/j.ydbio.2016.05.030

Hao, M. M., Lomax, A. E., McKeown, S. J., Reid, C. A., Young, H. M., & Bornstein, J. C. (2012). Early development of electrical excitability in the mouse enteric nervous system. *J Neurosci, 32*(32), 10949-10960. doi:10.1523/JNEUROSCI.1426-12.2012

Hao, M. M., Moore, R. E., Roberts, R. R., Nguyen, T., Furness, J. B., Anderson, R. B., & Young, H. M. (2010). The role of neural activity in the migration and differentiation of enteric neuron precursors. *Neurogastroenterol Motil, 22*(5), e127-137. doi:10.1111/j.1365-2982.2009.01462.x

Hao, M. M., & Young, H. M. (2009). Development of enteric neuron diversity. *J Cell Mol Med, 13*(7), 1193-1210. doi:10.1111/j.1582-4934.2009.00813.x

Heanue, T. A., & Pachnis, V. (2007). Enteric nervous system development and Hirschsprung's disease: advances in genetic and stem cell studies. *Nat Rev Neurosci, 8*(6), 466-479. doi:10.1038/nrn2137

Heanue, T. A., & Pachnis, V. (2011). Prospective identification and isolation of enteric nervous system progenitors using Sox2. *Stem Cells, 29*(1), 128-140. doi:10.1002/stem.557

Heanue, T. A., Shepherd, I. T., & Burns, A. J. (2016). Enteric nervous system development in avian and zebrafish models. *Dev Biol, 417*(2), 129-138. doi:10.1016/j.ydbio.2016.05.017

Hibberd, T. J., Feng, J., Luo, J., Yang, P., Samineni, V. K., Gereau, R. W. t., . . . Spencer, N. J. (2018). Optogenetic Induction of Colonic Motility in Mice. *Gastroenterology, 155*(2), 514-528 e516. doi:10.1053/j.gastro.2018.05.029

Hirano, T., Murata, T., & Hayashi, T. (2015). Physiological significance of recombination-activating gene 1 in neuronal death, especially optic neuropathy. *FEBS J, 282*(1), 129-141. doi:10.1111/febs.13109

Hirota, K., Duarte, J. H., Veldhoen, M., Hornsby, E., Li, Y., Cua, D. J., . . . Stockinger, B. (2011). Fate mapping of IL-17-producing T cells in inflammatory responses. *Nat Immunol, 12*(3), 255-263. doi:10.1038/ni.1993

Hirota, K., Turner, J. E., Villa, M., Duarte, J. H., Demengeot, J., Steinmetz, O. M., & Stockinger, B. (2013). Plasticity of Th17 cells in Peyer's patches is responsible for the induction of T cell-dependent IgA responses. *Nat Immunol, 14*(4), 372-379. doi:10.1038/ni.2552

Hoff, S., Zeller, F., von Weyhern, C. W., Wegner, M., Schemann, M., Michel, K., & Ruhl, A. (2008). Quantitative assessment of glial cells in the human and guinea pig enteric nervous system with an anti-Sox8/9/10 antibody. *J Comp Neurol, 509*(4), 356-371. doi:10.1002/cne.21769

Holmqvist, S., Chutna, O., Bousset, L., Aldrin-Kirk, P., Li, W., Bjorklund, T., . . . Li, J. Y. (2014). Direct evidence of Parkinson pathology spread from the gastrointestinal tract to the brain in rats. *Acta Neuropathol, 128*(6), 805-820. doi:10.1007/s00401-014-1343-6

Holzer, P., & Farzi, A. (2014). Neuropeptides and the microbiota-gut-brain axis. *Adv Exp Med Biol, 817*, 195-219. doi:10.1007/978-1-4939-0897-4_9

Human Microbiome Project, C. (2012). Structure, function and diversity of the healthy human microbiome. *Nature, 486*(7402), 207-214. doi:10.1038/nature11234

Husebye, E., Hellstrom, P. M., Sundler, F., Chen, J., & Midtvedt, T. (2001). Influence of microbial species on small intestinal myoelectric activity and transit in germ-free

rats. *Am J Physiol Gastrointest Liver Physiol, 280*(3), G368-380. doi:10.1152/ajpgi.2001.280.3.G368

Hyland, N. P., & Cryan, J. F. (2016). Microbe-host interactions: Influence of the gut microbiota on the enteric nervous system. *Dev Biol, 417*(2), 182-187. doi:10.1016/j.ydbio.2016.06.027

Ibiza, S., García-Cassani, B., Ribeiro, H., Carvalho, T., Almeida, L., Marques, R., . . . Veiga-Fernandes, H. (2016). *Glial cell-derived neuroregulators control type 3 innate lymphoid cells and gut defence*.

Ito, D., Imai, Y., Ohsawa, K., Nakajima, K., Fukuuchi, Y., & Kohsaka, S. (1998). Microglia-specific localisation of a novel calcium binding protein, Iba1. *Brain Res Mol Brain Res, 57*(1), 1-9.

Ivanov, II, Atarashi, K., Manel, N., Brodie, E. L., Shima, T., Karaoz, U., . . . Littman, D. R. (2009). Induction of intestinal Th17 cells by segmented filamentous bacteria. *Cell, 139*(3), 485-498. doi:10.1016/j.cell.2009.09.033

Jensen, V. S., Porsgaard, T., Lykkesfeldt, J., & Hvid, H. (2016). Rodent model choice has major impact on variability of standard preclinical readouts associated with diabetes and obesity research. *Am J Transl Res, 8*(8), 3574-3584.

Jessen, K. R., & Mirsky, R. (1980). Glial cells in the enteric nervous system contain glial fibrillary acidic protein. *Nature, 286*(5774), 736-737.

Jessen, K. R., & Mirsky, R. (1983). Astrocyte-like glia in the peripheral nervous system: an immunohistochemical study of enteric glia. *J Neurosci, 3*(11), 2206-2218.

Joseph, N. M., He, S., Quintana, E., Kim, Y. G., Nunez, G., & Morrison, S. J. (2011). Enteric glia are multipotent in culture but primarily form glia in the adult rodent gut. *J Clin Invest, 121*(9), 3398-3411. doi:10.1172/JCI58186

Kabouridis, P. S., Lasrado, R., McCallum, S., Chng, S. H., Snippert, H. J., Clevers, H., . . . Pachnis, V. (2015). Microbiota controls the homeostasis of glial cells in the gut lamina propria. *Neuron, 85*(2), 289-295. doi:10.1016/j.neuron.2014.12.037

Kabouridis, P. S., & Pachnis, V. (2015). Emerging roles of gut microbiota and the immune system in the development of the enteric nervous system. *J Clin Invest, 125*(3), 956-964. doi:10.1172/JCI76308

Kamm, K., Hoppe, S., Breves, G., Schroder, B., & Schemann, M. (2004). Effects of the probiotic yeast Saccharomyces boulardii on the neurochemistry of myenteric neurones in pig jejunum. *Neurogastroenterol Motil, 16*(1), 53-60.

Kane, J. S., & Ford, A. C. (2016). Rifaximin for the treatment of diarrhea-predominant irritable bowel syndrome. *Expert Rev Gastroenterol Hepatol, 10*(4), 431-442. doi:10.1586/17474124.2016.1140571

Kaplan, G. G. (2015). The global burden of IBD: from 2015 to 2025. *Nat Rev Gastroenterol Hepatol, 12*(12), 720-727. doi:10.1038/nrgastro.2015.150

Kashyap, P. C., Marcobal, A., Ursell, L. K., Larauche, M., Duboc, H., Earle, K. A., . . . Sonnenburg, J. L. (2013). Complex interactions among diet, gastrointestinal transit, and gut microbiota in humanized mice. *Gastroenterology, 144*(5), 967-977. doi:10.1053/j.gastro.2013.01.047

Kermarrec, L., Durand, T., Gonzales, J., Pabois, J., Hulin, P., Neunlist, M., . . . Naveilhan, P. (2018). Rat enteric glial cells express novel isoforms of Interleukine-7 regulated during inflammation. *Neurogastroenterol Motil*, e13467. doi:10.1111/nmo.13467

Kermarrec, L., Durand, T., Neunlist, M., Naveilhan, P., & Neveu, I. (2016). Enteric glial cells have specific immunosuppressive properties. *J Neuroimmunol, 295-296*, 79-83. doi:10.1016/j.jneuroim.2016.04.011

Kitamura, D., Roes, J., Kuhn, R., & Rajewsky, K. (1991). A B cell-deficient mouse by targeted disruption of the membrane exon of the immunoglobulin mu chain gene. *Nature, 350*(6317), 423-426. doi:10.1038/350423a0

Klose, C. S. N., Mahlakoiv, T., Moeller, J. B., Rankin, L. C., Flamar, A. L., Kabata, H., . . . Artis, D. (2017). The neuropeptide neuromedin U stimulates innate lymphoid cells and type 2 inflammation. *Nature, 549*(7671), 282-286. doi:10.1038/nature23676

Knowles, C. H., Lindberg, G., Panza, E., & De Giorgio, R. (2013). New perspectives in the diagnosis and management of enteric neuropathies. *Nat Rev Gastroenterol Hepatol, 10*(4), 206-218. doi:10.1038/nrgastro.2013.18

Kontoyiannis, D., Boulougouris, G., Manoloukos, M., Armaka, M., Apostolaki, M., Pizarro, T., . . . Kollias, G. (2002). Genetic dissection of the cellular pathways and signaling mechanisms in modeled tumor necrosis factor-induced Crohn's-like inflammatory bowel disease. *J Exp Med, 196*(12), 1563-1574.

Kontoyiannis, D., Pasparakis, M., Pizarro, T. T., Cominelli, F., & Kollias, G. (1999). Impaired on/off regulation of TNF biosynthesis in mice lacking TNF AU-rich elements: implications for joint and gut-associated immunopathologies. *Immunity, 10*(3), 387-398.

Koretz, K., Momburg, F., Otto, H. F., & Moller, P. (1987). Sequential induction of MHC antigens on autochthonous cells of ileum affected by Crohn's disease. *Am J Pathol, 129*(3), 493-502.

Krammer, H. J., Karahan, S. T., Rumpel, E., Klinger, M., & Kuhnel, W. (1993). Immunohistochemical visualization of the enteric nervous system using antibodies against protein gene product (PGP) 9.5. *Ann Anat, 175*(4), 321-325.

Krishnaswami, S. R., Grindberg, R. V., Novotny, M., Venepally, P., Lacar, B., Bhutani, K., . . . Lasken, R. S. (2016). Using single nuclei for RNA-seq to capture the transcriptome of postmortem neurons. *Nat Protoc, 11*(3), 499-524. doi:10.1038/nprot.2016.015

Kulkarni, S., Micci, M. A., Leser, J., Shin, C., Tang, S. C., Fu, Y. Y., . . . Pasricha, P. J. (2017). Adult enteric nervous system in health is maintained by a dynamic balance between neuronal apoptosis and neurogenesis. *Proc Natl Acad Sci U S A, 114*(18), E3709-E3718. doi:10.1073/pnas.1619406114

Kunze, W. A., & Furness, J. B. (1999). The enteric nervous system and regulation of intestinal motility. *Annu Rev Physiol, 61*, 117-142. doi:10.1146/annurev.physiol.61.1.117

Kunze, W. A., Mao, Y. K., Wang, B., Huizinga, J. D., Ma, X., Forsythe, P., & Bienenstock, J. (2009). Lactobacillus reuteri enhances excitability of colonic AH neurons by inhibiting calcium-dependent potassium channel opening. *J Cell Mol Med, 13*(8B), 2261-2270. doi:10.1111/j.1582-4934.2009.00686.x

Labosky, P. A., & Kaestner, K. H. (1998). The winged helix transcription factor Hfh2 is expressed in neural crest and spinal cord during mouse development. *Mech Dev, 76*(1-2), 185-190.

Lai, J. P., Douglas, S. D., & Ho, W. Z. (1998). Human lymphocytes express substance P and its receptor. *J Neuroimmunol, 86*(1), 80-86.

Lai, J. P., Douglas, S. D., & Ho, W. Z. (2002). Mimic-based RT-PCR quantitation of substance P mRNA in human mononuclear phagocytes and lymphocytes. *Methods Mol Biol, 193*, 129-147. doi:10.1385/1-59259-283-X:129

Landreth, K. S. (2002). Critical windows in development of the rodent immune system. *Hum Exp Toxicol, 21*(9-10), 493-498. doi:10.1191/0960327102ht287oa

Langley, J. N. (1921). *The Autonomic Nervous System* (Vol. Part I). Cambridge, England: W. Heffer & Sons LTD.

Laranjeira, C., Sandgren, K., Kessaris, N., Richardson, W., Potocnik, A., Vanden Berghe, P., & Pachnis, V. (2011). Glial cells in the mouse enteric nervous system can undergo neurogenesis in response to injury. *J Clin Invest, 121*(9), 3412-3424. doi:10.1172/JCI58200

Lasrado, R., Boesmans, W., Kleinjung, J., Pin, C., Bell, D., Bhaw, L., . . . Pachnis, V. (2017). Lineage-dependent spatial and functional organization of the mammalian enteric nervous system. *Science, 356*(6339), 722-726. doi:10.1126/science.aam7511

LeBien, T. W., & Tedder, T. F. (2008). B lymphocytes: how they develop and function. *Blood, 112*(5), 1570-1580. doi:10.1182/blood-2008-02-078071

Leng, Y. X., Wei, Y. Y., Chen, H., Zhou, S. P., Yang, Y. L., & Duan, L. P. (2010). Alteration of cholinergic and peptidergic neurotransmitters in rat ileum induced by acute stress following transient intestinal infection is mast cell dependent. *Chin Med J (Engl), 123*(2), 227-233.

Levite, M. (2016). Dopamine and T cells: dopamine receptors and potent effects on T cells, dopamine production in T cells, and abnormalities in the dopaminergic system in T cells in autoimmune, neurological and psychiatric diseases. *Acta Physiol (Oxf), 216*(1), 42-89. doi:10.1111/apha.12476

Li, B., & Dewey, C. N. (2011). RSEM: accurate transcript quantification from RNA-Seq data with or without a reference genome. *BMC Bioinformatics, 12*, 323. doi:10.1186/1471-2105-12-323

Lin, Z., Gao, N., Hu, H. Z., Liu, S., Gao, C., Kim, G., . . . Wood, J. D. (2002). Immunoreactivity of Hu proteins facilitates identification of myenteric neurones in guinea-pig small intestine. *Neurogastroenterol Motil, 14*(2), 197-204.

Linden, D. R., Couvrette, J. M., Ciolino, A., McQuoid, C., Blaszyk, H., Sharkey, K. A., & Mawe, G. M. (2005). Indiscriminate loss of myenteric neurones in the TNBS-inflamed guinea-pig distal colon. *Neurogastroenterol Motil, 17*(5), 751-760. doi:10.1111/j.1365-2982.2005.00703.x

Linden, D. R., Sharkey, K. A., & Mawe, G. M. (2003). Enhanced excitability of myenteric AH neurones in the inflamed guinea-pig distal colon. *J Physiol, 547*(Pt 2), 589-601. doi:10.1113/jphysiol.2002.035147

Liu, G. X., Yang, Y. X., Yan, J., Zhang, T., Zou, Y. P., Huang, X. L., & Gan, H. T. (2014). Glial-derived neurotrophic factor reduces inflammation and improves delayed colonic transit in rat models of dextran sulfate sodium-induced colitis. *Int Immunopharmacol, 19*(1), 145-152. doi:10.1016/j.intimp.2014.01.008

Liu, H., Rhodes, M., Wiest, D. L., & Vignali, D. A. (2000). On the dynamics of TCR:CD3 complex cell surface expression and downmodulation. *Immunity, 13*(5), 665-675.

Liu, T. C., & Stappenbeck, T. S. (2016). Genetics and Pathogenesis of Inflammatory Bowel Disease. *Annu Rev Pathol, 11*, 127-148. doi:10.1146/annurev-pathol-012615-044152

Lomasney, K. W., Houston, A., Shanahan, F., Dinan, T. G., Cryan, J. F., & Hyland, N. P. (2014). Selective influence of host microbiota on cAMP-mediated ion transport in mouse colon. *Neurogastroenterol Motil, 26*(6), 887-890. doi:10.1111/nmo.12328

Lomax, A. E., & Furness, J. B. (2000). Neurochemical classification of enteric neurons in the guinea-pig distal colon. *Cell Tissue Res, 302*(1), 59-72.

Lombardi, V. C., De Meirleir, K. L., Subramanian, K., Nourani, S. M., Dagda, R. K., Delaney, S. L., & Palotas, A. (2018). Nutritional modulation of the intestinal

microbiota; future opportunities for the prevention and treatment of neuroimmune and neuroinflammatory disease. *J Nutr Biochem, 61*, 1-16. doi:10.1016/j.jnutbio.2018.04.004

Love, M. I., Huber, W., & Anders, S. (2014). Moderated estimation of fold change and dispersion for RNA-seq data with DESeq2. *Genome Biol, 15*(12), 550. doi:10.1186/s13059-014-0550-8

Lovell, D. J., Johnson, A. L., Huang, B., Gottlieb, B. S., Morris, P. W., Kimura, Y., . . . Giannini, E. H. (2018). Risk, Timing, and Predictors of Disease Flare After Discontinuation of Anti-Tumor Necrosis Factor Therapy in Children With Polyarticular Forms of Juvenile Idiopathic Arthritis With Clinically Inactive Disease. *Arthritis Rheumatol, 70*(9), 1508-1518. doi:10.1002/art.40509

Luckensmeyer, G. B., & Keast, J. R. (1998). Projections of pelvic autonomic neurons within the lower bowel of the male rat: an anterograde labelling study. *Neuroscience, 84*(1), 263-280.

Luczynski, P., McVey Neufeld, K. A., Oriach, C. S., Clarke, G., Dinan, T. G., & Cryan, J. F. (2016). Growing up in a Bubble: Using Germ-Free Animals to Assess the Influence of the Gut Microbiota on Brain and Behavior. *Int J Neuropsychopharmacol, 19*(8). doi:10.1093/ijnp/pyw020

Makowska, K., & Gonkowski, S. (2018). The Influence of Inflammation and Nerve Damage on the Neurochemical Characterization of Calcitonin Gene-Related Peptide-Like Immunoreactive (CGRP-LI) Neurons in the Enteric Nervous System of the Porcine Descending Colon. *Int J Mol Sci, 19*(2). doi:10.3390/ijms19020548

Martins, P. R., Nascimento, R. D., Dos Santos, A. T., de Oliveira, E. C., Martinelli, P. M., & d'Avila Reis, D. (2018). Mast cell-nerve interaction in the colon of Trypanosoma cruzi-infected individuals with chagasic megacolon. *Parasitol Res, 117*(4), 1147-1158. doi:10.1007/s00436-018-5792-z

Mashaghi, A., Marmalidou, A., Tehrani, M., Grace, P. M., Pothoulakis, C., & Dana, R. (2016). Neuropeptide substance P and the immune response. *Cell Mol Life Sci, 73*(22), 4249-4264. doi:10.1007/s00018-016-2293-z

Maynard, C. L., Elson, C. O., Hatton, R. D., & Weaver, C. T. (2012). Reciprocal interactions of the intestinal microbiota and immune system. *Nature, 489*(7415), 231-241. doi:10.1038/nature11551

McAllister, A. K., & van de Water, J. (2009). Breaking boundaries in neural-immune interactions. *Neuron, 64*(1), 9-12. doi:10.1016/j.neuron.2009.09.038

McClain, J., Grubisic, V., Fried, D., Gomez-Suarez, R. A., Leinninger, G. M., Sevigny, J., . . . Gulbransen, B. D. (2014). Ca2+ responses in enteric glia are mediated by connexin-43 hemichannels and modulate colonic transit in mice. *Gastroenterology, 146*(2), 497-507 e491. doi:10.1053/j.gastro.2013.10.061

McClain, J. L., Fried, D. E., & Gulbransen, B. D. (2015). Agonist-evoked Ca2+ signaling in enteric glia drives neural programs that regulate intestinal motility in mice. *Cell Mol Gastroenterol Hepatol, 1*(6), 631-645. doi:10.1016/j.jcmgh.2015.08.004

McKeown, S. J., Stamp, L., Hao, M. M., & Young, H. M. (2013). Hirschsprung disease: a developmental disorder of the enteric nervous system. *Wiley Interdiscip Rev Dev Biol, 2*(1), 113-129. doi:10.1002/wdev.57

McVey Neufeld, K. A., Mao, Y. K., Bienenstock, J., Foster, J. A., & Kunze, W. A. (2013). The microbiome is essential for normal gut intrinsic primary afferent neuron excitability in the mouse. *Neurogastroenterol Motil, 25*(2), 183-e188. doi:10.1111/nmo.12049

McVey Neufeld, K. A., Perez-Burgos, A., Mao, Y. K., Bienenstock, J., & Kunze, W. A. (2015). The gut microbiome restores intrinsic and extrinsic nerve function in germ-free mice accompanied by changes in calbindin. *Neurogastroenterol Motil, 27*(5), 627-636. doi:10.1111/nmo.12534

Melzer, N., Meuth, S. G., & Wiendl, H. (2009). CD8+ T cells and neuronal damage: direct and collateral mechanisms of cytotoxicity and impaired electrical excitability. *FASEB J, 23*(11), 3659-3673. doi:10.1096/fj.09-136200

Memic, F., Knoflach, V., Morarach, K., Sadler, R., Laranjeira, C., Hjerling-Leffler, J., . . . Marklund, U. (2018). Transcription and Signaling Regulators in Developing Neuronal Subtypes of Mouse and Human Enteric Nervous System. *Gastroenterology, 154*(3), 624-636. doi:10.1053/j.gastro.2017.10.005

Menchen, L., Colon, A. L., Madrigal, J. L., Beltran, L., Botella, S., Lizasoain, I., . . . Lorenzo, P. (2004). Activity of inducible and neuronal nitric oxide synthases in colonic mucosa predicts progression of ulcerative colitis. *Am J Gastroenterol, 99*(9), 1756-1764. doi:10.1111/j.1572-0241.2004.40065.x

Meuth, S. G., Herrmann, A. M., Simon, O. J., Siffrin, V., Melzer, N., Bittner, S., . . . Wiendl, H. (2009). Cytotoxic CD8+ T cell-neuron interactions: perforin-dependent electrical silencing precedes but is not causally linked to neuronal cell death. *J Neurosci, 29*(49), 15397-15409. doi:10.1523/JNEUROSCI.4339-09.2009

Mills, C. D., Kincaid, K., Alt, J. M., Heilman, M. J., & Hill, A. M. (2000). M-1/M-2 macrophages and the Th1/Th2 paradigm. *J Immunol, 164*(12), 6166-6173.

Miyamoto, A., Wake, H., Ishikawa, A. W., Eto, K., Shibata, K., Murakoshi, H., . . . Nabekura, J. (2016). Microglia contact induces synapse formation in developing somatosensory cortex. *Nat Commun, 7*, 12540. doi:10.1038/ncomms12540

Mombaerts, P., Clarke, A. R., Rudnicki, M. A., Iacomini, J., Itohara, S., Lafaille, J. J., . . . et al. (1992). Mutations in T-cell antigen receptor genes alpha and beta block thymocyte development at different stages. *Nature, 360*(6401), 225-231. doi:10.1038/360225a0

Mombaerts, P., Iacomini, J., Johnson, R. S., Herrup, K., Tonegawa, S., & Papaioannou, V. E. (1992). RAG-1-deficient mice have no mature B and T lymphocytes. *Cell, 68*(5), 869-877.

Moran, C., Sheehan, D., & Shanahan, F. (2016). The Changing Phenotype of Inflammatory Bowel Disease. *Gastroenterol Res Pract, 2016*, 1619053. doi:10.1155/2016/1619053

Moreau, N. M., Champ, M. M., Goupry, S. M., Le Bizec, B. J., Krempf, M., Nguyen, P. G., . . . Martin, L. J. (2004). Resistant starch modulates in vivo colonic butyrate uptake and its oxidation in rats with dextran sulfate sodium-induced colitis. *J Nutr, 134*(3), 493-500. doi:10.1093/jn/134.3.493

Mowat, A. M., & Agace, W. W. (2014). Regional specialization within the intestinal immune system. *Nat Rev Immunol, 14*(10), 667-685. doi:10.1038/nri3738

Muller, P. A., Koscso, B., Rajani, G. M., Stevanovic, K., Berres, M. L., Hashimoto, D., . . . Bogunovic, M. (2014). Crosstalk between muscularis macrophages and enteric neurons regulates gastrointestinal motility. *Cell, 158*(2), 300-313. doi:10.1016/j.cell.2014.04.050

Mundell, N. A., Plank, J. L., LeGrone, A. W., Frist, A. Y., Zhu, L., Shin, M. K., . . . Labosky, P. A. (2012). Enteric nervous system specific deletion of Foxd3 disrupts glial cell differentiation and activates compensatory enteric progenitors. *Dev Biol, 363*(2), 373-387. doi:10.1016/j.ydbio.2012.01.003

Nagahama, M., Semba, R., Tsuzuki, M., & Aoki, E. (2001). L-arginine immunoreactive enteric glial cells in the enteric nervous system of rat ileum. *Biol Signals Recept, 10*(5), 336-340. doi:10.1159/000046901

Nagakura, Y., Naitoh, Y., Kamato, T., Yamano, M., & Miyata, K. (1996). Compounds possessing 5-HT3 receptor antagonistic activity inhibit intestinal propulsion in mice. *Eur J Pharmacol, 311*(1), 67-72.

Nasser, Y., Fernandez, E., Keenan, C. M., Ho, W., Oland, L. D., Tibbles, L. A., . . . Sharkey, K. A. (2006). Role of enteric glia in intestinal physiology: effects of the gliotoxin fluorocitrate on motor and secretory function. *Am J Physiol Gastrointest Liver Physiol, 291*(5), G912-927. doi:10.1152/ajpgi.00067.2006

Neild, T. O., Shen, K. Z., & Surprenant, A. (1990). Vasodilatation of arterioles by acetylcholine released from single neurones in the guinea-pig submucosal plexus. *J Physiol, 420*, 247-265.

Neumann, H., Cavalie, A., Jenne, D. E., & Wekerle, H. (1995). Induction of MHC class I genes in neurons. *Science, 269*(5223), 549-552.

Neunlist, M., Aubert, P., Toquet, C., Oreshkova, T., Barouk, J., Lehur, P. A., . . . Galmiche, J. P. (2003). Changes in chemical coding of myenteric neurones in ulcerative colitis. *Gut, 52*(1), 84-90.

Neunlist, M., Van Landeghem, L., Bourreille, A., & Savidge, T. (2008). Neuro-glial crosstalk in inflammatory bowel disease. *J Intern Med, 263*(6), 577-583. doi:10.1111/j.1365-2796.2008.01963.x

Nikolich-Zugich, J. (2018). Author Correction: The twilight of immunity: emerging concepts in aging of the immune system. *Nat Immunol, 19*(10), 1146. doi:10.1038/s41590-018-0205-0

Norouzinia, M., Chaleshi, V., Alizadeh, A. H. M., & Zali, M. R. (2017). Biomarkers in inflammatory bowel diseases: insight into diagnosis, prognosis and treatment. *Gastroenterol Hepatol Bed Bench, 10*(3), 155-167.

Norris, G. T., Smirnov, I., Filiano, A. J., Shadowen, H. M., Cody, K. R., Thompson, J. A., . . . Kipnis, J. (2018). Neuronal integrity and complement control synaptic material clearance by microglia after CNS injury. *J Exp Med, 215*(7), 1789-1801. doi:10.1084/jem.20172244

Nurgali, K., Nguyen, T. V., Thacker, M., Pontell, L., & Furness, J. B. (2009). Slow synaptic transmission in myenteric AH neurons from the inflamed guinea pig ileum. *Am J Physiol Gastrointest Liver Physiol, 297*(3), G582-593. doi:10.1152/ajpgi.00026.2009

Nurgali, K., Qu, Z., Hunne, B., Thacker, M., Pontell, L., & Furness, J. B. (2011). Morphological and functional changes in guinea-pig neurons projecting to the ileal mucosa at early stages after inflammatory damage. *J Physiol, 589*(Pt 2), 325-339. doi:10.1113/jphysiol.2010.197707

O'Donnell, A. M., Coyle, D., & Puri, P. (2016). Altered expression of retinoblastoma 1 in Hirschsprung's disease. *J Pediatr Surg, 51*(11), 1830-1833. doi:10.1016/j.jpedsurg.2016.07.020

Obata, Y., & Pachnis, V. (2016). The Effect of Microbiota and the Immune System on the Development and Organization of the Enteric Nervous System. *Gastroenterology, 151*(5), 836-844. doi:10.1053/j.gastro.2016.07.044

Oliveira, E. C., Fujisawa, M. M., Hallal Longo, D. E., Farias, A. S., Contin Moraes, J., Guariento, M. E., . . . Santos, L. M. (2009). Neuropathy of gastrointestinal Chagas' disease: immune response to myelin antigens. *Neuroimmunomodulation, 16*(1), 54-62. doi:10.1159/000179667

OpenStax. (2013). *Anatomy & Physiology*. In. Retrieved from http://cnx.org/contents/14fb4ad7-39a1-4eee-ab6e-3ef2482e3e22@8.24

Palleja, A., Mikkelsen, K. H., Forslund, S. K., Kashani, A., Allin, K. H., Nielsen, T., . . . Pedersen, O. (2018). Recovery of gut microbiota of healthy adults following antibiotic exposure. *Nat Microbiol, 3*(11), 1255-1265. doi:10.1038/s41564-018-0257-9

Palucka, A. K., & Coussens, L. M. (2016). The Basis of Oncoimmunology. *Cell, 164*(6), 1233-1247. doi:10.1016/j.cell.2016.01.049

Paolicelli, R. C., Bolasco, G., Pagani, F., Maggi, L., Scianni, M., Panzanelli, P., . . . Gross, C. T. (2011). Synaptic pruning by microglia is necessary for normal brain development. *Science, 333*(6048), 1456-1458. doi:10.1126/science.1202529

Papadakis, K. A., & Targan, S. R. (2000). Tumor necrosis factor: biology and therapeutic inhibitors. *Gastroenterology, 119*(4), 1148-1157.

Parisi, M. A. (1993). Hirschsprung Disease Overview. In M. P. Adam, H. H. Ardinger, R. A. Pagon, S. E. Wallace, L. J. H. Bean, K. Stephens, & A. Amemiya (Eds.), *GeneReviews((R))*. Seattle (WA).

Parkhurst, C. N., Yang, G., Ninan, I., Savas, J. N., Yates, J. R., 3rd, Lafaille, J. J., . . . Gan, W. B. (2013). Microglia promote learning-dependent synapse formation through brain-derived neurotrophic factor. *Cell, 155*(7), 1596-1609. doi:10.1016/j.cell.2013.11.030

Pattyn, A., Morin, X., Cremer, H., Goridis, C., & Brunet, J. F. (1999). The homeobox gene Phox2b is essential for the development of autonomic neural crest derivatives. *Nature, 399*(6734), 366-370. doi:10.1038/20700

Perez-Pardo, P., Dodiya, H. B., Engen, P. A., Naqib, A., Forsyth, C. B., Green, S. J., . . . Kraneveld, A. D. (2018). Gut bacterial composition in a mouse model of Parkinson's disease. *Benef Microbes, 9*(5), 799-814. doi:10.3920/BM2017.0202

Perrone-Bizzozero, N., & Bird, C. W. (2013). Role of HuD in nervous system function and pathology. *Front Biosci (Schol Ed), 5*, 554-563.

Pham, T. D., Gershon, M. D., & Rothman, T. P. (1991). Time of origin of neurons in the murine enteric nervous system: sequence in relation to phenotype. *J Comp Neurol, 314*(4), 789-798. doi:10.1002/cne.903140411

Phillips, R. J., Hargrave, S. L., Rhodes, B. S., Zopf, D. A., & Powley, T. L. (2004). Quantification of neurons in the myenteric plexus: an evaluation of putative pan-neuronal markers. *J Neurosci Methods, 133*(1-2), 99-107.

Phillips, R. J., & Powley, T. L. (2007). Innervation of the gastrointestinal tract: patterns of aging. *Auton Neurosci, 136*(1-2), 1-19. doi:10.1016/j.autneu.2007.04.005

Phillips, R. J., & Powley, T. L. (2012). Macrophages associated with the intrinsic and extrinsic autonomic innervation of the rat gastrointestinal tract. *Auton Neurosci, 169*(1), 12-27. doi:10.1016/j.autneu.2012.02.004

Piper, M., & Holt, C. (2004). RNA translation in axons. *Annu Rev Cell Dev Biol, 20*, 505-523. doi:10.1146/annurev.cellbio.20.010403.111746

Pochard, C., Coquenlorge, S., Jaulin, J., Cenac, N., Vergnolle, N., Meurette, G., . . . Rolli-Derkinderen, M. (2016). Defects in 15-HETE Production and Control of Epithelial Permeability by Human Enteric Glial Cells From Patients With Crohn's Disease. *Gastroenterology, 150*(1), 168-180. doi:10.1053/j.gastro.2015.09.038

Poole, D. P., Godfrey, C., Cattaruzza, F., Cottrell, G. S., Kirkland, J. G., Pelayo, J. C., . . . Corvera, C. U. (2010). Expression and function of the bile acid receptor GpBAR1 (TGR5) in the murine enteric nervous system. *Neurogastroenterol Motil, 22*(7), 814-825, e227-818. doi:10.1111/j.1365-2982.2010.01487.x

Powley, T. L. (2000). Vagal input to the enteric nervous system. *Gut, 47 Suppl 4*, iv30-32; discussion iv36.

Powrie, F. (1995). T cells in inflammatory bowel disease: protective and pathogenic roles. *Immunity, 3*(2), 171-174.

Powrie, F., Leach, M. W., Mauze, S., Menon, S., Caddle, L. B., & Coffman, R. L. (1994). Inhibition of Th1 responses prevents inflammatory bowel disease in scid mice reconstituted with CD45RBhi CD4+ T cells. *Immunity, 1*(7), 553-562.

Puig, K. L., Lutz, B. M., Urquhart, S. A., Rebel, A. A., Zhou, X., Manocha, G. D., . . . Combs, C. K. (2015). Overexpression of mutant amyloid-beta protein precursor and presenilin 1 modulates enteric nervous system. *J Alzheimers Dis, 44*(4), 1263-1278. doi:10.3233/JAD-142259

Rao, M., Nelms, B. D., Dong, L., Salinas-Rios, V., Rutlin, M., Gershon, M. D., & Corfas, G. (2015). Enteric glia express proteolipid protein 1 and are a transcriptionally unique population of glia in the mammalian nervous system. *Glia, 63*(11), 2040-2057. doi:10.1002/glia.22876

Rao, M., Rastelli, D., Dong, L., Chiu, S., Setlik, W., Gershon, M. D., & Corfas, G. (2017). Enteric Glia Regulate Gastrointestinal Motility but Are Not Required for Maintenance of the Epithelium in Mice. *Gastroenterology, 153*(4), 1068-1081 e1067. doi:10.1053/j.gastro.2017.07.002

Reardon, C., Duncan, G. S., Brustle, A., Brenner, D., Tusche, M. W., Olofsson, P. S., . . . Mak, T. W. (2013). Lymphocyte-derived ACh regulates local innate but not adaptive immunity. *Proc Natl Acad Sci U S A, 110*(4), 1410-1415. doi:10.1073/pnas.1221655110

Reardon, C., Murray, K., & Lomax, A. E. (2018). Neuroimmune Communication in Health and Disease. *Physiol Rev, 98*(4), 2287-2316. doi:10.1152/physrev.00035.2017

Reichardt, F., Chassaing, B., Nezami, B. G., Li, G., Tabatabavakili, S., Mwangi, S., . . . Srinivasan, S. (2017). Western diet induces colonic nitrergic myenteric neuropathy and dysmotility in mice via saturated fatty acid- and lipopolysaccharide-induced TLR4 signalling. *J Physiol, 595*(5), 1831-1846. doi:10.1113/JP273269

Rinner, I., Kawashima, K., & Schauenstein, K. (1998). Rat lymphocytes produce and secrete acetylcholine in dependence of differentiation and activation. *J Neuroimmunol, 81*(1-2), 31-37.

Roberts, R. R., Murphy, J. F., Young, H. M., & Bornstein, J. C. (2007). Development of colonic motility in the neonatal mouse-studies using spatiotemporal maps. *Am J Physiol Gastrointest Liver Physiol, 292*(3), G930-938. doi:10.1152/ajpgi.00444.2006

Robinson, A. M., Rahman, A. A., Miller, S., Stavely, R., Sakkal, S., & Nurgali, K. (2017). The neuroprotective effects of human bone marrow mesenchymal stem cells are dose-dependent in TNBS colitis. *Stem Cell Res Ther, 8*(1), 87. doi:10.1186/s13287-017-0540-3

Rogier, E. W., Frantz, A. L., Bruno, M. E., Wedlund, L., Cohen, D. A., Stromberg, A. J., & Kaetzel, C. S. (2014). Secretory antibodies in breast milk promote long-term intestinal homeostasis by regulating the gut microbiota and host gene expression. *Proc Natl Acad Sci U S A, 111*(8), 3074-3079. doi:10.1073/pnas.1315792111

Rolig, A. S., Mittge, E. K., Ganz, J., Troll, J. V., Melancon, E., Wiles, T. J., . . . Guillemin, K. (2017). The enteric nervous system promotes intestinal health by constraining microbiota composition. *PLoS Biol, 15*(2), e2000689. doi:10.1371/journal.pbio.2000689

Rooks, M. G., & Garrett, W. S. (2016). Gut microbiota, metabolites and host immunity. *Nat Rev Immunol, 16*(6), 341-352. doi:10.1038/nri.2016.42

Rosenbaum, C., Schick, M. A., Wollborn, J., Heider, A., Scholz, C. J., Cecil, A., . . . Metzger, M. (2016). Activation of Myenteric Glia during Acute Inflammation In Vitro and In Vivo. *PLoS One, 11*(3), e0151335. doi:10.1371/journal.pone.0151335

Roulis, M., Bongers, G., Armaka, M., Salviano, T., He, Z., Singh, A., . . . Kollias, G. (2016). Host and microbiota interactions are critical for development of murine Crohn's-like ileitis. *Mucosal Immunol, 9*(3), 787-797. doi:10.1038/mi.2015.102

Rousseaux, C., Thuru, X., Gelot, A., Barnich, N., Neut, C., Dubuquoy, L., . . . Desreumaux, P. (2007). Lactobacillus acidophilus modulates intestinal pain and induces opioid and cannabinoid receptors. *Nat Med, 13*(1), 35-37. doi:10.1038/nm1521

Ruhl, A. (2005). Glial cells in the gut. *Neurogastroenterol Motil, 17*(6), 777-790. doi:10.1111/j.1365-2982.2005.00687.x

Ruhl, A., Franzke, S., Collins, S. M., & Stremmel, W. (2001). Interleukin-6 expression and regulation in rat enteric glial cells. *Am J Physiol Gastrointest Liver Physiol, 280*(6), G1163-1171. doi:10.1152/ajpgi.2001.280.6.G1163

Ruhl, A., Franzke, S., & Stremmel, W. (2001). IL-1beta and IL-10 have dual effects on enteric glial cell proliferation. *Neurogastroenterol Motil, 13*(1), 89-94.

Ruhl, A., Hoppe, S., Frey, I., Daniel, H., & Schemann, M. (2005). Functional expression of the peptide transporter PEPT2 in the mammalian enteric nervous system. *J Comp Neurol, 490*(1), 1-11. doi:10.1002/cne.20617

Ruhl, A., Trotter, J., & Stremmel, W. (2001). Isolation of enteric glia and establishment of transformed enteroglial cell lines from the myenteric plexus of adult rat. *Neurogastroenterol Motil, 13*(1), 95-106.

Rusmini, M., Griseri, P., Lantieri, F., Matera, I., Hudspeth, K. L., Roberto, A., . . . Mavilio, D. (2013). Induction of RET dependent and independent pro-inflammatory programs in human peripheral blood mononuclear cells from Hirschsprung patients. *PLoS One, 8*(3), e59066. doi:10.1371/journal.pone.0059066

Sampson, T. R., Debelius, J. W., Thron, T., Janssen, S., Shastri, G. G., Ilhan, Z. E., . . . Mazmanian, S. K. (2016). Gut Microbiota Regulate Motor Deficits and Neuroinflammation in a Model of Parkinson's Disease. *Cell, 167*(6), 1469-1480 e1412. doi:10.1016/j.cell.2016.11.018

Samulski, R. J., & Muzyczka, N. (2014). AAV-Mediated Gene Therapy for Research and Therapeutic Purposes. *Annu Rev Virol, 1*(1), 427-451. doi:10.1146/annurev-virology-031413-085355

Sanders, K. M., Kito, Y., Hwang, S. J., & Ward, S. M. (2016). Regulation of Gastrointestinal Smooth Muscle Function by Interstitial Cells. *Physiology (Bethesda), 31*(5), 316-326. doi:10.1152/physiol.00006.2016

Sanovic, S., Lamb, D. P., & Blennerhassett, M. G. (1999). Damage to the enteric nervous system in experimental colitis. *Am J Pathol, 155*(4), 1051-1057. doi:10.1016/S0002-9440(10)65207-8

Sansonetti, P. J. (2004). War and peace at mucosal surfaces. *Nat Rev Immunol, 4*(12), 953-964. doi:10.1038/nri1499

Sant'Ana, D. M., Gois, M. B., Zanoni, J. N., da Silva, A. V., da Silva, C. J., & Araujo, E. J. (2012). Intraepithelial lymphocytes, goblet cells and VIP-IR submucosal neurons of jejunum rats infected with Toxoplasma gondii. *Int J Exp Pathol, 93*(4), 279-286. doi:10.1111/j.1365-2613.2012.00824.x

Sant'Ana, D. M. G., Gois, M. B., Hermes-Uliana, C., Pereira-Severi, L. S., Baptista, E. M., Mantovani, L. C., . . . de Almeida Araujo, E. J. (2017). Acute infection with an avirulent strain of Toxoplasma gondii causes decreasing and atrophy of nitrergic myenteric neurons of rats. *Acta Histochem, 119*(4), 423-427. doi:10.1016/j.acthis.2017.04.008

Saravia, J., Chapman, N. M., & Chi, H. (2019). Helper T cell differentiation. *Cell Mol Immunol*. doi:10.1038/s41423-019-0220-6

Sarnelli, G., De Giorgio, R., Gentile, F., Cali, G., Grandone, I., Rocco, A., . . . D'Argenio, G. (2009). Myenteric neuronal loss in rats with experimental colitis: role of tissue transglutaminase-induced apoptosis. *Dig Liver Dis, 41*(3), 185-193. doi:10.1016/j.dld.2008.06.004

Sasselli, V., Boesmans, W., Vanden Berghe, P., Tissir, F., Goffinet, A. M., & Pachnis, V. (2013). Planar cell polarity genes control the connectivity of enteric neurons. *J Clin Invest, 123*(4), 1763-1772. doi:10.1172/JCI66759

Schafer, D. P., Lehrman, E. K., Kautzman, A. G., Koyama, R., Mardinly, A. R., Yamasaki, R., . . . Stevens, B. (2012). Microglia sculpt postnatal neural circuits in an activity and complement-dependent manner. *Neuron, 74*(4), 691-705. doi:10.1016/j.neuron.2012.03.026

Schafer, D. P., Lehrman, E. K., & Stevens, B. (2013). The "quad-partite" synapse: microglia-synapse interactions in the developing and mature CNS. *Glia, 61*(1), 24-36. doi:10.1002/glia.22389

Scheperjans, F., Aho, V., Pereira, P. A., Koskinen, K., Paulin, L., Pekkonen, E., . . . Auvinen, P. (2015). Gut microbiota are related to Parkinson's disease and clinical phenotype. *Mov Disord, 30*(3), 350-358. doi:10.1002/mds.26069

Schneider, J., Jehle, E. C., Starlinger, M. J., Neunlist, M., Michel, K., Hoppe, S., & Schemann, M. (2001). Neurotransmitter coding of enteric neurones in the submucous plexus is changed in non-inflamed rectum of patients with Crohn's disease. *Neurogastroenterol Motil, 13*(3), 255-264.

Schneider, S., Wright, C. M., & Heuckeroth, R. O. (2018). Unexpected Roles for the Second Brain: Enteric Nervous System as Master Regulator of Bowel Function. *Annu Rev Physiol*. doi:10.1146/annurev-physiol-021317-121515

Schuchardt, A., D'Agati, V., Larsson-Blomberg, L., Costantini, F., & Pachnis, V. (1994). Defects in the kidney and enteric nervous system of mice lacking the tyrosine kinase receptor Ret. *Nature, 367*(6461), 380-383. doi:10.1038/367380a0

Semar, S., Klotz, M., Letiembre, M., Van Ginneken, C., Braun, A., Jost, V., . . . Schafer, K. H. (2013). Changes of the enteric nervous system in amyloid-beta protein precursor transgenic mice correlate with disease progression. *J Alzheimers Dis, 36*(1), 7-20. doi:10.3233/JAD-120511

Seth, A., Stemple, D. L., & Barroso, I. (2013). The emerging use of zebrafish to model metabolic disease. *Dis Model Mech, 6*(5), 1080-1088. doi:10.1242/dmm.011346

Shankle, W. R., Landing, B. H., Ang, S. M., Chui, H., Villarreal-Engelhardt, G., & Zarow, C. (1993). Studies of the enteric nervous system in Alzheimer disease and other dementias of the elderly: enteric neurons in Alzheimer disease. *Mod Pathol, 6*(1), 10-14.

Shea-Donohue, T., Notari, L., Stiltz, J., Sun, R., Madden, K. B., Urban, J. F., Jr., & Zhao, A. (2010). Role of enteric nerves in immune-mediated changes in protease-activated receptor 2 effects on gut function. *Neurogastroenterol Motil, 22*(10), 1138-e1291. doi:10.1111/j.1365-2982.2010.01557.x

Shinkai, Y., Rathbun, G., Lam, K. P., Oltz, E. M., Stewart, V., Mendelsohn, M., . . . et al. (1992). RAG-2-deficient mice lack mature lymphocytes owing to inability to initiate V(D)J rearrangement. *Cell, 68*(5), 855-867.

Smith, T. K., & Koh, S. D. (2017). A model of the enteric neural circuitry underlying the generation of rhythmic motor patterns in the colon: the role of serotonin. *Am J Physiol Gastrointest Liver Physiol, 312*(1), G1-G14. doi:10.1152/ajpgi.00337.2016

Smith, T. K., & Robertson, W. J. (1998). Synchronous movements of the longitudinal and circular muscle during peristalsis in the isolated guinea-pig distal colon. *J Physiol, 506 (Pt 2)*, 563-577.

Sofroniew, M. V. (2009). Molecular dissection of reactive astrogliosis and glial scar formation. *Trends Neurosci, 32*(12), 638-647. doi:10.1016/j.tins.2009.08.002

Sokol, H., Polin, V., Lavergne-Slove, A., Panis, Y., Treton, X., Dray, X., . . . Marteau, P. (2009). Plexitis as a predictive factor of early postoperative clinical recurrence in Crohn's disease. *Gut, 58*(9), 1218-1225. doi:10.1136/gut.2009.177782

Song, W. M., & Colonna, M. (2018). The identity and function of microglia in neurodegeneration. *Nat Immunol, 19*(10), 1048-1058. doi:10.1038/s41590-018-0212-1

Soret, R., Chevalier, J., De Coppet, P., Poupeau, G., Derkinderen, P., Segain, J. P., & Neunlist, M. (2010). Short-chain fatty acids regulate the enteric neurons and control gastrointestinal motility in rats. *Gastroenterology, 138*(5), 1772-1782. doi:10.1053/j.gastro.2010.01.053

Soufflet, F., Biraud, M., Rolli-Derkinderen, M., Lardeux, B., Trang, C., Coron, E., . . . Neunlist, M. (2018). Modulation of VIPergic phenotype of enteric neurons by colonic biopsy supernatants from patients with inflammatory bowel diseases: Involvement of IL-6 in Crohn's disease. *Neurogastroenterol Motil, 30*(2). doi:10.1111/nmo.13198

Southard-Smith, E. M., Kos, L., & Pavan, W. J. (1998). Sox10 mutation disrupts neural crest development in Dom Hirschsprung mouse model. *Nat Genet, 18*(1), 60-64. doi:10.1038/ng0198-60

Spencer, N. J. (2001). Control of migrating motor activity in the colon. *Curr Opin Pharmacol, 1*(6), 604-610.

Spits, H., & Cupedo, T. (2012). Innate lymphoid cells: emerging insights in development, lineage relationships, and function. *Annu Rev Immunol, 30*, 647-675. doi:10.1146/annurev-immunol-020711-075053

Stanisz, A. M., Befus, D., & Bienenstock, J. (1986). Differential effects of vasoactive intestinal peptide, substance P, and somatostatin on immunoglobulin synthesis and proliferations by lymphocytes from Peyer's patches, mesenteric lymph nodes, and spleen. *J Immunol, 136*(1), 152-156.

Starr, D. A., & Fischer, J. A. (2005). KASH 'n Karry: the KASH domain family of cargo-specific cytoskeletal adaptor proteins. *Bioessays, 27*(11), 1136-1146. doi:10.1002/bies.20312

Stavely, R., Robinson, A. M., Miller, S., Boyd, R., Sakkal, S., & Nurgali, K. (2015a). Allogeneic guinea pig mesenchymal stem cells ameliorate neurological changes in experimental colitis. *Stem Cell Res Ther, 6*, 263. doi:10.1186/s13287-015-0254-3

Stavely, R., Robinson, A. M., Miller, S., Boyd, R., Sakkal, S., & Nurgali, K. (2015b). Human adult stem cells derived from adipose tissue and bone marrow attenuate enteric neuropathy in the guinea-pig model of acute colitis. *Stem Cell Res Ther, 6*, 244. doi:10.1186/s13287-015-0231-x

Stevens, J. C., Banks, G. T., Festing, M. F., & Fisher, E. M. (2007). Quiet mutations in inbred strains of mice. *Trends Mol Med, 13*(12), 512-519. doi:10.1016/j.molmed.2007.10.001

Subramanian, A., Tamayo, P., Mootha, V. K., Mukherjee, S., Ebert, B. L., Gillette, M. A., . . . Mesirov, J. P. (2005). Gene set enrichment analysis: a knowledge-based approach for interpreting genome-wide expression profiles. *Proc Natl Acad Sci U S A, 102*(43), 15545-15550. doi:10.1073/pnas.0506580102

Sun, M., He, C., Cong, Y., & Liu, Z. (2015). Regulatory immune cells in regulation of intestinal inflammatory response to microbiota. *Mucosal Immunol, 8*(5), 969-978. doi:10.1038/mi.2015.49

Syken, J., & Shatz, C. J. (2003). Expression of T cell receptor beta locus in central nervous system neurons. *Proc Natl Acad Sci U S A, 100*(22), 13048-13053. doi:10.1073/pnas.1735415100

Szabolcs, M. J., Visser, J., Shelanski, M. L., O'Toole, K., & Schullinger, J. N. (1996). Peripherin: a novel marker for the immunohistochemical study of malformations of the enteric nervous system. *Pediatr Pathol Lab Med, 16*(1), 51-70.

Team, R. C. (2014). A Language and Environment for Statistical Computing. Vienna, Austria. Retrieved from http://www.R-project.org/

Tebaldi, T., Zuccotti, P., Peroni, D., Kohn, M., Gasperini, L., Potrich, V., . . . Quattrone, A. (2018). HuD Is a Neural Translation Enhancer Acting on mTORC1-Responsive Genes and Counteracted by the Y3 Small Non-coding RNA. *Mol Cell, 71*(2), 256-270 e210. doi:10.1016/j.molcel.2018.06.032

Teng, L., Mundell, N. A., Frist, A. Y., Wang, Q., & Labosky, P. A. (2008). Requirement for Foxd3 in the maintenance of neural crest progenitors. *Development, 135*(9), 1615-1624. doi:10.1242/dev.012179

Tilghman, J. M., Ling, A. Y., Turner, T. N., Sosa, M. X., Krumm, N., Chatterjee, S., . . . Chakravarti, A. (2019). Molecular Genetic Anatomy and Risk Profile of Hirschsprung's Disease. *N Engl J Med, 380*(15), 1421-1432. doi:10.1056/NEJMoa1706594

Timmermans, J. P., Hens, J., & Adriaensen, D. (2001). Outer submucous plexus: an intrinsic nerve network involved in both secretory and motility processes in the intestine of large mammals and humans. *Anat Rec, 262*(1), 71-78.

Timmermans, J. P., Scheuermann, D. W., Gabriel, R., Adriaensen, D., Fekete, E., & De Groodt-Lasseel, M. H. (1991). The innervation of the gastrointestinal tract of a chelonian reptile, Pseudemys scripta elegans. I. Structure and topography of the enteric nerve plexuses using neuron-specific enolase immunohistochemistry. *Histochemistry, 95*(4), 397-402.

Tordesillas, L., Berin, M. C., & Sampson, H. A. (2017). Immunology of Food Allergy. *Immunity, 47*(1), 32-50. doi:10.1016/j.immuni.2017.07.004

Turco, F., Sarnelli, G., Cirillo, C., Palumbo, I., De Giorgi, F., D'Alessandro, A., . . . Cuomo, R. (2014). Enteroglial-derived S100B protein integrates bacteria-induced Toll-like receptor signalling in human enteric glial cells. *Gut, 63*(1), 105-115. doi:10.1136/gutjnl-2012-302090

Tuttle, A. H., Philip, V. M., Chesler, E. J., & Mogil, J. S. (2018). Comparing phenotypic variation between inbred and outbred mice. *Nat Methods, 15*(12), 994-996. doi:10.1038/s41592-018-0224-7

Ueno, E., Hisajima, T., Nakano, M., Goris, R. C., & Funakoshi, K. (2011). Increased migration of IgA lymphocytes to VIP nerve fibers after DSS-induced colitis. *Histol Histopathol, 26*(10), 1317-1326. doi:10.14670/HH-26.1317

Uesaka, T., Nagashimada, M., & Enomoto, H. (2015). Neuronal Differentiation in Schwann Cell Lineage Underlies Postnatal Neurogenesis in the Enteric Nervous System. *J Neurosci, 35*(27), 9879-9888. doi:10.1523/JNEUROSCI.1239-15.2015

Vainchtein, I. D., Chin, G., Cho, F. S., Kelley, K. W., Miller, J. G., Chien, E. C., . . . Molofsky, A. V. (2018). Astrocyte-derived interleukin-33 promotes microglial synapse engulfment and neural circuit development. *Science, 359*(6381), 1269-1273. doi:10.1126/science.aal3589

van den Pol, A. N. (2012). Neuropeptide transmission in brain circuits. *Neuron, 76*(1), 98-115. doi:10.1016/j.neuron.2012.09.014

Vanderwinden, J. M., Timmermans, J. P., & Schiffmann, S. N. (2003). Glial cells, but not interstitial cells, express P2X7, an ionotropic purinergic receptor, in rat gastrointestinal musculature. *Cell Tissue Res, 312*(2), 149-154. doi:10.1007/s00441-003-0716-2

Vanner, S., & Surprenant, A. (1991). Cholinergic and noncholinergic submucosal neurons dilate arterioles in guinea pig colon. *Am J Physiol, 261*(1 Pt 1), G136-144. doi:10.1152/ajpgi.1991.261.1.G136

Veerkamp, J. H., & Zimmerman, A. W. (2001). Fatty acid-binding proteins of nervous tissue. *J Mol Neurosci, 16*(2-3), 133-142; discussion 151-137. doi:10.1385/JMN:16:2-3:133

Veiga-Fernandes, H., Coles, M. C., Foster, K. E., Patel, A., Williams, A., Natarajan, D., . . . Kioussis, D. (2007). Tyrosine kinase receptor RET is a key regulator of Peyer's patch organogenesis. *Nature, 446*(7135), 547-551. doi:10.1038/nature05597

Verdu, E. F., Bercik, P., Verma-Gandhu, M., Huang, X. X., Blennerhassett, P., Jackson, W., . . . Collins, S. M. (2006). Specific probiotic therapy attenuates antibiotic induced visceral hypersensitivity in mice. *Gut, 55*(2), 182-190. doi:10.1136/gut.2005.066100

Vicentino-Vieira, S. L., Gois, M. B., Trevizan, A. R., de Lima, L. L., Leatte, E. P., Nogueira de Melo, G. A., . . . Sant'Ana, D. M. G. (2017). Toxoplasma gondii infection causes structural changes in the jejunum of rats infected with different inoculum doses. *Life Sci, 191*, 141-149. doi:10.1016/j.lfs.2017.10.032

Vieten, D., & Spicer, R. (2004). Enterocolitis complicating Hirschsprung's disease. *Semin Pediatr Surg, 13*(4), 263-272.

Villanacci, V., Bassotti, G., Nascimbeni, R., Antonelli, E., Cadei, M., Fisogni, S., . . . Geboes, K. (2008). Enteric nervous system abnormalities in inflammatory bowel diseases. *Neurogastroenterol Motil, 20*(9), 1009-1016. doi:10.1111/j.1365-2982.2008.01146.x

von Boyen, G. B., Steinkamp, M., Reinshagen, M., Schafer, K. H., Adler, G., & Kirsch, J. (2004). Proinflammatory cytokines increase glial fibrillary acidic protein expression in enteric glia. *Gut, 53*(2), 222-228.

Vulchanova, L., Casey, M. A., Crabb, G. W., Kennedy, W. R., & Brown, D. R. (2007). Anatomical evidence for enteric neuroimmune interactions in Peyer's patches. *J Neuroimmunol, 185*(1-2), 64-74. doi:10.1016/j.jneuroim.2007.01.014

Wajant, H., Pfizenmaier, K., & Scheurich, P. (2003). Tumor necrosis factor signaling. *Cell Death Differ, 10*(1), 45-65. doi:10.1038/sj.cdd.4401189

Wallace, A. S., & Burns, A. J. (2005). Development of the enteric nervous system, smooth muscle and interstitial cells of Cajal in the human gastrointestinal tract. *Cell Tissue Res, 319*(3), 367-382. doi:10.1007/s00441-004-1023-2

Wan, Y. Y., & Flavell, R. A. (2005). Identifying Foxp3-expressing suppressor T cells with a bicistronic reporter. *Proc Natl Acad Sci U S A, 102*(14), 5126-5131. doi:10.1073/pnas.0501701102

Ward, S. M., Burns, A. J., Torihashi, S., & Sanders, K. M. (1994). Mutation of the proto-oncogene c-kit blocks development of interstitial cells and electrical rhythmicity in murine intestine. *J Physiol, 480 (Pt 1)*, 91-97.

Williams, E. K., Chang, R. B., Strochlic, D. E., Umans, B. D., Lowell, B. B., & Liberles, S. D. (2016). Sensory Neurons that Detect Stretch and Nutrients in the Digestive System. *Cell, 166*(1), 209-221. doi:10.1016/j.cell.2016.05.011

Winston, J. H., Li, Q., & Sarna, S. K. (2013). Paradoxical regulation of ChAT and nNOS expression in animal models of Crohn's colitis and ulcerative colitis. *Am J Physiol Gastrointest Liver Physiol, 305*(4), G295-302. doi:10.1152/ajpgi.00052.2013

Wraith, D. C., & Nicholson, L. B. (2012). The adaptive immune system in diseases of the central nervous system. *J Clin Invest, 122*(4), 1172-1179. doi:10.1172/JCI58648

Yano, J. M., Yu, K., Donaldson, G. P., Shastri, G. G., Ann, P., Ma, L., . . . Hsiao, E. Y. (2015). Indigenous bacteria from the gut microbiota regulate host serotonin biosynthesis. *Cell, 161*(2), 264-276. doi:10.1016/j.cell.2015.02.047

Yissachar, N., Zhou, Y., Ung, L., Lai, N. Y., Mohan, J. F., Ehrlicher, A., . . . Benoist, C. (2017). An Intestinal Organ Culture System Uncovers a Role for the Nervous System in Microbe-Immune Crosstalk. *Cell, 168*(6), 1135-1148 e1112. doi:10.1016/j.cell.2017.02.009

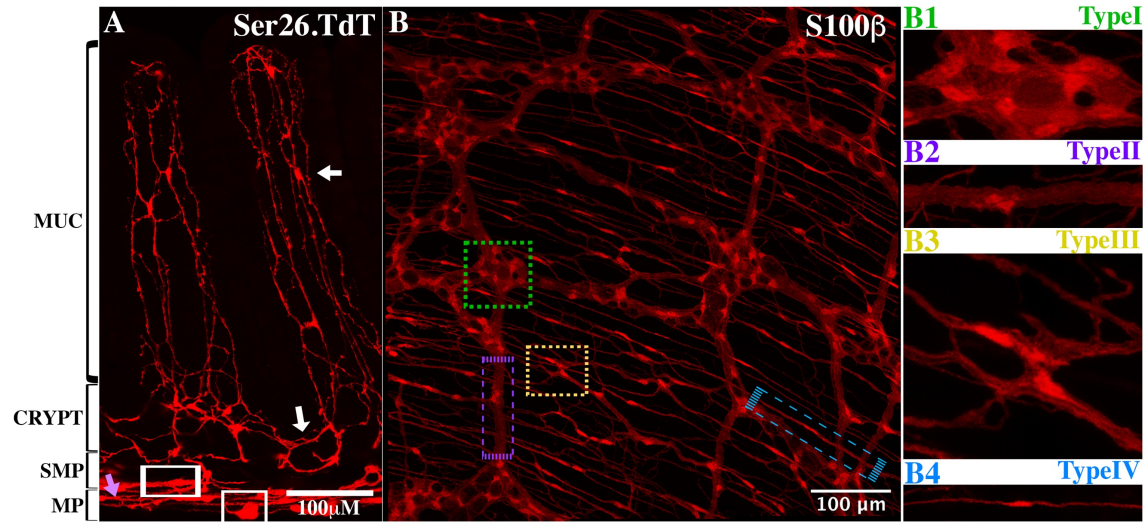
Young, H. M., Bergner, A. J., & Muller, T. (2003). Acquisition of neuronal and glial markers by neural crest-derived cells in the mouse intestine. *J Comp Neurol, 456*(1), 1-11. doi:10.1002/cne.10448

Young, H. M., Bergner, A. J., Simpson, M. J., McKeown, S. J., Hao, M. M., Anderson, C. R., & Enomoto, H. (2014). Colonizing while migrating: how do individual enteric neural crest cells behave? *BMC Biol, 12*, 23. doi:10.1186/1741-7007-12-23

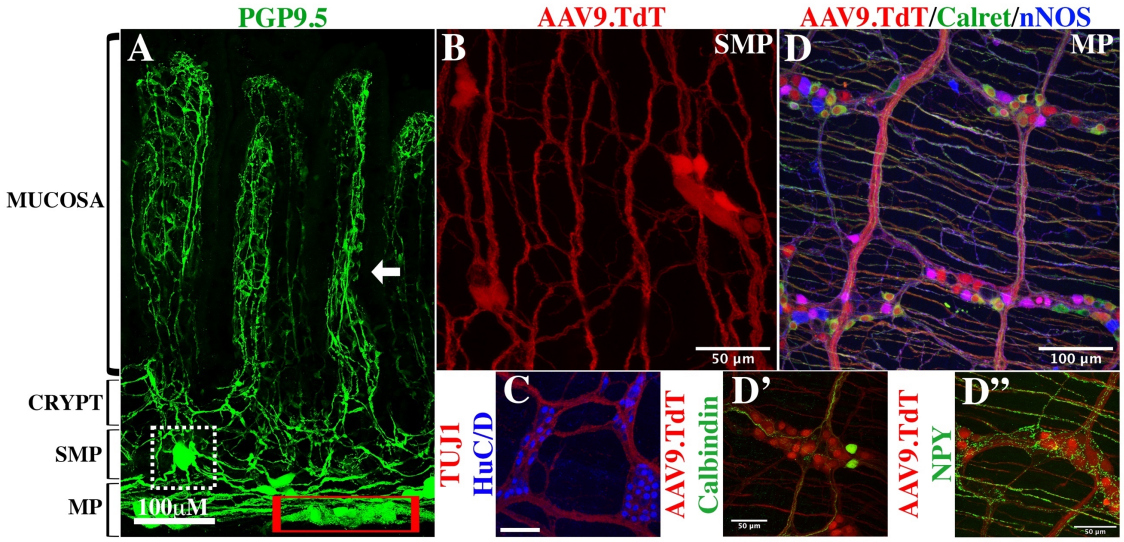
Zelikowsky, M., Hui, M., Karigo, T., Choe, A., Yang, B., Blanco, M. R., . . . Anderson, D. J. (2018). The Neuropeptide Tac2 Controls a Distributed Brain State Induced by Chronic Social Isolation Stress. *Cell, 173*(5), 1265-1279 e1219. doi:10.1016/j.cell.2018.03.037

Zhao, L. (2010). Genomics: The tale of our other genome. *Nature, 465*(7300), 879-880. doi:10.1038/465879a

Zhu, B., Wang, X., & Li, L. (2010). Human gut microbiome: the second genome of human body. *Protein Cell, 1*(8), 718-725. doi:10.1007/s13238-010-0093-z

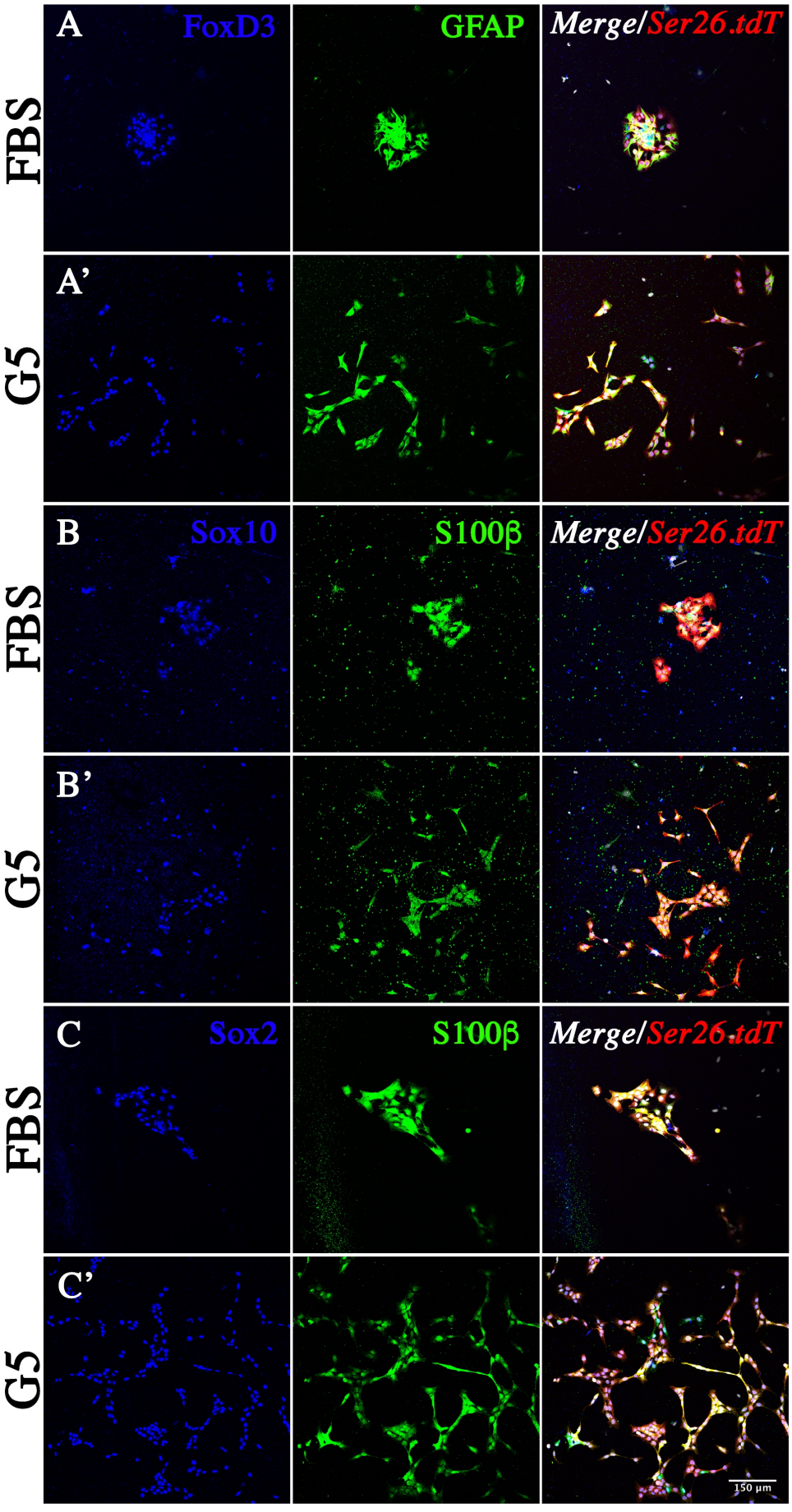


Appendix 1. Localisation and morphology of EGC subsets within the intestinal wall. MUC: Mucosal layer, MP: myenteric plexus, SMP: submucosal plexus. **(A)** Cross-section of ileum from the *Ser26.tdT* mice showing the **subepithelial** EGCs within the lamina propria and surrounding crypts (white arrows); **intramuscular** EGCs (lilac arrow) and **intraganglionic** EGCs within the SMP and MP (white squares). **(B)** Whole-mount preparation of LMMPs immunostained for S100β, highlighting the localisation of type I EGCs (green square), type II (purple rectangle), type III (yellow square) and type IV (blue rectangle). Higher magnification showing the morphology of type I EGCs **(B1)**, type II **(B2)**, type III **(B3)** and type IV **(B4)**. Scale bars: 100 µm.

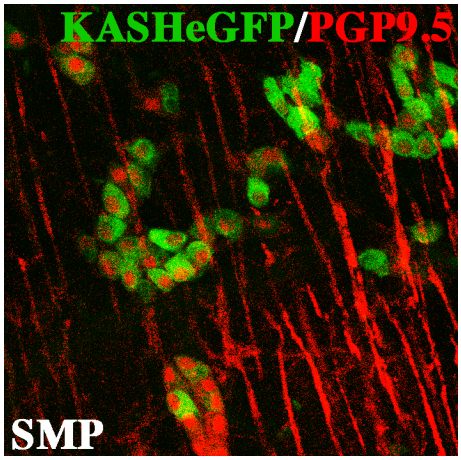


Appendix 2. Neuronal network within the gut. MP: myenteric plexus, SMP: submucosal plexus. **(A)** Cross-section of the ileum immunostained for the neuronal pan-marker PGP9.5 (green) showing neurons within the myenteric plexus (red rectangle) and the submucosal plexus (white square), and neuronal fibres within the mucosal layer (white arrow). **(B)** Whole-mount preparation of submucosal plexus from the ileum of

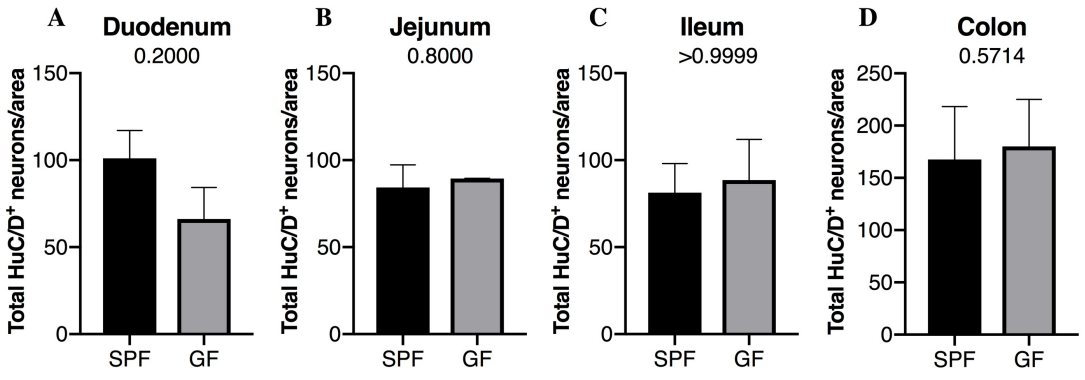
Rosa26.Td^{Tomato} mice transduced with AAV9.CaMKII.Cre showing neurons in red. **(C)** Whole-mount LMMP immunostaining for the pan-neuronal markers Tuj1 (red) and HuC/D (blue). Whole-mount preparation of LMMPs from the ileum of R26.Td^{Tomato} mice transduced with AAV9.CaMKII.Cre (red), and immunostained for the neuronal subtypes Calretinin (green) and nNos (blue) **(D)**, Calbindin (green) **(D')** and NPY (green) **(D")**. Scale bars: 100 μm **(A and D)** and 50 μm **(B, C, D' and D")**.


A
FoxD3
GFAP
Merge/Ser26.tdT
FBS
A'
G5
B
Sox10
S100β
Merge/Ser26.tdT
FBS
B'
G5
C
Sox2
S100β
Merge/Ser26.tdT
FBS
C'
G5
150 µm

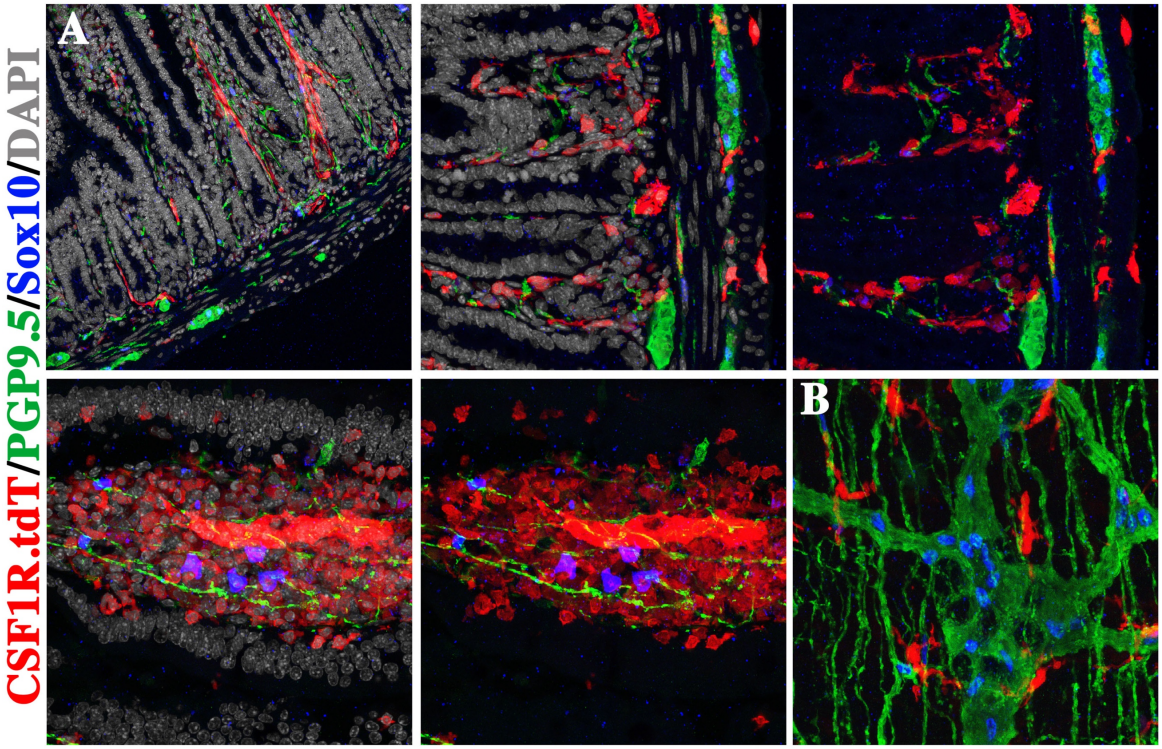
Appendix 3. *In vitro* expression of EGC markers in tdT$^+$ cells at DIV3. (A-C') Representative confocal images showing the expression of known EGC markers at DIV3 by tdT$^+$ cells (red) cultured in presence of FBS **(A, B and C)** or in G5 media **(A', B' and C')**. Immunocytochemistry to detect FoxD3 (blue) and GFAP (green) expression in tdT$^+$ cells in FBS **(A)** and G5 **(A')** culture conditions. Immunocytochemistry to identify Sox10 (blue) and S100β (green) expressing EGCs in cultures of *Ser26.tdT* mouse line in FBS **(B)** and G5 **(B')** media. Immunocytochemistry for the EGC markers Sox2 (blue) and S100β (green) in cultures of *Ser26.tdT* mouse line in FBS **(C)** and G5 **(C')** media. Nuclei were visualised by DAPI. Scale bar: 150 μm.



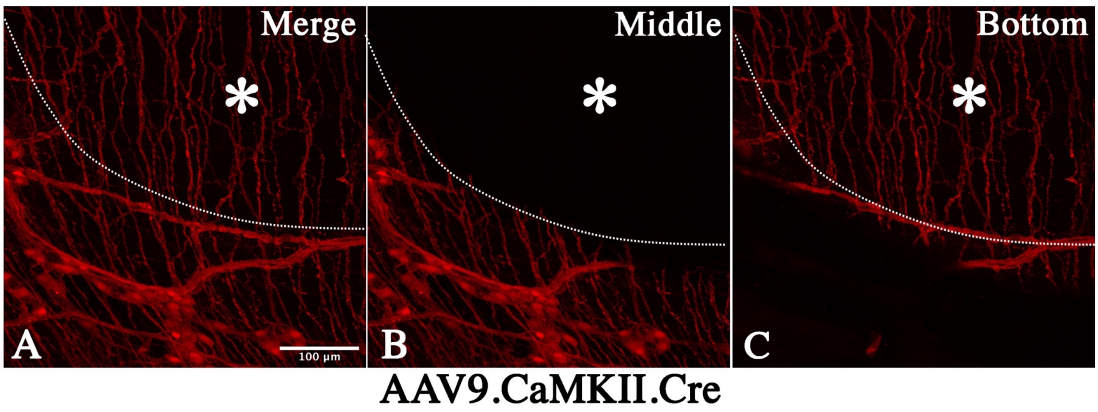
Appendix 4. eGFP expression in neurons from the SMP of the colon. Immunohistochemistry for PGP9.5 (red) in whole-mount colonic preparation from C57Bl/6 mice injected with AAV9.CaMKIIeGFP.



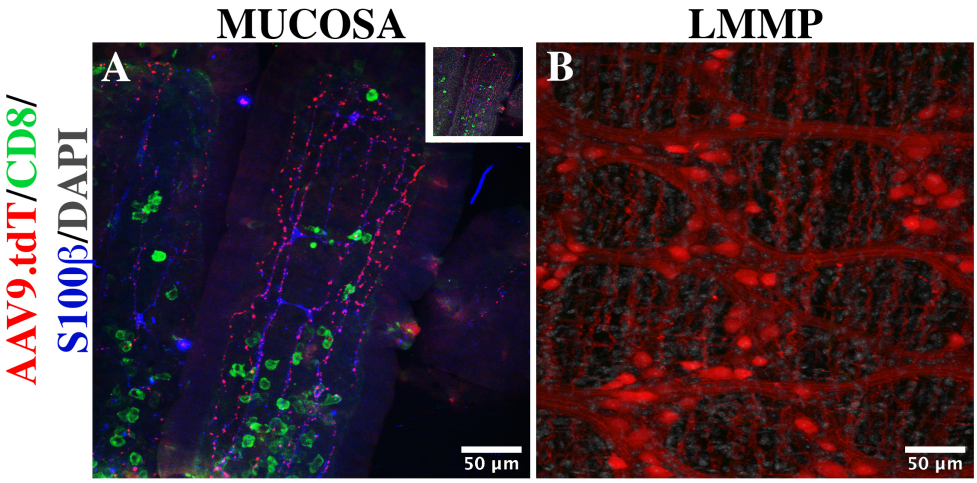
Appendix 5. Number of HuC/D$^+$ neurons within the MP of GF and SPF mice. (A-D) Graphs represent the average of the total number of HuC/D$^+$ neurons within the MP of GF and SPF mice in the duodenum **(A)**, jejunum **(B)**, ileum **(C)** and colon **(D)**. Bars represent SD. Duodenum (SPF: 101.1 ± 13.09 cells/area SD, GF: 66.17 ± 14.78), Jejunum (SPF: 84.25 ± 10.64, GF: 89.38 ± 0.125), Ileum (SPF: 81.33 ± 13.63, GF: 88.61 ± 19.03) and Colon (SPF: 167.5 ± 43.9, GF: 180 ± 36.77 SD).



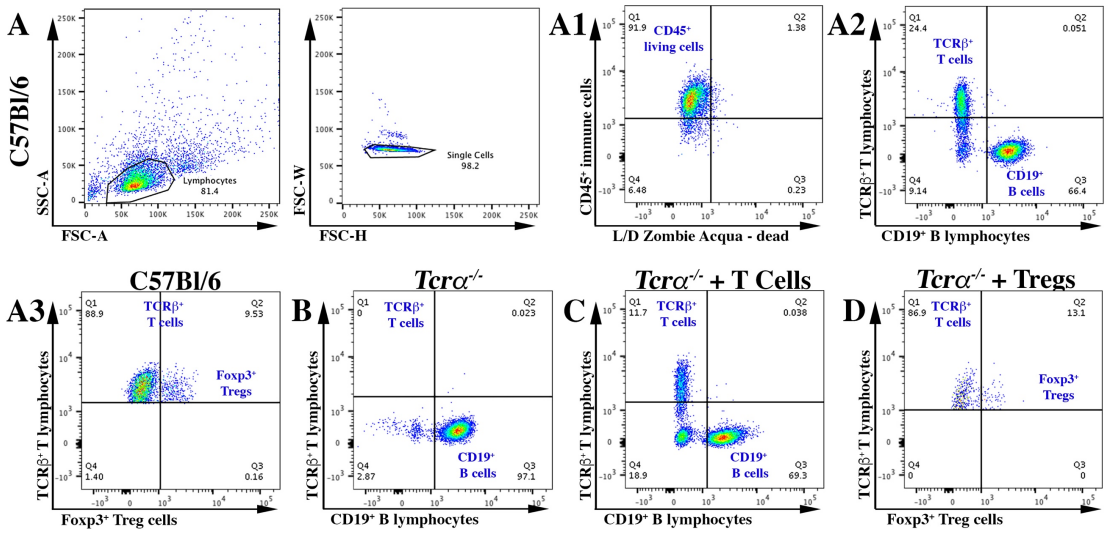
Appendix 6. Localisation of MMs relative to the ENS within different layers in the intestinal wall. Immunohistochemistry for the neuronal marker PGP9.5 (green), the EGCs marker Sox10 (blue) on 14 µm thick transverse sections **(A)** and LMMP preparations **(B)** of the ileum from the *Csf1r.tdT* mice in which macrophages express the tdT reporter (red). Nuclei were stained with DAPI.



Appendix 7. Neuronal network at the level of Peyer's Patches. Whole-mount preparation of ileum from the *Rosa26.TdT* mice injected with AAV9.CaMKII.Cre vector. Confocal images show stack of neuronal network (red) from different layers of the gut **(A)** and z-stacks at the level of PPs **(B)** and the bottom of PPs **(C)**. Asterisks represent PPs. Scale bar: 100 µm.

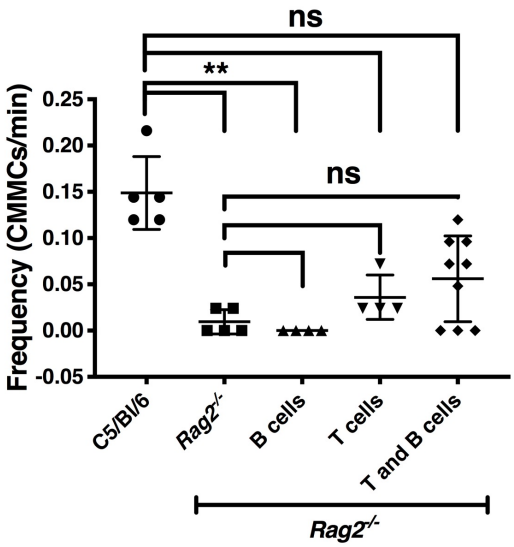


Appendix 8. CD8⁺ T cells localisation within the intestinal wall. Immunohistochemistry to detect CD8⁺ T cells (green), S100β EGCs (blue) on whole-mount preparations of the mucosal **(A)** and LMMP **(B)** layers from the *Rosa26.tdT* mice injected with AAV9.CaMKII.Cre to label neurons in red. Nuclei were stained with DAPI. Scale bar: 50 µm.



Appendix 9. Flow cytometry plots of spleen after adoptive transfer of lymphocytes into mice lacking T cells. (A) Representative flow cytometry plots of cell suspensions from the spleen in C57Bl/6 mice showing SSC-A vs FSC-A and FSC-W vs FSC-H gating strategy to exclude doublets. **(A1)** Representative gating to select live CD45⁺ immune cells (top left quadrant). **(A2)** Flow cytometry gating to separate TCRβ⁺ T cells (top left quadrant) and CD19⁺ B lymphocyte (bottom right quadrant) populations. **(A3)** Representative plot to identify Foxp3⁺TCRβ⁺ Tregs (top right quadrant). **(B)** Flow cytometry plot of spleen from the *Tcrα*$^{-/-}$ controls showing the absence of TCRβ⁺ T cells (top left quadrant) and the presence of CD19⁺ B lymphocytes (bottom right quadrant). **(C)** Flow cytometry plot of spleen from the *Tcrα*$^{-/-}$ transferred with naïve T cells showing TCRβ⁺ T lymphocytes (top left quadrant) and CD19⁺ B lymphocytes (bottom right quadrant). **(D)** Flow

cytometry plot of spleen from the *Tcrα*$^{-/-}$ transferred with regulatory T cells showing Foxp3^{+}TCRβ^{+} Tregs (top right quadrant).



Appendix 10. Neurogenic intestinal motility of mice lacking T and B cells after adoptive transfer of lymphocytes. (A) Graph shows the frequency of CMMCs (CMMCs/min) in C57Bl/6, *Rag2*$^{-/-}$ and *Rag2*$^{-/-}$ rescued with B, T and B and T lymphocytes. Kruskal Wallis, Dunn's Multiple Comparisons test, **p<0.01, n≥5mice/group.